

**UNIVERSITÀ DEGLI STUDI DI NAPOLI “FEDERICO II”**

*in consorzio con*  
**SECONDA UNIVERSITÀ DI NAPOLI**  
**UNIVERSITÀ “PARTHENOPE” NAPOLI**  
*in convenzione con*  
**ISTITUTO PER L’AMBIENTE MARINO COSTIERO – C.N.R.**  
**STAZIONE ZOOLOGICA “ANTON DOHRN”**

Dottorato in Scienze ed Ingegneria del Mare  
XVII ciclo

Tesi di Dottorato

**Ultraplankton in marine ecosystems:  
from seasonal cycle to short term responses**

Candidata:  
Dr. Immacolata Santarpia

Relatore:  
Dr. Vincenzo Saggiomo

Co-Relatore:  
Dr. Adriana Zingone

Il Coordinatore del Dottorato: Prof. Bruno D’Argenio

ANNO 2005

*“It is not the strongest of the species that survives,  
nor the most intelligent that survives.  
It is the one that is the most adaptable to change.”*  
*(C. Darwin)*

# **ABSTRACT**

A close relationship exists between phytoplankton size-class distribution and the carbon flow in the pelagic food webs. The smallest phytoplankton is esteemed to be responsible for about 38% of marine primary production (Agawin *et al.*, 2000). In spite of this, our knowledge of diversity, physiology and distribution of this size group is extremely fragmentary.

The broad aim of this project is a better understanding of the role of ultraphytoplankton (<5µm) in marine ecosystems. To this end, we have studied the distribution of this size fraction over an annual cycle at a long-term sampling station in the Gulf of Naples. The contribution to this fraction of different algal groups was evaluated by means of size-fractionated pigment analyses (HPLC). Further, experiments on the photophysiological responses of ultraphytoplankton (monospecific cultures and natural populations) were carried out in order to interpret its pattern of occurrence.

The results showed that the ultraphytoplankton, mainly small eukaryotes, is an abundant component of phytoplankton communities in Mediterranean coastal areas. The success of small eukaryotes may be explained by their high competitiveness in exploiting the episodic arrival of new nutrients. In addition, our observations on photoprotective mechanisms of the ultraphytoplankton showed that they have a very adaptable photosynthetic apparatus, where continuous regulation of antenna and reaction centers occur in order to avoid photodamage and to maximize carbon fixation rates in spite of both predictable (circadian cycle) and unpredictable (e.g. mixed water column) irradiance fluctuations. Thus, their productive capacity was similar to that of large cells. All these elements may suggest that the lower contribution of ultraphytoplankton during bloom periods could be related to an efficient grazing pressure from the microzooplankton.

Finally, the investigated species showed different responses in their photoprotective mechanisms, even within the same class, suggesting evolutionary constraints.

# Contents

<b>1. Introduction</b>	<b>p. 1</b>
1.1 Ultraphytoplankton in marine systems	p. 2
1.1.1 Definition	p. 2
1.1.2 Main features	p. 2
1.2 Aims of the project	p. 5
<b>2. Photosynthesis and controlling factors</b>	<b>p. 8</b>
2.1 Photosynthesis	p. 8
2.1.1 Photosynthetic pigments	p. 8
2.1.2 Photosynthetic units	p. 12
2.1.3 Electron transport chain	p. 12
2.1.4 Carbon organication	p. 14
2.2 Controlling factors	p. 16
2.2.1 Light	p. 16
2.2.2 Nutrients	p. 17
2.2.3 Temperature	p. 18
2.2.4 Grazing	p. 19
2.3 Phytoplankton response to light variability	p. 20
2.3.1 Photosynthesis-Irradiance curves	p. 21
2.3.2 Photoprotection	p. 23
2.3.3 Photoacclimation	p. 25
2.3.4 Circadian cycle	p. 27
<b>3. Materials and methods</b>	<b>p. 28</b>
3.1 <i>In situ</i> profiles	p. 28
3.2 Treatment and analyses of samples	p. 28
<b>4. Seasonal dynamics of fractionated phytoplankton pigments in a coastal environment</b>	<b>p. 34</b>
4.1 Study area	p. 34

4.1.1 Gulf of Naples	p. 34
4.1.2 Sampling strategies	p. 35
4.2 Hydrology	p. 36
4.3 Nutrients	p. 38
4.4 Phytoplankton biomass	p. 40
4.5 Primary production	p. 43
4.6 Pigments	p. 45
4.7 Discussion	p. 60
<b>5. Circadian patterns in natural ultraphytoplankton populations</b>	<b>p. 70</b>
5.1 TRI-1	p. 70
5.1.1 Physical parameters	p. 71
5.1.2 Pigments	p. 72
5.1.3 P <sub>vs</sub> E parameters	p. 75
5.1.4 Phyto-PAM coefficients	p. 77
5.1.5 FRRF parameters	p. 79
5.2 TRI-2	p. 81
5.2.1 Physical parameters	p. 81
5.2.2 Pigments	p. 83
5.2.3 P <sub>vs</sub> E parameters	p. 86
5.2.4 FRRF parameters	p. 88
5.3 TRI-3	p. 89
5.3.1 Physical parameters	p. 89
5.3.2 Pigments	p. 90
5.3.3 P <sub>vs</sub> E parameters	p. 92
5.3.4 Phyto-PAM coefficients	p. 94
5.4 Discussion	p. 97
<b>6. Photophysiological responses of five ultraphytoplankton species exposed to high irradiance</b>	<b>p. 103</b>
6.1 Species description	p. 103
6.1.1 culture conditions	p. 107

6.2 CULT-1	p. 108
6.2.1 Pigments	p. 108
6.2.2 Phyto-PAM coefficients	p. 111
6.3 CULT-2	p. 115
6.3.1 Pigments	p. 115
6.3.2 Phyto-PAM coefficients	p. 122
6.4 Discussion	p. 128
<b>Conclusions</b>	<b>p. 134</b>
<b>Appendix</b>	<b>p. 143</b>
<b>References</b>	<b>p. 147</b>
<b>Acknowledgements</b>	<b>p. 163</b>

## CHAPTER 1

### INTRODUCTION

The relevance of the carbon cycle to Earth climate and “global change” is a main topic for discussion in the scientific and social community nowadays (Hanson *et al.*, 1999; Chisholm *et al.*, 2001; Falkowski, 2002). Within this context, whether the oceans and their biome are a sink or a source for carbon dioxide is a major issue at the centre of a wide debate (Falkowski and Raven, 1997). Hence, a reliable estimate of primary production and respiration of marine phytoplankton over basin and regional scale are a fundamental achievement (Platt and Sathyendranath, 1988; Behrenfeld *et al.*, 2002).

Barber and Hilting (2002) have recently provided an exhaustive review of the available estimates of global primary productivity in the oceans, based on physical-biological models coupled with satellite images (CZCS, SeaWiFS). However, the need has been highlighted for a more accurate parameterization of phytoplankton physiology (Geider and MacIntyre, 2002) and its response to physical-chemical variables (e.g. light, temperature, nutrients) in order to improve these models (Riebesell and Wolf-Gladrow, 2002, Behrenfeld *et al.*, 2004). Since a close relationship exists between phytoplankton size-class distribution and the carbon flow in the pelagic food webs, the knowledge of the structure of phytoplankton assemblages by size is a relevant goal. In particular, the smallest phytoplankton is esteemed to be responsible for the 38% of the whole marine primary production (Agawin *et al.*, 2000) and this value rises up to the 90% in the oligotrophic areas (Li *et al.*, 1983). In spite of this, our knowledge of diversity, physiology and distribution of this size group is extremely fragmentary.

The broad aim of this project is a better understanding of the role of ultraphytoplankton in marine ecosystems. Particular attention has been devoted to small eukaryotes since their contribution would be more significant than previously suspected.

To this end, we have studied the distribution of this size fraction as compared to the rest of the phytoplankton populations over an annual cycle at a long-term sampling station in the Gulf of Naples. In addition, *in situ* and field experiments have been carried out on the photophysiological responses of the ultraphytoplankton; in order to interpret its patterns of occurrence. In fact, their spatial and temporal distribution could be partially explained by their specific responses to irradiance regime.

## 1.1 Ultraphytoplankton in marine ecosystems

### 1.1.1 Definition

As previously said, the size is a very relevant parameter in phytoplankton ecology. The cell size not only defines phytoplankton metabolic activity, growth rates and numerical abundance (Margalef, 1978; Falkowski *et al.*, 2004; Jiang *et al.*, 2005), but it also influences phytoplankton role in the biogeochemical cycles and the characteristics of community structure via size-dependent interactions (Kiørboe, 1993; Legendre and Michaud, 1998; Riebesell and Wolf-Gladrow, 2002). In spite of this, there is not a standardized classification of different dimensional classes accepted from the whole scientific community.

The term ultraphytoplankton was introduced for the first time by Nauman in the 1931 to define phytoplankton with dimension  $<5\mu\text{m}$ . Afterwards this definition has been used by other authors (Debres, 1974; Brunet and Lizon, 2003). However, some authors define ultraphytoplankton the organism  $<10\mu\text{m}$  (Li *et al.*, 1993), or, on the contrary, sometimes the fraction  $<5\mu\text{m}$  is called picoplankton (Stockner, 1988). In the present study I always used the term ultraphytoplankton for the fraction  $<5\mu\text{m}$ . This specific fraction has been chosen in order to study small eukaryotes. A lot of species of this group, in fact, have dimension between two and five  $\mu\text{m}$  (e.g. *Minidiscus comicus*, *Imantonia rotunda*).

### 1.1.2 Main features

The traditional fixatives such as formalin or Lugol, permit a good preservation of “robust” phytoplankton (e.g. diatoms), while the small and fragile species are not generally detected. As a consequence the recognition of the importance of delicates flagellates and minute coccoid forms ( $<2\mu\text{m}$ ) in the aquatic ecosystems has come only in the 1970s when more appropriate techniques (electron microscopy, flow cytometry, HPLC) were developed. Explicative is the discovery of the genus *Prochlorococcus* at the end of 1980s detected by cell flow-cytometry on ship-board (Chisholm *et al.*, 1988) and, afterwards, turned out a very widespread group (Jeffrey and Vesk, 1997).

To date, the picture of prokaryotic classification is quite clear. Good reviews were provided by Anagnostidis and Komárek (1990) for cyanobacteria and by Cox (1993) for prochlorophytes. In comparison the knowledge of the diversity of small eukaryotes is still very limited: only ~ 40 species belonging to nine classes of photosynthetic picoeukaryotes have been formerly described (Vaulot *et al.*, 2004). However, phylogenetic analyses have revealed much high diversity (Moon-van der Staay *et al.*, 2001; Zhu *et al.*, 2005) and

pigment signatures, electron microscopy and dilution cultures suggest that the classes Prasinophyceae, Pelagophyceae and Prymnesiophyceae are the major groups in different oceanic regions (Thomsen and Buck, 1998; Moon-van der Staay *et al.*, 2000). As consequence, to achieve a simple and reliable method to detect picoeukaryotes diversity is a crucial goal for understanding marine ecosystems. Recently a new technique based on taxon specific oligonucleotide probes in association with tyramide signal fluorescence *in situ* hybridization (TSA-FISH) and flow cytometry seems promising for quantitative assessment of picoeukaryotes (Biegala *et al.*, 2003; Not *et al.*, 2004).

As far as, the role of small phytoplankton in marine ecosystems has been recently reviewed by Agawin *et al.*, (2000) and by Bell and Kalf, (2001). Their data- set on abundance and production of small phytoplankton lead to the conclusion that these organisms play a much greater role in oligotrophic (chlorophyll a  $<0.3\text{mg m}^{-3}$ ), nutrient poor ( $\text{NO}_3+\text{NO}_2 < 1\mu\text{M}$ ) and warm ( $>26^\circ\text{C}$ ) waters, where they account for  $>50\%$  of total biomass. This dominance would be based on their major efficiency in nutrient uptake at low nutrient concentrations (Chisholm, 1992; Zubkov *et al.*, 2003) and in their rapid turnover (Raven, 1998). To demonstrate the validity of these assumptions recently Riebesell and Wolf-Gladrow (2002) have calculated the ratio of dissolved inorganic nitrogen (DIN) demand versus supply for phytoplankton cells as function of cell sizes, growth rates and DIN concentrations. As a consequence, they shown that only small phytoplankton could maintain a growth rate of  $1\text{d}^{-1}$  at the concentration usually present in oligotrophic waters. Agawin *et al.*, 2000 suggest that also temperature may favorite small phytoplankton, influencing the growth rate, but the strong co-variation between temperature and nutrients concentration and the small number of observation for both parameters affect the possibility to statistically separate their effects. On the other hand, though the absolute biomass and production of the small phytoplankton increase as total biomass increases, their relative contribution declines systematically (Agawin *et al.*, 2000; Bell and Kalf, 2001). Two linked hypotheses have been put forward to explain this relationship: the high small phytoplankton loss rate essentially due to predation by microzooplankton; the better competition of large cell in nutrient-rich waters and the little grazing pressure on them (Stockner, 1988; Bell and Kalf, 2001).

Otherwise, differences in the distribution of the different taxa may exist. For instance, small eukaryotes are generally more abundant in the coastal and nutrient rich waters (Courtiers *et al.*, 1994; Vaulot *et al.*, 2001). Furthermore, small eukaryotes and *Synechococcus* natural field populations show a positive relationship in terms of abundance and growth rate, which might be founded in similar response to relief from nutrient stress (Worden *et al.*, 2004). By

contrast *Prochlorococcus* and *Synechococcus* seem weak correlated. In particular, *Prochlorococcus* is generally dominant in systems based on recycled production since it turns out more efficient in  $\text{NH}_4$  and organic nitrogen compounds uptake (Zubkov *et al.*, 2003). Moreover, *Prochlorococcus* populations extend deeper in the water column than *Synechococcus*, probably since they are more efficient to absorb blue light (Ting *et al.*, 2002).

Obviously, to achieve a complete understanding of functional role of small phytoplankton in marine ecosystem a more complete knowledge of their physiology is desirable. Despite that, most of the detailed biochemical, molecular biological and physiological information about photosynthetic processes comes from studies of higher plants and few model micro-algae such as *Phaeodactylum tricornutum* for diatoms (e.g. Lohr and Wilhelm, 1999, 2001; Lavoud *et al.*, 2002a,b; Ruban *et al.*, 2004) and *Chlamydomonas reinhardtii* for green algae (e.g. Lin and Knox, 1991; Pineau *et al.*, 2001), generally chosen because they are easily grown rather than for their ecological role.

On the other hand, there is a great discrepancy in our knowledge about the different groups of small phytoplankton. In fact, the prokaryotes, above all the cyanobacteria (e.g. *Synechococcus*), have been more well studied than small eukaryotes, as it is demonstrated by the number of publications on their biology (Carr and Whitton, 1983; Fay and Van Baalen, 1987); molecular structure (Bryant, 1994; Jensen, 1993; Scanlan and West, 2002); photosynthesis (e.g. Bidigare *et al.*, 1989; Masojídek *et al.*, 2001; Palenik, 2001) and genomics (Palenik *et al.*, 2003; Rocap *et al.*, 2004).

By contrast, studies on small eukaryotes are fragmentary, probably in relation to their complexity and diversity, which is, as previous said, largely underestimated. An interesting exception is the small diatom *Thalassiosira pseudonana* (~5-7 $\mu\text{m}$  diameter), which was used in many physiological studies (e.g. Dortch *et al.*, 1991; Berges and Harrison, 1993; Thompson 1999). Further, this species was chosen as the first eukaryotic marine phytoplankton for whole genome sequencing because not only it has served as a model for diatom studies, but also the genus *Thalassiosira* is cosmopolitan throughout the world's oceans, and its genome is relatively small (34 mega base pairs). The complete *T. pseudonana* genome sequence will provide a foundation for interpreting the ecological success of these organisms and for better understanding phytoplankton physiology. The case of *T. pseudonana*, seems only the beginning of an increasing attention on small eukaryotes physiology and molecular biology as revealed by other recent studies (e.g. Jacquet *et al.*, 2001; DuRand *et al.*, 2002).

## 1.2 Aims of this project

The aim of this study is focused on the role of ultraphytoplankton (<5µm) in marine ecosystems: the contribution to phytoplankton biomass and productivity in a coastal environment and the attempt to correlate its patterns of occurrence to its photophysiology, through the responses to predictable (circadian patterns) and unpredictable (short term) changes in the irradiance regime.

As outlined in the previous section, only a few studies have been performed on the taxonomic composition and the contribution to total phytoplankton biomass of the smallest eukaryotes (most of them flagellated cells). This study works with the seasonal (over one year) and spatial (along the water column) ultraphytoplankton contributions (<5µm) to the entire phytoplankton biomass and productivity in a coastal environment and with the seasonal evolution of taxonomic composition (main algal groups) of this fraction by means of HPLC.

The use of signature pigments has been found to be very useful in outlining the main algal groups of phytoplankton communities, including the small and fragile forms generally underestimated by other methods (Jeffrey *et al.*, 1997). Another advantage is the capacity of HPLC analyses to detect pigments even when present at very low concentrations. In spite of these facts, only a few of the HPLC-based studies have performed pigment analyses on phytoplankton size fractions (Latasa and Bidigare, 1998; Ansotegui *et al.*, 2003; Rodriguez *et al.*, 2003).

The coastal study site was chosen on one hand to contribute to the knowledge of taxonomic composition of small eukaryotes (more abundant in coastal environments); on the other hand, the same sampling site has been sampled weekly by the researchers of the Zoological Station “A. Dohrn” from 1984 to present. This has allowed for comparing the results with a very reliable background of data. In particular, the role of ultraphytoplankton in this coastal marine ecosystem is discussed in relation to abiotic (e.g. nutrients) and biotic (e.g. “grazing”) factors, which may control its seasonal dynamics and composition.

In this context the responses to variations in light regime could be a key factor. Ultraphytoplankton photophysiology could be different from the “model” species and studying the characteristic of ultraphytoplankton responses to dark-light fluctuations in natural ultraphytoplankton populations could provide helpful instruments to working out these aspects.

To date, very few studies have been carried out to relate the characteristics of diel fluctuations (such as amplitude and timing) with algal size, obtaining contrasting results

(Glover *et al.*, 1985; Prezelin *et al.*, 1986, 1987). Moreover, in spite of the widely accepted significance of circadian cycles to phytoplankton physiology (see section 2.3.4) the interactions of the endogenous clock with the external environment (e.g. variability in the irradiance field) remain unclear. During the 1970-1980's several studies (Mac Caull and Platt, 1977; Prezelin and Ley, 1980; Forbes *et al.*, 1986; Vandeveldel *et al.*, 1989) were carried out on diel rhythm in phytoplankton photosynthesis in natural populations. However, they were aimed more at providing a good model to predict daily productivity (Vandeveldel *et al.*, 1989; Prezelin and Glover, 1991; Lizon *et al.*, 1995) than at understanding the physiological regulation of these rhythms (Kana *et al.*, 1985; Prezelin *et al.*, 1986).

So that, the second aim of this project was centred on test daily fluctuations of photophysiological parameters in a variety of natural ultraphytoplankton populations (where the  $<5\mu\text{m}$  fraction accounted for  $\geq 90\%$  of total biomass). Three experiments were carried out over a diel cycle (24h) in different ecological contexts (a coastal site, an offshore area and a Mediterranean lagoon), in different periods of the year (spring, early and late summer) and at different depths (i.e. different irradiance regimes).

In particular, the experiments were designed to allow detailed assessment of the circadian patterns not only in the photosynthetic coefficients and variable fluorescence parameters, but also in the pigment pool (with particular attention to the photoprotective pigments). In fact, the improvement of *in vivo* fluorescence techniques now permits to relate productivity with the organization of the photosynthetic apparatus and thus to provide a detailed picture of photophysiological regulations on a diel scale.

Finally, this work focused on the study of photoprotection mechanisms in some ultraphytoplankton species. In fact, the spatial distribution and the contribution to primary productivity of different ultraphytoplankton groups could be related to their capacity to acclimate to the fluctuations of natural light fields. Until now, many efforts have been made to understand the mechanisms of photoprotection adopted by the algae to limit the damage of excessive light (see sections 2.3.2 and 2.3.3 for a review). As mentioned above, the species used as a model for this type of studies were mainly large forms ( $> 20\mu\text{m}$ ), such as *P. tricornutum*, while the small size groups remain quite understudied. For instance, Glover *et al.* (1986, 1987) performed some comparative experiments on both small and large eukaryotes as well as on prokaryotes (i.e. *Synechococcus* spp.), but these experiments were focused in particular on the growth response to different intensities and qualities of light than on the photoprotective mechanisms themselves.

Thus, the third point of this project was to study the short term responses (min-hours) of five ultraphytoplankton (i.e. small eukaryotes) species exposed to excessive irradiance. In particular, the relationship between *in vivo* variable fluorescence parameters and changes in the de-epoxidative state of xanthophyll-cycle pigments was investigated. In fact, variable fluorescence parameters are a very reliable tool to estimate the energy distribution between photochemical activity and thermal dissipation during high irradiance conditions (Masojídek *et al.*, 1999), since they provide information on the status of photosystem II, one of the principal elements involved in photoprotection (see section 2.3 and 3.2). In addition, the role of the xanthophyll cycle in photoprotection and its relationship with fluorescence changes has yet to find a general consensus (Casper-Lindley and Björkman, 1998; Masojídek *et al.*, 1999; Garcia- Mendoza *et al.*, 2002; Ruban *et al.*, 2004) and, to date, it has not been investigated in the smallest eukaryotic species.

The experiments were performed on five monospecific cultures of marine ultraphytoplankton, chosen for their different pigment content (brown and green algae) and for their patterns of occurrence. For instance, the green algae *Micromonas pusilla* is a very widespread species (Not *et al.*, 2004), while *Minidiscus comicus* occasionally accounted for phytoplankton blooms in some Mediterranean areas, e.g. Northwestern Mediterranean (Sarno *et al.*, 2004).

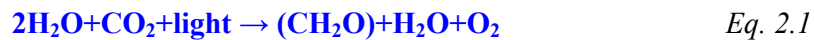
## CHAPTER 2

### PHOTOSYNTHESIS and CONTROLLING FACTORS

#### 2.1 Photosynthesis

In this chapter, a brief description of the principal processes involved in aquatic photosynthesis and its controlling factors is presented. These topics were extensively reviewed in Falkowski and Raven, (1997) and in Williams *et al.*, (2002).

Photosynthesis is the biological conversion of light energy to chemical bond energy that is stored in the form of organic carbon compounds. For phytoplankton it can be written as an oxidation-reduction reaction of the general form:



In this case the light is described as a substrate, because the energy of absorbed light is stored in the products. The process can be divided into two steps: the so called “*light reactions*” whereby light energy is used to oxidize water and the “*dark reactions*” that lead to carbon reduction. The first takes place within the thylakoids membranes and the second in the aqueous phase of chloroplasts (*stroma*); these two phases are coupled by common intermediates and by enzymes.

##### 2.1.1 Photosynthetic pigments

The first process of light reactions is the capture and transfer of light (photons) by photosynthetic pigments. These compounds have double bonds ( $\pi$  orbitals) able to absorb the radiations by means of transitions of their electronic state. Only photons with an energy exactly matching the difference between the ground state and excited state are absorbed. Conversely the relaxation of an electron to the lower energy level (de-excitation) is accompanied by the emission of energy (Falkowski and Raven, 1997). Different de-excitation pathways may occur: non-radiative emission: the energy is dissipated as heat; fluorescence: the transition proceeds from an excited state to a lower one, where no change in the spin direction of the electron has been induced; reemitting light ( $10^{-8}$ s); phosphorescence: if the spin direction is reversed, the electron must change it before returning to the ground state; excitation energy transfer: the energy is transferred to another

molecule which absorbs the same or a longer wavelength; photooxidation: the energy of excitation is converted in chemical energy by means of a charge separation. All these processes are in competition one with the other. Both the velocity and the presence of specific mechanisms will determine which de-excitation pathway will occur during photosynthesis.

On the basis of their molecular structure the photosynthetic pigments can be distinguished into three groups: chlorophylls, carotenoids and phycobilins.

Chlorophylls (Chls) are a group of magnesium coordination complexes of cyclic tetrapyrroles (Fig. 2.1). All Chls contain a fifth isocyclic ring often referred to as a phorbins (Porra *et al.*, 1997). Two basic types of closed rings are found: chlorins and porphyrins. Chlorins (Chlorophyll *a* and *b*) are distinguished from porphyrins (Chlorophyll *c*) by the saturation of a single C-C bond in ring 4, which break the symmetry of the molecule and lead to important spectral consequence (Falkowski and Raven, 1997). However, all Chls have two major absorption bands: the Soret bands in the blue to blue-green region and the Q bands in the red. All photochemical reactions in photosynthesis proceed from the de-excitation of the Q transition to the ground state. To allow excitation energy to be transferred efficiently from Chl *b* and *c* to Chl *a* the Q bands of Chlorophyll *b* and *c* are at higher energy levels than that of chlorophyll *a* with some overlapping in the Q absorption band of the three Chls.

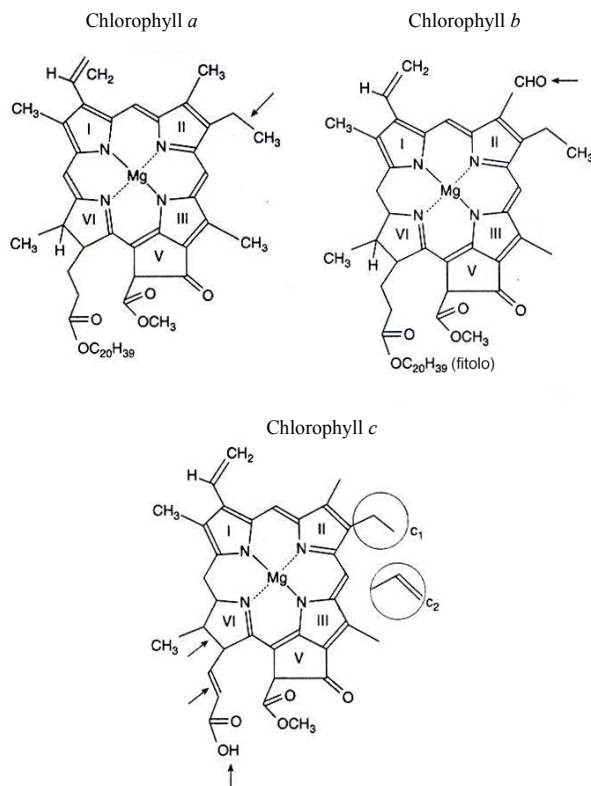


**Figure 2.1** – Structure of some Chlorophylls (from Falkowski and Raven, 1997).

Carotenoids are an extremely large group of pigments. The basic structural element consists of two unsaturated, 6-carbon rings joined by an 18-carbon, conjugated double-bond bridge (Fig. 2.2) (Porra *et al.*, 1997). They have a remarkable range of spectral characteristics, but always display a blue or blue green absorption bands that partially overlap the Soret bands of chlorophyll and, depending on the nature of the overlap, either facilitate the transfer of excitation energy to, or remove excitation energy from, Chlorophyll (Falkowski and Raven, 1997). The *Xanthophylls* are a family of carotenoids, where oxygen is bound to the ring forming an alcohol or epoxide (Young and Frank, 1996). Despite their role in photoprotection, knowledge about xanthophyll biosynthesis is still scarce. Recently Lohr and Wilhelm (1999, 2001) proposed an interesting pathway where violaxanthin is an intermediate in both Diadinoxanthin and Fucoxanthin synthesis.

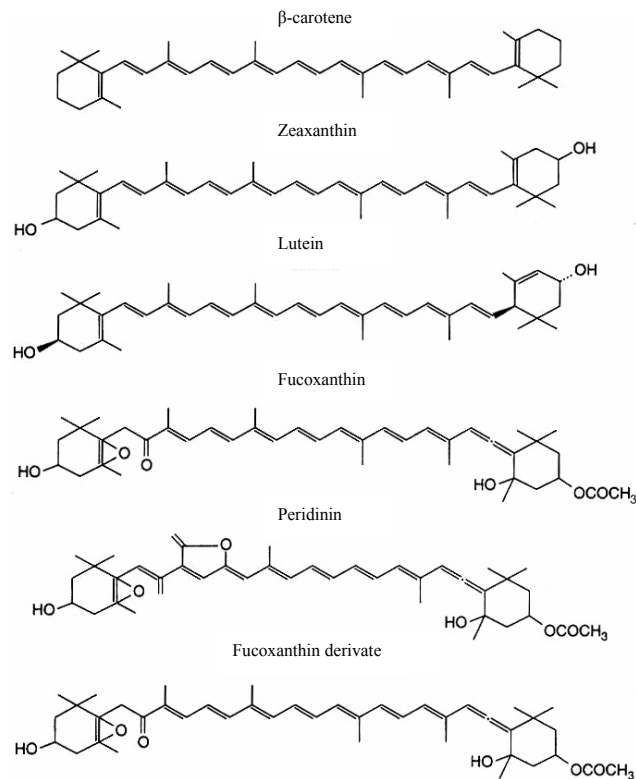


**Figure 2.2** – Some molecular structures of the principal carotenoids in algae (from Falkowski and Raven, 1997).

Phycobilins are open chain tetrapyrroles with extensive conjugated bond system and no associated metal (Fig. 2.3). These molecules absorb either blue-green, green, yellow, or orange light. Generally they are organized in poly-aggregates of phycobilin-protein complexes (phycobilisomes) attached to the outer face of the thylakoids of cyanobacteria and red algae. Three major phycobiliprotein families – the phycoerythrins, phycocyanins and allophycocyanins – are present in red algae and cyanobacteria, but only the first two are present in cryptomonads. However phycobilins are the major light harvesting pigments in these phytoplankton groups (Tandeau de Marsac, 2003).

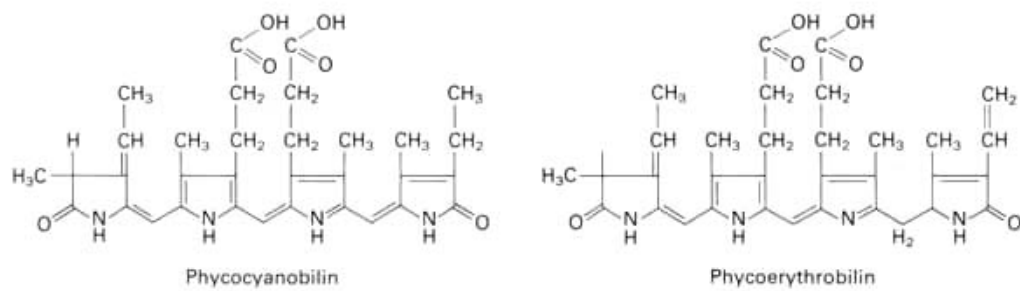


**Figure 2.3** –Structure of some phycobilins (from Falkowski and Raven, 1997).

Photosynthetic pigments can be used as markers for a chemotaxonomic assessment of natural phytoplankton populations. Some of them, as a matter of fact, are taxon-specific (Table-I in appendix). For example, Alloxanthin is found only in Cryptophyceae and Divinyl-Chlorophyll *a* and *b* are specific for Prochlorophyceae (Goericke and Repeta, 1992). Other pigments are recommended as markers of a certain taxon, only on the basis of the analysis of few species, but the pigment composition within the group may be more complex. One example is provided by the prymnesiophytes: the analyses of 50 strains clearly show four types of pigment distribution within the class (Jeffrey, 1997). Thus, some caution is needed when using marker pigment schemes to relate any particular pigment to an algal class. Some limitations have been recently resolved by means of a matrix factorisation program (CHEMTAX), which also allows for a quantitative estimation of algal class abundance (Mackey *et al.*, 1996). However, this approach is still controversial (Zapata *et al.* 2004; Wright, 2001), actually, pigment content can change, in relation, for example, to physiological conditions or light regime. As a consequence, a better knowledge of the

influence of light intensity and nutrient limitation on the Pigment/Chl *a* ratios of different species, is needed before CHEMTAX can be extensive applied (Schlüter *et al.*, 2000).

Jeffrey *et al.*, (1997) have published a comprehensive monograph in which both photosynthetic pigment analysis methods and their application to biological oceanography were reviewed.

### 2.1.2 Photosynthetic unit

Pigments will function in photosynthesis only when associated with specific *apoproteins* as Chl- and carotenoid-containing pigment-protein complexes. Their properties, above all their absorption spectra, are strongly modified by this association. The pigment-protein complexes are further organized into two photosystems, which span the thylakoid membrane from stroma to lumen. Each photosystem is made up of a Light Harvesting-Complex (LHC), a Core Protein (CP) and a Reaction Center (RC) (Fig. 2.4).

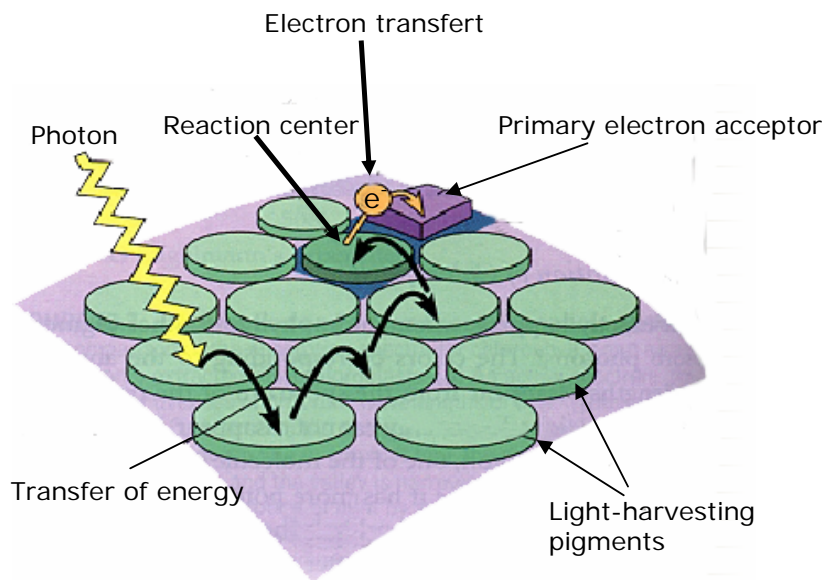


**Figure 2.4** – A schematic representation of photosystem organization (from [www.uqtr.ca/labcarpentier/eng/research.htm](http://www.uqtr.ca/labcarpentier/eng/research.htm)).

The former contains both chlorophyll and carotenoids, and play a central role in light absorption and transfer to the CP (chlorophyll *a* binding to proteins), which surround the RC. The Reaction Center contains essentially one molecule of chlorophyll *a*, which is different in the two photosystems. In the Photosystem I (PSI) the chlorophyll (P700) absorbs wavelengths longer than 700 nm, while in the Photosystem II (PSII) chlorophyll (P680)

absorbs at shorter wavelengths. These photosystems are not homogeneously distributed in the thylakoids: PSI is located in the membranes, while PSII is on the face exposed to the stroma (Porra *et al.*, 1997). Very recently, multiple types of PSII were found (Adir *et al.*, 2003): PSII $\alpha$ , located in the grana and PSII $\beta$  in the stroma lamella, with a limited antenna size. The concept of *photosynthetic unit*, introduced for the first time by Emerson and Arnold in 1932, involves both PSI and PSII as responsible of O<sub>2</sub> production (Falkowski and Raven, 1997) as described in the next section.

### 2.1.3 Electron transport chain

Hill and Bendel (1960) proposed for the first time that two photoreactions operate in series, with an electron transport between them (*Z-scheme*) (Fig. 2.5). Photons absorbed by PSII oxidize water and produce a weak reductant that is in turn oxidized by PSI, which produces a second stronger reductant. Based on this scheme, the photosynthetic electron transport chain (PET) can be divided into three segments: the donor side of PSII, which includes the reactions responsible for the transfer of electrons from water to PSII; the intersystem electron transport chain, which includes all the carriers between PSII and PSI; the acceptor side of PSI, in which the primary reducing agent, NADPH, is formed and exported to the carbon cycle (Falkowski and Raven, 1997).

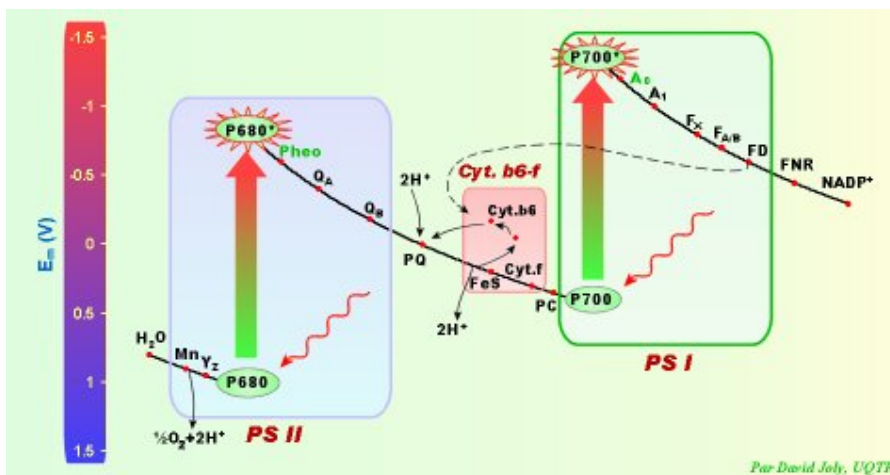


**Figure 2.5** – A schematic representation of electron transport chain, *Z-scheme* (from [www.uqtr.ca/labcarpentier/eng/research.htm](http://www.uqtr.ca/labcarpentier/eng/research.htm)).

Specifically, oxidation of  $2H_2O$  molecules, catalyzed by the S enzymatic complex, produces one molecule of O<sub>2</sub> and  $4H^+$  are released into the thylakoid lumen. The electrons produced

are donated to the P680, which in turn reduce an intermediate acceptor (Phaeophytin *a*). The life time of Phaeophytin *a* radicals is very short, thus its electron is rapidly passed on to a secondary acceptor,  $Q_A$  (a quinone). This stable acceptor is called “*fluorescence quencher*”, because when it is in the reduced state ( $Q^-$ ) the reaction center cannot use the photons absorbed for electron transfer (photochemistry), but the energy will be reemitted as fluorescence. It follows that the maximum quantum yield for photochemistry occurs when all  $Q$  molecules are oxidized and the maximum quantum yield for fluorescence occurs when all molecules are reduced. Thus, to a first order, the quantum yield of photochemistry and fluorescence are reversely related to each other. All the modern *in vivo* fluorescence techniques (see section 3.2) are based on this assumption.

In the electron chain an important step is the reduction of plastoquinone to  $PQH_2$  (plastoquinol). Actually  $PQH_2$  re-oxidation by cytochrome *b<sub>6</sub>f* is the slowest step ( $10^{-2}$ s) of the electron transport chain, so it can affect the efficiency of the photosynthetic machinery and regulate pigment synthesis (Durnford and Falkowski, 1997). Furthermore, this process requires the extraction of  $2H^+$  from the stromal fluid, which results in an increase in the protonic gradient. The last acceptor of PSII is a plastocyanin or a cytochrome *c<sub>6</sub>*, which reduces P700. The electron produced by the photoreaction in PSI is transferred from one carrier to the other and  $NADP^+$  is the terminal acceptor of the entire electron transport chain. NAPH is one of the principal stable products of photosynthesis (Geider and MacIntyre, 2002). Another one is ATP, formed by ATP synthase complex, utilizing the electrochemical gradient ( $\Delta pH$ ) between lumen and stroma of the thylakoids (*photophosphorylation*). Photophosphorylation can affect photosynthetic rate, because photons can be involved in a cycle around PSI to synthesize additional ATP (Falkowski and Raven, 1997). Such cyclic electron flow disconnected from the linear pathway apparently includes also PSII $\alpha$ , located in the grana (Adir *et al.*, 2003).

#### **2.1.4 Carbon organication**

Approximately 95% of the photosynthetically generated in the cell NADPH, and more than 60% of ATP, are used to assimilate and reduce inorganic carbon (Falkowski and Raven, 1997). Net photosynthetic carbon fixation involves a cycle of reactions named the photosynthetic carbon reduction cycle or Calvin Cycle. Carbon enters the cycle as  $CO_2$  and leaves it as sugar phosphate (Fig. 2.6). The energy is provided by ATP and the reducing form by NADPH. The central passage of the Calvin cycle is the carboxylation of ribulose 1,5-bisphosphate (RuBP) to form two molecules of glycerate 3-phosphate (G3P),

subsequently reduced to glyceraldehydes 3-phosphate (GA3P). The remaining steps of the cycle serve to regenerate RuBP (Geider and MacIntyre, 2002). The carboxylation of RuBP is catalysed by the enzyme RUBISCO. The rate of carbon fixation depends on the amount of RUBISCO in the cell, the proportion of active enzyme and on the intracellular concentration of CO<sub>2</sub> at the active site of RUBISCO. Therefore the enzyme plays a crucial role in maintaining a balance between the generation of NADPH and ATP and the synthesis of organic compounds. The active site of RUBISCO can also promote the oxygenation of RuBP (*photorespiration*) with formation of phosphoglycolate. Clearly the competition between O<sub>2</sub> and CO<sub>2</sub> may limit the carbon fixation rate. By contrast, the glycolate metabolism may provide a safety valve against photo-oxidative stress. A review of the mechanisms of regulation of RUBISCO activity *in vivo* is provided by Geider and MacIntyre (2002).

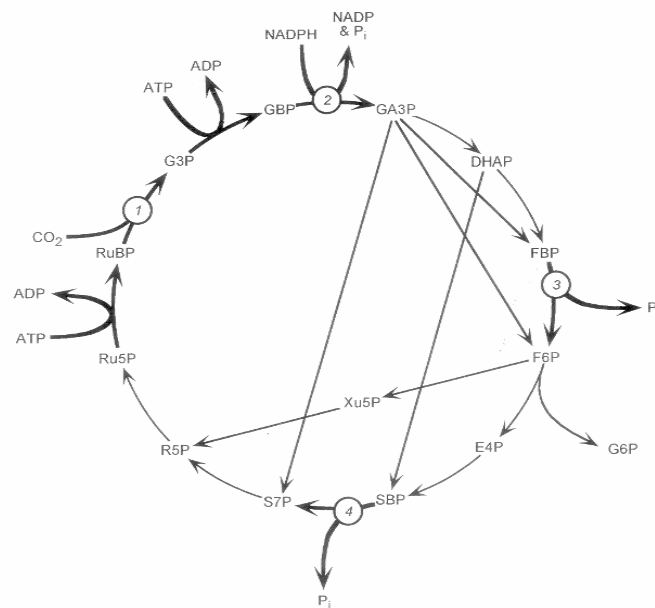


**Figure 2.6** – A schematic representation of Calvin cycle (from Geider and MacIntyre, 2002).

In a recent review of variability encountered in P-E experiments (see section 2.3) Behrenfeld *et al.* (2004) suggest that as growth rates decrease (e.g. due to nutrient stress) reductants, formed through photochemistry, are increasingly used for simple ATP generation through a fast (<1s) respiratory pathway involving mitochondrial metabolism, that skips the carbon reduction cycle. More generally they assert that the fundamental products of photosynthesis (ATP and NADPH) are available for the photoautotroph to spend on a

variety of secondary pathways (e.g. nitrogen assimilation and ATP production) in response to the changes in the cell's metabolic demands and coordinated by sophisticated regulatory mechanisms.

## 2.2 Controlling factors

Due to its unicellular structure phytoplankton is very vulnerable to bio-physical fluctuations in the environment. The cell is forced to continuous adjustments involving biophysical, biochemical, physiological, ecological and evolutionary components on very different time scales. As a consequence the spatial and temporal dynamics of environmental variables can provide crucial information on phytoplankton distribution and vice versa (Harris, 1986). The main factors controlling phytoplankton growth are common to all photosynthetic organisms: light, nutrients, temperature and grazing. A brief description of them is given in the following sections.

### 2.2.1 Light

According to their pigment composition, photosynthetic organisms are able to absorb only the part of the solar spectrum between 400 and 700nm, called Photosynthetically Available Radiation (PAR), i.e. about 50% of the total irradiance at the Earth's surface.

The total solar irradiance (*solar constant*), which arrives outside the Earth, is significantly reduced during its passage through the atmosphere. This reduction is due partly to scattering by air molecules and partly to absorption by water vapour, oxygen, ozone and carbon dioxide. The proportion of incident light removed by the atmosphere will change according to solar elevation, cloud cover and particle concentration. Solar irradiance is clearly influenced by diurnal and seasonal variations as well as by latitude (Kirk, 1992; Kirk, 1994). Furthermore the downward irradiance ( $E_d$ ) in a water body diminishes in an approximately exponential manner as described by the equation:

$$\ln E_d(z) = \ln E_d(0) - K_d z \quad \text{Eq. 2.2}$$

where  $E_d(z)$  and  $E_d(0)$  are the values of downward irradiance at  $z$  depth and just below the surface, respectively, and  $K_d z$  is the vertical attenuation coefficient of downward irradiance, due to the sum of absorption and scattering coefficients.

Except for a relatively small amount of light scattered back from the water surface, attenuation of PAR in water bodies is above all due to absorption. The relative contribution of the different components (water itself, particles and dissolved yellow substance) to light

absorption at any given wavelength is in proportion to their absorption coefficients (Kirk, 1992). A widely used albeit controversial rule in biological oceanography is that significant phytoplankton photosynthesis takes place only down to that depth, ( $z_{eu}$ ), at which the downwelling irradiance is 1% of PAR at surface (Kirk, 1994).  $Z_{eu}$  is also called *compensation depth* and represents the depth at which gross photosynthesis and respiration loss are equal, while the *euphotic zone* is the portion of water column that supports net primary production. However it is now acknowledged that net photosynthesis may occur at depths down to 0.1% of incident PAR (Sakshaug *et al.*, 1997). Clearly the depth of the euphotic zone changes according to different inherent properties of waters, such as the absorption coefficient. Modelling in detail the underwater light field is a crucial challenge of modern oceanography, because of its application in primary production models (Mobley, 1994).

The effects of irradiance level and its variations on photosynthesis will be discussed more in details in the section 2.3.

### **2.2.2 Nutrients**

The main building blocks (*macronutrients*) for the production of organic matter are the elements C, H, O, N, P, K, Na, Ca, Mg, Cl and Si (in species with a silica frustule or skeleton). In addition to these bulk elements, photoautotrophs have an absolute requirement for trace elements such as Fe, Mn, Cu, Zn (*micronutrients*) as well as for a few essential vitamins which some species are unable to synthesise themselves. Among the macronutrients only N and P (and at times Si) may be depleted through biological utilization and become limiting. However, inorganic carbon has also been suggested to potentially limit phytoplankton growth. Although its concentration in sea water by far exceeds phytoplankton carbon requirement, its biological availability can become rate-limiting under slow conversion between  $HCO_3^-$  and  $CO_2$  (Geider and MacIntyre, 2002; Riebesell and Wolf-Gladrow, 2002; Reinfelder *et al.*, 2000). Some of the micronutrients are also present at critically low concentrations and may become limiting in certain areas of the oceans. Interesting is the case of High Nutrient Low Chlorophyll (HNLC) areas, such as the Eastern Equatorial Pacific, where inorganic nitrogen and phosphate are in excess throughout the year, and the mixed layer is shallower than the critical depth, but the extremely low flux of aeolian iron limits phytoplankton production (Behrenfeld *et al.*, 1997).

Phytoplankton stoichiometry is generally considered to be rather uniform. For the major elements C, N, and P, it is defined by the Redfield ratio: C:N:P = 106:16:1 (Redfield *et al.*,

1963). Despite the large variability in phytoplankton elemental composition, there appears to be a remarkable uniformity in this ratio across time and space. Differences in elemental composition between major taxonomic phytoplankton groups originate essentially from the production of different cell coverings such as silica frustule, carbon platelet and organic walls. On the other hand, the composition of phytoplankton groups may have major effects on large scale elemental cycling.

On the size scale of microalgae, nutrient supply occurs primarily by means of molecular diffusion. The rate of diffusive transport thereby depends on the diffusion coefficient of the nutrient, the concentration gradient from the bulk medium to the algal surface and the thickness of the diffusive boundary layer (DBL) surrounding the alga. Phytoplankton cells are able to affect the flow of inorganic carbon and nutrients through the DBL in at least two ways. By controlling nutrient concentrations at the cell surface, phytoplankton determine the concentration gradient and thus the rate of diffusive transport across the DBL. Furthermore, the thickness of the DBL is to a certain extent under the influence of the organism (size, cell shape, motility). A review of processes of nutrient supply and their quantification is provided by Riebesell and Wolf-Gladrow, (2002). Nutrient replenishment in the microenvironment of the microalgal cell can also occur by advective transport due to water motion (Mann and Lazier, 1991).

A general feature of aquatic environments is that the pool of inorganic nutrients increases with depth, while light availability decreases. Therefore the inputs of “new” nutrients in the euphotic zone from the deep ocean (e.g. mesoscale activity, upwelling), the atmosphere, terrestrial run-off or biological N<sub>2</sub> fixation (cyanobacteria) are crucial for phytoplankton primary production (Mann and Lazier, 1991; Lewis, 2002). In the surface layer of a stratified water column the major source of nutrients is the local regeneration resulting from metabolic activity and microbial degradation (*recycled production*). Moreover the form of inorganic nitrogen (NO<sub>3</sub><sup>-</sup> in case of new production, NH<sub>4</sub><sup>+</sup> in recycled production) may affect the photosynthetic rate. In fact, nitrogen reduction involves oxidation of ferredoxin and hence competes with the carbon pathway (Behrenfeld *et al.* 2004).

### **2.2.3 Temperature**

Temperature affects phytoplankton productivity in at least two ways. First, the thermal vertical structure of the water column, such as the presence of a thermocline, regulate nutrient availability in the photic zone and the thermal exchanges with the atmosphere or

with other water masses drive ocean circulation, especially at mesoscale (Mann and Lazier, 1991).

On the other hand, temperature may also have a direct effect on photosynthesis. As a matter of fact, it influences the kinetics of reactions and enzyme activities, and, consequently, affect several processes such as nutrient uptake, growth rate (Harris, 1986), or electron transport rate (Geider and MacIntyre, 2002). For instance, at low temperatures the maximum rate of electron transport is generally lower and cells became photoinhibited at lower irradiance levels (Falkowski and Raven, 1997). A marked dependence of Chl<sub>a</sub>:C ratio on temperature was also found in some species such as *Chaetoceros calcitrans*, but not in *Phaeodactylum tricornutum*. Therefore a general assumption can not be made.

Furthermore, temperature affects the fluidity of cellular membrane; at low temperatures the membranes become rigid and there is a reduction of movement of the protein complexes through them. On the other hand, high temperatures make the membranes so fluid that the complexes lose their position and function. Phytoplankton species have evolved adaptative mechanism such as optimal temperatures for growth approximates the *in situ* temperatures. For instance, Crysophyceae are preferably found at temperatures around 15°C (Jeffery and Vesik, 1997). Clearly, more work is needed to unravel temperature acclimation of the photosynthetic apparatus, in particular in natural populations. This is important, since temperature is one of the variables that provide some power in predicting photosynthesis rates (Geider and MacIntyre, 2002).

#### **2.2.4 Grazing**

The predation of micro- and meso-zooplankton on phytoplankton, “*grazing*”, exerts the so called “top-down control” on phytoplankton abundance and composition (Banse, 1992).

Until the early 1970s, the view was widely held that the plankton had a relatively simple pyramidal structure with phytoplankton being exploited by zooplankton which in turn provided an energy source for fish or other predators. The introduction of the “microbial loop” concept (Azam *et al.*, 1983) expanded this traditional view of the pelagic ecosystem structure to include more trophic levels in which microorganism play a very important role.

A very significant portion of primary production is not consumed directly by zooplankton, but is instead channelled through the carbon pool. It is estimated that up to 50% of primary production is released in form of **D**issolved **O**rganic **C**arbon (**DOC**) and is used by bacteria. Other sources of DOC include excretion by zooplankton and viral lysis of bacterial cells. Production by heterotrophic bacteria averages around 20% of primary production and is

about twice that of mesozooplankton (Laybourn-Parry, 1992). It appears that a major part of the bacterial production is exploited by heterotrophic flagellates and ciliates, which provide an important energy source for the metazoan organisms of the zooplankton (Fig. 2.7).

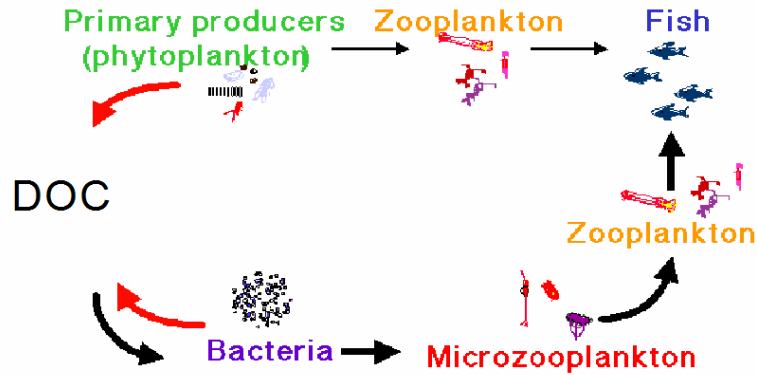


**Figure 2.7** – A schematic representation of microbial loop (modified from Lally and Parson, 1997).

Clearly the importance of the microbial loop may vary throughout the seasonal cycle or in relation to phytoplankton community structure. For example, where large cells are dominant (e.g. spring bloom in temperate areas) the food web is very simple (three-four trophic levels) and similar to the classic food chain. On the other hand, the microbial loop is a fundamental component in oligotrophic warm areas, where the small phytoplankton is dominant. An assemblage of small autotrophs is expected to leak more exudates than a community dominated by large cells, enhancing bacterial production; e.g. flagellate grazing on bacteria resulted in the remineralization of orthophosphate (Laybourn-Parry, 1992). Thus, the dominance of small phytoplankton cells will play a crucial role also for nutrient recycling. In spite of the importance of microzooplankton in the pelagic food web, its role in nutrient recycling as well as its productivity, particularly on a seasonal basis, are still poorly understood.

### 2.3 Phytoplankton responses to light variability

As irradiance regimes are continuously changing (see section 2.2.1), photosynthetic organisms have evolved mechanisms (such as biochemical feedback) to acclimate, insofar as possible, to such variability. Therefore the rate of photosynthesis is controlled by the efficiency of light utilization. To achieve a good parameterization of this light dependency

remain one of the most important goals of biological oceanography. The sections below provide a picture of the actual background.

### 2.3.1 Photosynthesis-Irradiance curve

To a first order the light dependency can be described as:

$$P_E = E_a \Phi_E \quad \text{Eq. 2.3}$$

Where  $P_E$  is a photosynthetic rate at any incident irradiance  $E$ ,  $E_a$  is the light absorbed by the organism and  $\Phi_E$  is the quantum yield at irradiance  $E$ . The absorbed light is measured from the incident spectral irradiance  $E_{0(\lambda)}$  in conjunction with the spectrally averaged optical absorption cross-section  $a^*$ :

$$E_a = E_{0(\lambda)} a^* \quad \text{Eq. 2.4}$$

The optical cross-section,  $a^*$ , describes the spectrally averaged target for the absorption of photons by all pigments in the photosynthetic apparatus.

At present, radioactive carbon incubation is the most commonly used method to determine photosynthesis-irradiance ( $P_{vs.E}$ ) relationships. It is preferred to oxygen measurements because of its higher sensitivity. On the other hand, the radiocarbon method gives an ambiguous estimate between net and gross photosynthetic rates and, depending on the length of incubation, acclimations may occur (Falkowski and Raven, 1997; Sakshaug *et al.*, 1997). Furthermore, the interpretation of  $P_{vs.E}$  curves depends critically on the currency in which mass is expressed (MacIntyre *et al.*, 2002). For these reasons, much attention is now focused on improving *in vivo* fluorescence approaches, which permit new insights into the physiology of PSII.

Independently from the parameters measured, a typical photosynthesis –irradiance curve may be divided into three distinct regions: a light-limited region, a light saturated region, and a photoinhibited region (Fig. 2.8) (Sakshaug *et al.*, 1997).

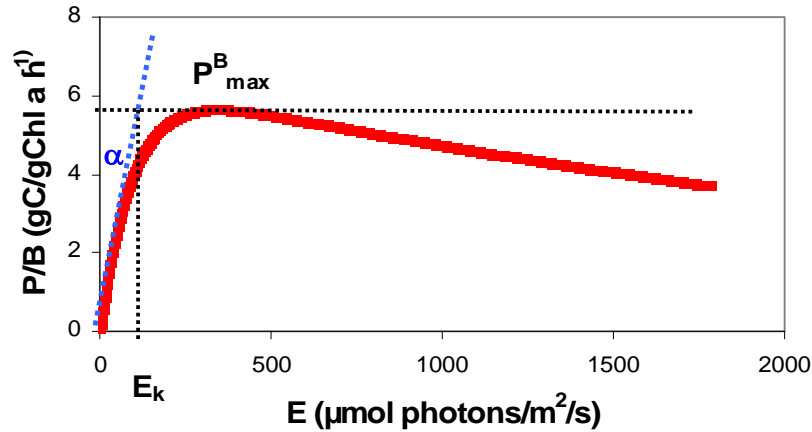


**Figure 2.8** – Scheme of a typical photosynthesis irradiance-curve (modified from Falkowski and Raven, 1997).

At low irradiance levels, photosynthetic rates are linearly proportional to irradiance and the rate of photon absorption determines the rate of steady-state electron transport (*light-limited region*). The initial slope of the  $P$  vs.  $E$  curve is often denoted by the symbol  $\alpha$  and is related to the maximum quantum yield  $\Phi_m$ ;  $B$  is added to denote the normalization to chlorophyll biomass:

$$\Phi_m = \alpha^B / a^* \quad \text{Eq. 2.5}$$

From Eq. 2.5 through a series of mathematical correlations (see Falkowski and Raven, 1997) we obtain the following relationship:

$$\alpha^B = n \sigma_{\text{PSII}} \quad \text{Eq. 2.6}$$

Eq. 2.6 reveals that the initial slope of the  $P$  vs.  $E$  curve is directly proportional to the functional absorption cross-section of PSII ( $\sigma_{\text{PSII}}$ ) and the numbers of photosynthetic units ( $n$ ). However, proper estimation of  $\Phi_m$  remains still controversial. In a recent study, Johnson and Barber (2003) showed that reductions in  $\Phi$  at low irradiances may occur that are not observable using conventional  $P$ - $E$  analyses and hence they suggest to determine  $\Phi_m$  by directly estimating the true maximum of an  $\Phi$ - $E$  curve.

At increasing irradiance levels, the increase in photosynthetic rate becomes non linear up to a saturation level (*light-saturated region*). By definition, at light saturation the rate of photon absorption exceeds the rate of steady-state electron transport. Therefore the maximum photosynthetic rate normalized to chlorophyll biomass ( $P_{\text{max}}^B$ ) is:

$$P_{\text{max}}^B = n(1/\tau) \quad \text{Eq. 2.7}$$

Where  $1/\tau$  is the maximum rate at which electrons are transferred from  $\text{H}_2\text{O}$  to the terminal electron acceptor in the steady state (Sakshaug *et al.*, 1997).

The intersection of  $\alpha^B$  and  $P_{\max}^B$  gives  $E_k$  (*light saturation index*):

$$E_k = P_{\max}^B / \alpha^B \quad \text{Eq. 2.8}$$

At irradiance levels lower than  $E_k$ , the rate of photon absorption is less than  $1/\tau$  and the quantum yield is higher but absolute photosynthetic rate is less than maximal. At higher irradiance levels, the rate of photon exceeds  $1/\tau$  and the quantum yield decreases. Hence, the optimum photosynthetic rate is achieved at  $E_k$  even if the quantum yield may not be maximal (Falkowski and Raven, 1997). The light saturation index is a very important tool in understanding phytoplankton physiology. For example, Behrenfeld *et al.* (2004) proposed to separate the variability of  $P_{vs.E}$  curves into two categories:

- “ $E_k$  dependent group”, associated with variations in  $E_k$  and mainly a result of photoacclimation;
- “ $E_k$  independent group”, where  $\alpha^B$  and  $P_{\max}^B$  co-varied in relation to alternative metabolic pathways (see section 2.1.4).

In the *photoinhibited region* the further increase of irradiance leads to a reduction in photosynthetic rate, dependent on both light intensity and duration of exposure. This reduction often called photoinhibition (PI) is due to lower efficiency of PSII. There are two types of photoinhibition: acceptor side induced PI, characterized by an over reduction of the plastoquinone pool and a donor side induced PI. In this case the potential of PSII leads to the formation of a number of transiently short-lived radical species, which could oxidize the RC II either directly or by the production of singlet oxygen or hydroxyl radicals (Adir *et al.*, 2003). However, the efficiency of photosynthetic electron transfer decreases markedly only when the rate of damage exceeds the rate of its repair, which requires *de novo* PSII proteins synthesis, especially D1 protein. Adir *et al.*, (2003) provided a good review, and a historical perspective, of over a century of studies on photoinhibition.

### 2.3.2 Photoprotection

Photosynthetic organisms have developed pathways to re-equilibrate imbalances between absorption and utilisation of light to cope with the effect of short- and medium-term irradiance fluctuations. A brief description of the major ones is given in this section.

#### *Cyclic electron pathways*

Photo-oxidative damage of both acceptor and donor side of PSII might be prevented by an electron transfer cycle around PSII (*chlororespiration*) involving the plastoquinone pool and the donor side of PSII. This cycle, found for example in diatoms, (Lavaud *et al.*, 2002a) is insignificant at limiting light intensity but it becomes important at excessive light

intensity. Another pseudo-cyclic electron pathway (*Mehler reaction*) is proposed by Behrenfeld *et al.* (2004) to play a protective role at very high levels.

#### *State transition*

A redistribution of excitation energy between the photosystems probably occurs as a first line of regulation to small changes in irradiance level (such as the passage of a cloud). A state transition leads to changes in effective absorption cross-sections of PSII of about 10% to 20% and simultaneously affects the PSI cross-section in the opposite way. Such changes would produce a corresponding shift in  $E_k$  and thus help to balance light absorption with electron transport. The changes in the effective cross-sections appear related to phosphorylation of pigment-protein complexes of LHC, which consequently detach from PSII and migrate to PSI (Falkowski and Raven, 1997, Garcia-Mendoza *et al.*, 2002).

#### *Non photochemical Quenching (NPQ) - Xanthophyll cycle*

An alternative mechanism for altering the effective absorption cross-section of the antennae is to dissipate absorbed excitation energy thermally. It is called *non photochemical quenching* (NPQ) as it is accompanied by a reduction of chlorophyll fluorescence that is not due to photochemical reactions. The change in PSII absorption cross-section due to the non photochemical quenching can approach 50% and results in an increase in  $E_k$  (Falkowski and Raven, 1997). The most common mathematical expression of NPQ is the Stern Volmer equation:

$$NPQ = F_m / F_m' - 1 \quad \text{Eq. 2.9}$$

Where  $F_m$  and  $F_m'$  are the maximum fluorescence of PSII in the dark adapted state and in the light adapted state, respectively.

NPQ is a complex phenomenon that involves the formation of a transthylakoidal proton gradient ( $\Delta pH$ ) and xanthophyll cycle activity (Garcia-Mendoza *et al.*, 2002). Two different xanthophyll cycles (Fig. 2.9) were found in photoautotrophic organism, both involving an enzymatic de-epoxidative reaction:

- “Violaxanthin cycle”: at high light the epoxidated xanthophylls (Violaxanthin) is de-epoxidated to Zeaxanthin through an intermediate form (Antheraxanthin). This cycle is present in all higher plants (Young and Frank, 1996) and in chlorophytes (Casper-Lindley and Björkman, 1998; Garcia-Mendoza *et al.*, 2002), and has been reported also in some golden- brown algae (Lohr and Wilhelm, 1999).
- “Diadinoxanthin cycle”: the monoepoxide Diadinoxanthin is converted to the de-epoxidated form Diatoxanthin. It is typical of cromophyte algae (Olaizola *et al.*, 1994; Casper-Lindley and Björkman, 1998).

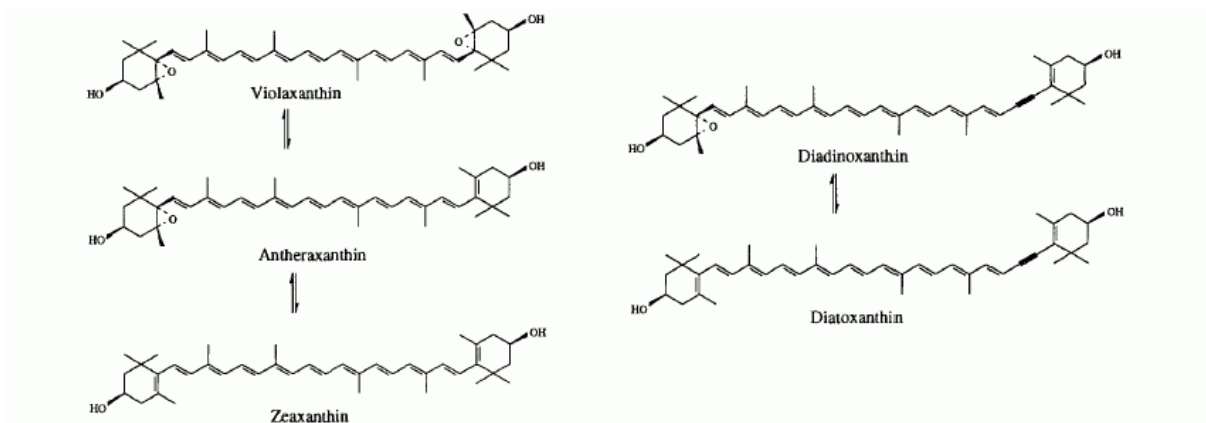


**Fig. 2.9-** A schematic representation of xanthophyll cycles (modified from Young and Frank, 1996).

In both cases, the de-epoxidation occurs at high light and very rapidly (min), while the inverse reaction is enzymatically catalyzed in the dark. However, the kinetics of the Diadinoxanthin cycle is very fast as it is a one-step reaction (Lohr and Wilhelm, 1999).

The exact molecular mechanism involved in the energy dissipation is still not clear. Two hypotheses have been proposed: a direct de-epoxidated pigment-chlorophyll interaction, involving singlet-singlet energy transfer and resulting in a direct quenching of Chl fluorescence, or, alternatively, an indirect process where xanthophyll formation promotes the aggregation of light-harvesting pigment-protein complexes (Young and Frank, 1996).

Furthermore, the relationship between changes in NPQ and in xanthophylls is still disputed. In fact, while a linear relationship appears to occur in higher plants (Young and Frank, 1996; Demming-Adams, 2003), experiments on different phytoplankton classes gave controversial results, especially on the role of the proton gradient (Casper-Lindley and Björkman, 1998; Garcia-Mendoza *et al.*, 2002; Lavoud *et al.*, 2002b; Ruban *et al.*, 2004). To this end, the exact determination of the binding sites of each xanthophyll species on LHC polypeptides will be helpful, as NPQ is strictly related both to the position of xanthophylls within the light harvesting complexes (Young and Frank, 1996; Pineau *et al.*, 2001) and to the size and stability of the antenna (Lokstein *et al.*, 2002).

### 2.3.3 Photoacclimation

It is generally accepted that the term *photoacclimation* refers to phenotypic adjustments (macromolecular composition and ultrastructure of the photosynthetic apparatus) in

response to variations of environmental factors, above all light (Falkowski and La Roche 1991). By contrast, the term *photoadaptation* is reserved for changes in the genetic structure, which clearly occur on long temporal scale (Falkowski and Raven 1997).

Typically photoacclimation involves changes in the pigment content. In particular, the chlorophyll *a* content per cell or per unit surface area increases with irradiance reduction; the opposite is clearly observed at increasing irradiance (Falkowski and Raven 1997; MacIntyre *et al.*, 2002). Also the cell content of *accessory photosynthetic pigments* (PSP) declines at high irradiance. This pattern is observed in all phytoplankton groups, but appears more marked in cyanobacteria (MacIntyre *et al.*, 2002). The decline in accessory pigments may be parallel to the decline in Chl *a*, so that there is a limited variability in the PSP: Chl *a* ratios. However, the overall decrease in cellular pigment content with irradiance is due to a decrease in the number of PSI and PSII reaction centers and in the ratio of light-harvesting antennae and reaction centers. Furthermore, the proportion of *photoprotective carotenoids* (PPC) is high in cells acclimated to high irradiance levels. The term photoprotective pigments is applied to carotenoids which do not transfer ( $\beta$ -carotene and Zeaxanthin) or transfer with reduced efficiency (Lutein) excitation energy to the reaction center, thus protecting it from excess light (Falkowski and Raven 1997). As these carotenoids absorb light without a corresponding increase in the functional absorption cross-section of PSII a decline of quantum yield may occur.

Another central point is the so called *package effect* that reduces the effectiveness of increased pigmentation in light harvesting at low irradiance (Kirk, 1994). In fact, as cells accumulate chlorophyll each chlorophyll molecule become less effective in light absorption due to *self-shading* and to the increase in the number of thylakoid membranes. Package effect is also a function of cell size: the larger the cell the more important this effect (Falkowski and Raven 1997).

Understanding the physiology of photoacclimation is central to aquatic primary production models. To date, two different approaches have been explored: the determination of acclimation kinetics (e.g. Cullen and Lewis, 1988; Geider *et al.*, 1996) and the direct measurements of photoacclimation states in variable light regime (e.g. Fietz and Nicklish, 2002; Havelková-Doušova *et al.*, 2004). A good review of the models based on the first approach is proposed by MacIntyre *et al.*, 2002. The authors assume light-limited photosynthesis rates to be proportional to the cellular Chl *a* content, whereas light-saturated rates are proportional to cellular carbon content. In addition, their analysis indicates that maximizing the rate of carbon assimilation is not the only criterion governing

photoacclimation, but costs associated with photoinhibition and photooxidative stress and their repair may also play an important role.

### **2.3.4 Circadian cycles**

Circadian or diel cycles, i.e. periodical variations occurring in the 24 hour period (day/night alternation), involve essentially all the principal activities of the organism (e.g. cell division, nutrient uptake, metabolic pathways) (Sournia, 1974). Some of these processes, such as cellular cycle or chlorophyll *a* content, appear to be under endogenous control (genetically encoded). In fact, circadian rhythms are expressed for some time even in constant illumination or darkness (Owens *et al.*, 1980). One adaptive advantage of such internal control is the temporal separation of incompatible processes (i.e. nitrogen fixation and oxygen evolution in cyanobacteria) or the possibility to synchronize physiological activities in order to match the optimal use of resources according to their availability. An outstanding example is photosynthetic capacity that is elevated during the photoperiod and decreases at night (Kaftan *et al.*, 1999). The higher diurnal photosynthetic capacity may be related to an increase in the number of active reaction centers and/or to a change in the ratio of Rubisco to reactions centers. Circadian variations in photosynthesis occur in all major taxonomic groups (see Prezelin, 1992 for a review), but are particularly pronounced in diatoms (Harding *et al.*, 1981). In addition to species-specific differences, the amplitude of diel photosynthetic oscillation is correlated with nutrient availability and growth rate (Behrenfeld *et al.* 2004).

Furthermore, circadian oscillations of pigment content have been observed in different phytoplankton groups, such as diatoms (Marra and Heinemann, 1982; Post *et al.*, 1984); prasinophytes (Kohata and Watanabe, 1988) and dinoflagellates (Latasa *et al.*, 1992). Experiments performed on prasinophytes have shown that pigments are synthesized at different times, in order to maintain an optimal amount of each pigment pool during the day (Kohata and Watanabe, 1988). For instance, chlorophyll *a* content is generally highest at the end of photoperiod (Post *et al.*, 1984), presumably in relation to the cell division cycle.

## CHAPTER 3

### **MATERIALS and METHODS**

In this chapter a general description of the procedures used for samples collection and analyses is provided, both for *in situ* and culture measurements. Instead, the scheme and relative sampling strategies of each experiment is explained more in details at the beginning of the following chapters.

#### **3.1 *In situ* profiles**

##### *Hydrology*

Down- and upwelling profiles of the most important chemical-physical parameters were performed at the stations of the *in situ* experiments, utilizing a SBE 911plus CTD equipped with salinity, temperature and oxygen sensors as well as a SCUFA fluorometer. The data were processed (mediated to one meter) using the SeaSave Data Processing Software. The CTD was connected to an automatic Carousel sampler of SeaBird Electronics, equipped with 12 Niskin bottles (12L); water samples for salinity and oxygen analyses were drawn from the Niskin bottles.

##### *Irradiance*

Supporting primary production measurements, up- and downwelling profiles of underwater PAR (Photosynthetically Active Radiation) were obtained utilizing a photoprobe equipped with three underwater quanta meters (Chelsea Instrument ltd). Moreover, incident PAR had been recorded during the entire day by means of a LI-COR quanta meter (mod. 1400).

#### **3.2 Treatment and analyses of samples**

##### *Nutrients*

Discrete samples for nitrate ( $\text{NO}_3^-$ ), nitrite ( $\text{NO}_2^-$ ), ammonium ( $\text{NH}_4^+$ ), orthophosphate ( $\text{PO}_4^{3-}$ ) and silicate ( $\text{SiO}_4$ ) determination were collected in high density polyethylene vials directly from Niskin bottles and immediately stored at  $-20^\circ\text{C}$  until the analysis. The analyses were performed by technicians of Zoological Station “A. Dohrn” of Naples utilizing an Autoanalyzer Technicon II series (five continuous flux channels), according to Scotto *et al.* (1985).

### Spectrofluorimetry

For determination of total chlorophyll a (as a proxy for phytoplankton biomass), an aliquot of water sample was filtered on glass-fibre filters (GF/F, Ø 25mm) of Whatman. In addition, to determine the contribution of the <math><5\mu\text{m}</math> chlorophyll fraction, water samples were filtered sequentially on polycarbonate membrane (porosity of  $5\mu\text{m}$ , Ø 47mm) and on glass-fibre filters (GF/F, Ø 25mm). The filters were immediately stored in liquid nitrogen until the analysis. In the laboratory the samples were extracted in 90% neutralized acetone and analyzed utilizing a Spex Fluoromax spectrofluorometer, according to Holm-Hansen *et al.*, (1965). The instrument was calibrated daily with a solution of pure chlorophyll a, extracted from *Anacystis nidulans* (Sigma).

### High pressure liquid chromatography (HPLC)

The major photosynthetic pigments were determined using High Performance Liquid Chromatography (HPLC). For natural samples a variable aliquot of seawater (depending on phytoplankton concentration) was collected from the Niskin bottles at each sampling depth and filtered sequentially on polycarbonate membrane (porosity of  $5\mu\text{m}$ , Ø 47mm) to determine the fraction  $> 5\mu\text{m}$  and on glass-fibre filters (GF/F, Ø 47mm) for the fraction  $< 5\mu\text{m}$ . For culture samples a small volumes (20-30 ml) was filtered directly on glass-fibre filters (GF/F, Ø 25mm) of Whatman. In both case filters were immediately stored in liquid nitrogen until analysis. Filters were subsequently extracted in methanol and analysed according to Vidussi *et al.* (1996) with a Hewlett Packard HPLC 1100 Series. The instrument was supplied of a spectrophotometer with diodes array detector (DAD) and a fluorometer (Fig. 3.1). The column was a reverse phase column Hypersil MOS C8 (Sigma-Aldrich,  $3\mu\text{m}$ , 100x4, 6mm). For pigments quantification the instrument was calibrated with external standards according to Mantoura and Repeta (1997). The 20 different pigments utilized were provided by the International Agency for  $^{14}\text{C}$  Determination, VKI Water Quality Institute.

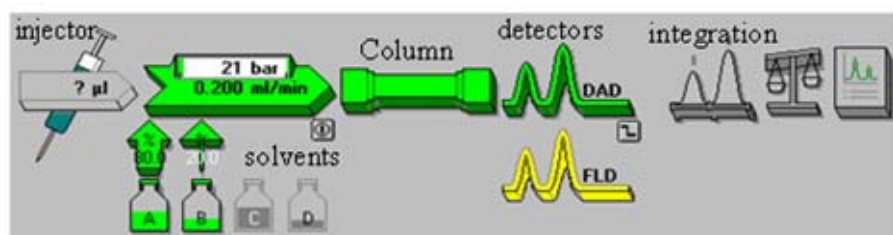


**Figure 3.1** - Scheme of HPLC phases.

*In vivo fluorescence*

*In vivo* variable fluorescence techniques allow obtaining rapid, real-time and non-invasive measurements of photosynthetic characteristics of phytoplankton. In this study, they were carried out with an FRRF (Fast Repetition Rate Fluorometer) and a Phyto-PAM (Pulse Amplitude Modulated). The first was used essentially in a profile mode for *in situ* measurements during circadian experiments while the Phyto-PAM was used both in the photoacclimation and in the circadian experiments. For each of the two instruments, particular attention was placed to work out suitable protocols, before routine measurements.

*FRRF*

This technique induce a saturation profile of PSII variable fluorescence and its following decay (Fig. 3.2), by exposing the sample to a series of short (microseconds) sub saturating flashes of blue light. The parameters measured are the minimal ( $F_0$ ) and maximal ( $F_m$ ) fluorescence, the functional absorption cross-section of the PSII ( $\sigma_{PSII}$ ) and a time constant of the  $Q_A^-$  reoxidation ( $\tau$ ). During the experiments these parameters were measured both on dark adapted and ambient irradiated samples. The adopted protocol planned two acquisitions for each measurement, delayed by 5 minutes one from another. Moreover the number of sequences for each acquisition was 10 (1 second delay between each) and each sequence was made up of about 100 flashes of 1.10 $\mu$ s, and an interval of delay of 2.8 $\mu$ s. The instrument utilized was a Fast Tracka FRR fluorometer (Chelsea Instruments Ltd) and the data were elaborated using the Frs software (version 1.8) provided by the same Chelsea and according to Kolber and Falkowski (1993) and Kolber *et al.* (1998).

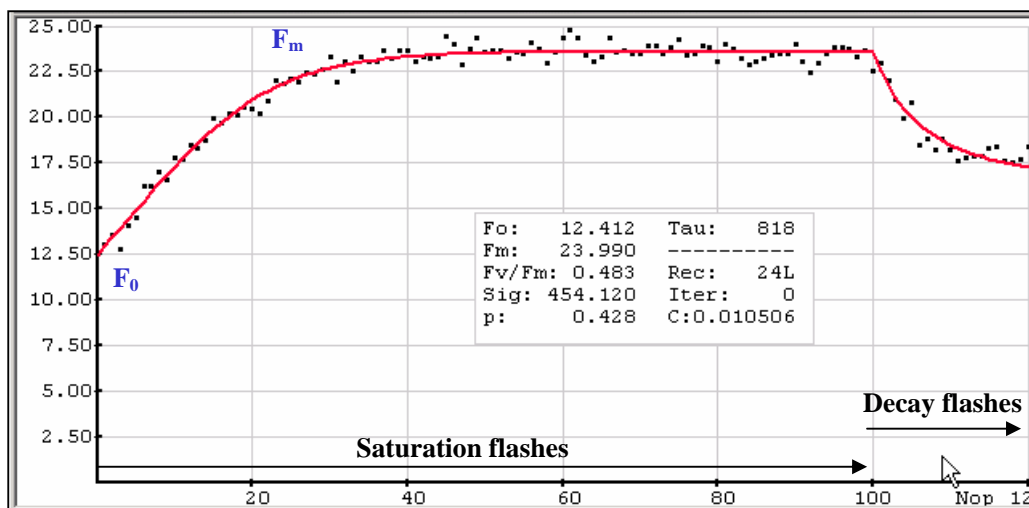


**Figure 3.2** – Example of variable fluorescence profile obtained with FRRF.

*Phyto-PAM*

The Pulse Amplitude Modulated (PAM) technique use a more intense and longer pulse (45 $\mu$ s) as compared to the FRRF. The pulse is generated by an array of light-emitting diodes (LED) in 4 different colours: blue (470 nm), green (520nm) light red (645nm) and dark red (665nm). The induced fluorescence signal is detected by a photomultiplier. For each measurement 3 ml of sample were injected into a quartz cuvette (10mm) and dark adapted for 5 minutes, before the saturation pulse. In this way the maximum quantum yield ( $F_v/F_m$ ) of photochemical energy conversion in PSII was determined. The product of quantum yield and quantum flux density of absorbed PAR provides a relative measurement of the electron transport rate (rETR) in the electron transport chain. In addition, light response curves were performed, increasing progressively the light intensity to predefined levels (up to 10). The sample was illuminated by each background irradiance for a fixed time (2 minutes for natural samples, 1 for cultures) and after that a new saturation pulse permitted to determine the quantum yield. At the end, a light response curve of rETR and of quantum yield was obtained (Fig. 3.3). The first have a shape similar to PvsE curves and in analogy with them the following coefficients can be determined:

- $\alpha_{PAM}$ , the slope of rETR vsE curves
- $rETR_{max}$  the value of rETR at saturating light
- $E_{kPAM}$  (compensation irradiance), the ratio between  $rETR_{max}$  and  $\alpha_{PAM}$ .

The coefficients derived fitting the data with a theoretical light response function according to the photosynthesis model of Eilers and Peeters (1993):

$$ETR = \frac{PAR}{a*PAR^2 + b*PAR + c} \quad Eq. 3.1$$

Where a, b, c are coefficients fitted for least square deviation.

The instrument used was a Walz Phyto-PAM provided with PhytoWIN software for data elaboration and fitting.

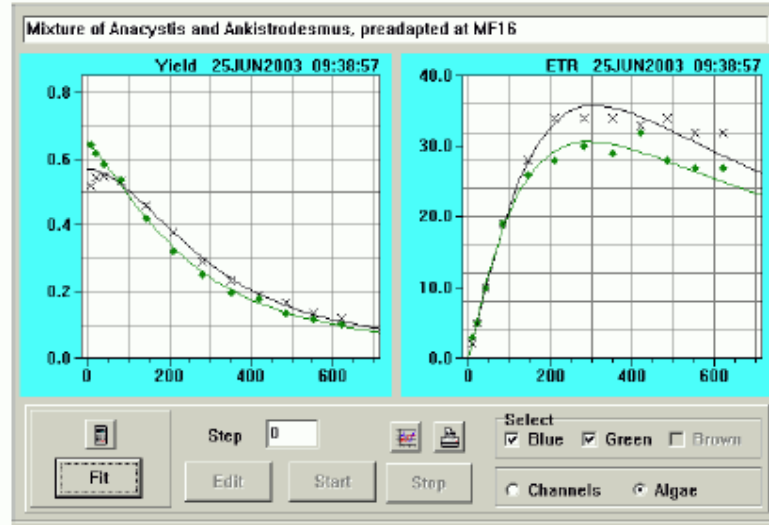


**Figure 3.3** – Example of light response curves obtained with the Phyto-PAM.

#### *Photosynthetic parameters*

*PvsE* experiments were performed in order to determine the main photosynthetic parameters. For each sampling depth, twelve subsamples were pored in 50-ml Pyrex bottles, inoculated with 1 ml of  $\text{NaH}^{14}\text{CO}_3$  (10-15  $\mu\text{Ci}$ ) and incubated for 1h, utilizing a radial incubator (photosynthetron), according to Babin *et al.* (1994). The light source was a HQI-T 250W/D lamp (Osram) and the light extinction curve was determined with a PAR  $4\pi$  sensor of Biospherical Instruments (mod. QSL-101). The circulating water was temperature controlled. Filtration on 25 mm Whatman GF/F filters was carried out immediately after incubation under dim light conditions. Radioactive content of each sample was measured, after acidification with 200  $\mu\text{l}$  of HCL 0.1 N, in a Packard Tricarb (mod.2100TR) liquid scintillator, using 10 ml of Aquasol II scintillation cocktail.

The data were fitted with the model of Platt *et al.* (1980):

$$P^B(E) = P^B_S [1 - \exp(-\alpha E / P^B_S)] \exp(-\beta E / P^B_S) \quad \text{Eq. 3.2}$$

Where:

$P^B_S$  is the potential light-saturated Chl-specific rate of photosynthesis in the absence of photoinhibition (photosynthetic capacity), in  $\text{mgC} (\text{mgChl}a)^{-1}\text{h}^{-1}$ ;

$\alpha$  is the initial slope of *PvsE* curves, in  $\text{mgC} (\text{mgChl}a)^{-1}\text{h}^{-1}(\mu\text{mol photons m}^{-2}\text{s}^{-1})^{-1}$ ;

$\beta$  is the index of photoinhibition (same units of  $\alpha$ ).

From the Eq.3.2 we also obtain other important photosynthetic coefficients:

$$E_m = P_s^B / \alpha \log_e [(\alpha + \beta) / \beta], \text{ in } \mu\text{mol photons m}^{-2}\text{s}^{-1}$$

$$E_k = P_m^B / \alpha \text{ in } \mu\text{mol photons m}^{-2}\text{s}^{-1}$$

The first is the optimal irradiance for photosynthesis (saturation irradiance); the second is the index of photoacclimation.

#### *Primary Production measurements*

For primary production measurements sampling depths were selected according to optical levels equivalent to 100%, 65%, 33%, 20%, 12%, 9%, 5%, 3%, 1.3% and 0.6% of incident irradiance. The measurements were performed under *in situ* simulated conditions. Each sample was poured into polycarbonate (Nalgene) 300 ml bottles, inoculated with 1-2 ml of  $\text{NaH}^{14}\text{CO}_3$  (10-20  $\mu\text{Ci}$ ) and incubated for 4-6 h. Incubations were made on deck in incubators cooled by circulation of temperature controlled water. The different light levels were obtained by means of neutral light screen (Veco Int. Co. USA). After incubation, differential filtration was realized in order to separate size fractions (total,  $>5\mu\text{m}$ ). To this end, sub-samples of 150 ml were filtered on Nucleopore polycarbonate membranes (porosity of  $5\mu\text{m}$ ,  $\varnothing$  25mm) for the  $>5\mu\text{m}$  fraction and on GF/F filters ( $\varnothing$  25mm) for the whole sample (total). Radioactive content of each sample was measured according to the procedure described above for the PvsE experiments.

#### *Flow cytometry (FCM)*

For flow cytometry determination of cell counts, one ml of each sample was fixed in a mixture of paraformaldehyde and glutaraldehyde (1% and 0.05% final concentration respectively) for 15 minutes according to Biegala *et al.* (2003). Samples were stored in liquid nitrogen and analysed a few days after the experiments utilizing a FACS calibur flow-cytometer (Becton-Dickinson) according to Marie *et al.*, (1999).

A list of the principal used symbols and abbreviations was provided in the Tab. I and Tab. II of Appendix.

## CHAPTER 4

### **Seasonal dynamics of fractionated phytoplankton pigments in a coastal environment**

The temporal variations in the abundance, production and taxonomic composition of two phytoplankton size classes ( $<5\mu\text{m}$  and  $>5\mu\text{m}$ ) was investigated at a coastal site in the Gulf of Naples during one year (July 2004-July 2005). A chemotaxonomic approach based on HPLC analysis was applied on a weekly time scale, whereas primary production measurements were carried out monthly. The study area and the sampling strategies are described in section 4.1, while the results are presented in the following sections.

#### **4.1 Study area**

##### **4.1.1 Gulf of Naples**

The Gulf of Naples (Southern Tyrrhenian Sea) is a SW oriented coastal embayment with a very complex morphology, an average depth of 170 m, an area of  $\sim 870 \text{ km}^2$  and a surface/volume ratio of 5.8 (Fig.4.1). From the environmental point of view, the Gulf can be subdivided into two subsystems: a coastal and an “open water” one (Carrada *et al.*, 1980). The former occupies the eastern and north-western shores and is heavily influenced by land runoff (urban and industrial discharges) from an overpopulated region (Carrada *et al.*, 1981; Ribera d'Alcalà *et al.*, 1989). In addition, the Northern part is sometimes affected by the diluted waters of the Volturno River and by the sewage plumes of Cuma, while the polluted Sarno river flows in the Southern part of the Gulf. The open water system, located in the central part of the Gulf, is strongly influenced by the oligotrophic Tyrrhenian waters entering through Bocca Grande. In particular, the Gulf is characterized by the mixture of four different water masses: The Coastal Surface Water (CSW), The Tyrrhenian Surface Water (TSW), The Tyrrhenian Intermediate Water (TIW) and the Levantine Intermediate Water (LIW). The properties and dynamics of these water masses are described in details by Carrada (1983), Carrada *et al.* (1980) and Hopkins (1986).

As a result of the general topography, the inner shelf and the offshore areas are strictly coupled, the boundary between these two subsystems being variable in location and extension; no stable frontal structure has been observed between the two subsystems (Modigh *et al.*, 1996). Thus, the Coastal Surface Waters present a wide range of values for

physical and chemical parameters (salinity, temperature, nutrients) due to changes in land run-off and exchange with off-shore waters.

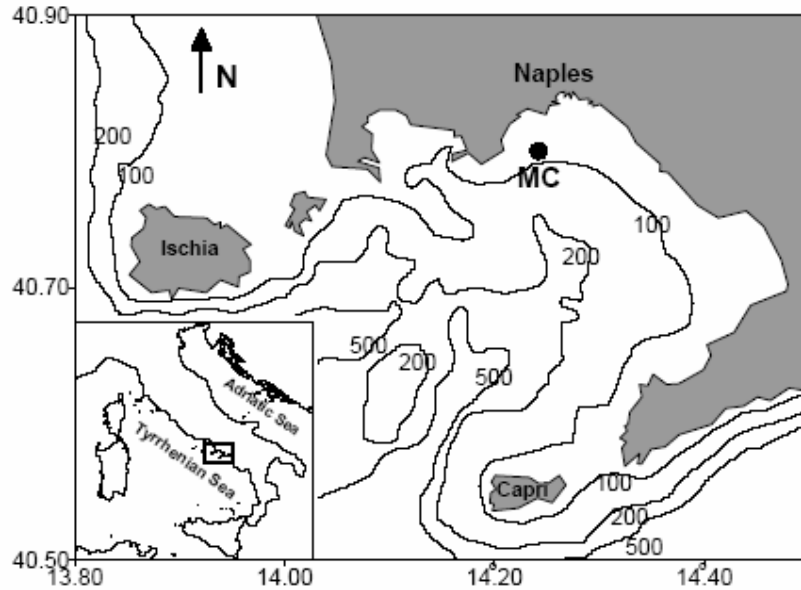


**Figure 4.1** – Sampling site (st. MC) in the Gulf of Naples (Tyrrhenian Sea).

Biological studies have been carried out in the Gulf of Naples since the end of the nineteenth century at the Zoological Station “A. Dohrn, yet it was not until the 1980’s that an ecological approach was applied, essentially focused on plankton communities (e.g. Carrada *et al.*, 1981; Marino *et al.*, 1984, Ianora *et al.*, 1985; Zingone *et al.*, 1990; Modigh, 2001). To this end, a coastal long-term station, called Marechiarà (st. MC), is regularly sampled since January 1984 (Ribera d’Alcalà *et al.*, 2004) for plankton and associated environmental variables. This station has also been chosen for the present investigation in order to exploit the base of knowledge accumulated over the years and better interpret the data obtained in this project.

#### 4.1.2 Sampling strategies

The sampling site, st. MC, is located at 40°48.5’N and 14°15’E, two nautical miles from the coastline, in proximity of the 80m isobath (Fig. 4.1). Sampling was carried out weekly between July 2004 and July 2005. Profiles of physical parameters (temperature, salinity, density, oxygen) and fluorescence were determined with a CTD (see section 3.1), while water samples for nutrient determinations were collected at 0.5, 2, 5, 10, 20, 30, 40, 50, 60,

70 m. The water samples for the determination of pigment content in the fractions  $< 5\mu\text{m}$  and  $> 5\mu\text{m}$ , were collected at four depths: 0-10-20-40m.

Fractionated primary production measurements (total and  $> 5\mu\text{m}$ ) were carried out monthly, from March 2004 to May 2005. The sampling depths were selected each time according to optical levels as determined by means of underwater irradiance profiles. In addition, incident PAR irradiance was recorded over the sampling days (see section 3.1).

All the analytical procedures are reported with more details in the section 3.2 of the previous chapter.

## **4.2 Hydrology**

The vertical distribution of salinity during the investigated period showed the presence of fresher waters in the surface layer especially during spring, probably in relation with rain and land-runoff (Fig. 4.2a). Low-salinity water came from the coast by means of lateral advection and determined a sharp halocline. In particular, the salinity minimum (36.204) was recorded on 14 October 2004 at 0m, and the maximum (38.124) on 2 February 2005 at 20m.

The vertical distribution of temperature was similar to that of a typical temperate region: a pronounced thermocline in summer and a homothermal water column in winter (Fig. 4.2b). The lowest annual value (12.36 °C) was recorded on 8 March 2005 at 6m, and the highest (26.65 °C) on 20 August 2004 at 0m.

The vertical distribution of density indicated the driving role of temperature in the alternation of stratification and mixing of the water column (Fig. 4.2c). The seasonal stratification started at the end of March, and was completely disrupted in December. However, the pycnocline recorded at the end of March 2005 was probably more related to the low salinity than to the temperature increase. The stratification reached the maximum in August, when density values along the water column ranged between 23.63 and 28.41 kg m<sup>-3</sup>.

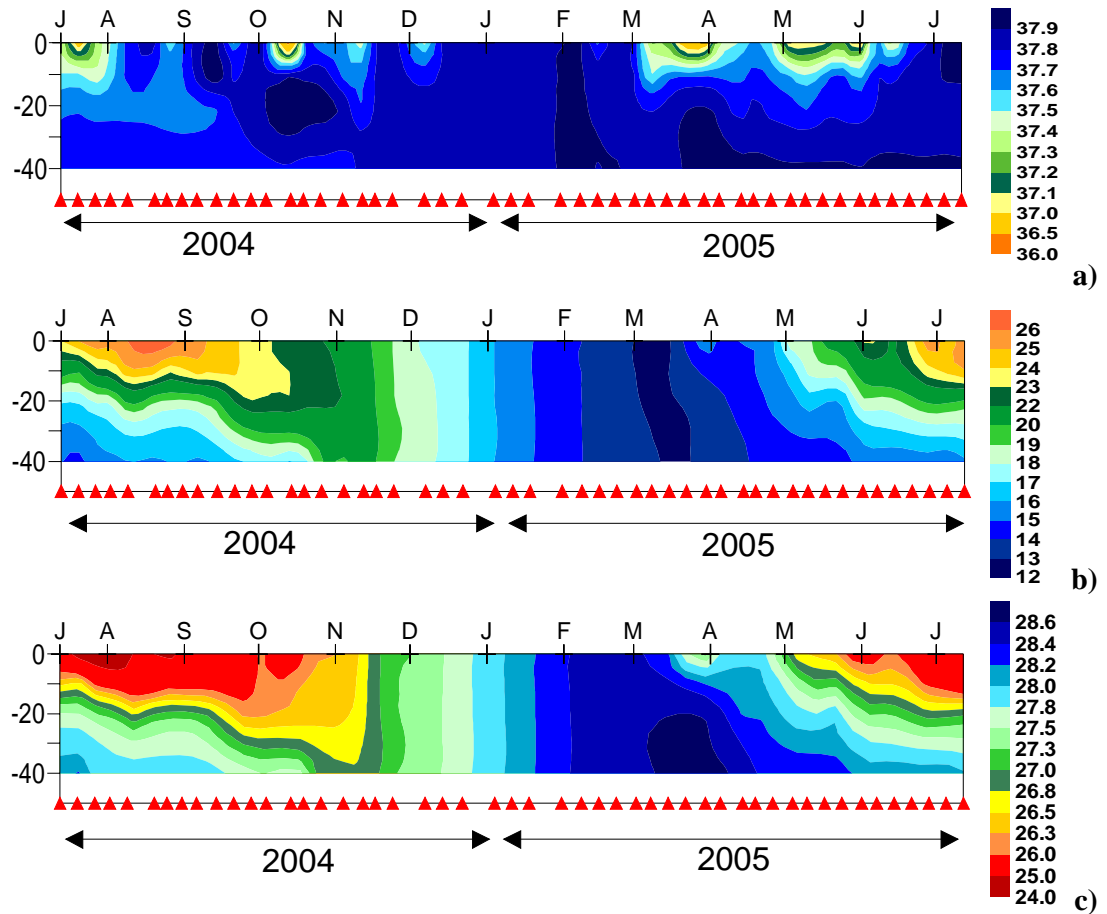


**Figure 4.2** – Vertical distribution (0-40m) of salinity (a), temperature (b) and density (c) at st. MC during the sampling period.

The annual cycle of stratification can be represented as the depth of the mixed layer (Fig. 4.3), here defined as the thickness of the layer down to an anomaly in density  $\geq 0.01 \text{ Kg m}^{-3}$  in one meter. The amplitude of the standard deviation between weekly records averaged over one month, reflected the presence of episodic input of less dense waters especially in November and March.

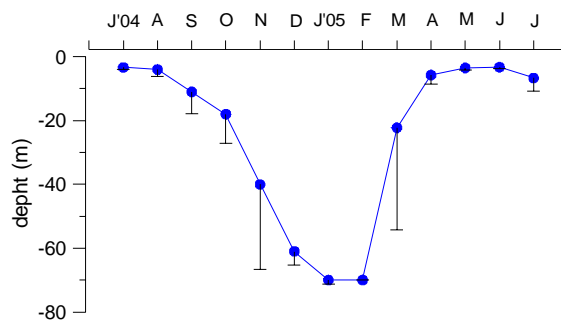


**Figure 4.3** – Monthly averages and standard deviation of the upper mixed layer depth at st. MC for the sampling period.

### 4.3 Nutrients

All the analyzed nutrients presented the highest values in the first 10 meters of the water column (Fig. 4.4- 4.6) and their variations in time showed a pattern quite similar to that of salinity, thus confirming their terrestrial origin. For instance, nitrate ( $\text{NO}_3^-$ ) showed a significant correlation with salinity in winter and spring ( $r = 0.64$ ,  $P < 0.05$ ,  $n = 200$ ).

The vertical distribution of nitrate ( $\text{NO}_3^-$ ) and ammonium ( $\text{NH}_4^+$ ) during the sampling period is shown in Fig. 4.4. These nutrients displayed a quite similar pattern, with maxima in spring and minima in summer.

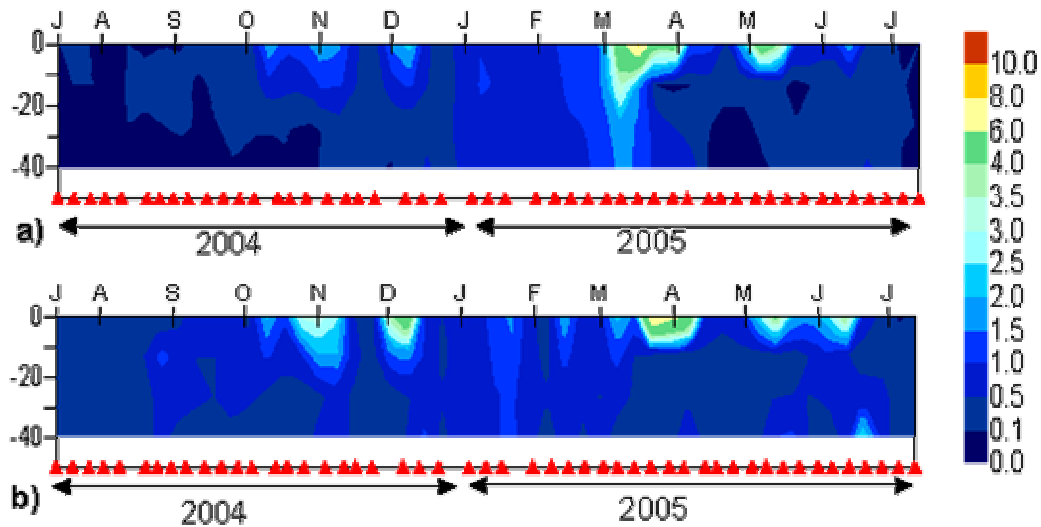


**Figure 4.4** – Vertical distribution (0-40m) of nitrate (a), and ammonium (b) at st. MC during the sampling period.

Nitrate concentrations were below detection only occasionally (in summer), while the highest value ( $8.64 \mu\text{mol l}^{-1}$ ) was recorded on 8 March 2005 at surface. Ammonium was never below the detection limit, ranging between  $8.24$  and  $0.05 \mu\text{mol l}^{-1}$ . The maximum value was recorded at surface on 15 March 2005 and the minimum also at surface on 8 August 2004.

The variations in time of phosphates ( $\text{PO}_4^-$ ) displayed the same patterns as that described for the nitrogen compounds (Fig. 4.5). The concentrations reached the highest value ( $0.43 \mu\text{mol l}^{-1}$ ) at surface on 10 May 2005, while they decreased below the detection limit in a few occasions (generally in summer).

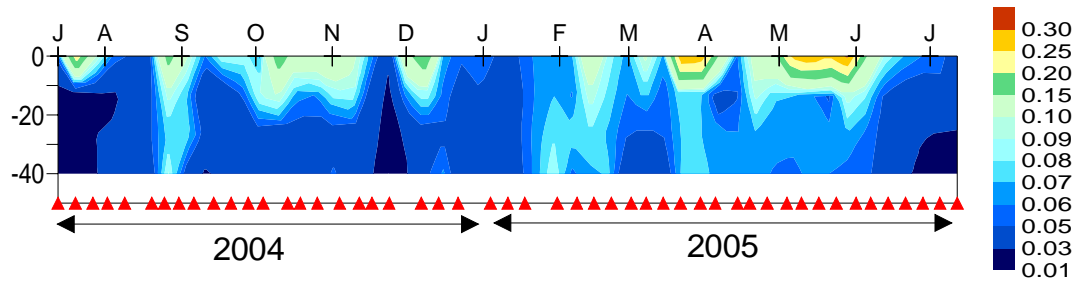


**Figure 4.5** – Vertical distribution (0-40m) of phosphate ( $\text{PO}_4^-$ ) at st. MC during the sampling period.

Silicate ( $\text{SiO}_4$ ) concentrations also confirmed the importance of terrestrial run-off at the station Marechiara, their maximum occurring mainly in correspondence with salinity minima. The highest value was recorded at surface in May 2005, along with the phosphate maximum, while the lowest was found on 27 July 2004 again in the surface layer (Fig. 4.6).

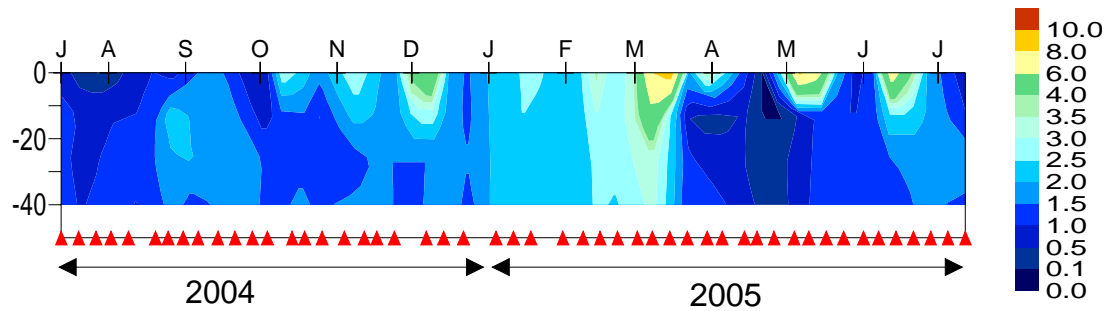


**Figure 4.6** – Vertical distribution (0-40m) of silicate ( $\text{SiO}_4$ ) at st. MC during the sampling period.

#### 4.4 Phytoplankton Biomass

Chlorophyll *a* is used as index of phytoplankton biomass and the total chlorophyll *a* content (TChl *a*) is given by the sum of Chl *a* and div-Chl *a*.

The seasonal changes of TChl *a* of the whole phytoplankton community (sum of the  $>5\mu\text{m}$  and the  $<5\mu\text{m}$  fractions) showed two main periods of high concentrations, in autumn 2004 and spring 2005, as well as sporadic peaks in summer. The highest value of the whole sampling period was recorded:  $7.59\text{ mg m}^{-3}$  at 0m on 20 July 2004 (Fig. 4.7a).

The thickness of the layer affected by the biomass increase seems to depend on the mixed layer depth. The peak in July 2004 only affected the water layers over 10 m, whereas the blooms in the following autumn reached down to about 20 m depth.

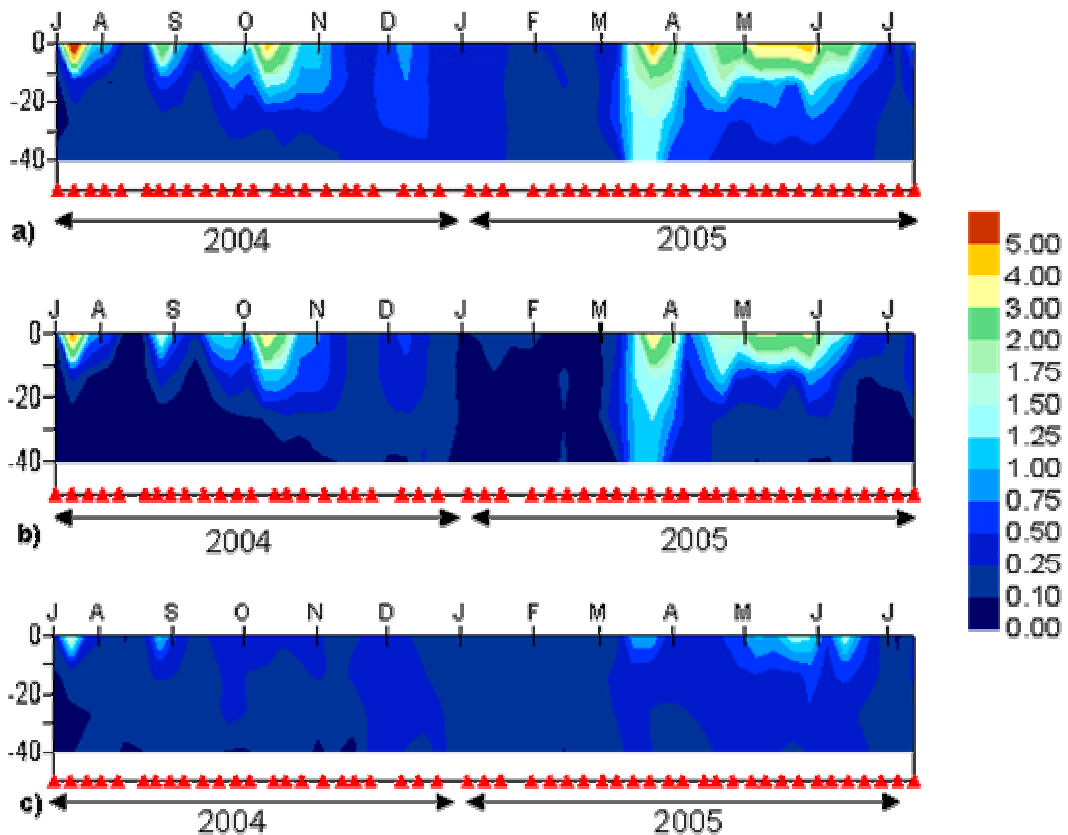


**Figure 4.7** – Vertical distribution (0-40m) of total TChl *a* (a), TChl *a*  $>5\mu\text{m}$  (b), TChl *a*  $<5\mu\text{m}$  (c) at st. MC during the sampling period.

The March bloom in 2005 occurred over the entire water column. The maximum was recorded at surface ( $5.45 \text{ mg m}^{-3}$ ), but the values remained high down to 40 m ( $1.88 \text{ mg m}^{-3}$ ). In relation to seasonal thermal stratification of the water column, the layer with high phytoplankton biomass became thinner in May and June. This pattern was reflected also in the time distribution of integrated TChl *a* (Fig.4.8), which showed the highest values ( $88.5 \text{ mg m}^{-2}$ ) in March 2005, while in July 2004 in spite of the chlorophyll maximum recorded in the surface layer, the integrated TChl *a* was only  $55.10 \text{ mg m}^{-2}$ .

The vertical distribution of TChl *a* for the fraction  $>5\mu\text{m}$  followed that of total TChl *a*, in particular during bloom periods (Fig. 4.7b). In fact, the average value was  $0.53 \pm 1.15 \text{ mg m}^{-3}$ , while the maximum ( $6.45 \text{ mg m}^{-3}$ ) was recorded on 14 October at surface and the minimum ( $0.01 \text{ mg m}^{-3}$ ) on 7 December at 40m. Variations in the concentrations of ultraphytoplankton TChl *a* were instead much less pronounced over the annual cycle, ranging between 0.050 and  $1.98 \text{ mg m}^{-3}$  (average value  $0.31 \pm 0.29 \text{ mg m}^{-3}$ ). The highest values were reached in surface layers during TChl *a* peaks in July 2004 and in late spring-summer 2005, whereas value increased only slightly during the autumn 2004 peak of the TChl *a* (Fig. 4.7c).

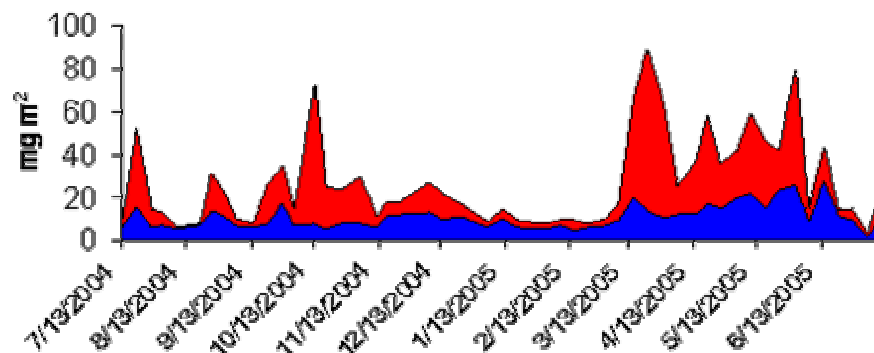


**Figure 4.8** – Seasonal distribution of integrated TChl *a* (0-40m) for the fraction  $<5\mu\text{m}$  (blue area), and the fraction  $>5\mu\text{m}$  (red area) at st. MC during the sampling period.

An opposite trend between the two size fractions was evident along the water column, whereby the contribution of ultraphytoplankton was higher in the 20-40m layer than in the upper, 0-10m layer, which was interested more frequently by the biomass increase (Table 4.1). Therefore, despite the conspicuous blooms of larger cells, the ultraphytoplankton contributed on average  $\approx 50\%$  to the total TChl *a* recorded over the year (Fig. 4.9; Tab. 4.1).

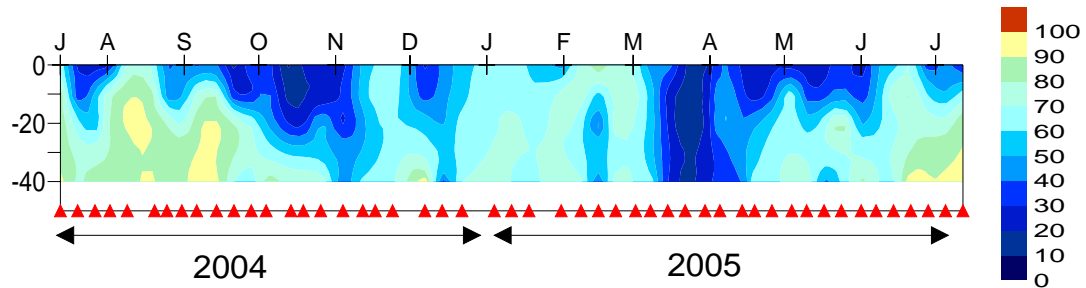


**Figure 4.9** – Vertical distribution of the relative contribution of ultraphytoplankton to total Chl *a* at st. MC during the sampling period.

The highest contribution of the ultraphytoplankton fraction (99.01%) was found on 21 June 2005 at 40m, while the minimum one (5.20%) was recorded on 14 October at 0m.

	0-40m	0-10 m	20-40 m
%<5	51.4±19.4	44.7±19.67	63.1±20.0
%>5	48.6±19.3	55.3±19.52	36.9±20.0

**Table 4.1** - Average percentage values of the two size fractions for the layer 0-40m, 0-10 m and 20-40m at st. MC, during the sampling period.

## 4.5 Primary production

Some interesting features emerged as to the annual cycle of phytoplankton productivity at Station Marechiara, though the monthly measurements (see section 4.1.2) did not allow for a very detailed reconstruction.

Integrated carbon assimilation in the 0-40m layer is reported in Fig. 4.10.

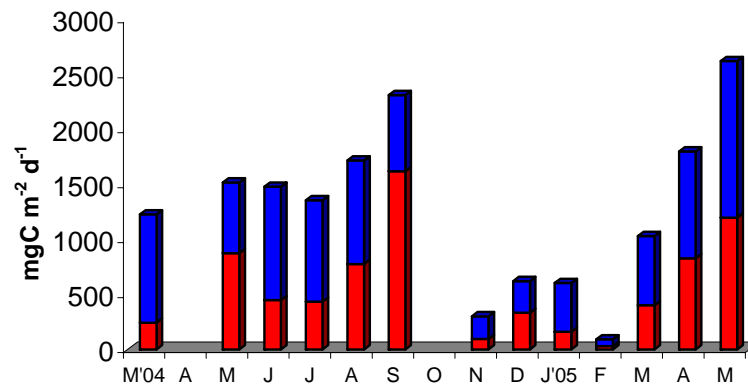


**Figure 4.10** – Evolution in time of integrated primary production (0-40m) for the fraction <5µm (blue area), and the fraction >5µm (red area) at st. MC during the sampling period.

The average integrated carbon assimilation value was  $1307 \pm 766$  mgC m<sup>-2</sup> d<sup>-1</sup>, with the highest values (up to 2624 mgC m<sup>-2</sup> d<sup>-1</sup>, May 2005) recorded in spring and summer and the lowest in winter (92 mgC m<sup>-2</sup> d<sup>-1</sup>, February 2005).

In Fig. 4.11 four primary production profiles are showed. They have been chosen since representative of different situation occurring trough the seasonal cycle, such as summer bloom (Fig. 4.11a) or winter condition (Fig. 4.11c).

Generally, highest carbon assimilation rates were recorded in the surface layer (first 10 meters). These maxima were again related to the >5µm fraction, but especially in summer and in autumn, also the ultraphytoplankton fraction showed high surface values: 58.5 mgC m<sup>-3</sup> d<sup>-1</sup> at 5m in July 2004 and 45.1 mgC m<sup>-3</sup> d<sup>-1</sup> at 10m in September 2004 (Fig. 4.11a,b). On the other hand, in winter, when the carbon assimilation values were lower the ultraphytoplankton productivity was slightly higher than that of the >5µm fraction (Fig. 4.11c). Moreover, the carbon assimilation rate of the ultraphytoplankton fraction was always higher than the fraction >5µm at depth.

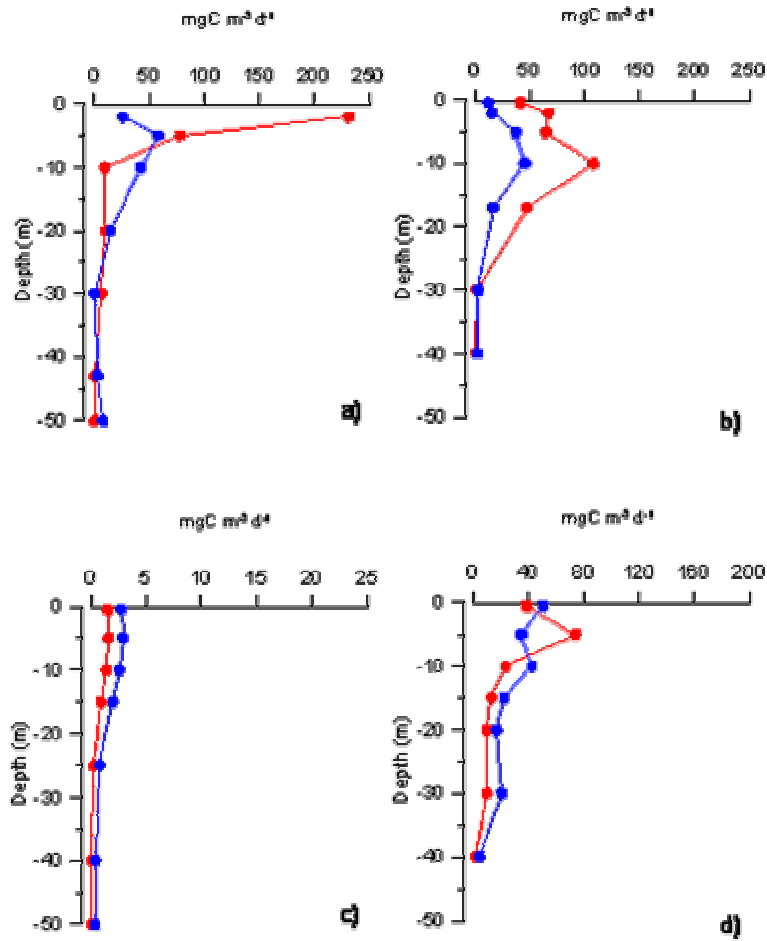


**Figure 4.11** – Vertical profiles of daily primary production on 27 July 2004 (a), 28 September 2004 (b), 12 February 2005 and on 14 May 2005 for the <5µm fraction (●), and the >5µm fraction (●) at st. MC.

The average contribution of ultraphytoplankton to the integrated total primary production was more than 50% (see Tab. 4.2); this contribution, however, was lower in the surface layer (0-10m):  $38.7 \pm 13.8$  %, while it reached  $71.3 \pm 14.3$ % in the layer 20-40m.

	0-40m	0-10 m	20-40 m
%<5	55.8±13.0	41.5±13.8	71.3±14.3
%>5	44.2±14.0	58.5±13.8	28.7±14.3

**Table 4.2** - Average contributions of the two size fractions to total primary production for the 0-40m, the 0-10 m and the 20-40m layers at st. MC, during the sampling period.

## 4.6 Pigments

The HPLC data of the main diagnostic photosynthetic pigments showed notable differences between the two size fractions during the seasonal cycle. The percentage of each pigment found in the two fractions was quite variable too. However, some pigments (e.g. Div-chl *a*) were exclusive of a size class (Tab. 4.3).

<b>Pigments</b>	<b>% &gt;5<math>\mu</math>m</b>	<b>% &lt;5<math>\mu</math>m</b>	<b>SD</b>
19'Bf	8.7	91.3	14.4
19'Hf	27.0	73.0	18.2
Allo	7.1	92.9	16.1
Chl <i>b</i>	8.9	91.1	0.263
Chl <i>c</i> <sub>3</sub>	30.2	69.8	0.135
Chl <i>c</i> <sub>1</sub> + <i>c</i> <sub>2</sub>	49.8	50.2	0.261
Diado	53.1	46.9	21.7
Diato	49.2	50.8	0.030
Div- Chl <i>a</i>	0	100	-
Fuco	63.3	36.7	19.9
Lut	5.9	94.1	13.9
Neox	10.2	89.8	23.2
Perid	91.5	8.5	13.9
Prasino	0	100	-
Viola	9.7	90.3	19.7
Zea	6.2	93.8	14.0
$\beta$ - carot	56.1	43.9	30.5

**Table 4.3**– Average percentage and standard deviation (SD) of main pigments in the >5 $\mu$ m and <5 $\mu$ m fraction, at st. MC.

In Tab. 4.4 the average, minimum and maximum concentration values of the principal diagnostic pigments are reported for the > 5 $\mu$ m and <5 $\mu$ m fraction.

Pigments	AVG		MIN		MAX	
	>5µm	<5µm	>5µm	<5µm	>5µm	<5µm
19'Bf	<b>0.004±0.010</b>	<b>0.024±0.021</b>	0.000	0.000	0.072	0.174
19'Hf	<b>0.040±0.106</b>	<b>0.066±0.0566</b>	0.000	0.000	1.259	0.359
Allo	<b>0.003±0.010</b>	<b>0.013±0.020</b>	0.000	0.000	0.100	0.199
Chl <i>b</i>	<b>0.006±0.021</b>	<b>0.028±0.032</b>	0.000	0.000	0.158	0.263
Chl <i>c</i> <sub>3</sub>	<b>0.021±0.039</b>	<b>0.031±0.021</b>	0.006	0.000	0.394	0.135
Chl <i>c</i> <sub>1</sub> + <i>c</i> <sub>2</sub>	<b>0.120±0.238</b>	<b>0.044±0.040</b>	0.000	0.000	1.809	0.261
Diado	<b>0.051±0.132</b>	<b>0.021±0.032</b>	0.000	0.000	0.862	0.241
Diato	<b>0.005±0.013</b>	<b>0.002±0.024</b>	0.000	0.000	0.112	0.030
Div- Chl <i>a</i>	<b>0.000</b>	<b>0.004±0.007</b>	0.000	<b>0.000</b>	<b>0.000</b>	0.050
Fuco	<b>0.293±0.524</b>	<b>0.071±0.084</b>	0.005	0.000	3.533	0.866
Lut	<b>0.001±0.003</b>	<b>0.001±0.004</b>	0.000	0.000	0.027	0.045
Neox	<b>0.003±0.015</b>	<b>0.004±0.005</b>	0.000	0.000	0.150	0.032
Perid	<b>0.016±0.053</b>	<b>0.001±0.007</b>	0.000	0.000	0.407	0.085
Prasino	<b>0.000</b>	<b>0.001±0.005</b>	0.000	<b>0.000</b>	<b>0.000</b>	0.047
Viola	<b>0.001±0.004</b>	<b>0.003±0.006</b>	0.000	0.000	0.032	0.032
Zea	<b>0.002±0.007</b>	<b>0.023±0.024</b>	0.000	0.000	0.052	0.177
β - carot	<b>0.020±0.037</b>	<b>0.008±0.012</b>	0.000	0.000	0.283	0.101

**Table 4.4** – AVG, MIN and MAX pigments concentration (mg m<sup>-3</sup>) of the <5µm and <5µm fractions at st. MC, during the sampling period.

*Golden-brown algae pigments*

The vertical distribution of Fucoxanthin (Fuco) concentrations, a diagnostic pigment of diatoms, showed maximum values at surface in correspondence with blooms (Fig. 4.12a). A positive correlation was found between Fuco and TChl *a* both in the  $> 5\mu\text{m}$  ( $r = 0.97$ ,  $P < 0.01$ ,  $n=200$ ) and in the ultraphytoplankton fraction ( $r = 0.81$ ,  $P < 0.01$ ,  $n=200$ ).

Fuco was always the most important carotenoid in the  $>5\mu\text{m}$  fraction. It was not detected only in rare occasions (e.g. July 2004). The high standard deviation on the mean value reflects the considerable temporal variability of phytoplankton populations at st. MC (Tab. 4.3).

On the contrary, the changes in Fuco concentrations in the ultraphytoplankton fraction were less pronounced and the pigment was always detected in this fraction (Tab. 4.4). The minima values were recorded in the layer 20-40m and in winter, while the maxima were associated with the summer bloom in July 2004 (Fig. 4.12b).

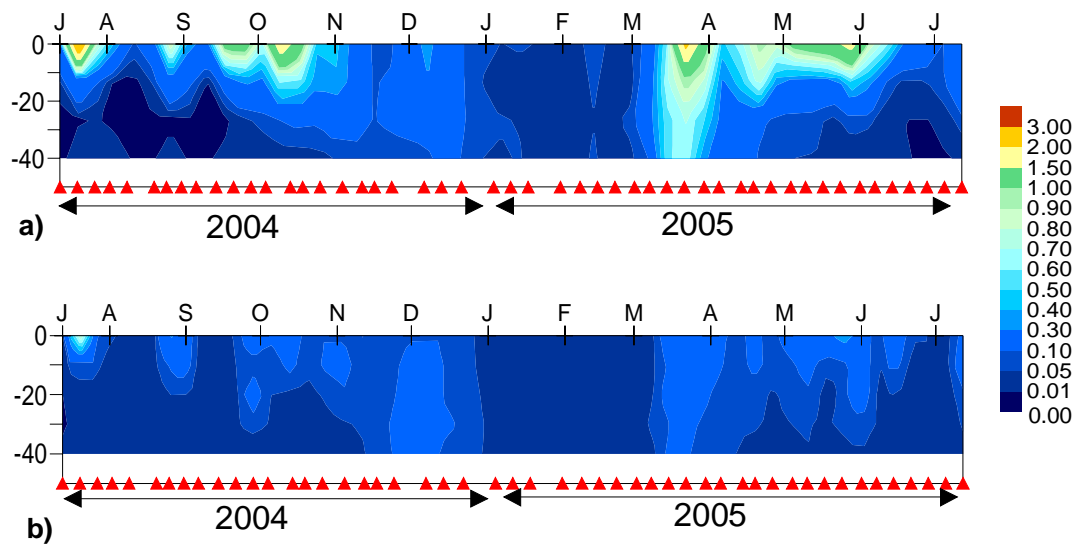


**Figure 4.12** – Vertical distribution (0-40m) of the Fuco concentration ( $\text{mg m}^{-3}$ ) for the fraction  $>5\mu\text{m}$  (a), and  $<5\mu\text{m}$  (b) at st. MC during the sampling period.

On average  $\sim 60\%$ , of Fuco was found in  $>5\mu\text{m}$  fraction, in all samples (Tab. 4.5). In the 0-10m layer this percentage reached 80-90%, during phytoplankton blooms, by contrast in the 20-40m layer,  $\sim 60\%$  of Fuco was in the ultraphytoplankton fraction.

The variations in time of Chlc<sub>1</sub>+c<sub>2</sub> pigments, which are typical of golden-brown algae, were significantly correlated with Fuco in both the ultraphytoplankton ( $r = 0.83$ ,  $P < 0.01$ ,  $n=200$ ) and the  $>5\mu\text{m}$  fraction ( $r = 0.95$ ,  $P < 0.01$ ,  $n=200$ ) (data not shown).

The vertical distribution of 19'Hexanoylfucoxanthin (19'Hf) concentrations during the sampling period is shown in Fig. 4.13. This pigment is considered diagnostic of prymnesiophytes, though it may be lacking in some species of this group and present also in other golden-brown algae (see section 2.1.1).

In the fraction  $>5\ \mu\text{m}$ , 19'Hf distribution showed the highest values during bloom periods. In contrast to the observations on the vertical distribution of Fuco, this pigment was often not detected below 20m in late summer and early autumn 2004 (Fig. 4.13a),

In the ultraphytoplankton fraction, the 19'Hf concentrations were quite constant from August 2004 to March 2005 (average  $0.042\pm 0.018\ \text{mg m}^{-3}$ ), thereafter an increase in this pigment was recorded throughout the 0-40m layer in spring and early summer 2005 (average  $0.12\pm 0.07\ \text{mg m}^{-3}$ ) (Fig. 4.13b).

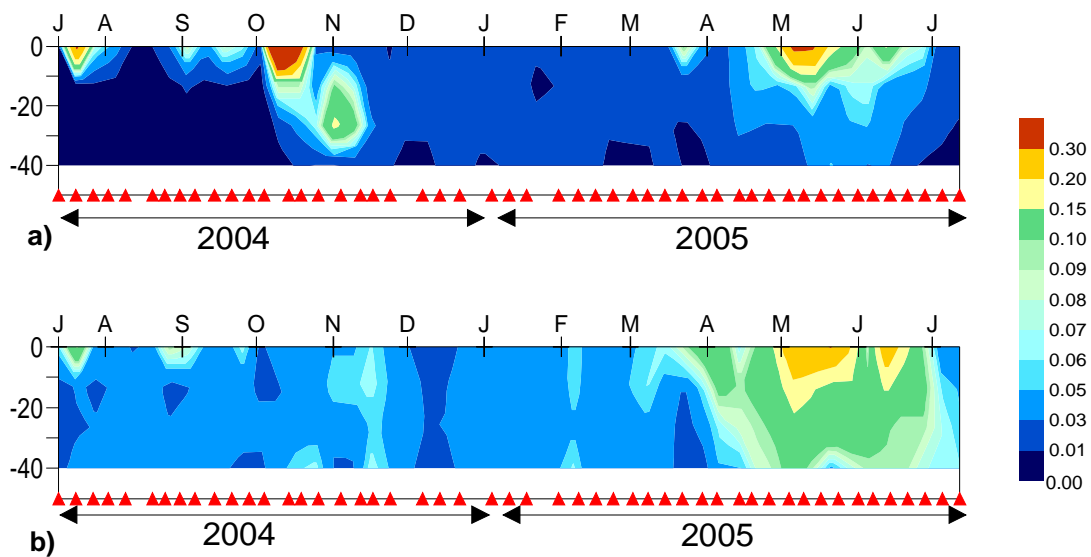


**Figure 4.13** – Vertical distribution (0-40m) of the 19'Hf concentration ( $\text{mg m}^{-3}$ ) for the fraction  $>5\ \mu\text{m}$  (a), and  $<5\ \mu\text{m}$  (b) at st. MC during the sampling period.

Again in contrast to the occurrence of Fuco, the 19'Hf was essentially found in the ultraphytoplankton fraction (Tab. 4.5). However, during the autumn bloom ~80% of this pigment occurred in the  $>5\ \mu\text{m}$  fraction at surface.

The variations in time of Chlc<sub>3</sub> concentrations (data not shown) were significantly correlated with 19'Hf both in the ultraphytoplankton ( $r = 0.91$ ,  $P < 0.01$ ,  $n = 200$ ) and in the  $>5\ \mu\text{m}$  fraction ( $r = 0.72$ ,  $P < 0.01$ ,  $n = 200$ ).

Peridinin (Perid), a marker of autotrophic dinoflagellates, did not occur in either size fractions for most of the sampling period (Fig. 4.14). This pigment was not detected in the  $>5\mu\text{m}$  fraction in  $\sim 70\%$  of the samples and in  $\sim 90\%$  of the samples as regards the ultraphytoplankton fraction. When present, Perid was essentially associated with the  $>5\mu\text{m}$  fraction. In this size-fraction, high concentrations of Perid occurred in summer 2004, when the highest TChl *a* value was recorded. A second peak, up to  $0.26\text{ mg m}^{-3}$ , occurred in early spring 2005 again within the first 10 meters. Finally, during the late spring-early summer bloom higher Perid values showed a wide vertical extension and persisted for several months, (Fig. 4.14a).

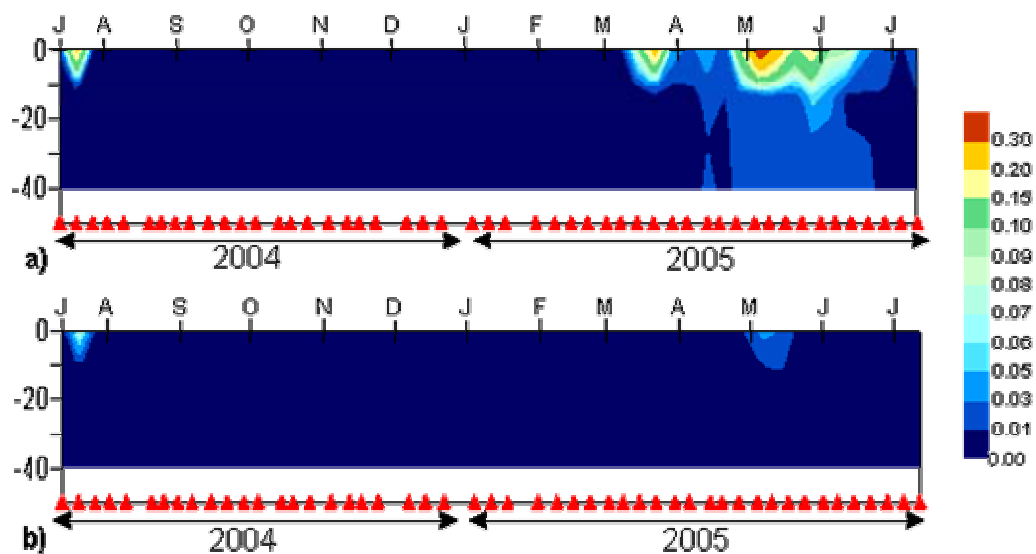


**Figure 4.14** – Vertical distribution (0-40m) of Perid concentrations ( $\text{mg m}^{-3}$ ) for the fraction  $>5\mu\text{m}$  (a), and  $<5\mu\text{m}$  (b) at st. MC during the sampling period.

19'Butanoiloxifucoxanthin (19'Bf) is a diagnostic pigment of pelagophytes, but it may also occur in some species of prymnesiophytes. Low concentrations of 19'Bf, occurred in the  $>5\mu\text{m}$  fraction during the spring-summer blooms (April-June 2005) and the highest value was found at surface. However, this pigment was often not detected at all in the  $>5\mu\text{m}$  fraction during the sampling period (Fig. 4.15a).

In the ultraphytoplankton fraction 19'Bf concentrations were low and fairly constant throughout the sampling period (Tab. 4.5). This pigment was not detected between October and November 2004 in the surface layer, while a small peak was recorded in summer 2005 (Fig. 4.15b). In contrast to the other pigments, the 19'Bf maxima were not correlated with maximum TChl *a* concentrations.

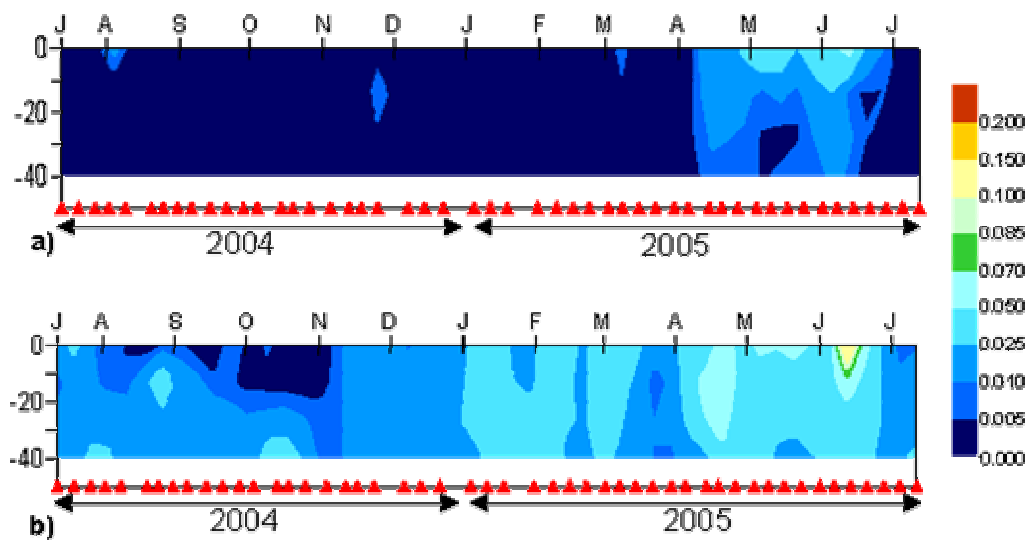


**Figure 4.15** – Vertical distribution (0-40m) of 19'Bf concentrations ( $\text{mg m}^{-3}$ ) for the  $>5\mu\text{m}$  fraction (a), and the  $<5\mu\text{m}$  fraction (b) at st. MC during the sampling period.

Essentially all of the 19'Bf was detected in the ultraphytoplankton fraction (Tab. 4.5).

Alloxanthin (Allo) is a specific marker of cryptophytes. Its vertical distribution during the sampling period is shown in Fig. 4.16. In the  $>5\mu\text{m}$  fraction Allo was only occasionally detected. This pigment was recorded in summer 2004 (up to  $0.1\text{ mg m}^{-3}$ ), in correspondence to the maximum TChl *a* value. A second peak, which lasted for several weeks, occurred in spring 2005. The extension of the presence of Allo along the water column was apparently related to the depth of the mixed layer, as already observed for the distribution of phytoplankton biomass (Fig. 4.16a). Since Allo is also present in the ciliate *Mesodinium rubrum*, a species frequently recorded with high numbers at st. MC (Modigh, 2001), a certain amount of the Allo recorded in the larger size fraction may be due to this ciliate. However, no significant correlation was found between Allo concentrations and *M. rubrum* cell numbers during the sampling period (Modigh personal communication).

Allo was generally present, though at low concentrations in the ultraphytoplankton fraction; with the highest values in the spring-summer 2005 (Fig. 4.16b). Allo did not occur only in 8% of the samples and similarly to the findings reported for 19'Bf, it was almost exclusively recorded in the ultraphytoplankton fraction (Tab. 4.5).

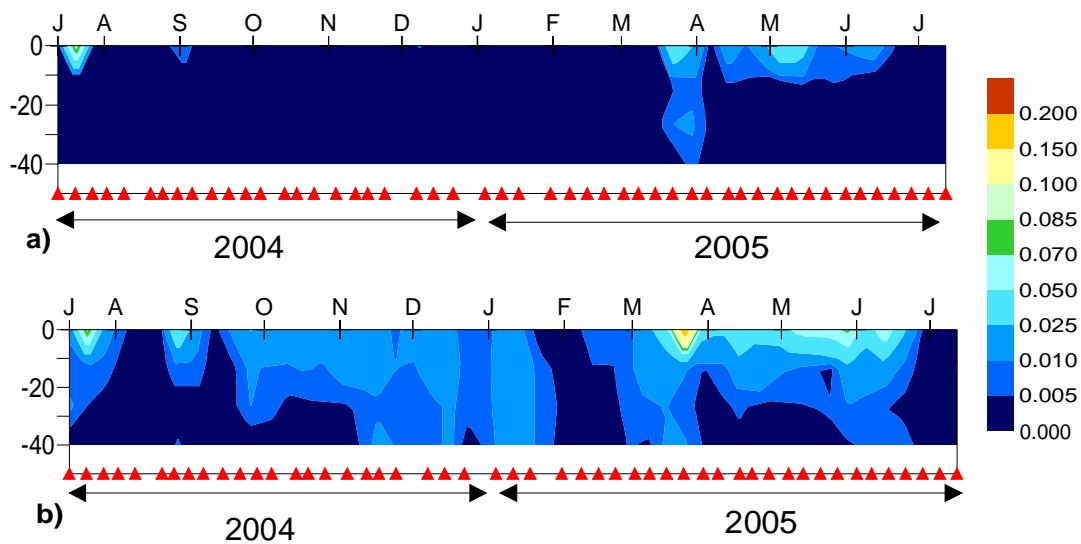


**Figure 4.16** – Vertical distribution (0-40m) of Allo concentrations ( $\text{mg m}^{-3}$ ) in the  $>5\mu\text{m}$  (a), and in the  $<5\mu\text{m}$  fraction (b) at st. MC during the sampling period.

*Green algae pigments*

Chlorophyll *b* (Chl *b*) is a pigment diagnostic of the group of green algae. In the  $>5\mu\text{m}$  fraction Chl *b* was detected albeit in low values in summer-autumn 2004, associated with episodic increments in TChl *a* concentrations, always limited to the surface layer. Slightly higher Chl *b* concentrations were recorded in spring and early summer 2005 (Fig. 4.17a). In the ultraphytoplankton fraction, Chl *b* displayed quite low and uniform values ( $0.018\pm 0.015\text{ mg m}^{-3}$ ) between July 2004 and February 2005, while values exceeding  $0.15\text{ mg m}^{-3}$  were recorded in March and in June 2005 (Fig. 4.17b).

Chl *b* was a pigment of the ultraphytoplankton fraction. In this fraction, it was not detected in only 11% of samples; while it was often absent in the fraction  $>5\mu\text{m}$  (73% of samples).

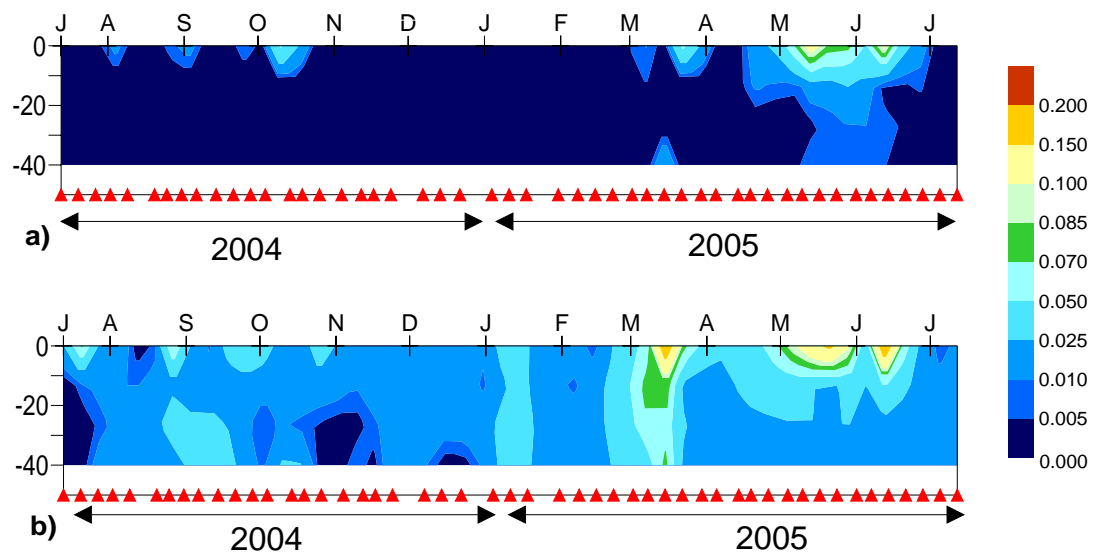


**Figure 4.17** – Vertical distribution (0-40m) of Chl *b* concentrations ( $\text{mg m}^{-3}$ ) in the  $>5\mu\text{m}$  (a), and in the  $<5\mu\text{m}$  fraction (b) at st. MC during the sampling period.

Violaxanthin (Viola) is another diagnostic pigment of green algae; in fact, its distribution was strongly correlated with Chl *b* in both the ultraphytoplankton ( $r = 0.86$ ,  $P < 0.01$ ,  $n = 200$ ) and in the  $>5\mu\text{m}$  fraction ( $r = 0.84$ ,  $P < 0.01$ ,  $n = 200$ ). The vertical distribution of Viola concentrations shows that Violaxanthin occurred only between May and July 2005 in the  $>5\mu\text{m}$  fraction at very low concentrations (Fig. 4.18a). Similar concentrations (average  $0.003\pm 0.006\text{ mg m}^{-3}$ ) were found also in the ultraphytoplankton in spring-summer 2005 (Fig. 4.18b). Viola was never detected below 20 m in either of the two size fractions, probably because of its role as a photoprotective pigment.

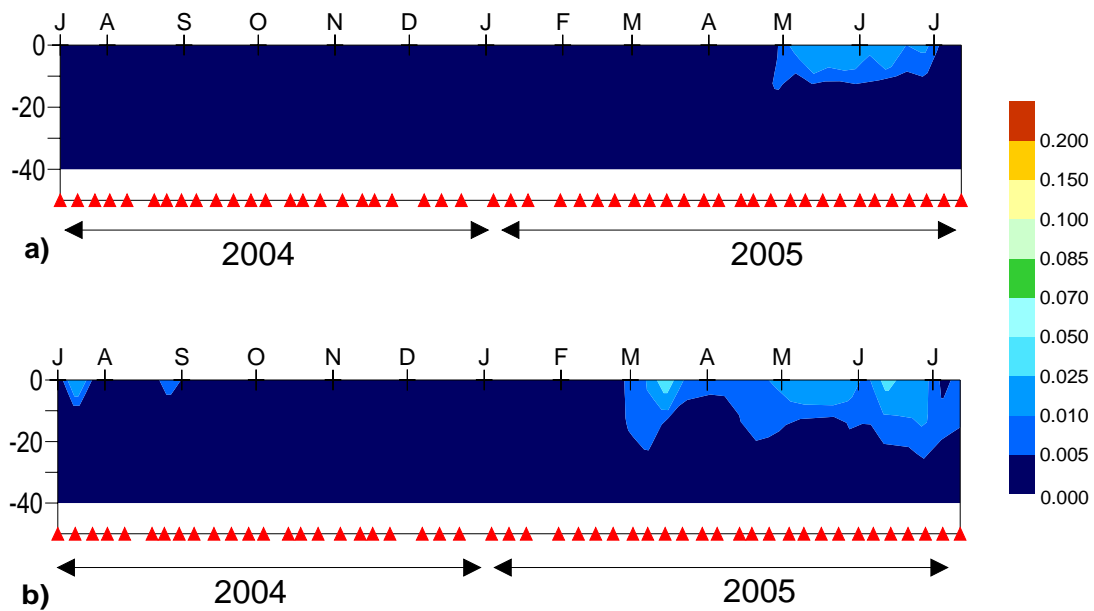


**Figure 4.18** – Vertical distribution (0-40m) of the Viola concentration ( $\text{mg m}^{-3}$ ) for the fraction  $>5\mu\text{m}$  (a), and  $<5\mu\text{m}$  (b) at st. MC during the sampling period.

In March 2005 Prasinocyanin (Prasino), a diagnostic pigment of prasinophytes, was recorded in the ultraphytoplankton fraction throughout the 0-40m layer, associated with the first phytoplankton spring bloom (Fig. 4.19).

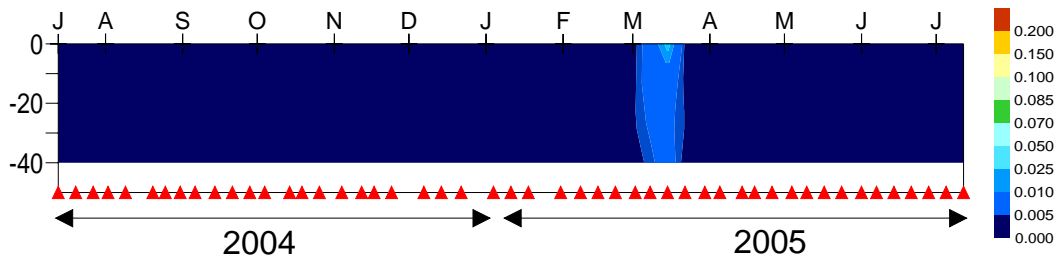


**Figure 4.19** – Vertical distribution (0-40m) of the Prasino concentration ( $\text{mg m}^{-3}$ ) in the  $<5\mu\text{m}$  fraction, at st. MC during the sampling period.

Finally, small amounts of Neoxanthin, another pigment that is typical of green algae, were only occasionally recorded, generally in samples where Chl *b* was also recorded (data not shown).

*Prokaryotes pigments*

Zeaxanthin (Zea) is a marker of prokaryotes; it is synthesized by both cyanobacteria and prochlorophytes. In order to estimate the contribution to total Zea concentrations of these two groups, we calculated the content of Zea in the prochlorophytes using the Zeaxanthin/Divinyl Chl *a* ratio of 0.32 as suggested by Barlow *et al.*, (1999) and Marty *et al.* (2002). The Zeaxanthin due to cyanobacteria ( $Zea_{syn}$ ) was obtained by subtracting this portion from the Zea concentration measured. Vertical distributions of Zea and  $Zea_{syn}$  concentrations in the ultraphytoplankton fraction clearly show that the major part of Zeaxanthin was associated to cyanobacteria during the entire sampling period (Fig. 4.20). The highest concentrations of Zea were recorded in summer, while the lowest occurred in winter. This pigment was not detected only in 3% of the samples.

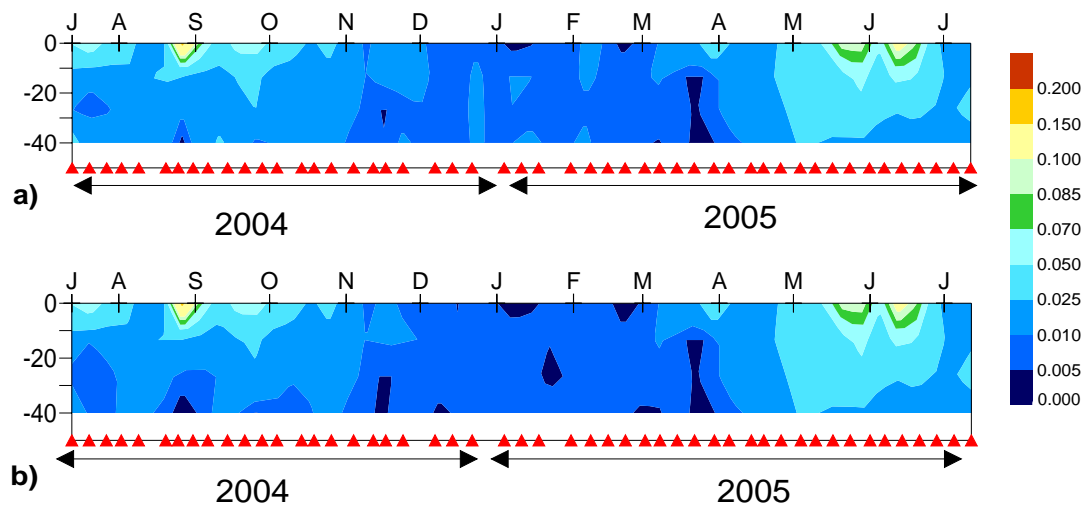


**Figure 4.20** – Vertical distribution (0-40m) of Zea (a), and of  $Zea_{syn}$  (b) concentrations ( $\text{mg m}^{-3}$ ) in the  $<5\mu\text{m}$  fraction at st. MC during the sampling period.

Zea was detected in the  $>5\mu\text{m}$  fraction only on a few occasions in summer and spring generally at surface and associated with Chl *b* (data not shown). Thus, the presence of Zeaxanthin in the larger size fraction may be related to its role as a photoprotective pigment in green algae. The same hypothesis may also explain the presence again in the  $>5\mu\text{m}$  fraction of small amounts of Lutein (data not shown).

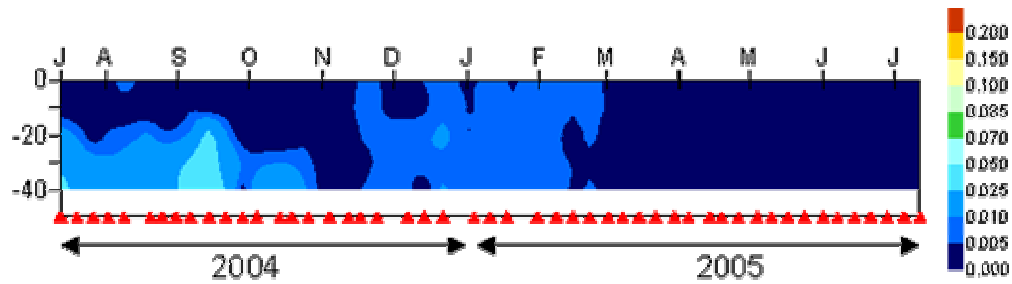


**Figure 4.21** – Vertical distribution (0-40m) of div-Chl *a* concentration ( $\text{mg m}^{-3}$ ) in the fraction  $<5\mu\text{m}$  at st. MC during the sampling period.

Div-Chl *a* is a specific marker pigment of prochlorophytes and, in agreement with the small size of this group, this pigment was found exclusively in the ultraphytoplankton fraction (Tab. 4.4). In particular, the highest values of div-Chl *a* were recorded in summer and autumn 2004 in the 20-40m layer, with a vertical distribution opposite to that of Zeaxanthin. In contrast, div-Chl *a* was recorded along the entire water column during winter and subsequently disappeared at the onset of the spring bloom (Fig. 4.21).

#### *Photoprotective carotenoids*

The vertical distribution of Diadinoxanthin (Dd) concentrations of the two size fractions showed the highest values at surface during the spring and summer bloom, while the lowest values were recorded in winter and at depth (Fig. 4.22). These results were well in agreement with the role of Diadinoxanthin in the photoprotection of golden-brown algae. A strong positive correlation was found between Fucoxanthin and Diadinoxanthin both in the ultraphytoplankton ( $r = 0.84$ ,  $P < 0.01$ ,  $n = 200$ ) and in the  $>5\mu\text{m}$  fraction ( $r = 0.78$ ,  $P < 0.01$ ,  $n = 200$ ).

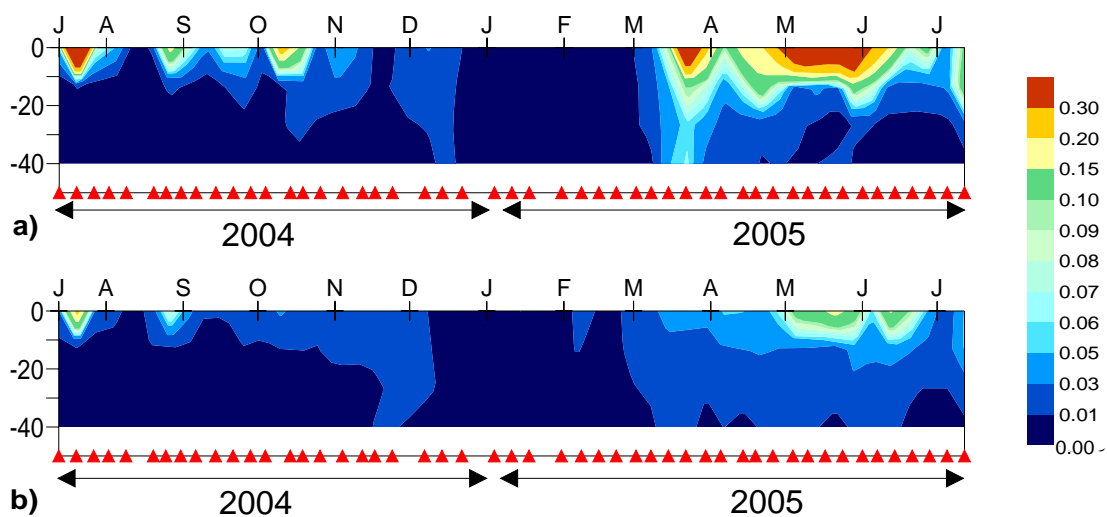


**Figure 4.22** – Vertical distribution (0-40m) of Dd concentration ( $\text{mg m}^{-3}$ ) for the fraction  $>5\mu\text{m}$  (a), and  $<5\mu\text{m}$  (b) at st. MC during the sampling period.

The seasonal occurrence of  $\beta$ -carotene, another photoprotective carotenoid, was similar to that described for Diadinoxanthin. Highest concentrations of  $\beta$ -carotene were recorded at surface in spring and summer in both studied fractions; in winter this pigment was often not detected at all or occurred at very low concentrations (data not shown).

In order to investigate the seasonal patterns of the photoprotective pigments, we considered a ratio between photoprotective and photosynthetic pigments, according to Gibb *et al.*, (2000), the PPC/(PPC+PSP) ratio. PPC is the sum of the photoprotective carotenoids Diado, Allo, Zea and  $\beta$ -carotene, while PSP is the sum of the photosynthetic pigments Perid, 19'Bf, 19'Hf, Fuco and Prasino. The PPC/ (PPC+PSP) ratio showed a seasonal pattern, with the highest values recorded in summer in the surface layer (Fig. 4.23). This pattern was more evident in the ultraphytoplankton fraction (Fig. 4.23b), where the highest value (0.47) was recorded at 0m on 14 June 2005, and the lowest (0.003) at 40m on 12 November 2004.

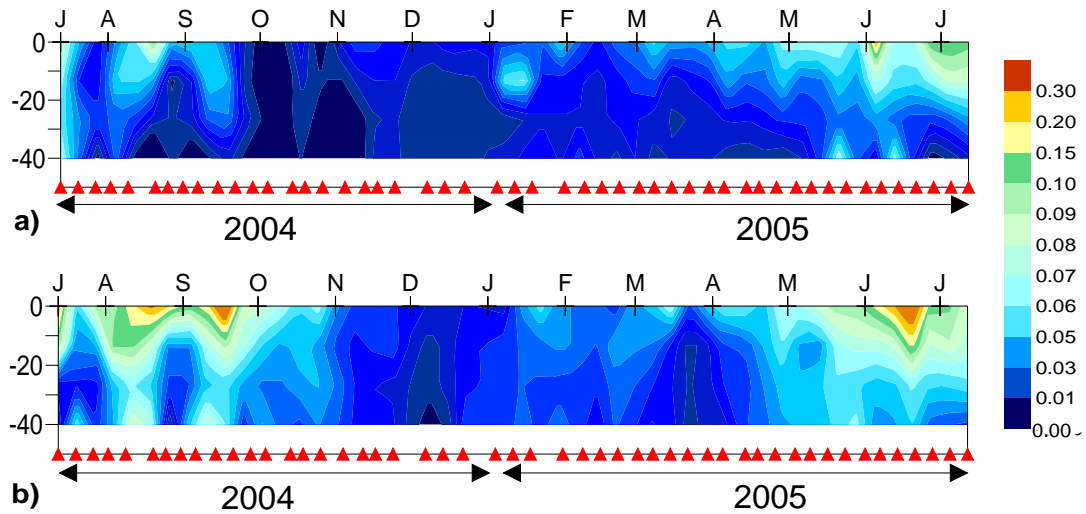


**Figure 4.23**– Vertical distribution (0-40m) of the PPC/(PPC+PSP) ratio (photoprotective/photoprotective carotenoids+ photosynthetic pigments see text) in the  $>5\mu\text{m}$  (a), and in the  $<5\mu\text{m}$  fraction (b) at st. MC during the sampling period.

The relative contributions of pigments (except Chl *a*) in the two sampling fractions were showed in Fig. 4.24 (layer 0-10m) and in Fig. 4.25 (layer 20-40m). The six sampling dates were chosen as significant of different situations, occurring at MC during the seasonal cycle: a summer bloom (20 July 2004), summer oligotrophic conditions (9 August 2004), autumn bloom (14 October 2004), winter condition (11 January 2005), late-winter bloom (22 March 2005) and a late-spring early summer bloom (1 June 2005), see Fig. 4.7 for TChl *a* distribution.

The >5 $\mu$ m fraction displayed a quite constant pigment composition trough the year, with Fuco as main pigment in the two layers. The only exception was recorded in summer oligotrophic condition (on 9 August 2004), when 19'Hf and Fuco showed quite similar values (Fig. 4.24b, 4.25b). In the two layers the Perid contribution was quite low (<8%) and limited to the spring-summer blooms.

The ultraphytoplankton fraction showed a more variable pigment composition. The Fuco was the main pigment during the bloom periods in the layer 0-10m (e.g. on 20 July and 14 October 2004), while in summer oligotrophic condition 19Hf and Zea were well represented (Fig. 4.24b). In winter, instead the main pigments were 19'Hf, Chl *b* and 19'Bf (Fig. 4.24d). In the late-winter bloom (22 March 2005) the Fuco was again the main pigment, but followed by Allo, more than by 19'Hf.

In the layer 20-40m the pigment composition of ultraphytoplankton fraction showed a high diversity, with clear changes in time. The 19'Hf was generally the main pigment (>20%), with the only exception of early –spring bloom, when the Fuco was by far the dominant pigment (Fig. 4.25e). In summer, the 19'HF, Zea, 19'Bf and div-Chl *a* were the well represented pigments, in both high-biomass and oligotrophic conditions (Fig. 4.25a,b).

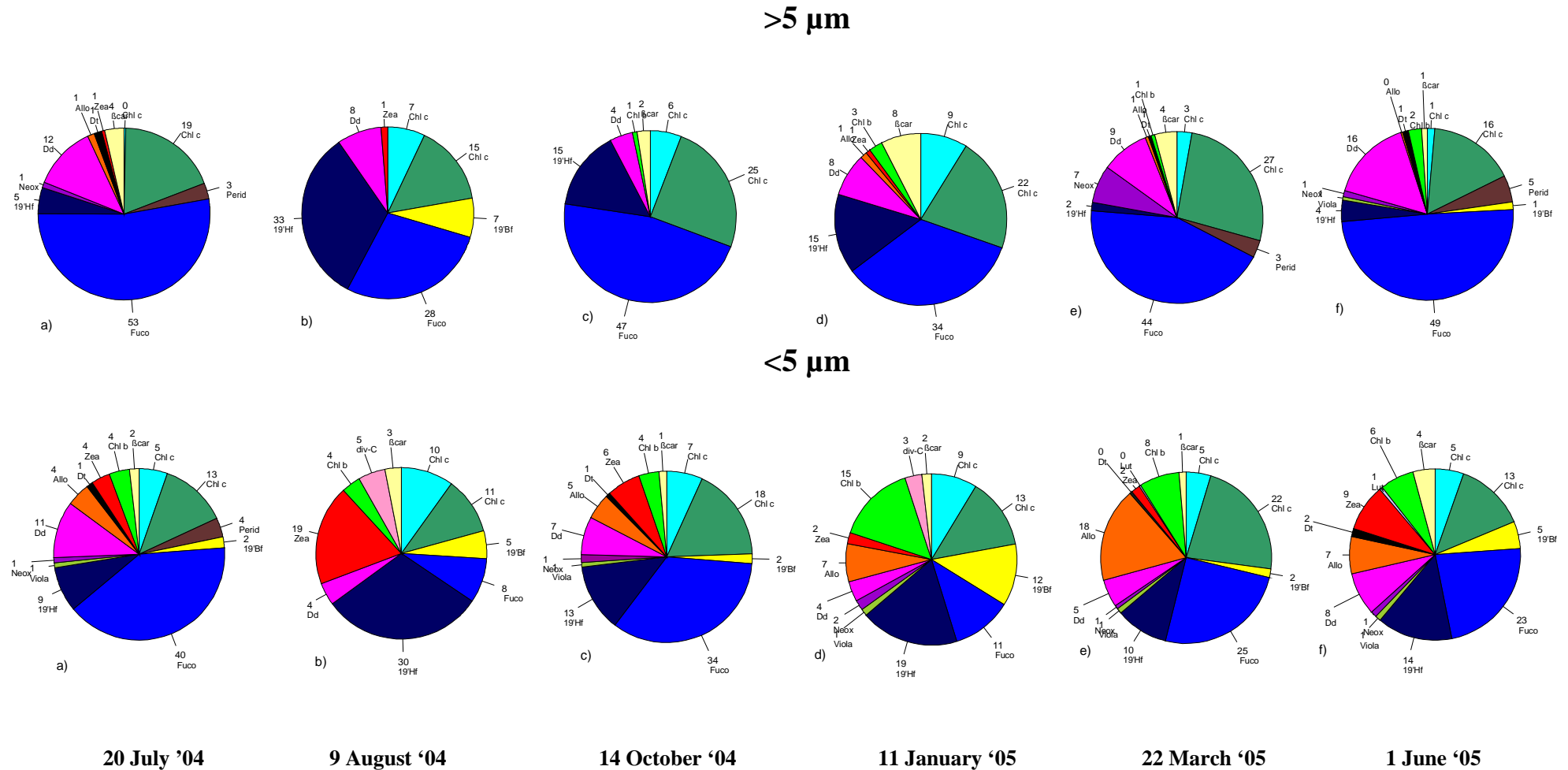


**Figure 4.24** – Average relative contribution of HPLC pigments (except Chl *a*) on 20 July 2004 (a.), on 9 August 2004 (b), on 14 October 2004 (c), on 11 January 2005 (d), 22 March 2005 (e) and 1 June 2005 for the two sampling fraction, in the layer 0-10m at st. MC.

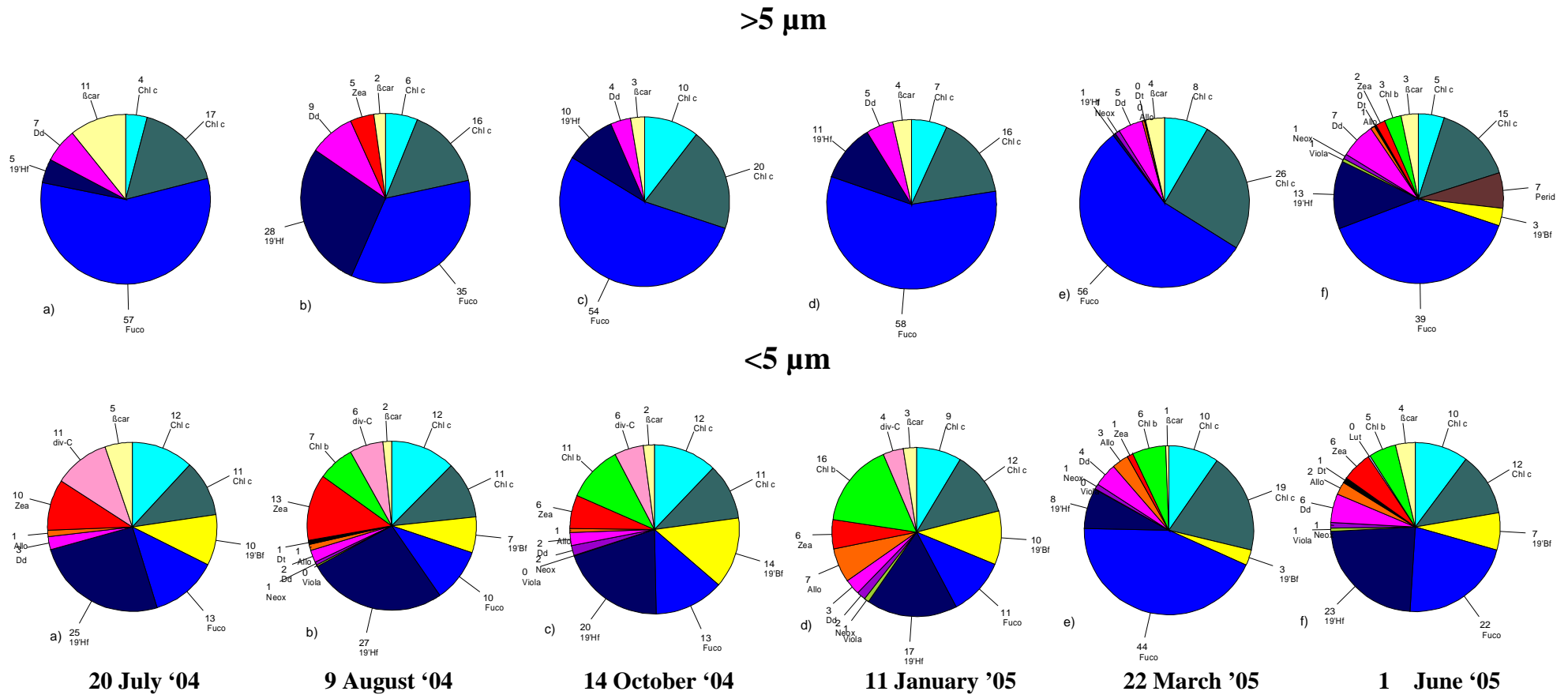


**Figure 4.25** – Average relative contribution of HPLC pigments (except Chl *a*) on 20 July 2004 (a), on 9 August 2004 (b), on 14 October 2004 (c), on 11 January 2005 (d), 22 March 2005 (e) and 1 June 2005 for the two sampling fraction, in the layer 20-40m at st. MC.

## 4.7 Discussion

The mean both TChl *a* ( $0.83 \pm 1.15 \text{ mg m}^{-3}$ ) and integrated daily primary production ( $1307 \pm 766 \text{ mg C m}^{-2} \text{ d}^{-1}$ ) values indicated the general mesotrophic conditions of the area.

On the other hand, they were within the ranges reported for this area in previous studies (Marino *et al.*, 1984; Scotto di Carlo *et al.* 1985; Modigh *et al.*, 1996; Zingone *et al.* 1995; Ribera d'Alcalà *et al.*, 2004). In particular during summer, these values were higher than those reported for the Western Mediterranean (Moutin and Raimbault, 2002) and similar to those of eutrophic coastal environments, such as the Northern Adriatic Sea (Mangoni *et al.*, 2004; Pugnetti *et al.*, in press).

The ultraphytoplankton accounted on average for ~50% of both phytoplankton biomass and primary production. So, it turned out a fundamental component of phytoplankton community, although seasonal differences in ultraphytoplankton contribution to total biomass were also evident. In terms of both chlorophyll *a* concentration and carbon assimilation rate, the highest values recorded during the sampling period were associated to the  $>5\mu\text{m}$  fraction. In fact, as showed in Fig. 4.26a, when TChl *a* increased, the  $>5\mu\text{m}$  fraction increased quite at the same level (slope = 0.80;  $r = 0.98$ ,  $P < 0.01$ ,  $n = 200$ ), while the ultraphytoplankton fraction also increased, but increased slower (slope = 0.23;  $r = 0.86$ ,  $P < 0.01$ ,  $n = 200$ ). This indicated that the mean percentage contribution of ultraphytoplankton to total phytoplankton biomass decreased significantly during bloom conditions.

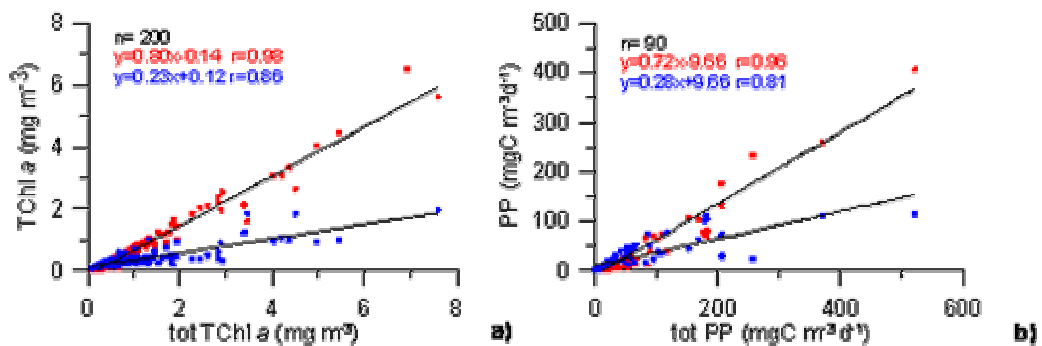


**Figure 4.26** – Correlation between total TChl *a* and TChl *a* of  $>5\mu\text{m}$  (●) and  $<5\mu\text{m}$  (●) fraction (a) and correlation between daily primary production total and of the  $>5\mu\text{m}$  (●) and  $<5\mu\text{m}$  (●) (b) at st. MC, for all the sampling depths.

In fact, ultraphytoplankton accounted for  $80 \pm 10.8\%$ , when tot TChl *a* concentration was lower than  $0.1 \text{ mg m}^{-3}$ , while the percentage decreased to  $23.7 \pm 13.4\%$  when tot TChl *a* concentration was higher than  $1 \text{ mg m}^{-3}$ .

The same relationship was found for the primary production measurements (Fig. 4.26b):  $>5\mu\text{m}$  fraction increased when total carbon assimilation increased (slope =0.72;  $r = 0.96$ ,  $P<0.05$ ,  $n=90$ ) on the contrary ultraphytoplankton did not change so much (slope =0.28;  $r = 0.81$ ,  $P<0.05$ ,  $n=90$ ).

These results were in agreement with the general trend described by Agawin *et al.* (2000) and Bell and Kalff (2001) for the picoplankton ( $<2\mu\text{m}$ ) on world data sets.

As reported in section 1.1.2, two main hypotheses have been proposed to explain the lower increase of small phytoplankton in area with high chlorophyll values: a) the faster up-take of large cells at high nutrient concentrations; b) the grazing pressure on small ones (Bell and Kalff, 2001).

During the bloom phases (tot TChl  $a > 1 \text{ mg m}^{-3}$ ) our results showed a mean ratio between carbon assimilation and biomass (P/B) quite similar in the two fractions (9.3 and 10.9  $\text{mg C (mg Chl } a)^{-1} \text{ h}^{-1}$  in the  $>5\mu\text{m}$  fraction and ultraphytoplankton respectively) in the surface layer. Though we did not performed estimate of phytoplankton growth rate, the P/B seems to indicate a virtually identical growth capacity. On the other hand, at surface a positive correlation between TChl  $a$  and microzooplankton cell number (Modigh personal communication) was found during the sampling period for both fractions ( $r = 0.72$ ,  $P<0.05$ ,  $n=42$  for ultraphytoplankton). In addition, studies on surface microzooplankton community at st. MC indicated that phytoplankton cells  $<10 \mu\text{m}$  are the favourite preys of microzooplankton groups (e.g. ciliate and tintinnids), and there is no lag in the time response of microzooplankton to variations in chlorophyll  $a$  concentration (Modigh 2001; Modigh and Castaldo, 2001). Although our data did not permit to exclude that the success of large phytoplankton cell was partially due to their faster growth capacity in responses to nutrient pulses, however they suggest a crucial role of microzooplankton grazing in controlling ultraphytoplankton growth. The impact of size-selective microzooplankton grazing on small cells was demonstrated in recent studied in different costal sites (Jochem 2003; Mousseau *et al.*, 1996). For the Mediterranean Sea an interesting study of Bec *et al.*, (2005) found that microzooplankton grazers removed on average 71% of picoplankton production throughout the year, suggesting a high transfer efficiency to higher trophic levels. In line with these observations and confirming the importance of grazing to define phytoplankton size structure are the results of simulations of an Evolutionary Nutrient-Phytoplankton-Zooplankton (ENPZ) model proposed by Jiang *et al.* (2005). They showed that increasing nutrient flux tends to increase phytoplankton cell size in the presence of phytoplankton-zooplankton coevolution, but have no effect in the absence of zooplankton.

The seasonal phytoplankton dynamics at st. MC was clearly influenced by the input of fresher waters with their load of nutrients, as demonstrated by the negative correlation of salinity with both biomass and primary production (Fig. 4.27). In particular, according with its lower increase compared with the total phytoplankton community, ultraphytoplankton, showed lower yet significant correlations with salinity ( $r = -0.62$ ,  $P < 0.01$ ,  $n = 198$  for the biomass and  $r = -0.69$ ,  $P < 0.01$ ,  $n = 90$  for primary production).

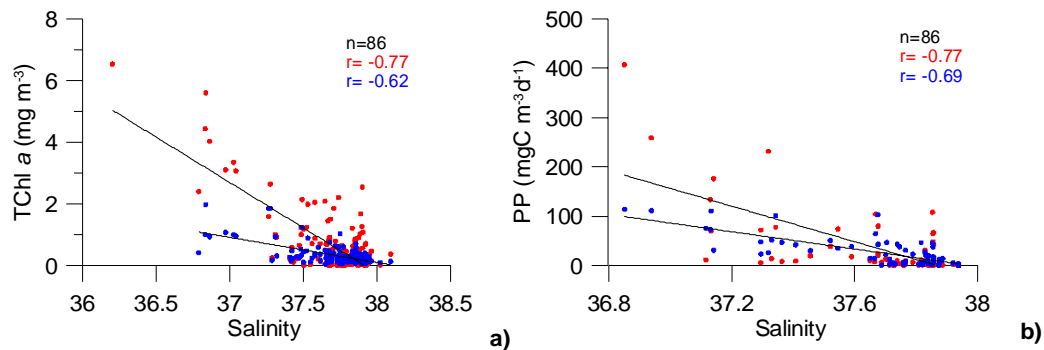


**Figure 4.27** – Correlation between TChl *a* of  $>5\mu\text{m}$  (●) and  $<5\mu\text{m}$  (●) fraction (a) and daily primary production and of the  $>5\mu\text{m}$  (●) and  $<5\mu\text{m}$  (●) (b) with salinity at st. MC.

As reported in the section 1.1.2, a positive correlation between small phytoplankton and temperature was found both for the Mediterranean Sea (Agawin *et al.*, 1998) and world data set (Agawin *et al.*, 2000). By contrast, our data did not show a positive correlation between ultraphytoplankton contribution and temperature. In our opinion, an explanation of this discrepancy is the presence at st. MC of episodic and variable arrivals of new nutrients even in summer. As a consequence warmer temperatures often do not coincide with low nutrients concentrations and, more in general, oligotrophic conditions; instead blooms may occur with a dominance of large cells. This hypothesis further highlights the importance of nutrients in organizing the phytoplankton community at st. MC.

To obtain a rough estimate of the frequency of sampling where nutrient concentrations may have controlled phytoplankton biomass, we calculated the number of samplings in which each nutrient was below a threshold chosen within the range of half saturation constants ( $K_s$ ) reported in literature (e.g. Goldman *et al.*, 1983, Ragueneau *et al.*, 2000). As a consequence of their terrestrial origin, the nutrient concentrations were only occasionally under the saturation level in the layer 0-10m, with the only exception of nitrates (51.0%) (Tab. 4.5).

On the other hand, TChl *a* of both studied fractions did not show direct significant correlations with the nutrients analyzed.

	<b>NO<sub>3</sub></b>	<b>NO<sub>2</sub></b>	<b>NH<sub>4</sub></b>	<b>PO<sub>4</sub></b>	<b>SiO<sub>4</sub></b>
<b>K<sub>s</sub></b>	<b>0.5</b>	<b>0.03</b>	<b>0.3</b>	<b>0.03</b>	<b>0.5</b>
<b>% Samplings (0-10m)</b>	<b>51.0</b>	<b>8.2</b>	<b>16.3</b>	<b>10.2</b>	<b>10.2</b>
<b>% Samplings (20-40m)</b>	<b>73.5</b>	<b>32.7</b>	<b>26.5</b>	<b>30.6</b>	<b>6.1</b>

**Table 4.5** - Half-saturation constant (K<sub>s</sub>) for phytoplankton uptake and percentage of sampling when depth integrated (0-10m and 20-40m) concentrations of each nutrient was lower than K<sub>s</sub>.

#### *Phytoplankton composition*

The seasonal cycle of phytoplankton biomass at st. MC was quite different from the “classical scheme” proposed for the temperate area, since it was characterized by four main “bloom” periods. We have just widely pointed out that the >5µm fraction was dominant in these conditions and that the pigment composition indicated Fuco as the main pigment of this fraction. On the other hand, the previous microscopic studies (Marino *et al.*, 1984, Zingone *et al.*, 1990) indicated that diatoms were the dominant group of these blooms. Hence, using a Fuco/Chl *a* ratio of 0.75, chosen within the range reported in literature (e.g. Schlüter *et al.*, 2000; Ansotegui *et al.*, 2003; Rodriguez *et al.*, 2003) we estimated roughly the diatoms contribution to total biomass (TChl *a*) during blooming conditions. The results showed that this group may account for >80% of TChl *a*.

However, the composition of large phytoplankton at st. MC has been widely explored and to date well known (Marino *et al.*, 1984, Scotto di Carlo *et al.*, 1985; Zingone *et al.*, 1990; Zingone *et al.*, 1995; Ribera d’Alcalà *et al.*, 2004) while it is more interesting to explore the composition, even for main groups, of ultraphytoplankton fraction, trying to single out possible patterns of occurrence. In particular, one of the aims of this project was to determine the role of small eukaryotes within the ultraphytoplankton community. So, in order to estimate the contribution of small eukaryotes to ultraphytoplankton TChl *a*, we considered the prokaryote proportion as the sum of div-Chl *a*- and Chl *a*<sub>syn</sub>- containing microalgae. Chl *a*<sub>syn</sub> was calculated using a Chl *a*/Zea<sub>syn</sub> ratio of 1.65 according to Kana *et al.*, (1988), Morel *et al.*, (1993) and Marty *et al.*, (2002).

Then, we calculated the eukaryote proportion by the difference between TChl *a* and prokaryote Chl *a*, as suggested by Marty *et al.*, (2002).

The eukaryotes accounted on average for  $84.1 \pm 11.0\%$  of the ultraphytoplankton biomass, ranging between 35.42% and 98.6%. The minimum value was recorded at 40m on 13 July 2004, while the maximum at 10m on 22 March 2005 (Fig. 4.28). Clearly the highest values were recorded during blooming conditions, while the prokaryotes proportion was more important in the “oligotrophic” ones, such as summer. In particular, the percentage of prokaryotes decreased at higher nitrate concentration as showed in Fig. 4.29. This relationship highlights that prokaryotes more than eukaryotes are favoured at low nutrient concentrations, probably due to a higher efficiency in nutrient uptake.

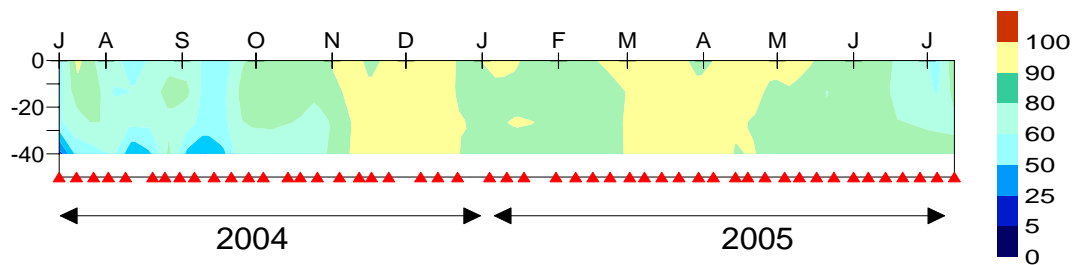


**Figure 4.28** – Percentage of eukaryote contribution to ultraphytoplankton TChl *a*, at st. MC during the sampling period.

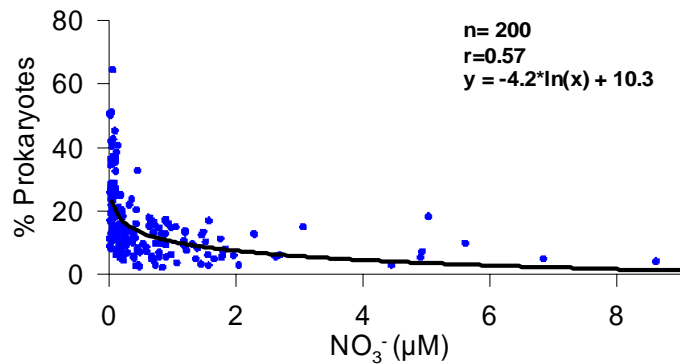


**Figure 4.29** – Relationship between percentage of prokaryotes contribution to ultraphytoplankton TChl *a* and nitrate concentration, at st. MC, during the sampling period.

Secondly, in order to estimate roughly the contribution of main groups to ultraphytoplankton TChl *a*, we used diagnostic pigment/Chl *a* ratios, chosen within the range reported in literature (Ansotegui *et al.*, 2003; Rodriguez *et al.*, 2003).

In particular, we calculated the Cyanobacteria and Prochlorophytes contributions as previous described. The cryptophytes, the Perid-containing dinoflagellates, the prasinophytes and the all green algae contribution were calculated using the following ratio:

Allo/Chl  $a = 0.19$ ; Perid/Chl  $a = 0.32$  Prasino/Chl  $a = 0.20$ , Chl  $b$ /Chl  $a = 0.84$ .

The green algae Chl  $a$  contribution, except the prasinophytes, was calculated by the difference between all green algae and prasinophytes.

Since the difficulty of recognize a precise rule in 19Bf, 19'Hf and Fuco distribution within diatoms, prymnesiophytes and pelagophytes (see section 2.1.2) we simply calculated the contribution of these golden-brown algae by the difference between TChl  $a$  and the sum of all the other groups. Although the results are clearly a simplification, some interesting feature in ultraphytoplankton seasonal dynamic emerged (Fig. 4.30).

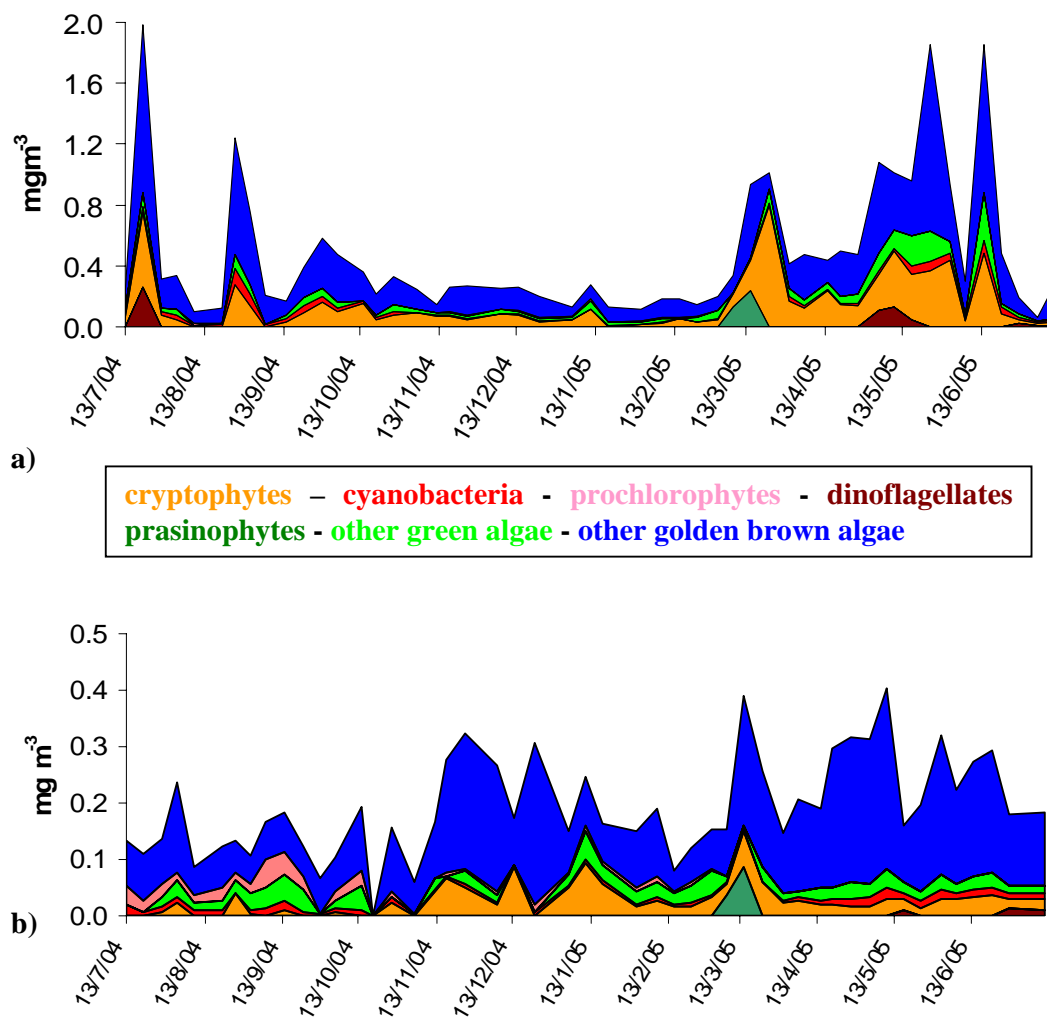


**Figure 4.30** – Main algae groups contribution to ultraphytoplankton TChl  $a$  at surface (a) and at 40m (b), at st. MC during the sampling period.

During the sampling period a first peak was recorded on 20 July 2004, confined to the layer 0-10m. The lateral transport of nutrients from land was one of the mechanisms invoked to

explain these summer blooms (Modigh *et al.*, 1985; Zingone *et al.*, 1990). At surface, ultraphytoplankton fraction (accounting for only 20% of TChl *a*) was made up mainly of golden-brown algae (55%) and cryptophytes (25%), while the contributes of Cyanobacteria and prochlorophytes were inconsistent. In particular, div-Chl *a* was never recorded under high TChl *a* concentrations ( $>1 \text{ mg m}^{-3}$ ), according with the results of other areas (Gibb *et al.*, 2000; Marty *et al.*, 2002). By contrast, these two groups became more important at 40m. Excluding these episodic events, the TChl *a* in summer was low and ultraphytoplankton dominant (on average  $75.2 \pm 18.1\%$  of the total TChl *a*). The composition of this fraction was quite similar trough the water column. The other golden brown algae remained the most important group, accounting on average for  $>50\%$ , while cyanobacteria and prochlorophytes were the other components. As just showed in Fig. 4.20 and 4.21 cyanobacteria ( $Zea_{syn}$ ) and prochlorophytes (div-Chl *a*) presented an opposite distribution in summer. In fact, the prochlorophytes were almost all absent in the surface layer, while they accounted on average for  $10 \pm 8\%$  of the ultraphytoplankton TChl *a* in the layer 20-40m. On the other hand, the contribution of cyanobacteria to TChl *a*, was on average  $22.2 \pm 10.3\%$  and slight decrease in the 20-40m layer. A similar pattern of occurrence with cyanobacteria at surface and prochlorophytes placed deeper was reported in the Gulf of Naples by Casotti *et al.*, (2000) and also in other different ecological contexts (Ting *et al.*, 2002; Worden *et al.*, 2004) (see section 1.1.2). This distribution is partially explained by the higher sensitivity of prochlorophytes to UV radiations, as Sommaruga *et al.*, (2005) demonstrated with a series of short experiments on picoplankton population of Mediterranean coastal waters. Furthermore, our data were within the range of prochlorophytes contribution to phytoplankton biomass reported in the Western Mediterranean (Bustillos-Guzman *et al.*, 1995; Barlow *et al.*, 1997; Marty *et al.*, 2002).

The match between stable meteorological conditions (the so called “St. Martin’s summer”) and nutrient made available by seasonal rains and consequent runoff would be responsible for biomass increase in autumn (Zingone *et al.*, 1995), as observed on 14 October 2004. Again the thickness of the layer involved in the bloom depended on water column stratification. Some differences were noticed in the ultraphytoplankton compared with the summer blooms. At first the biomass increase of this fraction was less pronounced and a change there was in the composition: cryptophytes accounted alone for  $\sim 40\%$  of ultraphytoplankton biomass at surface, while the other golden-brown algae made up the remaining part. These data were partially in agreement with the results of Zingone *et al.*

(1995), which showed the presence of small flagellates (<10µm) and coccolithophorids in the Gulf of Naples in autumn blooms. On the other hand, the autumnal peak of small cryptophytes was unknown.

Except the peaks episodes, in autumn the values of TChl *a* and the average ultraphytoplankton composition were very similar to that found in “oligotrophic” summer conditions through the whole 0-40m layer.

In winter, the lowest biomass (mean  $0.29 \pm 0.11 \text{ mg m}^{-3}$ ) and primary production (mean  $405.7 \pm 255.6 \text{ mg C m}^{-2} \text{ d}^{-1}$ ) values were recorded, in relation to both weather conditions (low light availability) and structure of the water column (deep mixed layer). Hence, ultraphytoplankton accounted for  $67.0 \pm 10.6\%$  of the total biomass. According with the homogeneity of the water column no significant differences were recorded in the ultraphytoplankton composition of the whole 0-40m layer and a high diversity was found: green algae, except prasinophytes (not detected), accounted for ~ 20 % of the TChl *a*, while the cryptophytes contributed to ~ 25%. Instead, the contribution of cyanobacteria and prochlorophytes decreased in winter, accounting for ~ 8% and 4% of the TChl *a* respectively. However, in this season the prochlorophytes were recorded also at surface, in relation to the homogeneity of the water column. The winter presence of prochlorophytes in coastal site was previously recorded by Vaultot *et al.*, (1990) and seems a recurrent feature in the Mediterranean distribution of this group (Marty *et al.*, 2002). Also the other golden-brown algae in winter were less important, especially in the 20-40m layer.

A late winter-early spring (March 2005) biomass increase, involving almost all the 0-40m layer, was recorded. This occurred later as compared to the phytoplankton growth phase preceding the spring stratification which is a recurrent feature at MC site (Ribera d’Alcalà *et al.*, 2004) as well as other sites of the Mediterranean Sea coasts (Mura *et al.*, 1996; Caroppo *et al.*, 1999; Psarra *et al.*, 2000).

The golden-brown algae were the most important group in the ultraphytoplankton fraction. Cryptophytes accounted for 40% of the TChl *a*. These data were in agreement with the previous studied on cryptophytes carried out at st. MC, which indicated peaks of this group in early spring-summer (Cerino, 2004). Small green algae accounted for ~13% of TChl *a* in this fraction. Furthermore, as showed in the results (section 4.6) only in March the Prasi, marker of Prasinophyceae was recorded. Small amounts of some carotenoides of uriolide serie, generally found in the order *Mamiellales*, which included the specie *Micromonas pusilla* (Egeland and Liaaen-Jensen, 1995; Egeland *et al.*, 1995), were always associated to

Prasino. Since peaks of *M. pusilla* were frequently recorded at st. MC in this period (Zingone *et al.*, 1999a), we determine the *M. pusilla* contribution using a Prasino/Chl *a* ratio of 0.20 (derived from our cultures). On 8 March 2005, *M. pusilla* accounted for 30% of the TChl *a* at surface and for 25% at 40m. These value is considerable lower that the values (>50% of total phytoplankton biomass) calculated based on MPN counts (Thronsen & Zingone, 1994). This difference could be due to the different method used or to a different dynamics of *M. pusilla* in the two years under investigation (1990 vs 2005). However, these results confirms that *M. pusilla* can play a key role in the ecology of coastal waters, as revealed by studied in other areas (Not *et al.*, 20004, 2005). The prochlorophytes practically disappeared with this bloom and remained undetected until the summer.

The last bloom period (tot TChl *a* =  $2.4 \pm 1.5 \text{ mg m}^{-3}$ ) was recorded in late spring-early summer (May and June 2005), probably in relation with the load of nutrients of terrestrial origin. The duration of this bloom was probably related to a continuous arrival of newland inputs. The thickness of water column involved became thinner as the thermal stratification proceeded. Again, the cryptophytes and the other golden-brown algae were the most important ultraphytoplankton groups at surface (Fig. 4.29a). In May also dinoflagellates and green algae, except prasinophytes were present, accounted for ~6% and 10% respectively.

Summarizing, ultraphytoplankton results a structural elements of phytoplankton community of coastal areas, even in sites subjected to important land run-off as the case of st. MC. Its lower contribution during bloom periods seems related more to the grazing control than to a less productivity capacity.

On the other hand, small eukaryotes are the dominant part of ultraphytoplankton. We may hypothesize that these small eukaryotes are more competitive in exploiting the episodic arrivals of new nutrients as compared to prokaryotes. Further, the eukaryotes may have a more adaptable photosynthetic apparatus (e.g. xanthophylls cycle), which is more successful in a water column subjected to alternation between stratification and mixing (e.g. in spring and autumn) as it will point out in the chapter VI.

The ultraphytoplankton fraction showed a higher diversity than the >5 $\mu\text{m}$  fraction. In fact, it presented almost the main diagnostic pigments (especially in the layer 20-40m and in the oligotrophic period), while in the other fraction the Fuco was by far the dominant pigment. On one hand, this richness may be related to a complex and stable community based on

microbial loop, on the other one the changes in light quality and intensity at depth may create new niches requiring different pigment assemblage (e.g. capacity of use blue light).

On a methodological point of view, the use of fractionated pigments HPLC method turned out to be a good and rapid tool to outline the phytoplankton assemblage of smallest size class. For instance, it has been possible to exploit the fundamental contribution of cryptophytes to this fraction at different moments of the seasonal cycle.

On the other hand, the HPLC remains quite inadequate to explore and correctly separate the high diversity of diatoms and prymnesiophytes. The situation found at Mc on 20 July 2004 was clarifying: the Fuco accounted for the 40% of total ultraphytoplankton pigment at surface, while the 19'Hf for the 9%; but the microscopic analysis showed a large numbers of small flagellates and no diatoms (Sarno, personal communication). Hence, these results suggested the presence of small flagellates containing as main carotenoid Fucoxanthin rather than 19'Hf. Alternatively, as proposed by Not *et al.*, (2005), the high Fuco values found in the ultraphytoplankton fraction could be partially due to cell debris, induced by zooplankton grazing. Actually, during the bloom recorded on 20 July 2004, high levels of phaeophorbides, which are known to be a marker of grazing activity, were detected in the surface layer.

Further, the application of size-fractionated HPLC has highlighted that the use of pigments as size indicators can imply significant errors in the estimate of size-classes contribution, since they are generally not confined in a specific size-class. Indeed, ~ 60% of total Fucoxanthin was found in the ultraphytoplankton fraction in the 20-40m layer, in contrast with its common use (Gibb *et al.*, 2000) as a marker of microphytoplankton (cells >20µm).

Being able to improve HPLC techniques and realizing comparing studied with other methods, such as the use of molecular marker is a very deliverable achievement of modern oceanography.

## CHAPTER 5

### Circadian Patterns in Natural Ultraphytoplankton Populations

In order to test the occurrence and the characteristics of circadian patterns in photophysiological parameters of natural ultraphytoplankton populations, three *in situ* experiments were carried out in different ecological contexts (Fig. 5.1). The first experiment was carried out in a coastal site in spring (TRI-1), the second in an oligotrophic area in late summer (TRI-2) and the third in a Mediterranean lagoon in early summer (TRI-3). In all three experiments the percentage of ultraphytoplankton (fraction  $< 5\mu\text{m}$ ) was  $\geq 90\%$  of total biomass. The most relevant results are presented in the following sections, while the sampling and analytical procedures were reported in the Chapter III.

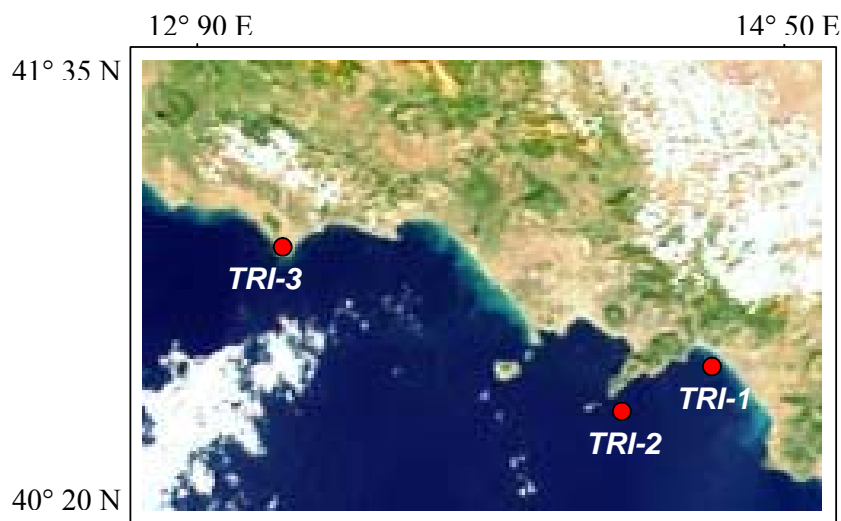


**Figure 5.1** – Location of sampling stations of the three TRI experiments.

#### 5.1 TRI 1

The first experiment TRICICLO 1 (**TRI-1**) was carried out from 9:00 AM of 22 April to 9:00 AM of 23 April 2004, on board the ship “Coopernaut Franca”, in coastal waters of the Gulf of Salerno (South Tyrrhenian Sea); the sampling station (Lat.  $40^{\circ} 33.95$  N, Long.  $14^{\circ} 47.83$  E) was 70 meters deep. The weather was clear and sunny throughout the period of investigation. The natural light:dark cycle was 14:10 and the maximum incident irradiance was  $1690 \mu\text{mol photons m}^{-2} \text{s}^{-1}$  recorded at 1:00 PM (local time).

Water samples were taken from two depths: 5 and 42 meters. The choice of the sampling depths was aimed at studying the effect of sun light on populations exposed to very different irradiance: ca 30% of the solar incident PAR at 5m (ranging between 0 and 450  $\mu\text{mol photons m}^{-2}\text{s}^{-1}$ ) and ca 1% at 42m (ranging between 0 and 15  $\mu\text{mol photons m}^{-2}\text{s}^{-1}$ ). The sampling strategy and the parameters recorded are reported in Tab. 5.1.

Parameters	Sampling Depth	Sampling interval
Incident solar irradiance (PAR)	surface	5min over 24h
Underwater irradiance (PAR)	0-50 m (profile)	2h
CTD parameters	0-50 m (profile)	2h
Nutrients	5 and 42m	6h
Pigment composition (HPLC)	5 and 42 m	2h
Fractionated HPLC (< and > 5 $\mu\text{m}$ )	5 and 42 m	4h
Spectrofluorometric Chl <i>a</i> (< and > 5 $\mu\text{m}$ )	5 and 42 m	6h
In-vivo fluorescence -FRRF	5 and 42 m	2h
In-vivo fluorescence –Phyto-PAM	5 and 42 m	2h
Pvs.E curves	5 and 42m	6h

**Table 5.1** – Sampling strategy during TRI 1 experiment.

### 5.1.1 Physical parameters

The water column showed a typical spring condition with an initial stratification in the first meters (average  $\Delta\sigma = 0.13$  at 5m). The lowest values of density recorded in the afternoon were due to an increase in temperature in the upper layer of the water column.

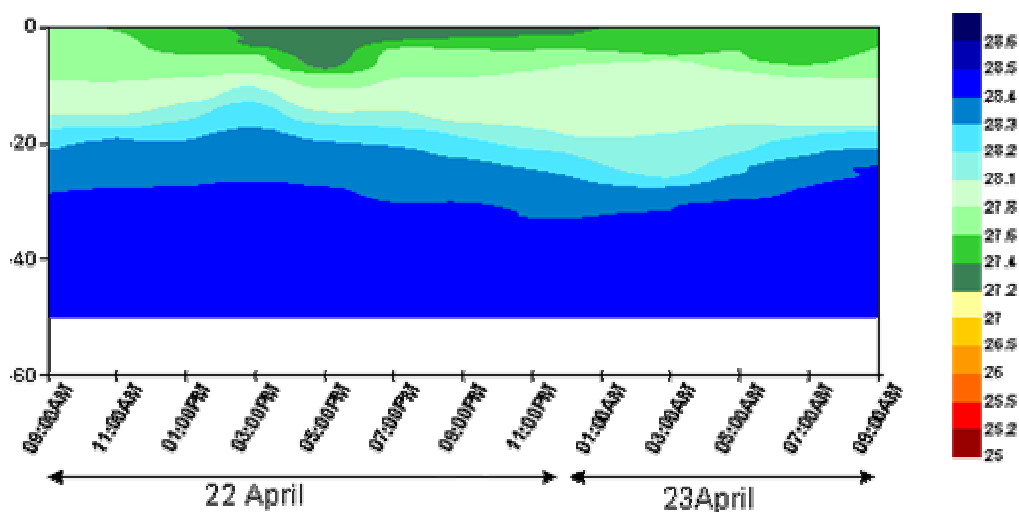


**Figure 5.2** – Variations in density ( $\sigma_t$ ) over the 24h of the TRI-1 experiment.

The resolution of nutrient sampling during the TRI-1 experiment did not allow to test for the presence of circadian patterns in nutrient concentrations. However, it is important to note that  $\text{NO}_3+\text{NO}_2$  and  $\text{PO}_4^-$  concentrations were never limiting at the two sampling depths (Fig. 5.3).

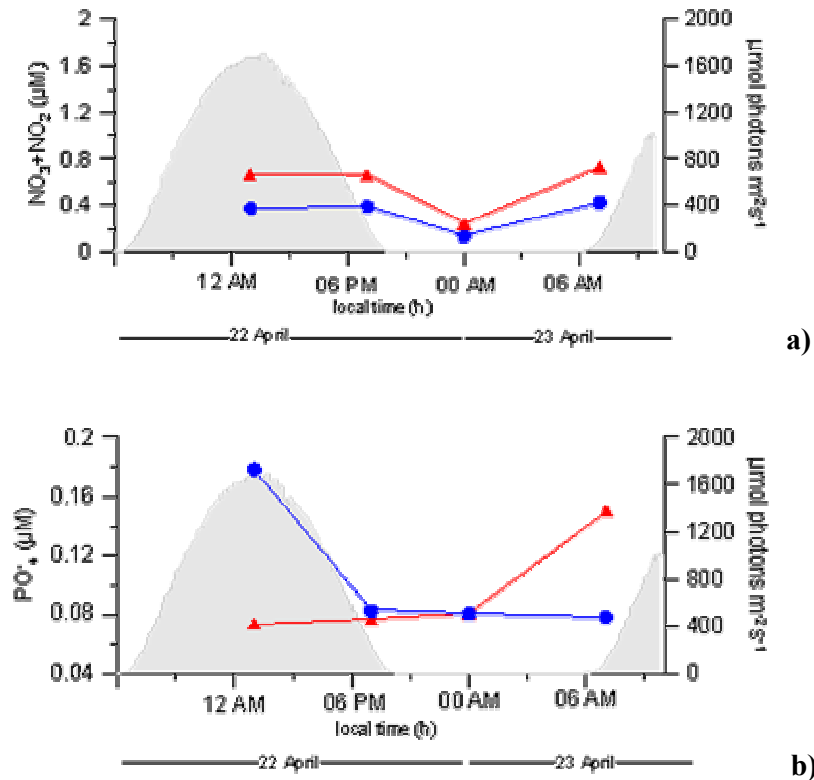


**Figure 5.3** – Variations in incident solar irradiance (grey area),  $\text{NO}_3+\text{NO}_2$  concentration (a) and  $\text{PO}_4^-$  concentration (b) at 5m (●) and at 42m (▲) over the 24h of the TRI-1 experiment.

### 5.1.2 Pigments

Total TChl *a* concentrations were similar at the two sampling depths; the mean value was  $0.26 \text{ mg m}^{-3}$  at 5m and  $0.27 \text{ mg m}^{-3}$  at 42m. The ultraphytoplankton fraction ( $< 5\mu\text{m}$ ) accounted for  $\approx 90\%$  of total biomass in both cases.

Golden-brown algae dominated the ultraphytoplankton as well as the  $> 5\mu\text{m}$  fractions at both sampling depths as shown by the pigment spectra (Fig. 5.4). Moreover, the same pigments were recorded at surface and at depth for the ultraphytoplankton fraction suggesting a similar algal assemblage.

In particular, the 19'Hf-containing algae were the most abundant ultraphytoplankton group (average 19'Hf=25% at 5m and 30% at 42m), followed by 19'Bf-containing (average 19'Bf=10% at 5m and 13% at 42m) and Fuco-containing (average Fuco=8% at both 5m and

42m). The average value of Zea (8% and 7% at 5m and 42m respectively) revealed the presence of cyanobacteria, while prochlorophytes were not detected. Finally, Allo (5% at 5m and 1% at 42m) and Chl *b* (5% at 5m and 7% at 42m) indicated the presence of cryptophytes and small green algae, respectively.

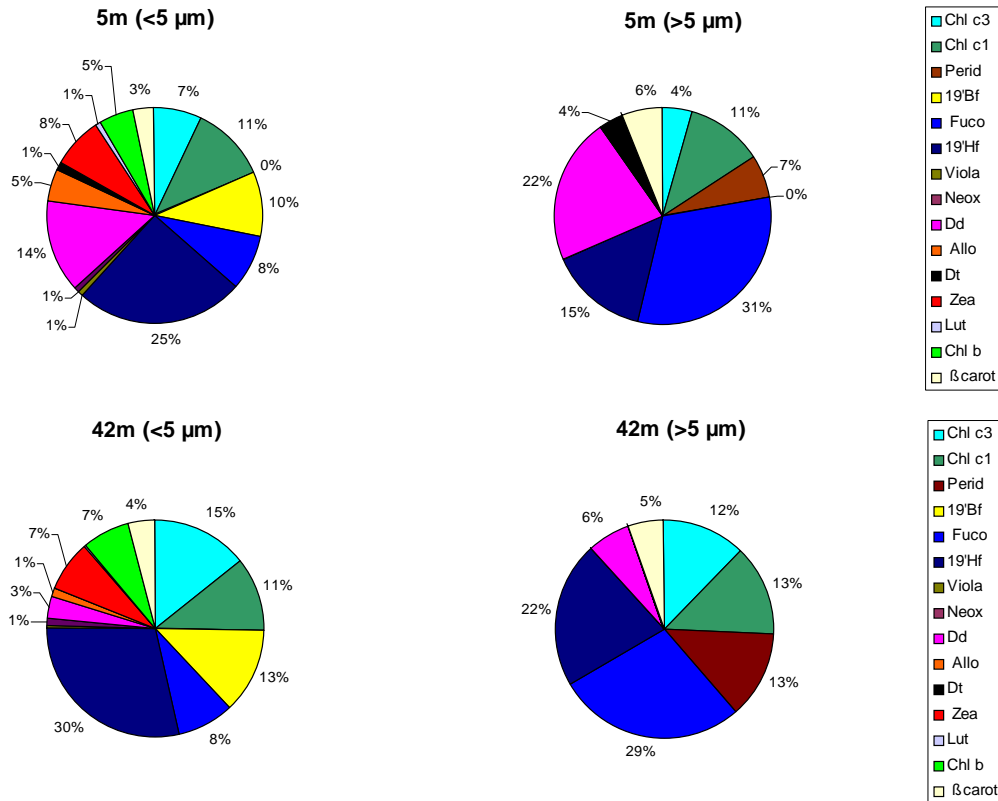


**Figure 5.4** – Average contribution of HPLC pigments (except Chl *a*) at the two sampling depths during the TRI-1 experiment.

On the other hand, the pigment composition of the > 5μm fraction (ca 10% of total biomass) was slight different at the two sampling depths. Fuco containing algae dominated at 5m (average Fuco=31%) followed by 19'Hf containing (average 19'Hf=15%), and dinoflagellates (average Perid=7%). At 42m, Fuco containing algae were still the most abundant phytoplankton group (average Fuco=29%), but as compared to the surface layer, the contribution of 19'Hf containing algae (average 19'Hf=22%), and of dinoflagellates (average Perid=7%) was higher; crysophytes and the green algae were practically absent.

The results presented in Fig. 5.5 and 5.6 refer to the entire phytoplankton population (TChl *a*, as the sum of the ultraphytoplankton and the >5μm fractions); the ultraphytoplankton fraction always accounted for ≈90% of total chlorophyll a concentrations.

Only minor variations occurred in TChl *a* concentration (Chl *a*+div-Chl *a*) at both sampling depths over the diel cycle, from 0.17 to 0.36 mg m<sup>-3</sup> at 5m and from 0.23 to 0.31 mg m<sup>-3</sup> at 42 m (Fig. 5.5). In addition, the ratios between the major accessory pigment and chlorophyll *a* did not show any clear pattern of variation during the 24h experiment (data not shown).

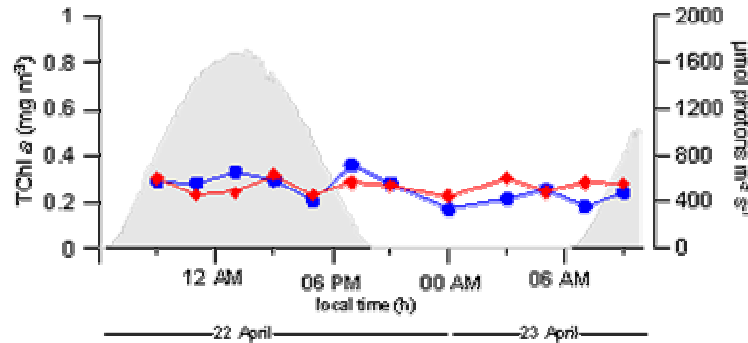


**Figure 5.5** – Incident solar irradiance (grey area), and Chl *a* concentration at 5m (●) and at 42m (▲) over the 24h of the TRI-1 experiment.

As expected, differences between the surface and the deep populations occurred in the ratio between photoprotective and photosynthetic carotenoids (PPC/PSP). Higher PPC/PSP ratio was recorded at 5m from 8:00AM to 12:00 AM and thereafter slightly lower values were recorded, while an invariably low ratio occurred at 42m (Fig.5.6a). In addition, the contribution of Diadinoxanthin (Fig.5.4) was higher at surface (on average 14% for the ultraphytoplankton fraction) than at 42m (3%).

Furthermore, the evolution in time of the Dt/Dd+Dt ratio showed a clear circadian pattern (Fig. 5.6b). This ratio provides information on the photoacclimation of phytoplankton populations, since it indicates de-epoxidation state of the xanthophylls. In particular, at 5m, the maximum value (0.44) was recorded at 10.00 AM, and the minimum (0.001) at 5.00 AM, just before dawn. Again, at 42m the Dt/Dd+Dt ratio did not show any significant variability; very small amounts of Dt were detected only around midday.

No particular pattern of variation could be found for the other photoprotective pigments, such as β-carotene (data not shown).

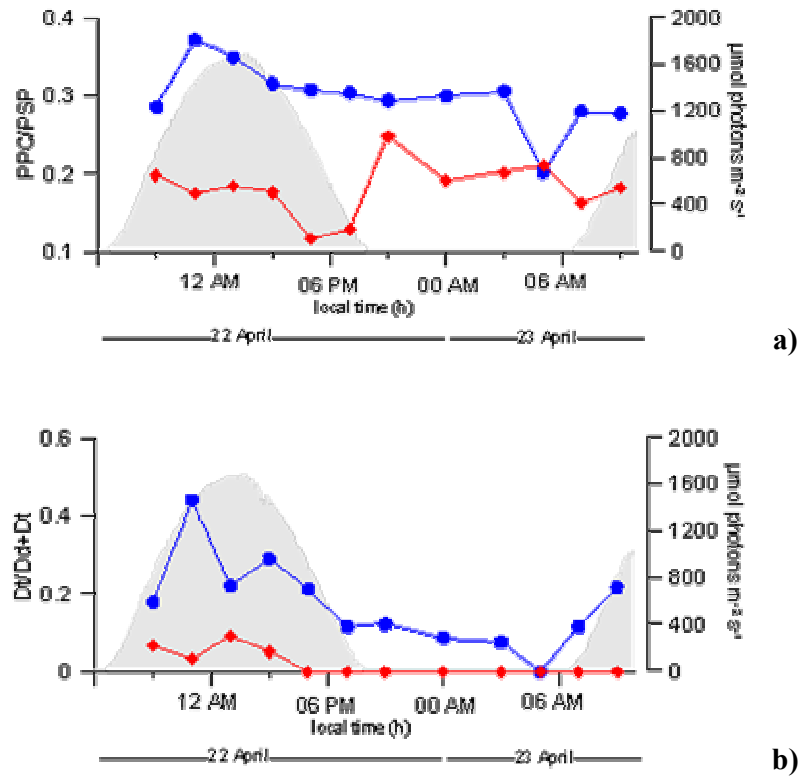
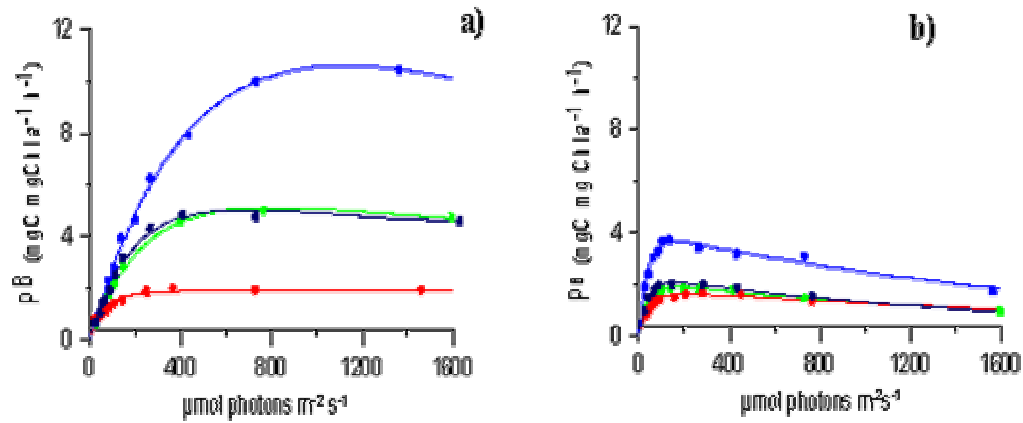


**Figure 5.6** – Incident solar irradiance (grey area), PPC/PSP ratio (a) and Dt/Dd+Dt ratio (b) at 5m (●) and at 42m (▲) over the 24h of the TRI-1 experiment.

### 5.1.3 $P_{vs.E}$ parameters

$P_{vs.E}$  experiments were performed on both surface and deep populations four times during the TRI-1: dawn, midday, dusk, night (Table 5.1). The coarse resolution of the  $P_{vs.E}$  measurements did not allow for a detailed reconstruction of the circadian variability, even though some interesting features emerged.

The curves constructed for the two sampling depths displayed clear differences as related to the different light history of the two populations (fig.5.7). In particular, the photosynthetic capacity ( $P_{max}^B$ ) was higher at surface than at depth, while the opposite occurred for the photosynthetic efficiency ( $\alpha^B$ ) that was higher at depth.



5m	$P^B_{\max}$	$\alpha^B$	$E_k$	42m	$P^B_{\max}$	$\alpha^B$	$E_k$
1:00 PM	10.6	0.031	343	1:00 PM	3.7	0.096	38
7:00 PM	5.1	0.026	198	7:00 PM	1.9	0.049	39
0:00 AM	1.9	0.027	70	0:00 AM	1.6	0.035	47
7:00 AM	5.0	0.031	162	7:00 AM	2.1	0.055	37

**Figure 5.7** –  $P_{vs.E}$  curves and photosynthetic parameters at 5m (a) and 42m (b) during the TRI-1 experiment.

On the other hand, the evolution in time of  $P^B_{\max}$  was similar in the two populations: highest values occurred at midday, lowest at night and intermediate as well as practically identical values were recorded at dawn and dusk (Fig. 5.8a). However, the amplitude of  $P^B_{\max}$  variations was considerably higher at surface ranging from 10.6 to 1.9 mgC mgChl  $a^{-1} h^{-1}$  than at depth where  $P^B_{\max}$  varied between 3.7 and 1.6 mg C mg Chl  $a^{-1} h^{-1}$ .

The photosynthetic efficiency ( $\alpha^B$ ) did not show any circadian pattern at 5m, while at 42m higher values occurred during daytime as compared to the evening and night (Fig. 5.8b).

The photoacclimation index ( $E_k$ ) showed the same diel pattern of variation as  $P^B_{\max}$  at 5m, while  $E_k$  was fairly constant at depth (Fig. 5.8c).

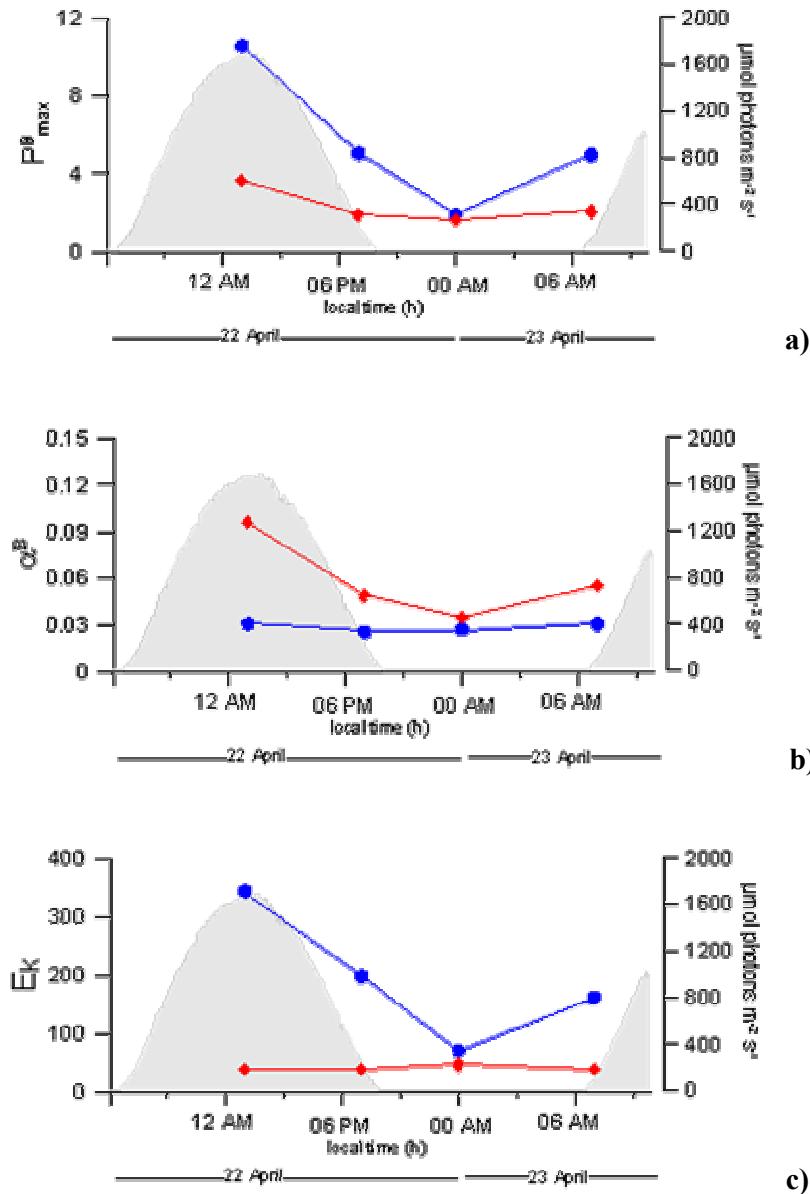


**Figure 5.8** - Incident solar irradiance (grey area),  $P^B_{max}$  (a),  $\alpha^B$  (b) and  $E_k$  (c) at 5m (●) and at 42m (▲) over the 24h of the TRI-1 experiment.

#### 5.1.4 Phyto-PAM coefficients

The evolution in time of the photosynthetic coefficients as derived from the Phyto-PAM measurements at the two sampling depths are reported in Fig. 5.9.

As already reported for the PvsE experiments, all the Phyto-PAM coefficients displayed higher variability at 5m as compared to the 42m samples. In particular,  $rETR_{max}$  values (Fig. 5.9a) were higher during daytime (maximum  $60.6 \mu\text{mol e}^{-} \text{m}^{-2} \text{s}^{-1}$  at 7:00 AM of 23 April) and decreased during the night (minimum  $11.9 \mu\text{mol e}^{-} \text{m}^{-2} \text{s}^{-1}$  at 03:00 AM of 23 April) in the surface layer.

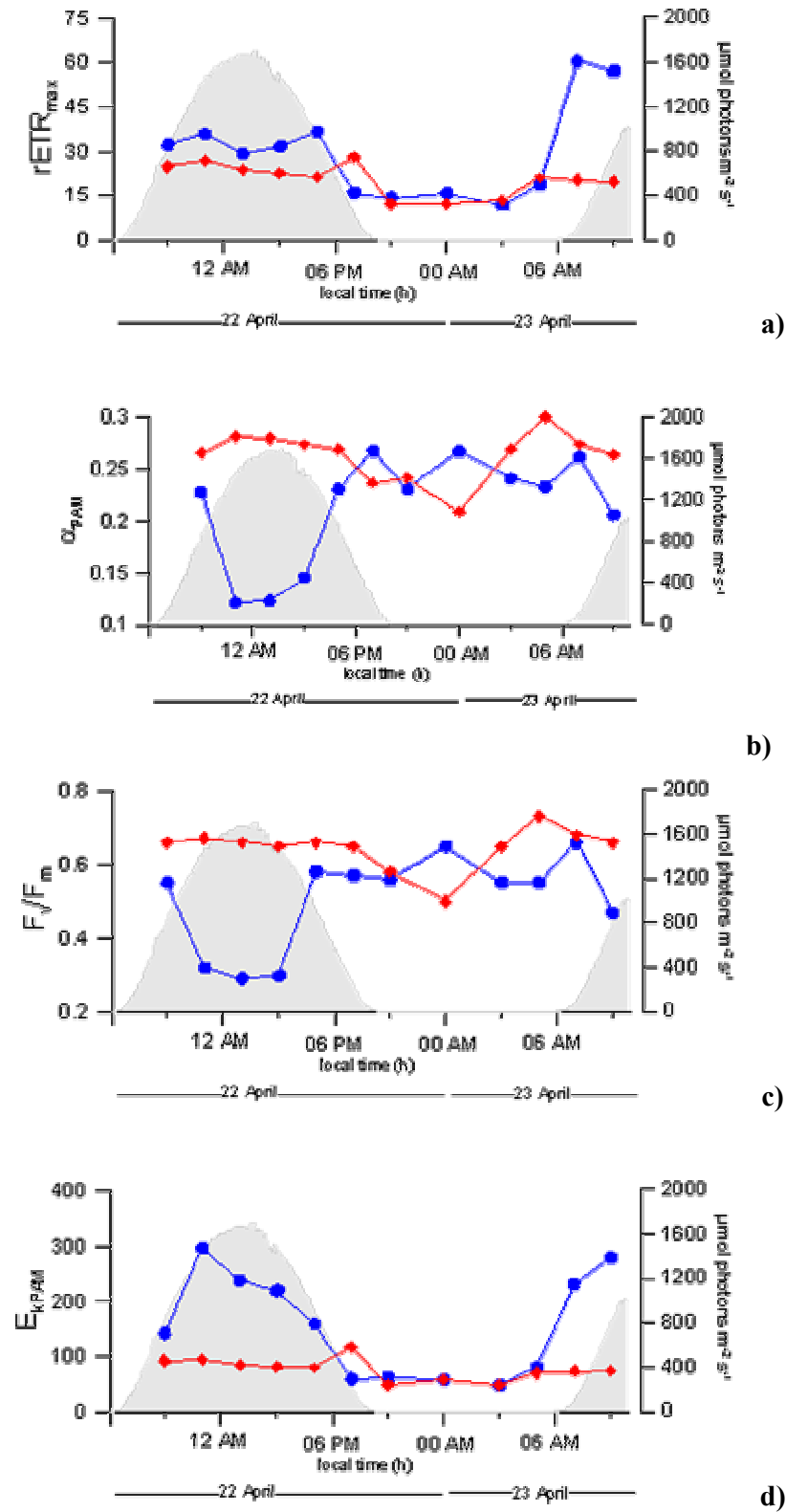


**Figure 5.9** – Incident solar irradiance (grey area),  $rETR_{\text{max}}$  (a),  $\alpha_{\text{PAM}}$  (b),  $F_v/F_m$  (c) and  $E_{k\text{PAM}}$  (d) at 5m (●) and at 42m (▲) over the 24h of the TRI-1 experiment.

The pattern was the same for the sample at 42m, but the amplitude of variation was less pronounced, ranging between 26.9 and 19.1  $\mu\text{mol e}^- \text{m}^{-2} \text{s}^{-1}$ .

In contrast,  $\alpha_{\text{PAM}}$  and  $F_v/F_m$  (Fig. 5.9b,c) showed minimum values at maximum sun irradiance and the maxima at night in the surface layer, while the opposite was found for the samples at 42m.

As in the case of the  $P_{\text{vs.E}}$  parameters, the  $E_{\text{kPAM}}$  (Fig. 5.9d) followed the time distribution of  $r\text{ETR}_{\text{max}}$  ranging between 296 and 49  $\mu\text{mol photons m}^{-2} \text{s}^{-1}$  at 5m and between 50 and 100  $\mu\text{mol photons m}^{-2} \text{s}^{-1}$  at 42m.

### 5.1.5 FRRF parameters

*In vivo* fluorescence measurements were performed also *in situ* with a Fast Repetition Rate Fluorometer (FRRF) at both sampling depths. Unfortunately, data are available only until 00:00 AM of 23 April, due to a technical problem that occurred during the recordings.

However, variations in time of  $F_v/F_m$  were similar to that observed with Phyto-PAM: a daylight depression, though less marked, was recorded at 5m and no diel pattern could be described at 42m (fig. 5.10a).

The absorption cross-section of PSII ( $\sigma_{\text{PSII}}$ ) displayed a diurnal depression and higher values during the night at both sampling depths, but the pattern was more evident in surface sample: the lowest value ( $645 \text{ m}^{-2} \text{s}^{-1}$ ) occurred under maximum irradiance, while the highest value ( $755 \text{ m}^{-2} \text{s}^{-1}$ ) was recorded at midnight (Fig. 5.10b). This pattern was to a certain extent in phase with  $\alpha_{\text{PAM}}$  and  $F_v/F_m$ , suggesting that the energy dissipation of excess light involved also the light harvesting complexes.

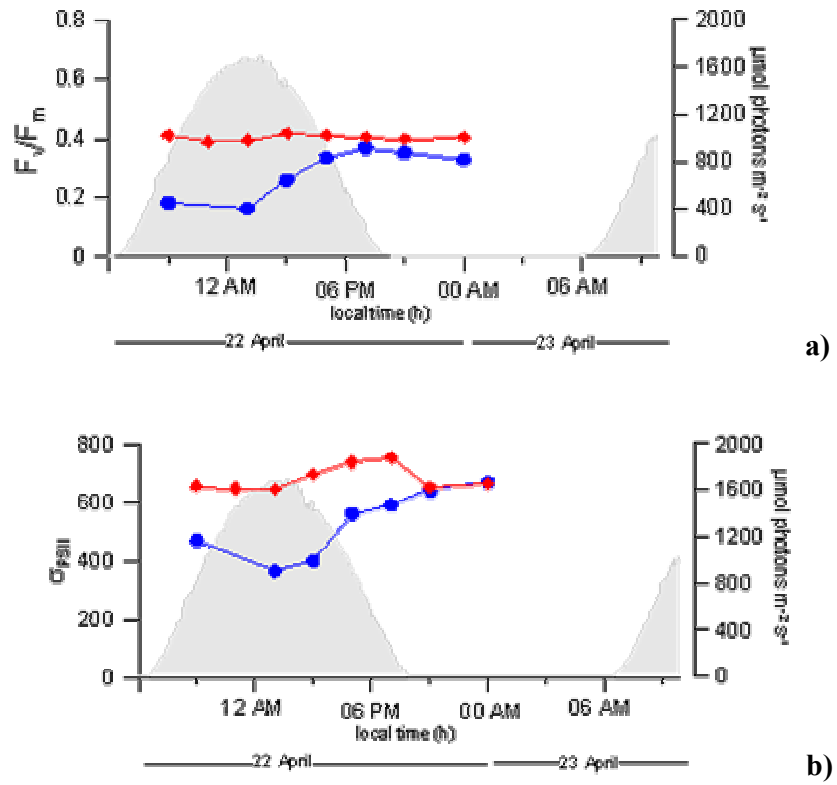


**Figure 5.10** – Incident solar irradiance (grey area),  $F_v/F_m$  (a) and  $\sigma_{PSII}$  (b) at 5m ( $\bullet$ ) and at 42m ( $\blacktriangle$ ) over the 24h of the TRI-1 experiment.

## 5.2 TRI 2

The second experiment, **TRI-2**, was carried out from 9:00 PM of August 3 to 9:00 PM of August 4, 2004, on board the ship “Urania”, in the Gulf of Naples (South Tyrrhenian Sea) (Lat. 40° 29'.52 N Long. 14°17'.01 E). The sampling station, 2000 meters depth, was located in offshore waters. The weather was clear and sunny; the natural light:dark cycle was 15:9 and the maximum incident irradiance, 1880  $\mu\text{mol photons m}^{-2} \text{s}^{-1}$ , was recorded at 1:30 PM (local time).

Water samples were taken from two depths: 5 and 80 meters. As in the case of TRI-1, the choice of the sampling depths was aimed at studying populations exposed to very different irradiance regimes: ca 40% of the incident PAR at 5m (ranging between 0 and 800  $\mu\text{mol photons m}^{-2} \text{s}^{-1}$ ) and ca 0.1% at 80m (ranging between 0 and 2  $\mu\text{mol photons m}^{-2} \text{s}^{-1}$ ). In particular, the population at 80 m was located within a Deep Chlorophyll Maximum (DCM), indicated by the CTD fluorescence profiles (data not shown).

The sampling strategy and the parameters recorded are reported in Tab. 5.2.

Parameters	Sampling Depth	Sampling interval
Incident solar irradiance (PAR)	surface	5min over 24h
Underwater irradiance (PAR)	0-90 m (profile)	2h
CTD parameters	0-90 m (profile)	2h
Nutrients	5 and 80m	2h
Fractionated HPLC (< and > 5 $\mu\text{m}$ )	5 and 80 m	2h
Spectrofluorometric Chl <i>a</i> (< and > 5 $\mu\text{m}$ )	5 and 80 m	4h
<i>In-vivo</i> fluorescence -FRRF	5 and 80 m	2h
Pvs.E curves	5 and 80m	4h

**Table 5.2** – Sampling strategy during TRI-2 experiment.

### 5.2.1 Physical parameters

The water column profiles showed a marked pycnocline in the upper layer (Fig. 5.11) due to summer thermal stratification; temperature and salinity remained fairly constant during the diel cycle.

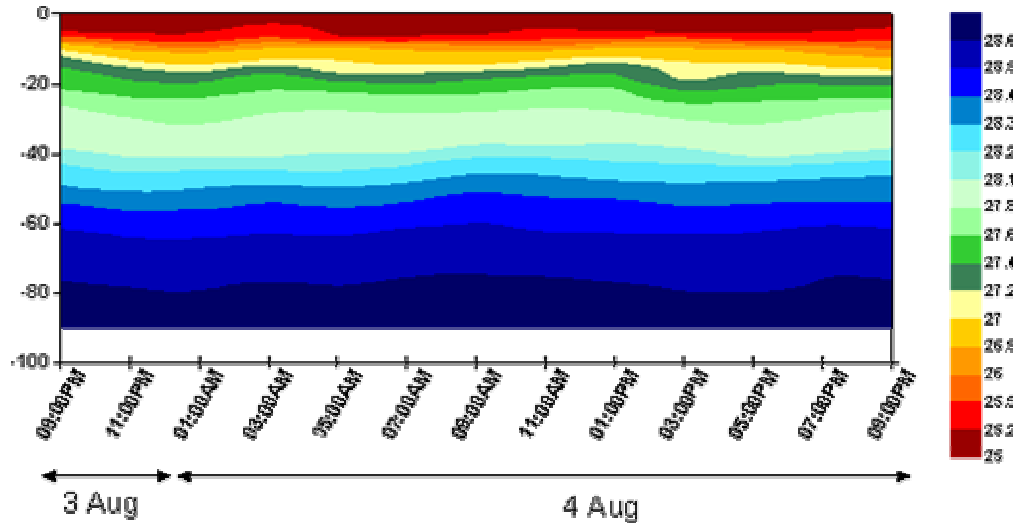


Figure 5.11 – Density ( $\sigma_t$ ) over the 24h of the TRI-2 experiment.

Nutrient concentrations did not display any systematic variations. In particular,  $\text{NO}_3+\text{NO}_2$  concentrations ranged between 0.05 and 0.1  $\mu\text{M}$  at 5m and between 0.95 and 2.38  $\mu\text{M}$  at 80m (Fig. 5.12a). Inorganic phosphate concentrations were very low and ranged between 0.03 and 0.07  $\mu\text{M}$  at 5m and between 0.04 and 0.05  $\mu\text{M}$  at 80m (Fig. 5.12b).

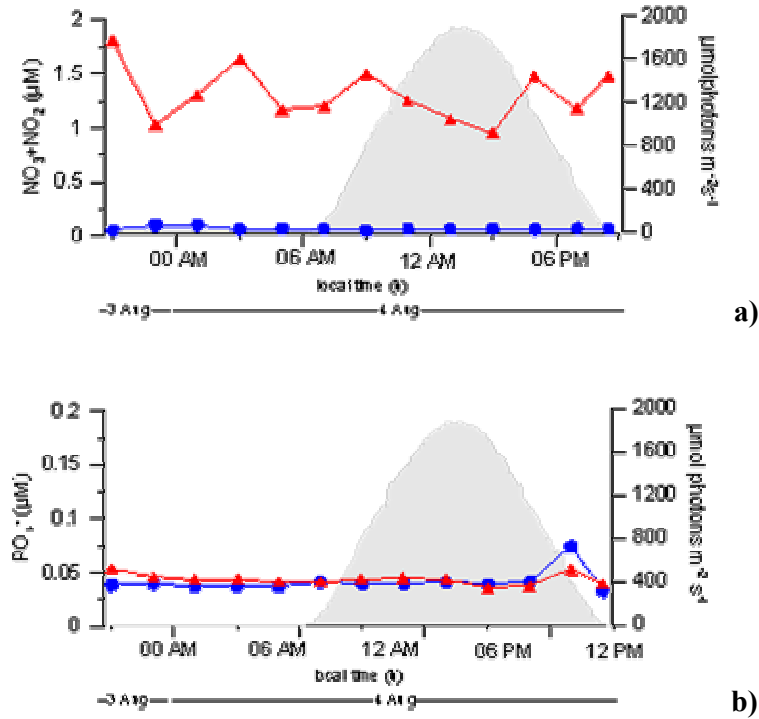


Figure 5.12 – Incident solar irradiance (grey area),  $\text{NO}_3+\text{NO}_2$  concentration (a) and  $\text{PO}_4^{3-}$  concentration (b) at 5m (●) and at 80m (▲) over the 24h of the TRI-2 experiment.

The data of NO<sub>3</sub>+NO<sub>2</sub> concentrations indicated the presence of a nutricline at depth, though the PO<sub>4</sub><sup>-</sup> values were low also at 80m.

### 5.2.2 Pigments

The total Chlorophyll *a* concentration was relatively higher at 80m than at 5m, the mean value was 0.07 mg Chl*a* m<sup>-3</sup> at 5m and 0.27 mg Chl*a* m<sup>-3</sup> at 80m. However, also in this experiment, the ultraphytoplankton fraction (<5µm) accounted for ≈ 90% of total biomass at 5m and 88% at 80m.

As shown in Fig. 5.13, the pigment composition was very different at the two sampling depths and the contribution of prokaryotes to the ultraphytoplankton fraction was more relevant than during the TRI-1 experiment.

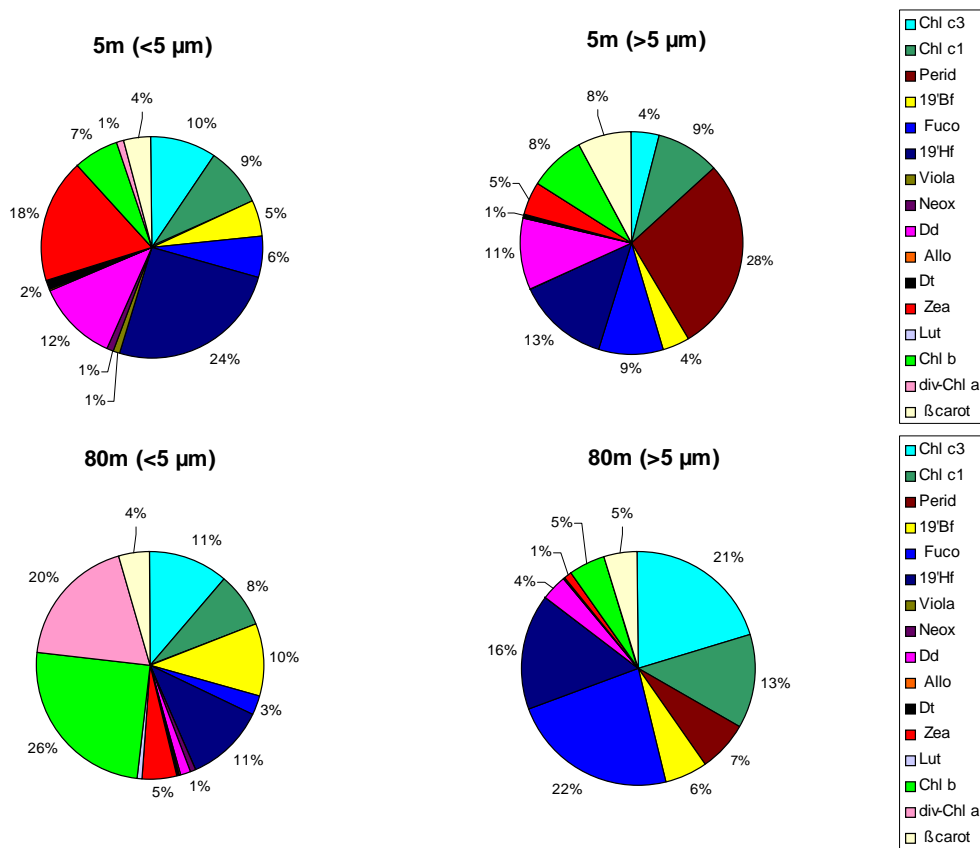


**Figure 5.13** – Average contribution of HPLC pigments (except Chl *a*) for the two sampling depths during the TRI-2 experiment.

In particular, ultraphytoplankton pigment composition displayed a dominance of 19'Hf-containing algae (average 19'Hf=24%) and cyanobacteria (average Zea=18%) at 5m. However, other groups, such as small green algae (average Chl *b*=7%), Fuco-containing

algae (average Fuco=6%). The prochlorophytes were present at 5m, but their contribution to the ultraphytoplankton community was very small (average div-Chl *a*=1%). On the contrary, small green algae (average Chl *b*=26%) and prochlorophytes (average div-Chl *a*=20%) were the dominant groups of the ultraphytoplankton fraction at 80 m. Further, the golden-brown algae were represented essentially by 19'Hf-containing groups (average 19'Hf=11%) and 19'Bf-containing groups (average 19'Bf=10%) and the contribution of cyanobacteria was relatively small (average Zea=5%).

Clearly the golden-brown algae groups were the most abundant in the fraction >5 $\mu$ m, but also in this case the two sampling depths were quite different. The Perid-containing dinoflagellates were dominant (average Perid=28%) at 5m, followed by 19'Hf-containing groups (average 19'Hf=13%) and Fuco containing groups (average Fuco=9%). At 80m, on the other hand, these two groups were relatively more abundant (average Fuco=22% and average 19'Hf=16%).

The results presented in Fig. 5.14 and 5.15 refer to the entire phytoplankton populations (sum of ultraphytoplankton and >5 $\mu$ m fraction); the ultraphytoplankton fraction accounted for  $\approx$ 90% of total TChl *a* concentrations at the two sampling depth throughout the experiment.

Also in this experiment, the time distribution of TChl *a* concentration (Fig. 5.14) did not show any significant diel fluctuations at the two sampling depths, ranging between 0.07 and 0.10 mg m<sup>-3</sup> at 5m and between 0.19 and 0.34 mg m<sup>-3</sup> at 80 m.

Again, no clear diel trend was found in the ratios between the major accessory pigment and chlorophyll (data not shown).

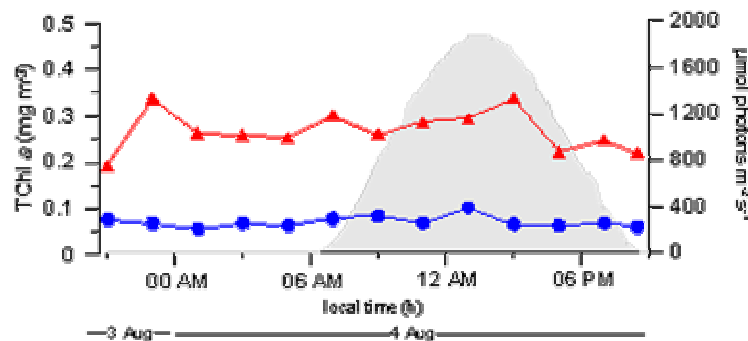


**Figure 5.14** – Incident solar irradiance (grey area), and Chl *a* concentration at 5m (●) and at 80m (▲) over the 24h of the TRI-2 experiment.

The ratio between photoprotective and photosynthetic carotenoids (PPC/PSP) differed between the two sampling depths in relation to the different irradiance regimes (Fig. 5.15a),

as already observed in the TRI-1 experiment. However, the PPC/PSP ratio was higher in this experiment as compared to the values recorded in TRI-1, probably due to both a longer photoperiod and to higher irradiance values in August than in April. In particular, a clear circadian pattern could be described in the PPC/PSP ratio at 5m; highest values occurred during daytime and the lowest during the night. Again, no diel pattern was found to occur in the population at 80m.

The contribution of Diadinoxanthin (Fig. 5.13) was higher at surface (12% for the ultraphytoplankton fraction) than at 80m (1%) and the diel periodicity in the Dt/Dd+Dt ratio was very pronounced (Fig. 5.15b) in the surface layer: the maximum value (0.26) was recorded at 3:00 PM, and the minimum (0.02) occurred at 9:00 PM. A slight increase in the Dt/Dd+Dt ratio during daytime was recorded also at 80m. However, the concentrations of Dd and Dt were always very low throughout the sampling period (Dd+Dt ranged between 0.006 and 0.009 mg m<sup>-3</sup>), due to the very low abundances of golden-brown algae.

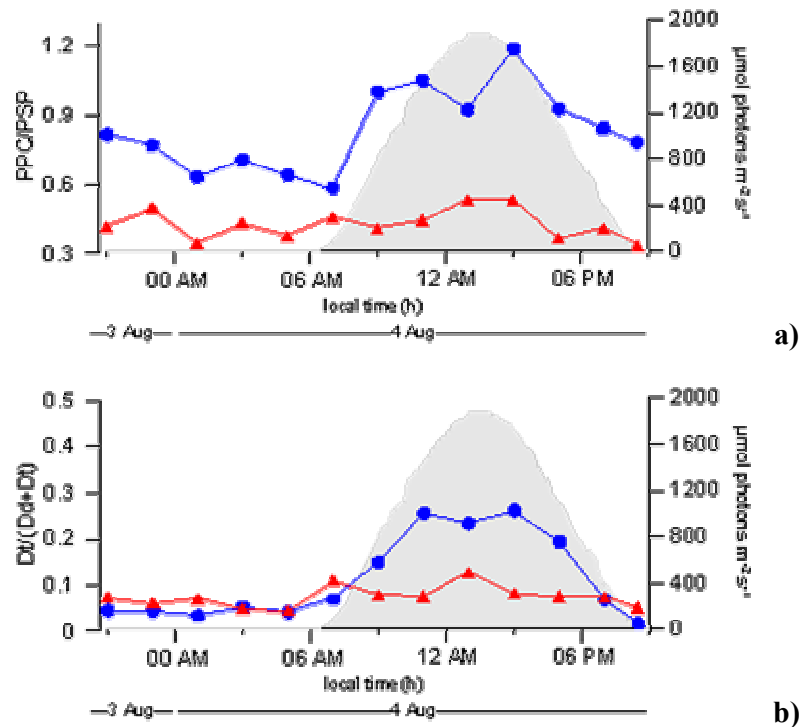


**Figure 5.15** – Incident solar irradiance (grey area), PPC/PSP ratio (a) and Dt/Dd+Dt ratio (b) at 5m (●) and at 80m (▲) over the 24h of the TRI-2 experiment.

As already observed in the TRI-1 experiment, the concentrations and ratios of other photoprotective pigments, such as  $\beta$ -carotene, did not display any particular pattern of variation neither along the water column nor in time (data not shown).

### 5.2.3 P<sub>vs.E</sub> parameters

P<sub>vs.E</sub> experiments were performed on both surface and deep populations approximately every four hours, in order to obtain a more accurate reconstruction of circadian variability (Table 5.2). The characteristic features were similar to those described for the TRI-1 experiment, with differences between P<sub>vs.E</sub> curves for the two depths (Fig. 5.16), clearly related to the different light regimes. Also in the TRI-2 experiment, the photosynthetic capacity ( $P_{\max}^B$ ) was higher at 5m than at depth, and an opposite pattern was found for photosynthetic efficiency ( $\alpha^B$ ).

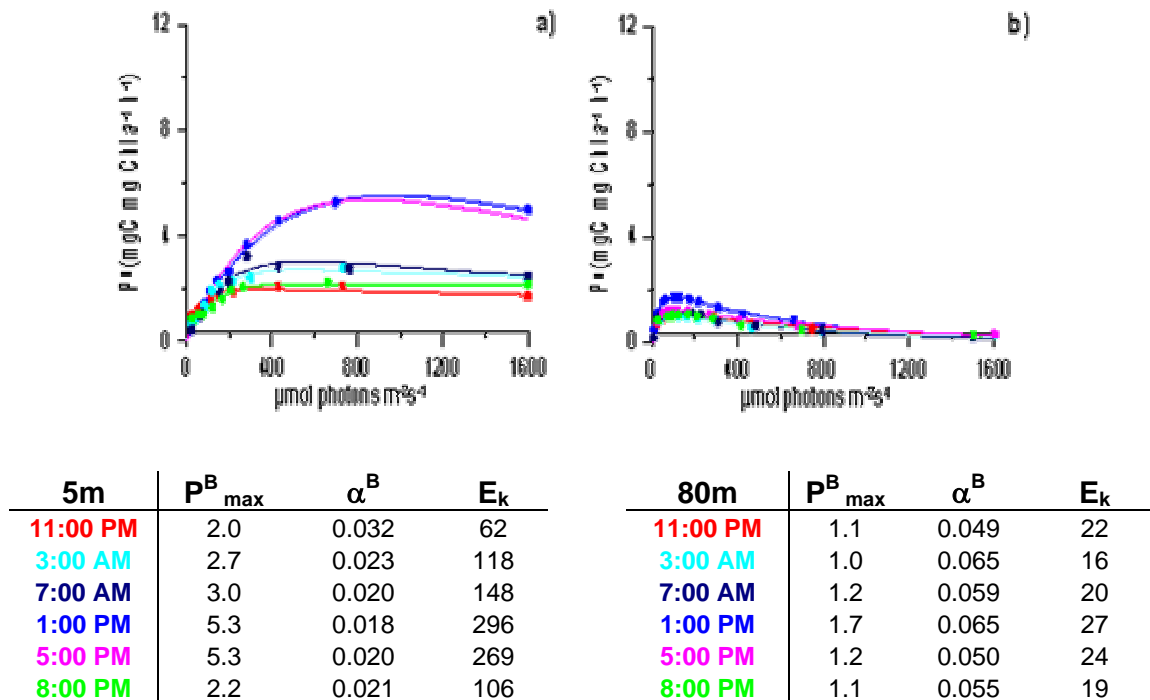


**Figure 5.16** – P<sub>vs.E</sub> curves and photosynthetic parameters at 5m (a) and 80m (b) over the 24h of the TRI-2 experiment.

For the population at 5m, the variation in time of the photosynthetic capacity,  $P_{\max}^B$ , showed the minimum value (2.0 mgC mgChl  $a^{-1} h^{-1}$ ) at 11:00 PM of the 3<sup>rd</sup> August; maximum photosynthetic capacity (5.3 mgC mgChl  $a^{-1} h^{-1}$ ) was recorded at 1:00 PM and at 05:00 PM of the 4<sup>th</sup> August (Fig. 5.17a). The high value in the afternoon may be related to the length of the photoperiod. As compared to the recordings in the surface population in the TRI-1

experiment, the amplitude of oscillation was considerably smaller, which may be related to the low nutrients concentrations that characterized the site of the TRI-2 experiment.

The circadian pattern at 80m was less evident than at surface:  $P^B_{\max}$  ranged from 1.7  $\text{mgC mgChl } a^{-1} \text{ h}^{-1}$  and 1.0  $\text{mgC mgChl } a^{-1} \text{ h}^{-1}$  at 1:00 PM and 11:00 PM, respectively.

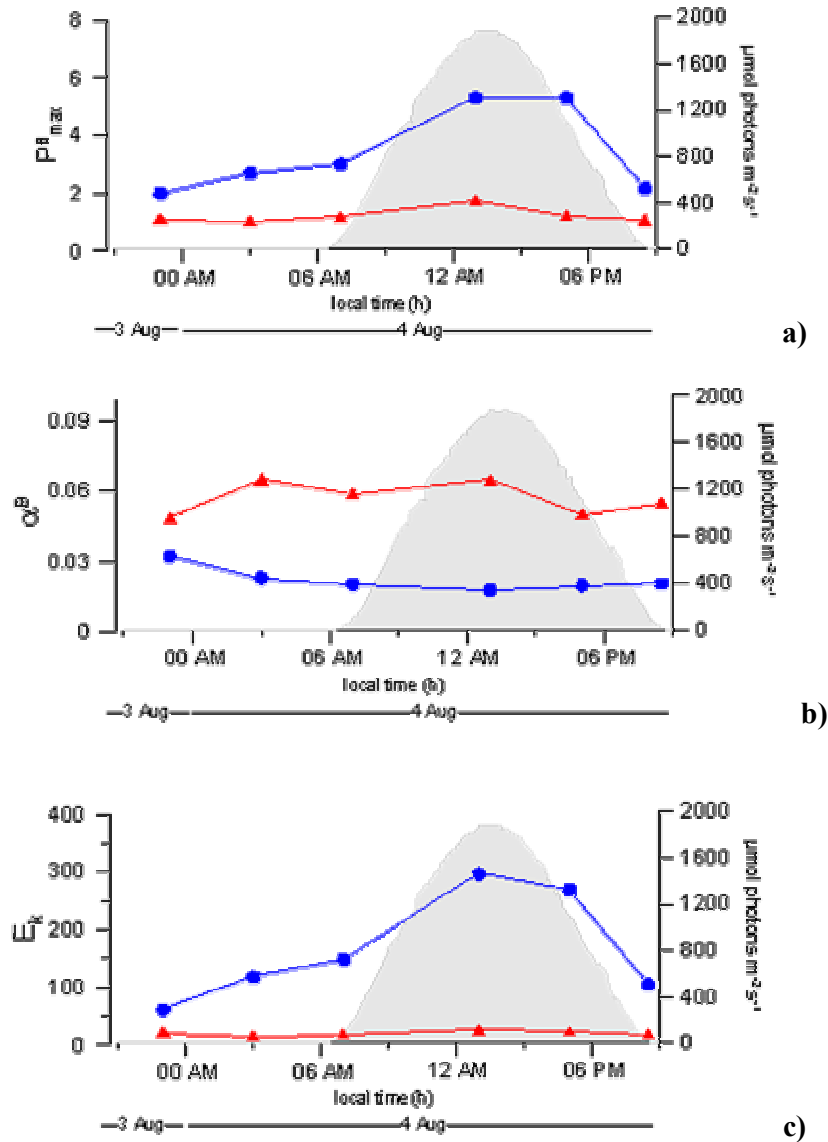


**Figure 5.17** – Incident solar irradiance (grey area),  $P^B_{\max}$  (a),  $\alpha^B$  (b) and  $E_k$  (c) at 5m (●) and at 80m (▲) over the 24h of the TRI-2 experiment.

The photosynthetic efficiency,  $\alpha^B$ , ranged between 0.018 and 0.32  $\text{mgC mgChl } a^{-1} \text{ h}^{-1} (\mu\text{mol photons m}^{-2} \text{ s}^{-1})^{-1}$  at 5m and between 0.049 and 0.065  $\text{mgC mgChl } a^{-1} \text{ h}^{-1} (\mu\text{mol photons m}^{-2} \text{ s}^{-1})^{-1}$  at 80m (Fig. 5.17b). Thus, only minor variations occurred in  $\alpha^B$  at the two sampling

depths, and although a diel pattern could not be discerned, a slight decrease in  $\alpha^B$  was observed during daytime in the surface population.

The variations in the photoacclimation index,  $E_k$ , followed that of  $P^B_{\max}$  at 5m, showing maximum values during daytime and minimum values at night, while it was lower and quite constant at 80m (Fig. 5.17c).

### 5.2.4 FRRF parameters

During the TRI-2 experiment, *in vivo* fluorescence measurements were performed every 2h at both sampling depths, by means of a Fast Repetition Rate Fluorometer (FRRF). The variations in time of  $F_v/F_m$  and of the absorption cross section  $\sigma_{PSII}$  indicated, as in the first circadian experiment, the presence of a diel periodicity at 5m. During daytime, a decrease in  $F_v/F_m$  was recorded that was very pronounced at 5m and much less so at 80m;  $\sigma_{PSII}$  showed a slight increase at 5m but remained constant throughout the diurnal cycle (Fig. 5.18 a, b). Some caution must be taken, however, when interpreting the data recorded in the surface layer as the FRRF measurements might be partially invalidated due to technical problems when performed at high irradiance levels.

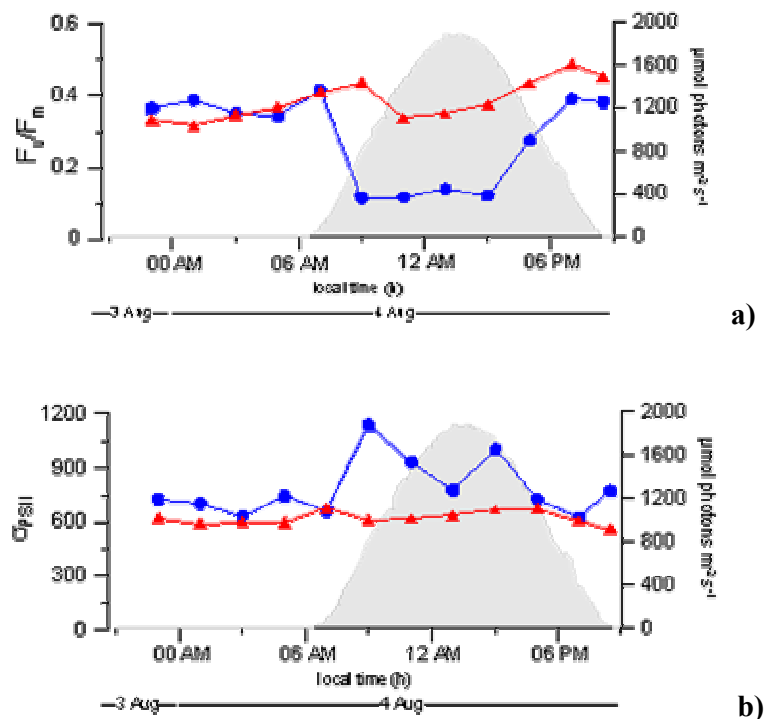


**Figure 5.18** – Incident solar irradiance (grey area),  $F_v/F_m$  (a) and  $\sigma_{PSII}$  (b) at 5m (●) and at 42m (▲) over the 24h of the TRI-2 experiment.

### 5.3 TRI-3

The third experiment, **TRI-3**, was carried out from 8:45 AM of June 29 to 6:00 AM of June 30 2005, in the Sabaudia lagoon (Tyrrhenian Sea) (Lat. 41° 16'.05 N, Long. 13° 01'.27 E). The weather was clear and sunny; the natural light:dark cycle was 16:8 and the maximum incident irradiance was 1830  $\mu\text{mol photons m}^{-2} \text{s}^{-1}$  recorded at 1: 10 PM (local time).

Water samples were taken at 0.5m. The choice of the sampling depth was aimed on one hand at studying phytoplankton population exposed to very high irradiance, and, on the other hand, at avoiding the problem of fitobenthos suspension during sampling; the Sabaudia lagoon is only ~ 4m deep.

The sampling strategy and the parameters recorded are reported in Tab. 5.3.

Parameters	Sampling Depth	Sampling interval
Incident solar irradiance (PAR)	surface	5min over 24h
salinity, temperature	0.5 m	2h
Nutrients	0.5m	2h
Fractionated HPLC (<5 $\mu\text{m}$ and > 5 $\mu\text{m}$ )	0.5m	2h
Spectrofluorometric Chl <i>a</i>	0.5m	2h
In-vivo fluorescence –Phyto-PAM	0.5m	2h
Pvs.E curves	0.5m	≈ 2h

**Table 5.3** – Sampling strategy for the TRI-3 experiment.

#### 5.3.1 Physical parameters

Temperature (Fig. 5.19) varied between during the night 29.0 °C and 32.2 °C in the afternoon; salinity remained constant, 35.04 to 35.06, throughout the sampling period (data not shown).

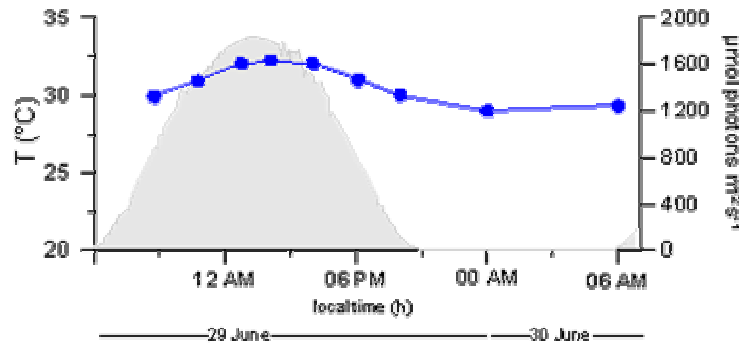


**Figure 5.19** – Incident solar irradiance (grey area) and temperature at 0.5m (●) over the 24h of the TRI-3 experiment.

Nutrient concentrations were low,  $\text{NO}_3+\text{NO}_2$  ranged between 0.09 and 0.61  $\mu\text{M}$  (Fig. 5.20a),  $\text{PO}_4^-$  ranged between 0.01 and 0.08  $\mu\text{M}$  (Fig. 5.20b) and the oscillations did not seem related to the L:D cycle.

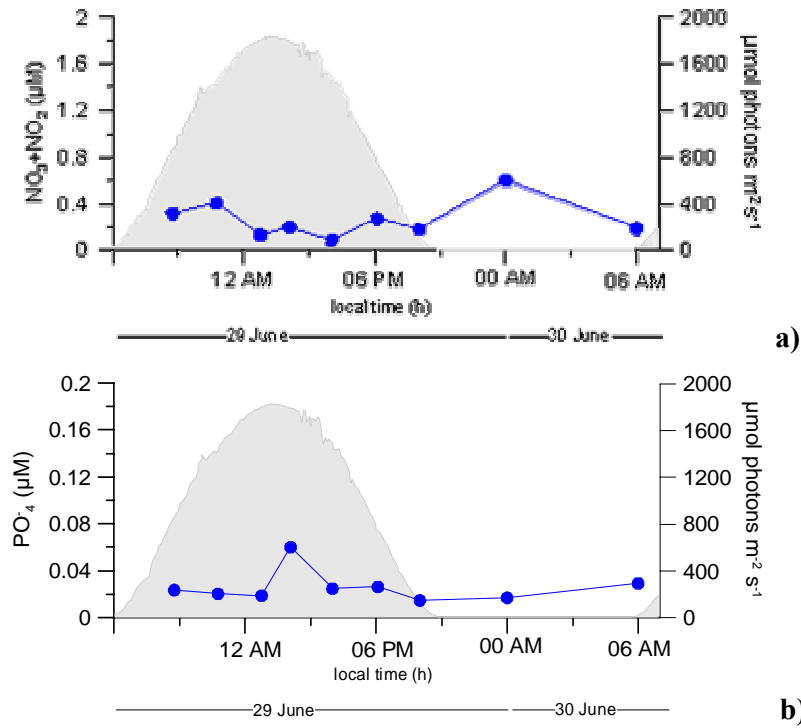


**Figure 5.20** – Incident solar irradiance (grey area),  $\text{NO}_3+\text{NO}_2$  concentration (a) and  $\text{PO}_4^-$  concentration (b) at 0.5m (●) over the 24h of the TRI-3 experiment.

### 5.3.2 Pigments

The total Chlorophyll *a* concentration,  $7.62\pm 0.93 \text{ mgm}^{-3}$ , was very high as compared to the other two experiments. Such values are typical for a Mediterranean lagoon in summer. Yet the ultraphytoplankton fraction ( $< 5\mu\text{m}$ ) accounted for  $\approx 95\%$  of total chlorophyll concentrations.

The average pigment composition of the ultraphytoplankton and the  $>5\mu\text{m}$  fractions during TRI-3 experiment are shown in Fig. 5.21.

The ultraphytoplankton population was strongly dominated by cyanobacteria (average Zea= 71%), with only minor contributions of small green algae (average Chl *b*= 4%) and Fuco-containing algae (average Fuco= 3%). On the other hand, this group was the most abundant in the  $>5\mu\text{m}$  fraction (average Fuco= 37%), followed by Perid-containing dinoflagellates (average Perid= 9%) and green algae (average Chl *b*= 4%).

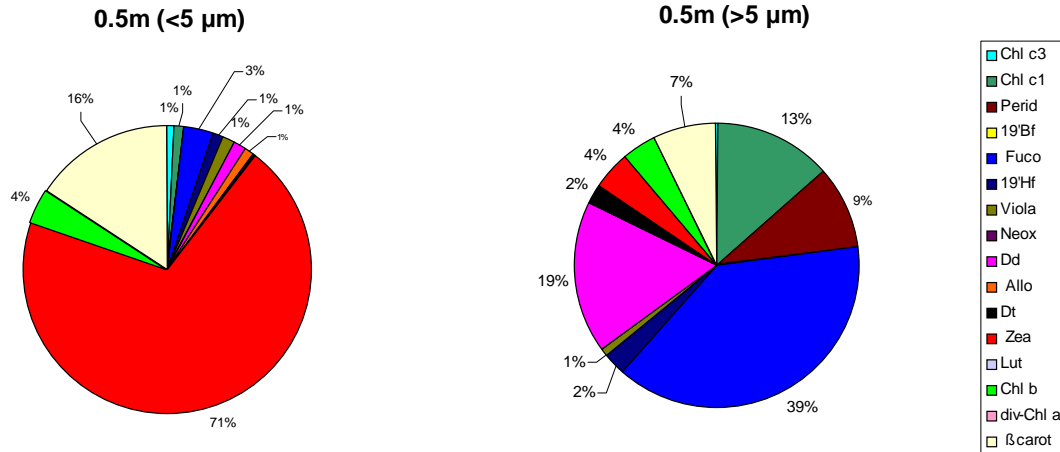


**Figure 5.21** – Average contribution of HPLC pigments (except Chl a) at the two sampling depths during the TRI-3 experiment.

As already underlined for the other circadian experiments, the results presented in Fig. 5.22 and Fig. 5.23 refer to the whole phytoplankton populations, but it should be kept in mind that the ultraphytoplankton fraction accounted for c.a. 95% of the phytoplankton in terms of chlorophyll.

A circadian pattern in TChl a concentration was not found; the values ranged between 6.10 and 8.32 mg m<sup>-3</sup> (Fig. 5.22). Also the ratios between the major accessory pigments and chlorophyll did not show any diel pattern of variation (data not shown).

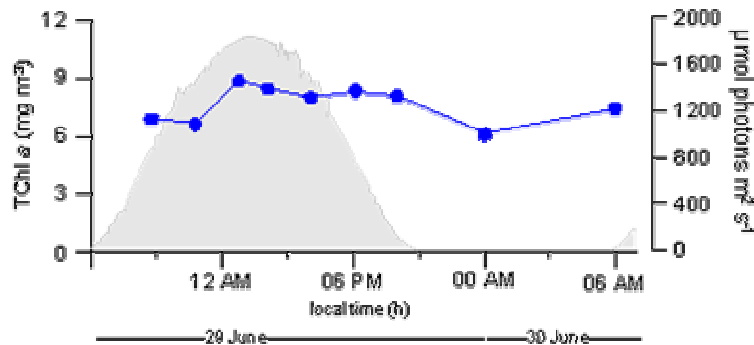


**Figure 5.22** – Incident solar irradiance (grey area), and Chl a concentration at 0.5m (●) over the 24h of the TRI-3 experiment.

As regards the photoprotective pigments, the Dt/Dd+Dt ratio (Fig. 5.23b) showed a slight increase at maximum irradiance. In this experiment, the concentrations of Dd and Dt were related essentially to the golden-brown algae in the >5μm fraction. Further, the Zea/Chl a ratio increased during the daytime, though the maximum value was recorded in the afternoon. However, the HPLC method used in this study did not separate the phycobilins,

the main pigments of cyanobacteria, thus there is a gap in the information on the pigment pool of this group.

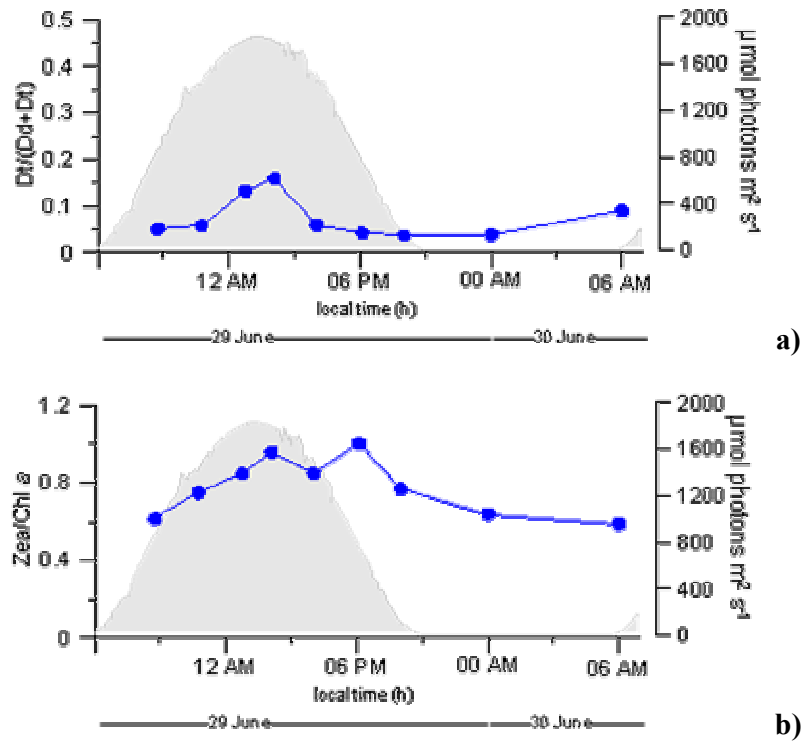


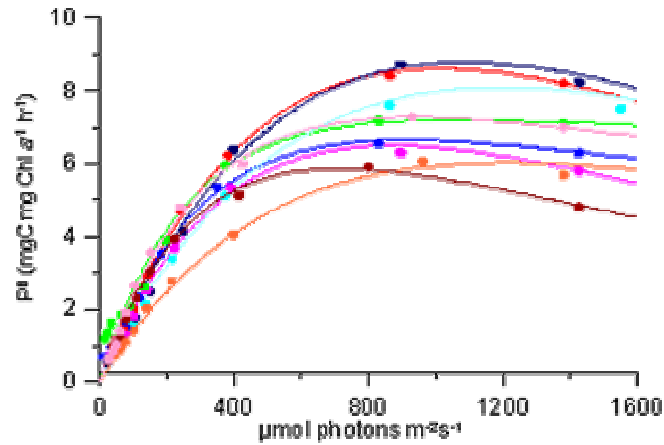
**Figure 5.23** – Incident solar irradiance (grey area),  $Dt/Dd+Dt$  ratio (a) and Zea/Chl *a* ratio (b) at 0.5m (●) over the 24h of the TRI-3 experiment.

### 5.3.3 Pvs.E parameters

To allow for a detailed reconstruction of the diurnal cycle of photosynthetic parameters, Pvs.E experiments were performed every two hours between 8:45 AM and 8:00 PM of 29 June and two PvsE experiments were performed during the dark hours, at midnight and at dawn.

In spite of the very different environmental conditions, the family of Pvs.E curves (Fig. 5.24) showed the same circadian patterns observed in the surface populations of the TRI-1 and TRI-2 experiments.

The photosynthetic capacity,  $P_{\text{max}}^B$ , (Fig. 5.25a) was higher during daytime than at night. The maximum value ( $8.7 \text{ mgC mgChl } a^{-1} \text{ h}^{-1}$ ) was found at 2:10 PM of the June 29, and the minimum ( $5.8 \text{ mgC mgChl } a^{-1} \text{ h}^{-1}$ ) was recorded at midnight. Notably, the night minimum was higher than the minima recorded in surface populations in the TRI-1 and TRI-2 experiments ( $1.9$  and  $2.0 \text{ mgC mgChl } a^{-1} \text{ h}^{-1}$ , respectively).



0.5m	$P_{\max}^B$	$\alpha^B$	$E_k$
8:45 AM	6.6	0.026	254
10:45 AM	7.2	0.030	238
12:45 AM	8.6	0.024	358
2:10 PM	8.7	0.022	396
4:00 PM	7.7	0.019	407
6:00 PM	6.4	0.022	293
8:00 PM	6.0	0.020	300
12:00 PM	5.8	0.026	224
6:00 AM	7.3	0.028	260

**Figure 5.24** –  $P_{\text{vs.}}E$  curves and photosynthetic parameters at 0.5m during the TRI-3 experiment.

The photosynthetic efficiency,  $\alpha^B$  (Fig. 5.25b), ranged between 0.019 and 0.030  $\text{mgC mgChl } a^{-1} \text{ h}^{-1} (\mu\text{mol photons m}^{-2}\text{s}^{-1})^{-1}$  and the slightly lower values were recorded at maximum irradiance levels as observed also in the TRI-2 experiment at 5m.

The pattern of variation in time of the photoacclimation index,  $E_k$  was similar to that recorded for  $P_{\max}^B$ ; very high values occurred during daytime reaching 407  $\mu\text{mol photons m}^{-2}\text{s}^{-1}$  in the afternoon. (Fig. 5.25c).

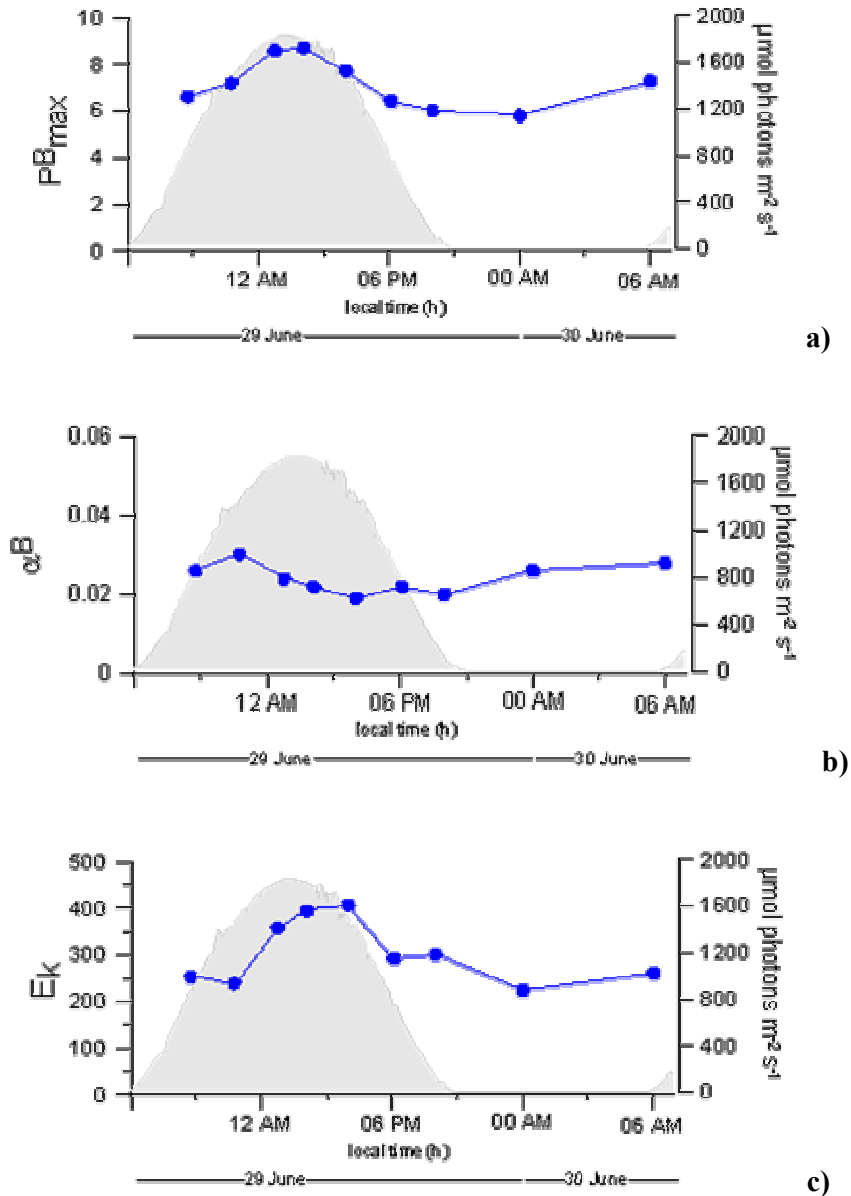


**Figure 5.25** – Incident solar irradiance (grey area),  $P^B_{max}$  (a),  $\alpha^B$  (b) and  $E_k$  (c) at 5m (●) and at 80m (▲) over the 24h of the TRI-3 experiment.

### 5.3.4 Phyto-PAM coefficients

The circadian pattern of all the Phyto-PAM derived coefficients (Fig. 5.26) was similar to that observed during the TRI-1 experiment at 5m, though the amplitude of the oscillations was less pronounced.

In particular, the  $rETR_{max}$  values (Fig. 5.26a) were higher during daytime (maximum  $32.45 \mu\text{mol e}^- \text{m}^{-2} \text{s}^{-1}$  at 8:45 AM) and decreased during the night (minimum  $23.25 \mu\text{mol e}^- \text{m}^{-2} \text{s}^{-1}$  at 00:00 AM).

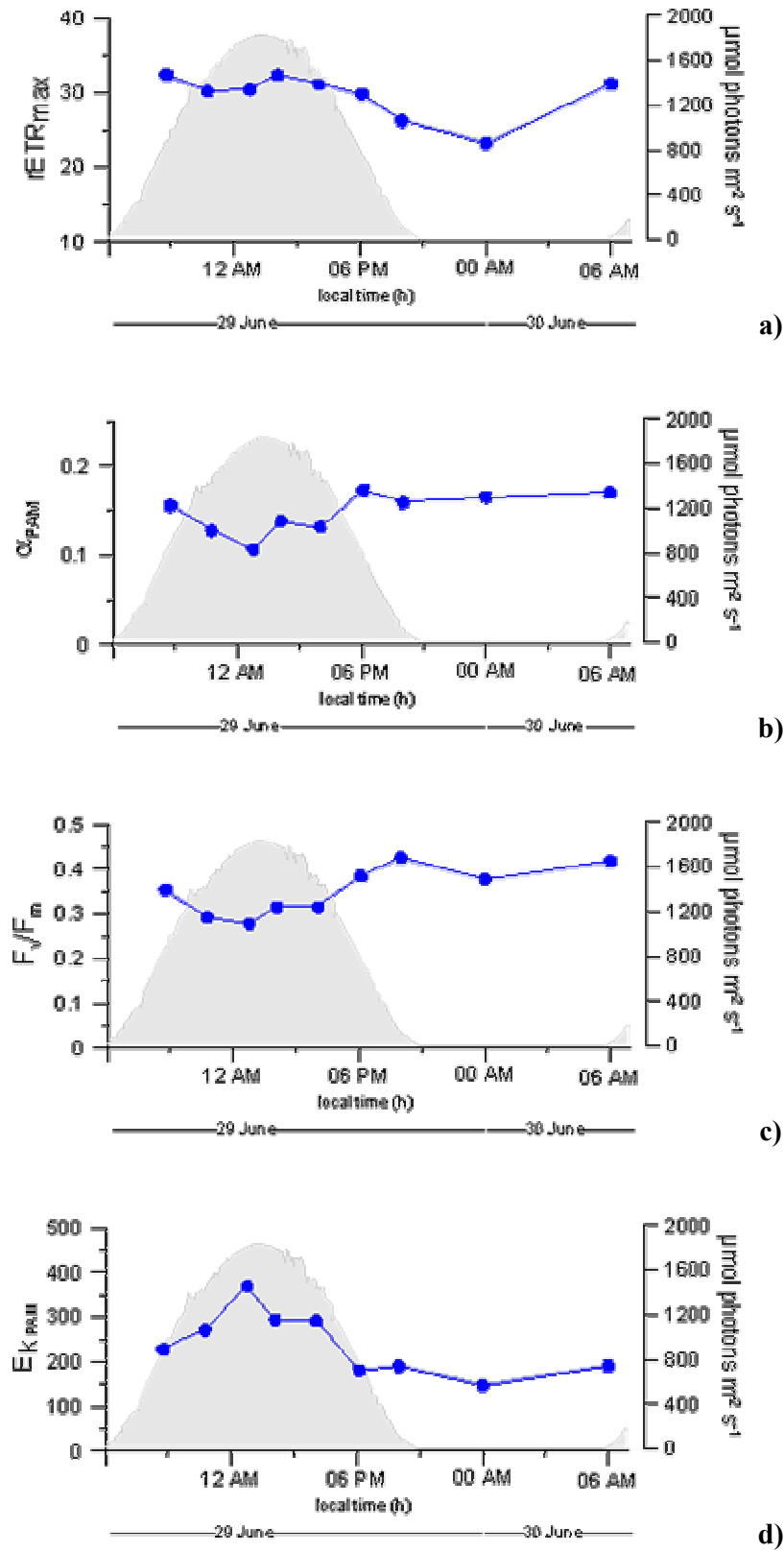


**Figure 5.26** – Incident solar irradiance (grey area),  $rETR_{\text{max}}$  (a),  $\alpha_{\text{PAM}}$  (b),  $F_v/F_m$  (c) and  $E_{k\text{PAM}}$  (d) at 0.5m (●) over the 24h of the TRI-3 experiment.

On the contrary,  $\alpha_{\text{PAM}}$  and  $F_v/F_m$  (Fig. 5.26b,c) showed minimum values at maximum sun irradiance and the highest values at night. In particular,  $\alpha_{\text{PAM}}$  ranged between 0.11 and 0.17 electrons photons<sup>-1</sup>, and  $F_v/F_m$  ranged between 0.28 and 0.42.

As in the case of the Pvs.E parameters, the  $E_{\text{kPAM}}$  (Fig. 5.26d) showed the same variation in time as that recorded for  $\text{rETR}_{\text{max}}$  with the maximum value (368  $\mu\text{mol photons m}^{-2} \text{s}^{-1}$ ) registered at 00:45 PM of the June 29 and the minimum, 146  $\mu\text{mol photons m}^{-2} \text{s}^{-1}$ , at midnight.

## 5.4 Discussion

The phytoplankton assemblages were very different in the three experiments, though the ultraphytoplankton fraction was by far the dominant component. In the TRI-1 experiment, where the station was located in a coastal area, small golden-brown algae were the most abundant at both sampling depths, revealing a condition similar to that found in spring at MC, when the TChl *a* was quite low (see chapter IV). These results again confirm the importance of small eukaryotes in coastal sites. The situation was quite different in the TRI-2 experiment, when the prokaryotes dominated the phytoplankton populations at both sampling depths. In particular, cyanobacteria and 19'Hf-containing golden-brown algae were the most abundant groups at surface (5m), while prochlorophytes and small green flagellates dominated in the Deep Chlorophyll Maximum (80m). This opposite distribution between cyanobacteria and prochlorophytes, also recorded at MC in summer, was in agreement with the hypothesis that prochlorophytes will prevail over the cyanobacteria at depth, probably because they are more efficient in absorbing blue light (Ting *et al.*, 2002). Finally, the HPLC pigment analyses in the third experiment (TRI-3) showed the presence of a cyanobacteria bloom. A summer bloom of cyanobacteria is a recurrent feature in the Sabaudia lagoon, as observed by our group in previous years (unpublished data).

Despite these differences in the composition of the phytoplankton community, some general features emerged in the diel variability of the physiological response of the algae during the three experiments.

First of all, the circadian patterns were much more pronounced in the surface samples, in almost all the photophysiological parameters studied though a linear relationship between the amplitude of the oscillations of cellular response and the diel excursion of irradiance did not occur. That is, the widest range in photophysiological parameters was not recorded in TRI-3 where extremely high irradiance levels were encountered. On the other hand, only minor oscillations were encountered for these parameters in the deeper phytoplankton populations that experienced much less variation in the irradiance regime (e.g. the irradiance ranged between 0 and 2  $\mu\text{mol photons m}^{-2}\text{s}^{-1}$  during TRI-2).

### *Photoprotective pigments*

The higher values of photoprotective/photosynthetic carotenoids (PPC/PSP) at surface in all the three experiments, indicated that the phytoplankton was “ready” to deal with excessive light; however, different photoprotective mechanisms could be described.

In the TRI-1 experiment, carried out in April 2004, golden-brown algae dominated the phytoplankton assemblage. The photoprotection mechanism of these algal groups is based on the Diadinoxanthin cycle that provides prompt changes, within minutes, in pigment composition thus switching between transfer of excitation energy to the reaction centers and photoprotection, when needed. In particular, a high proportion of Diadinoxanthin would allow for a rapid transformation in the de-epoxidated form (Diatoxanthin) and, therefore an almost immediate protection, thus reducing the photodamage. The increase in the de-epoxidative state of the Diadinoxanthin cycle during daytime (Fig. 5.6 and 5.15) clearly confirm this hypothesis. This flexibility in the function of pigments is particularly needed in spring, when weather conditions might change rapidly. The Diadinoxanthin cycle of golden-brown algae may be one explanation for the spring bloom in temperate waters being generally dominated by diatoms.

In the TRI-2 experiment, carried out in August 2004, photoprotection was more due to pigments, such as Zeaxanthin and  $\beta$ -carotene that do not transfer the excitation energy to the reaction centers, than to xanthophylls-cycle-pigments. Also in this case, phytoplankton adopted the solution that appears better suited the mean weather conditions.

The TRI-3 experiment was carried out in end June 2005 in shallow waters and thus at extremely high irradiance and long photoperiod. A cyanobacteria bloom was observed and, unfortunately, the main pigments (phycobilins) of this taxon were not eluted by the HPLC method employed in this study as already explained in section 5.3.2.

#### *Photosynthetic machinery*

In all the experiments, evidence of diel fluctuations in the photosynthetic capacity,  $P_{\max}^B$  were recorded both in the surface and in the deeper phytoplankton populations. A similar pattern was often reported in the study on diel periodicity of  $P_{vs.E}$  response in natural phytoplankton populations (MacCaull and Platt, 1977; Gargas *et al.*, 1979; Kana *et al.*, 1985; Prezelin *et al.*, 1986, 1987; .Putt *et al.*, 1988; Lizon *et al.*, 1995).

However, the amplitude of oscillations differed significantly between the phytoplankton in the upper and in the deeper layer; at surface the maximum value of  $P_{\max}^B$  was on average 3.2 fold higher than the minimum value, while at depth was 1.9.

Furthermore, the amplitude of diel fluctuations in  $P_{\max}^B$  values at surface was probably influenced also by other environmental factors in addition to the irradiance regime. In particular, during the TRI-1 experiment the ratio between maximum and minimum  $P_{\max}^B$  was 5.4, while during the TRI-2 experiment only a 2.8 fold change in  $P_{\max}^B$  was recorded. In the latter experiment the low nitrate concentrations (see section 5.2.1) suggest

that nutrient limitation may have affected the photosynthetic capacity. An impact of the nutritional status on diel fluctuations of photosynthetic parameters was already hypothesized by Malone (1971) and by Kana *et al.*, (1985).

During the third experiment (TRI-3) the maximum photosynthetic capacity exceeded by 1.5 fold minimum, in fact in this case  $P_{\max}^B$  remained quite high also during the night (see Fig. 5.25a). It may be hypothesized that the cyanobacteria population maintained always “ready” their photosynthetic machinery, in relation to the length of photoperiod and the very high irradiance level that they experienced (e.g. the incident irradiance was  $1000 \mu\text{mol photons m}^{-2}\text{s}^{-1}$  already at 8:00 AM).

As diel oscillations in photosynthetic efficiency ( $\alpha^B$ ) were small compared with the photosynthetic capacity,  $P_{\max}^B$ , these two parameters did not covaried. As a consequence, the photoacclimation index,  $E_k$ , showed a positive correlation with  $P_{\max}^B$  (Fig. 5.27) in all the three experiments ( $r = 0.94$ ,  $p < 0.05$ ,  $n = 28$ ). Behrenfeld *et al.* (2004) suggest that the lack of covariance between  $\alpha^B$  and  $P_{\max}^B$  in the  $P_{\text{vs.}}E$  response (the so-called “ $E_k$  dependent” group) is mainly a result of photoacclimation.

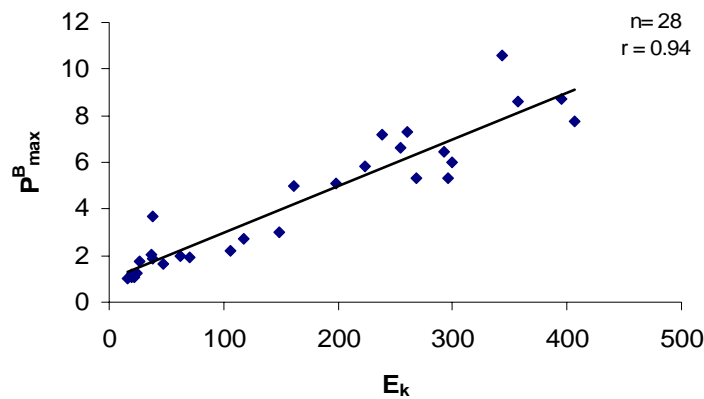


**Figure 5.27** – Correlation between  $P_{\max}^B$  and  $E_k$  from all the  $P_{\text{vs.}}E$  experiments.

By contrast, experiments carried out in our laboratory (Ragni, 2005) on cultures of *Phaeodactylum tricornutum*, grown under constant irradiance (“block mode”) showed a covariation between  $\alpha^B$  and  $P_{\max}^B$ . In our opinion, this discrepancy further highlights the role of field irradiance variations in tuning the diel responses of photosynthetic machinery of natural phytoplankton populations.

The coefficients obtained by means of the Phyto-PAM,  $\alpha_{\text{PAM}}$  and  $F_v/F_m$ , showed, especially in the surface samples, a depression in the central part of the day (i.e. under the maximal

irradiance). This finding indicates the action of light dissipation processes involving the Photosystem II. Furthermore, the changes in time of the absorption cross-section of PSII ( $\sigma_{\text{PSII}}$ ) during TRI-1 was to a certain extent in phase with  $\alpha_{\text{PAM}}$  and  $F_v/F_m$  suggesting that non photochemical quenching (NPQ) occurred both in the antenna and in the reaction center. The role of the antenna is also confirmed by the increase of de-epoxidation state of the xanthophyll pool, discussed above. Further, the photosynthetic apparatus was brought back in the second part of day and, in particular, at night.

However, these patterns were less pronounced during the TRI-3 experiment, probably in relation to phytoplankton composition (i.e. a cyanobacteria bloom). In fact, the state transitions are the most rapid and effective light adaptation processes in cyanobacteria (Masojídek *et al.*, 2001). As described in section 2.3.2, these mechanisms provide a redistribution of excitation energy between the photosystems to avoid imbalance in the photosynthetic electron transport.

The electron transport rate derived from Phyto-PAM measurements,  $r\text{ETR}_{\text{max}}$ , showed the highest values in the first part of the day both in the TRI-1 and the TRI-3 experiments. In particular it dramatically increased at dawn during TRI-1, suggesting that the presence of light, even at low levels, acts as a signal for the “wake up” of the photosynthetic machinery. This hypothesis is partially confirmed by experiments on monospecific culture. In fact, the same pattern was observed in a culture of *Phaeodactylum tricorutum* exposed to natural light (Ragni, 2005).

Furthermore, in phase with the depression of quantum yield ( $F_v/F_m$ ),  $r\text{ETR}_{\text{max}}$  showed a slight decrease under maximum irradiance levels. On the contrary, the photosynthetic capacity,  $P_{\text{max}}^{\text{B}}$ , presented maxima rates around noon (Fig. 5.28). The data available in literature on diel oscillation of  $P_{\text{max}}^{\text{B}}$  in some cases showed a similar pattern (e.g. Prezelin and Ley, 1980; Beherfield *et al.*, 1998), while in other cases (e.g. Kana *et al.*, 1985; Lizon *et al.*, 1995) the photosynthetic capacity showed a decrease in the central part of day, the so called midday depression. In our opinion, high  $P_{\text{max}}^{\text{B}}$  at noon indicated an efficient photosynthetic machinery in which the above described changes in antenna and reaction center were able to maintain high carbon assimilation levels as well as to minimize photoinhibition, even under excessive irradiance. Beherfield *et al.* (1998) suggest that, under excessive irradiance, compensatory changes in the electron turnover rate may occur too. By contrast, the midday depression indicated that the answers of photosynthetic machinery were not sufficient to prevent photodamage. The reason would be clearly various: from physiological conditions (e.g. nutrient stress) to pigment composition.

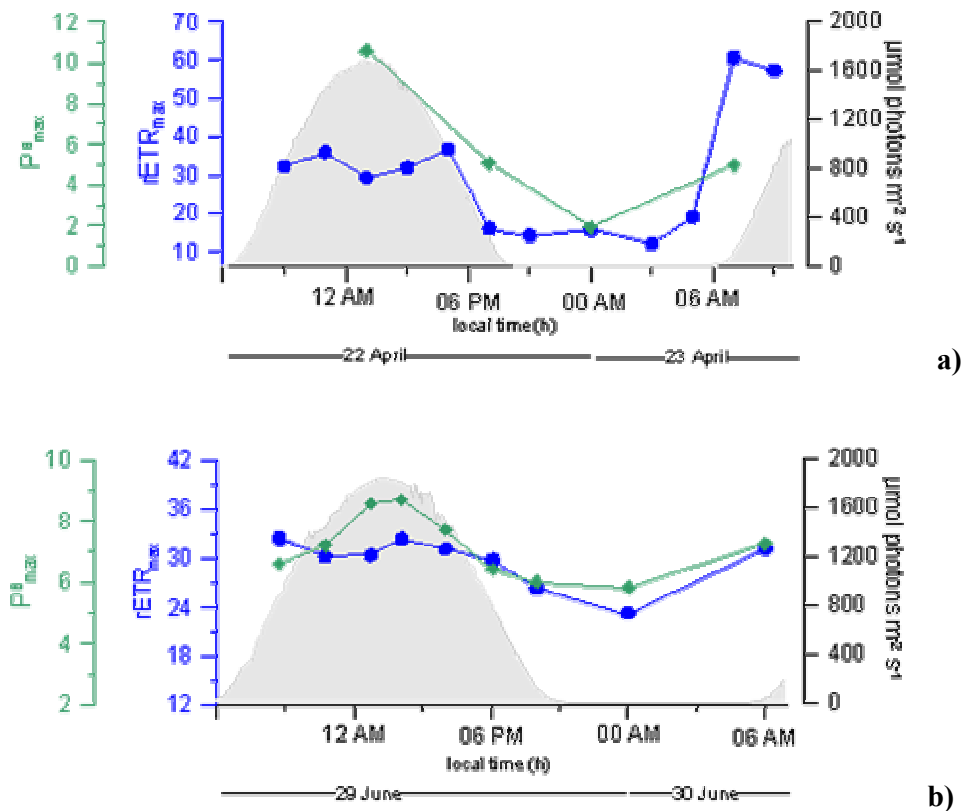


**Figure 5.28** – Incident solar irradiance (grey area),  $rETR_{max}$  (●) and  $P^B_{max}$  (◆) over TRI-1 (a) and TRI-3 (b) experiments.

As said in the chapter 1, the second aim of this project was focused on study the ultraphytoplankton photophysiology in order to interpret its patterns of occurrence and the possible differences compared to the “model” species. During our experiments on circadian cycles the ultraphytoplankton fraction always accounted for  $\geq 90\%$  of total phytoplankton biomass; it was thus not possible to discern directly any differences in photophysiological response as related to cell size. However, our data compared to the circadian fluctuations of photosynthetic parameters reported in literature (Prezelin *et al.*, 1987; Putt *et al.*, 1988) do not suggest the presence of differences related to the size. In addition, the observed diel fluctuations of *in vivo* fluorescence and photoprotective pigments pool are quite similar to that found in *Phaeodactylum tricornerutum* (Ragni, 2005). For instance, the pattern of Diadinoxanthin – Chlorophyll *a* ratio in *P. tricornerutum* cultures indicated that the pigment synthesis is modulated by variations in light intensity. *P. tricornerutum* cultures grown under

low light intensities did not show diel variations in Diadinoxanthin content as the deeper ultraphytoplankton natural populations.

As a general future, all the photophysiological parameters studied showed circadian patterns more pronounced in the surface samples than the deeper ones, during the three TRI experiments. The experimental evidence suggests that the irradiance regime experienced by ultraphytoplankton populations is the most important factor to trigger the cellular response; however other parameters, such as nutrient limitation, may have an impact modulating the circadian patterns, as in the case of photosynthetic capacity.

Ultraphytoplankton populations in the surface layer showed a photosynthetic machinery “ready” to answer to environmental changes, through the regulation of both antenna and reaction center systems. As a consequence, they were able to avoid photodamage and to maximize carbon fixation rates also at excessive light levels. Further, the organization and timing over the day of the different cellular activities (such as pigments synthesis) not only would increase the efficiency in responding to environmental perturbation but in the use of the resources too. Clearly this efficiency and flexibility could be ones of the elements to explain the observed importance of ultraphytoplankton in the coastal areas, such as st. MC. On the other hand, it again suggest that a biotic control (such as grazing) more than a physic one is responsible of the less contribution of this fraction during the bloom periods.

## CHAPTER 6

### **Photophysiological responses of five ultraphytoplankton species exposed to high irradiance**

The mechanisms of photoprotection were investigated on five ultraphytoplankton monospecific cultures, with different pigments content (i.e. golden-brown and green algae), in order to explore their characteristics and possible peculiarities related to the size (see section 1.2). The selected species were: two Bacillariophyceae (*Papiliocellulus simplex*, *Minidiscus comicus*), two Prymnesiophyceae (*Imantonia rotunda* and *Phaeocystis* sp.) and a Prasinophyceae (*Micromonas pusilla*), chosen for their ecological relevance and/or their pattern of occurrence.

Two short experiments (CULT-1 and CULT-2) were carried out to test photoprotective pigments (e.g. xanthophylls cycle) changes under high irradiance and their relationship with variable fluorescence parameters. Since the adopted frequency of sampling did not permit to determine contemporary the photosynthetic coefficients (e.g. electron transport rate) and *non-photochemical quenching* (NPQ) we chose to focus our attention on the first ones. This choice was aimed at outlining the changes in the photophysiological state of the cells more than the extent of dissipative processes, making the most of the improvement in the new Phyto-PAM technique (see section 3.2).

In the first experiment CULT-1, we investigated the answers of cultures grown at different irradiance regimes when they are exposed to excessive light. In the second (CULT-2), we studied the possible differences in photoprotection occurring in culture pre-adapted to variable light-regime.

A short description of the morphological and ecological characteristics of the five studied species is provided in the section below, while the experimental protocol and the most relevant results were presented in the sections 6.2 and 6.3.

#### **6.1 Species description**

Unialgal cultures of each species were obtained from Serial Dilution Cultures (SDC) of natural samples collected during the cruises Norbal4 and Norbal5 (March -April 2003; NW Mediterranean Sea). The list of species and the location of the stations where the samples were collected are shown in Table 6.1. The isolation of the five monospecific cultures was

performed by the researchers of the Marine Botany laboratory of the Zoological Station “A. Dohrn” of Naples.

Species	Class	Station Location
<i>Papiliocellulus simplex</i>	Bacillariophyceae	Lat. 41° 27 N Long. 5° 22 E
<i>Minidiscus comicus</i>	Bacillariophyceae	Lat. 41° 10 N Long. 5° 15 E
<i>Imantonia rotunda</i>	Prymnesiophyceae	Lat. 41° 35 N Long. 4° 09 E
<i>Phaeocystys</i> sp.	Prymnesiophyceae	Lat. 41° 40N Long. 4° 86 E
<i>Micromonas pusilla</i>	Prasinophyceae	Lat. 41° 35 N Long. 4° 09 E

**Table 6.1** – List of species cultures used for experiments.

### *Papiliocellulus simplex*

This small diatom (family Cymatosiraceae) was described for the first time by Gardener and Crawford (1992) from British coastal waters. The cells are elliptical in valve view (about 2µm wide and 5µm long) and rectangular in girdle view (about 4µm thick) (Fig. 6.1a). They are heterovalvate for the presence of a tubular process at the centre of one valve only. The frustule is siliceous and at each apex there is an ocellulus with 4-5 porelli. The girdle bands lacks pores. Non-dividing cells present only one plastid partly against valve face, partly against the girdle surface. The ecology and distribution of this species is basically unknown. The light harvesting complexes (LHC) of *P. simplex* have Chlorophyll  $c_1+c_2$ , Fucoxanthin (the principal carotenoid),  $\beta$ -carotene and xanthophylls cycle containing Diadinoxanthin and Diatoxanthin.

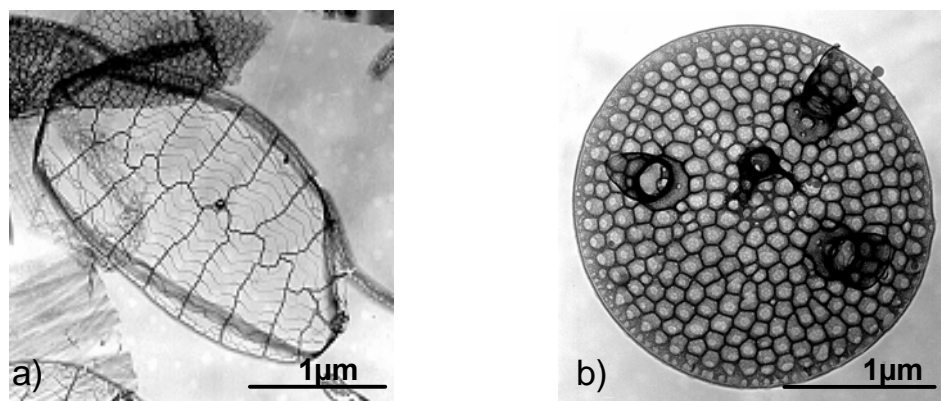


**Figure 6.1** – Transmission Electron Micrographs (TEM) of *P. simplex* (a) and *M. comicus* (b) - Valve view.

*Minidiscus comicus*

The genus *Minidiscus* (family Thallasiosiraceae) include the smallest centric diatoms of marine phytoplankton, with diameters ranging from 1.90 to 7.5  $\mu\text{m}$ . *Minidiscus comicus* was first observed in Japanese waters by Takano (1981). The cells are circular in valve view (diameter 2-3.5  $\mu\text{m}$ ) and possess three satellite pores (Fig. 6.1b). The cribrum is scarcely perforated. Each cell has one or two chloroplast. *M. comicus* usually consists of a single cell, but it can form aggregate flocks (Takano 1981). This species has a wide distribution in subtropical-temperate waters (Akè-Castillo *et al.*, 2001). For instance, it may be very important in phytoplankton blooms, occurring in the North-Western Mediterranean (Sarno *et al.*, 2004) as well as in the coastal area of the Gulf of Naples (Ribera d'Alcalà *et al.*, 2004). *M. comicus* have almost the main pigment composition of the other diatom species, *P. simplex*.

*Imantonia rotunda*

This species was described for the first time by Reynolds (1974). The cells are motile, more or less spherical, diameter 3-4 $\mu\text{m}$  (Fig. 6.2a). The two flagella are smooth and equal, a haptonema is absent. The chloroplasts are parietal and usually two in young cells, sometimes four-five in older ones. Opposite to the flagellar pole there are two or three vesicles containing leucosin. Little is know about the ecology and distribution of this small flagellate. The light harvesting complexes (LHC) of *I. rotunda* have again chlorophyll  $c_1+c_2$ , but also chlorophyll  $c_3$ . On the other hand, 19'Hexanoylfucoxanthin is the main carotenoid, though Fucoxanthin and 19'Butanoiloxifucoxanthin are even present. The other pigments are:  $\beta$ -carotene, Lutein and xanthophylls cycle containing Diadinoxanthin and Diatoxanthin.

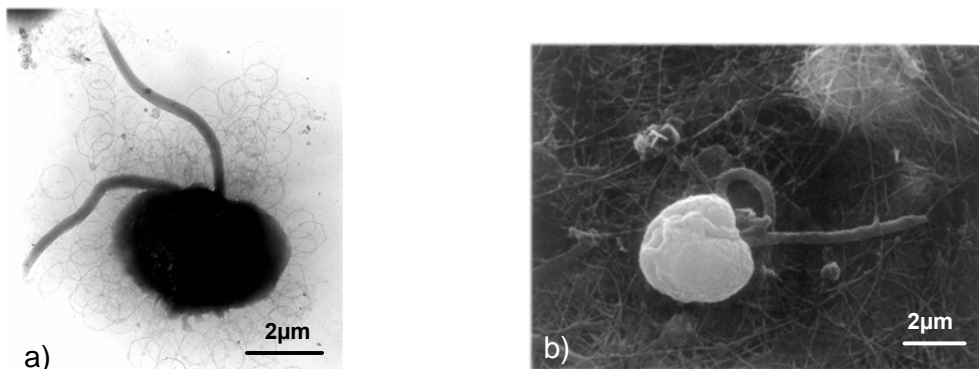


**Figure 6.2** – Transmission Electron Micrographs (TEM) of *I. rotunda* (a) and Scanning Electron Micrographs (SEM) of *Phaeocystis* sp.(b).  
*Phaeocystis* sp.

*Phaeocystis* is recognized both as a nuisance and as an ecologically important phytoplankter species. Its polymorphic life cycle with both colonial and flagellated cells causes many taxonomic problems.

This taxon includes strains isolated from the North-Western Mediterranean Sea during the Norbal cruise of spring 2003. It is very similar to strains MEDNS2 and MEDNS3 (Zingone *et al.* 1999b) isolated by Natalie Simon in the same area. Being single-celled and similar in scale morphology, it was preliminarily attributed to *P. cordata*, but it has morphological differences that were initially unappreciated. As compared to *P. cordata*, *Phaeocystis* sp. is somewhat larger, has a rounded body, shorter flagella and the larger body scales are circular rather than oval. In addition, it forms huge amounts of mucus that have so far hindered molecular analyses.

*Phaeocystis* sp. has a pigment composition similar to *I. rotunda*, except that the main carotenoid is Fucoxanthin.

#### *Micromonas pusilla*

It is one of the smallest known flagellates, described for the first time by Butcher (1952) with the name of *Chromulina pusilla*. The actual name is due to Manton and Parke (1960), who described more in details the cell ultrastructure. The cells are 1-3  $\mu\text{m}$  long, with a single posterior flagellum divided into a very short basal part and a longer hairpoint which contains only the central pair of flagellar axoneme microtubules. There is a single chloroplast with a pyrenoid, while an eyespot is lacking. Both the flagellum and the cell wall are naked. *M. pusilla* is distributed in all seas and often occurs in very large numbers (Guillou *et al.*, 2004).



**Figure 6.3** – Scanning Electron Micrographs (SEM) of *M. pusilla*.

*M. pusilla* has a light harvesting complex similar to plants, containing Chlorophyll *b*,  $\beta$ -carotene, Lutein and a xanthophylls cycle with Violaxanthin, Antheraxanthin and Zeaxanthin. Furthermore, this species contains Prasinoxanthin, Neoxanthin, a Chlorophyll *c*-like (MgDVP) and small amounts of urolide serie pigments just reported by Egeland *et al.*, 1995.

### 6.1.1 Culture conditions

The cultures were grown in Nalgene sterile square media bottles, bubbled with filtered air. The medium was 0.22  $\mu\text{m}$ -filtered and sterilized seawater, enriched with f/2 Guillard nutrients for diatoms (Guillard, 1983) and with K for the other species (Keller *et al.*, 1987). All cultures were frequently examined by means of light microscopy to exclude the presence of contaminating algae and sterile technique was employed to minimize bacterial contamination. Cultures of each species, kept in turbidostat-like conditions, were generally pre-adapted to experimental settings for at least three weeks in controlled culture chambers with a temperature of 20°C and a 14:10 LD cycle. Growth irradiance was provided by fluorescing lamps and dosed to the cells as a “block” regime (i.e. a rectangular on/off light climate). The photon flux density (PFD) was measured inside the Nalgene bottles filled with filtered seawater, utilizing a PAR  $4\pi$  sensor of Biospherical Instruments (mod. QSL-101).

The “block” mode, which we used to light supply, may affect the photoprotective carotenoids content, as recently showed in some studies, comparing different ways of light supply (Garcia-Mendoza *et al.*, 2002). For instance, it is probably responsible for the high DPS state found in the ML cultures before CULT-1 experiment started. On the other hand, we can reasonably exclude interference in the CULT-2 experiment, since HPLC samples taken immediately before and after the on/off switch show negligible variations in xanthophylls pool content and DPS state.

Notwithstanding the care to homogenize the culture suspensions during the experiments and to dilute them, when working in turbidostat-like mode, we can not rule out errors in the estimates of pigment content and cell concentration due to an inefficient mixing or inexact dilution. However, some replicate samples of HPLC and FCM were taken, revealing relatively low variance in pigments content and cells number, so that we can at least exclude large errors due to sampling or analytical procedures. Furthermore, the pigments content was averaged over the Chlorophyll *a* and/or cells number to mitigate the eventual differences between sub-samples.

## 6.2 CULT-1

The CULT-1 experiment was carried out on cultures grown at different irradiance regimes. In particular, for each studied species, one culture, called Low Light (LL), was acclimated at a PFD of  $80\mu\text{mol photons m}^{-2} \text{ s}^{-1}$ , the other one, called Medium Light (ML), was acclimated at a PFD of  $300\mu\text{mol photons m}^{-2} \text{ s}^{-1}$  for at least three weeks. When the experiment started, the two cultures were exposed for 4 hours to a high light (PFD =  $1200\mu\text{mol photons m}^{-2} \text{ s}^{-1}$ ), provided by a HQI-T 250W/D lamp (Osram). The temperature was kept constant ( $20 \pm 0.1^\circ \text{C}$ ) by a controlled water bath and the cultures were under aeration. No further dilution (batch mode) was provided when the experiment took place. Samples for pigment determination (HPLC) and for *in vivo* variable fluorescence measurements (Phyto-PAM) were taken at 0, 5, 15, 60, 120, 240 min. Sampling and technical procedures were described in detail in the section 3.2. During the experiment the de-epoxidation state of the xanthophylls cycle (DPS) was calculated as the ratio between Diatoxanthin and the sum of Diadinoxanthin and Diatoxanthin,  $Dt/(Dd+Dt)$ , for the golden-brown algae and as the ratio between the sum of Zeaxanthin and  $0.5 \times$  Antheraxanthin and all the xanthophyll cycle pool,  $Z+0.5A/(V+A+Z)$ , for the green algae, according to Casper-Lindley and Björkman, (1998). The photoprotective carotenoids (PPC) were calculated as the sum of the pigments of xanthophyll cycle (Dd, Dt, V, A, Z),  $\beta$ -carotene and Lutein.

### 6.2.1 Pigments

Before the high-light treatment, all the five species showed, a higher photoprotective carotenoids (PPC)/ Chl *a* ratio in the ML cultures than in the LL ones (Table 6.2). The lowest difference was recorded between the two cultures of *P. simplex* and the highest in *I. rotunda*.

Species	LL	ML
<i>P. simplex</i>	0,19	0,25
<i>M. comicus</i>	0,23	0,49
<i>I. rotunda</i>	0,22	0,55
<i>Phaeocystis</i> sp.	0,21	0,41
<i>M. pusilla</i>	0,22	0,35

**Table 6.2** – Photoprotective carotenoids / Chlorophyll *a* ratio (PPC/Chl *a*) in the LL and ML cultures, before CULT-1 experiment.

These differences were essentially due to an increase of xanthophyll cycle pigments in the ML cultures (Fig. 6.4).

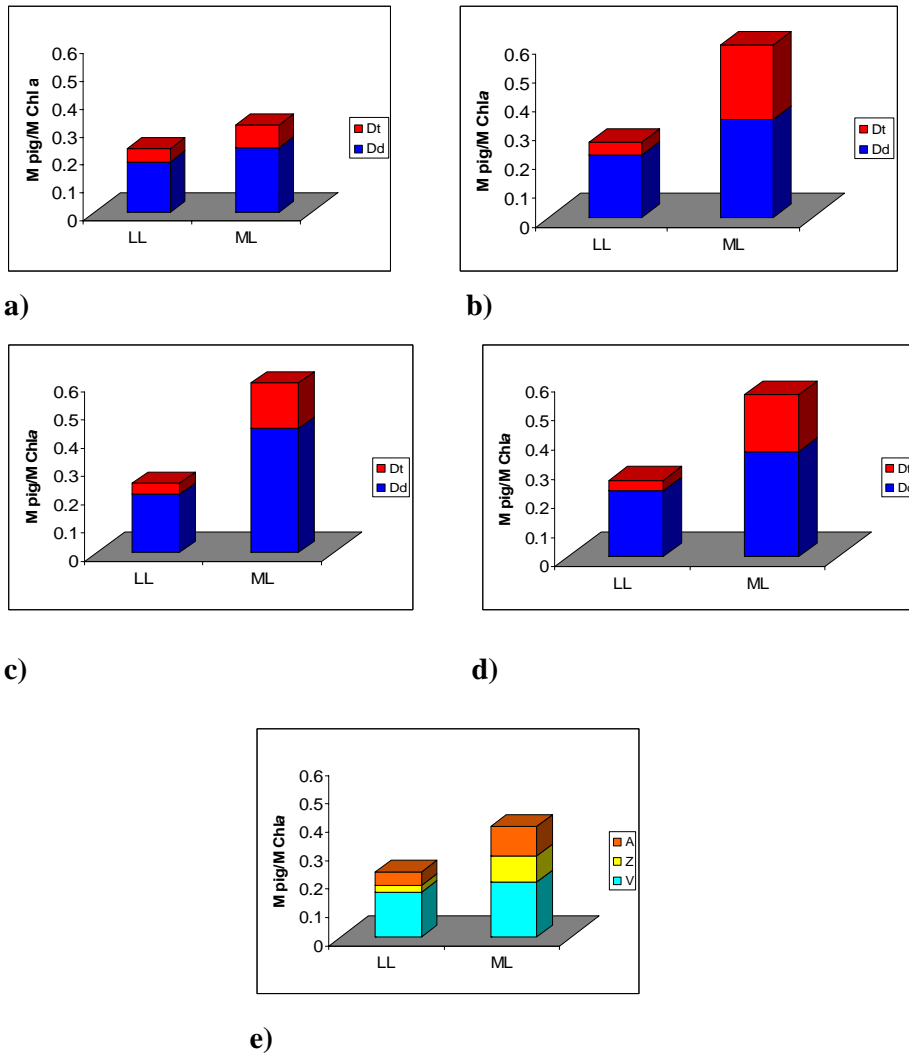


**Figure 6.4** – Pigments /Chlorophyll *a* ratio (Mpig/MChl *a*) l in the LL and ML cultures of *P. simplex* (a), *M. comicus* (b), *I. rotunda* (c), *Phaeocystis* sp. (d) and *M. pusilla* (e), before CULT-1 experiment.

The highest increase was observed in *I. rotunda*, where Diatoxanthin (Dt) content per Chl *a* in the ML culture exceeded by ~ 10 fold that of LL culture (Fig. 6.4c) and the lowest increment was observed in *P. simplex* (only 20% of increase in the ML culture) (Fig. 6.4a). In *M. pusilla*, the de-epoxidized form (Zeaxanthin) showed the highest increase (0.04 and 0.10 in LL and ML cultures respectively) (Fig. 6.4e).

The photosynthetic pigment content per Chl *a* did not present significant changes between the ML and LL cultures of each investigated species (data not shown).

Before the high-light treatment the DPS state of the ML cultures was higher than the LL one, while they displayed quite similar values at the end of the experiment (Tab.6.3, Fig. 6.5).

	LL		ML	
	DPS-0h	DPS-4h	DPS-0h	DPS -4h
<i>P. simplex</i>	0.20	0.71	0.28	0.68
<i>M. comicus</i>	0.16	0.51	0.43	0.72
<i>I. rotunda</i>	0.15	0.85	0.44	0.81
<i>Phaeocystis</i> sp.	0.14	0.79	0.34	0.75
<i>M. pusilla</i>	0.15	0.50	0.38	0.65

**Table 6.3** – DPS state in the LL and ML cultures, before and after CULT-1 experiment.

In the golden-brown algae, DPS increase was very rapid, with more than 80% of increment after only 5 min, then the values remained quite constant (Fig. 6.5a,b). In the green algae *M. pusilla* the changes were less pronounced, above all in the ML culture. However, in the LL culture the increase was again rapid (~60% of increment after 5min) (Fig. 6.5c).

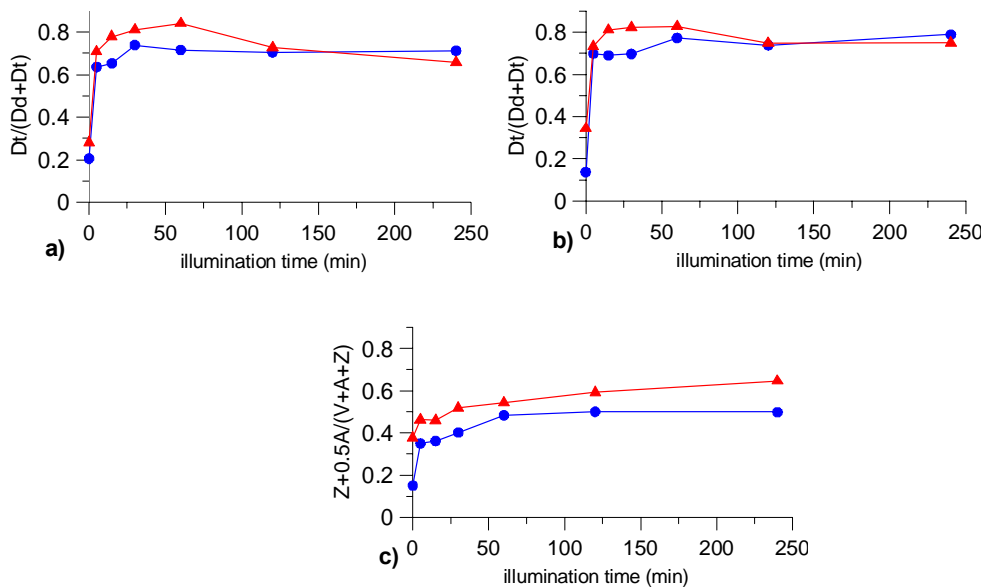


**Figure 6.5** – DPS state in LL (●) and ML (▲) cultures of *P. simplex* (a), *Phaeocystis* sp. (b) and *M. pusilla* (c) during CULT-1 experiment.

In all the species a *de novo* synthesis of xanthophyll cycle pigments occurred during the high-light treatment and was higher in the ML cultures than in the LL ones (data not shown).

In all the species, the other photoprotective carotenoids and the photosynthetic pigments of all the cultures did not change during CULT-1 experiment (data not shown). The only exception was Lutein in *M. pusilla*: at the end of the experiment the content of Lutein per Chl *a* exceeded the initial value by 5 folds in both the grown cultures (Fig. 6.6).

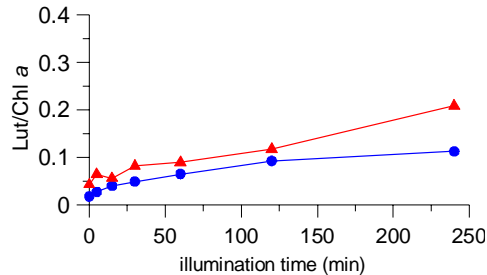


**Figure 6.6** – Lutein/Chl *a* ratio (MLut/MChl *a*) of LL (●) and ML (▲) cultures of *M. pusilla* during CULT-1 experiment.

On the other hand, small amounts of V- cycle pigments were recorded in both LL and ML cultures of golden-brown algae, accounted for less than 5% of the PPC pool. In particular, Zeaxanthin showed a slight increase at the end of the high light treatment, though a clear pattern was not evident (data not shown).

### 6.2.2 Phyto-PAM coefficients

The photosynthetic coefficients as derived from the Phyto-PAM measurements showed clear changes during the high-light exposure in both LL and ML cultures (Tab. 6.4 and 6.5, Fig. 6.7).

In ML culture of *I. rotunda* all the Phyto-PAM derived coefficients became undetermined after 2h of exposure. It is probably due to a stress condition of the culture, since it had not been diluted for the two days before the experiment.

A very rapid decrease of  $F_v/F_m$  ratio and  $\alpha_{PAM}$  values was observed in all the cultures (>75% of reduction after only 5 min). In particular, in the two diatoms the pre-treatment and the final (after 4h) values were quite similar in both LL and ML cultures (Tab. 6.4 and 6.5). In the other species  $F_v/F_m$  and  $\alpha_{PAM}$  was higher and decreased more in the LL cultures than in the ML one (Fig. 6.7).

The pre-treatment  $rEtr_{max}$  values of the two diatoms *P. simplex* and *M. comicus*, were higher than the other species. A decrease of  $rEtr_{max}$  was observed during the experiment, though less rapid than observed for the other coefficients. Again, the variations were quite similar in both LL and ML cultures of the two diatoms, while in the other specie the LL

cultures showed a more pronounced decrease (Fig. 6.7c,g,m). The smallest change was observed in the green algae *M. pusilla*.

The  $E_{kPAM}$  values during the high-light exposure were characterized by an increase in the two diatoms species and in the LL culture of *I. rotunda*. The changes were less pronounced in *M. pusilla* (Fig. 6.7n). By contrast, in both *Phaeocystis* sp. cultures  $E_{kPAM}$  showed a slight decrease (Fig. 6.7h).

**LL (Phyto-PAM coefficients)**

Species	$F_v/F_m$		$\alpha_{PAM}$		$rE_{tr_{max}}$		$E_{kPAM}$	
	0h	4h	0h	4h	0h	4h	0h	4h
<i>P. simplex</i>	0.58	0.10	0.27	0.07	25.0	14.7	93	210
<i>M. comicus</i>	0.57	0.16	0.24	0.10	25.3	16.0	104	170
<i>I. rotunda</i>	0.50	0.04	0.27	0.02	10.3	0.2	38	200
<i>Phaeocystis</i> sp.	0.54	0.05	0.25	0.03	13.9	0.5	55	30
<i>M. pusilla</i>	0.63	0.06	0.26	0.03	12.1	1.6	47	79

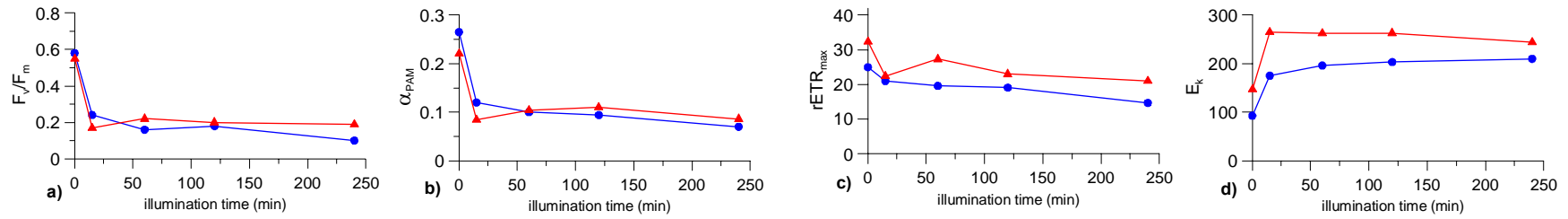
**Table 6.4** – Phyto-PAM derived coefficients in the LL cultures, before (0h) and after (4h) CULT-1 experiment.

**ML (Phyto-PAM coefficients)**

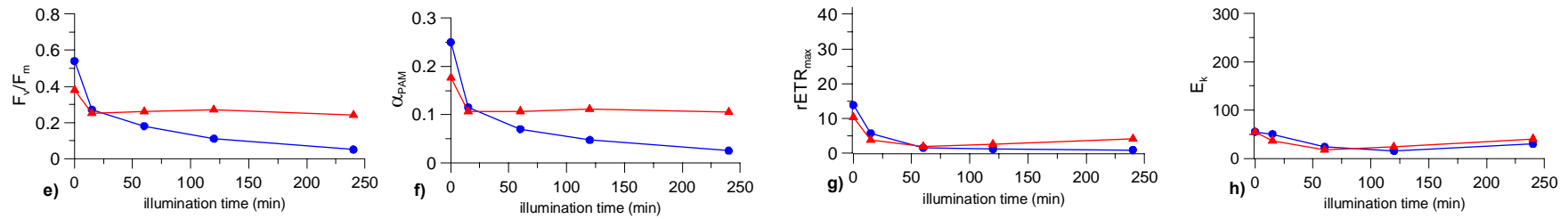
Species	$F_v/F_m$		$\alpha_{PAM}$		$rE_{tr_{max}}$		$E_{kPAM}$	
	0h	4h	0h	4h	0h	4h	0h	4h
<i>P. simplex</i>	0.55	0.19	0.22	0.09	32.4	21.0	146	243
<i>M. comicus</i>	0.50	0.15	0.22	0.10	28.4	20.7	131	200
<i>I. rotunda</i>	0.28	-	0.13	-	8.0	-	62	-
<i>Phaeocystis</i> sp.	0.38	0.24	0.18	0.10	10.4	4.2	55	40
<i>M. pusilla</i>	0.47	0.21	0.21	0.09	11.4	8.6	54	71

**Table 6.5** – Phyto-PAM derived coefficients in the ML cultures, before (0h) and after (4h) CULT-1 experiment.

*P. simplex*



*Phaeocystis* sp.



*M. pusilla*

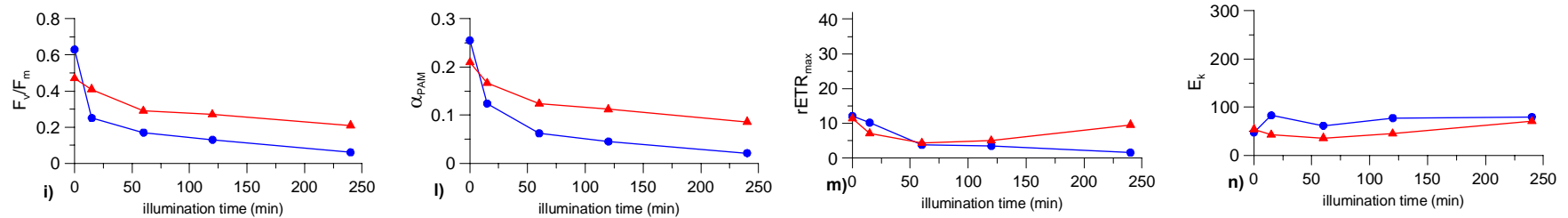


**Figure 6.7** – Variations in time of F<sub>v</sub>/F<sub>m</sub>, α<sub>PAM</sub>, rETR<sub>max</sub> and E<sub>kPAM</sub> of *P. simplex* (a,b,c,d), *Phaeocystis* sp. (e,f,g,h) and *M. pusilla* (i,l,m,n) in LL (●) and ML (▲) cultures during CULT-1 experiment.

### 6.3 CULT-2

The CULT-2 experiment aimed at testing the possible differences in photoprotection responses in cultures experiencing periodical high irradiance. In addition, the possibly more effective role in golden-brown algae photoprotection of Violaxanthin cycle was investigated.

For each species, one culture, called Pre-Adapted (PA), was adapted for one month at  $40\mu\text{mol photons m}^{-2} \text{s}^{-1}$ , and then it was exposed to a high-light cycle of 4 hours per day (for at least 10 days), to allow acclimation before the experiment started. Another culture, called Control Culture (CC) was only adapted at a growth irradiance of  $40\mu\text{mol photons m}^{-2} \text{s}^{-1}$  for at least one month and used as control. During the 4h high-light cycles the PFD was  $700\mu\text{mol photons m}^{-2} \text{s}^{-1}$  provided by a HQI-T 250W/D lamp (Osram). A controlled water bath kept the temperature constant ( $20 \pm 0.1^\circ \text{C}$ ) and the cultures were aerated and kept in turbidostat-like conditions. When the experiment started, the two cultures (CC and PA) were exposed to high light (PFD=  $700\mu\text{mol photons m}^{-2} \text{s}^{-1}$ ) for 4h, without further dilution (batch mode). In this experiment the sampling were collected with an higher frequency than the previous one, to allow a better definition of the photoprotection mechanisms involved. Samples for cell counting (FCM) and pigment content determination (HPLC) were taken at 0-1-2-3-5-6-8-10-15-20-25-30-45-60-120-240 min, while the samples for Phyto-PAM measurements were taken at 0-10-30-45-60-120-240 min. After the high-light treatment the two cultures were put back to the initial growth irradiance ( $40\mu\text{mol photons m}^{-2} \text{s}^{-1}$ ) and samples were taken in order to study the epoxidation kinetics as well as the recovery of the photosynthetic apparatus after the stress. Again, samples for cell counting (FCM) and pigment content determination (HPLC) were taken at 0-1-2-3-5-6-8-10-15-20-25-30-45-60-150 min, while the samples for Phyto-PAM measurements were taken at 0-10-30-45-60-150 min.

The sampling and technical procedures were described in detail in the section 3.2. The de-epoxidation state (DPS) and the photoprotective carotenoids (PPC) were calculated as described in the section 6.2.

#### 6.3.1 Pigments

Before the exposure to the high-light cycles, PPC/Chl *a* ratio showed quite similar values in the CC and PA cultures of each species (data not shown). By contrast, after the ten cycles of 4h high-light treatment, all the PA cultures showed a higher PPC/ Chl *a* ratio (Table 6.6).

The lowest difference in the PPC/ Chl *a* ratio was recorded, between the two cultures of *P. simplex* and the highest in *M. pusilla*.

Species	CC	PA
<i>P. simplex</i>	0.12	0.14
<i>M. comicus</i>	0.08	0.18
<i>I. rotunda</i>	0.11	0.17
<i>Phaeocystis</i> sp.	0.11	0.16
<i>M. pusilla</i>	0.10	0.21

**Table 6.6** – Photoprotective carotenoids Chlorophyll *a* ratio (PPC/Chl *a*) in CC and PA cultures, before CULT-2 experiment started.

The pigment content per cell indicated that in the PA cultures there was a contemporary increase of the xanthophyll pool and a reduction of Chlorophyll *a* (data not shown).

*P. simplex* showed little differences between the two cultures: Dd/Chl *a* rose from 0.09 to 0.12, while Dt/Chl *a* from 0.02 to 0.04 (Fig. 6.8a). By contrast, a greater increase was observed in *M. comicus*, where Dd and Dt of PA culture exceeded by 5 and 7 fold respectively the CC values (data not shown). In *Phaeocystis* sp., the increase involved essentially the Dd pool (Dd/Chl *a* = 0.10 and 0.16 in the CC and PA respectively) (Fig. 6.8c) and *I. rotunda* showed a very similar pattern (data not shown).

In all the golden-brown algae the PA cultures showed an increase in the Violaxanthin-cycle content, though its contribute remained negligible (<10% of the PPC pool) and was an order of magnitude lower than that of the Diadinoxanthin cycle (Fig. 6.8). The highest V-cycle pool increase was observed in the two diatoms (Fig. 6.8a). Also *M. pusilla* showed a marked increase of both Violaxanthin (from 0.06 to 0.21) and Zeaxanthin (from 0.005 to 0.019) (Fig. 6.8e).

As in CULT-1 experiment, the pre-treatment values of the other photoprotective pigments and of photosynthetic pigments did not display significant differences between CC and PA cultures (data not shown).

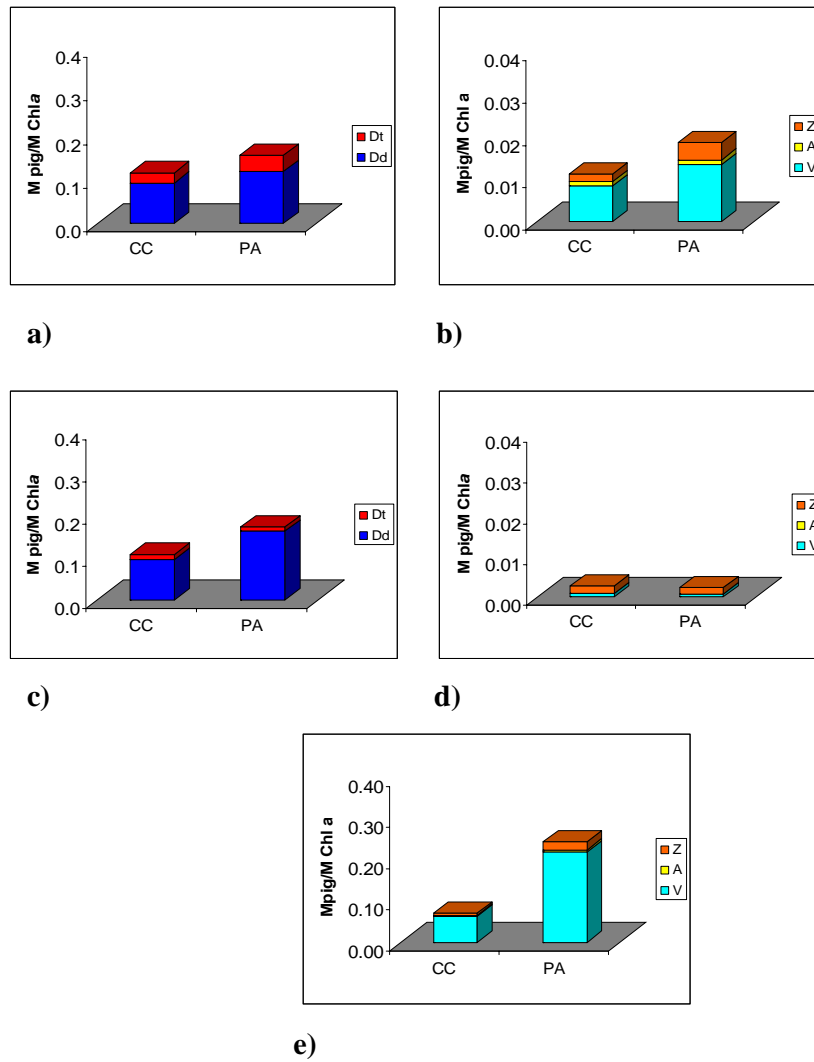


**Figure 6.8** – Pigments /Chlorophyll *a* ratio (Mpig/MChl *a*) of Diadinoxanthin cycle (a) and Violaxanthin cycle (b) in *P. simplex* and of Diadinoxanthin cycle (c) and Violaxanthin cycle in *I. rotunda* (d) and in *M. pusilla* (e) before CULT-2 experiment.

Each species showed a quite similar DPS state between the CC and PA cultures, with the lowest values recorded in *I. rotunda* (Tab. 6.7). When the experiment began, DPS increased very rapidly in all the species (Fig. 6.9) though with significant differences between CC and PA cultures.

	CC			PA		
	DPS 0h	DPS 4h	DPS -AI	DPS 0h	DPS 4h	DPS -AI
<i>P. simplex</i>	0.20	0.79	0.23	0.24	0.70	0.20
<i>M. comicus</i>	0.11	0.60	0.21	0.18	0.68	0.19
<i>I. rotunda</i>	0.03	0.54	0.21	0.02	0.67	0.05
<i>Phaeocystis</i> sp.	0.11	0.66	0.16	0.08	0.60	0.14
<i>M. pusilla</i>	0.09	0.41	0.15	0.09	0.22	0.13

**Table 6.7** – DPS state in the CC and PA cultures, at 0h, after 4h of high-light and after 150 min (AI) at growth irradiance (see text), CULT-2 experiment.

For instance, in *P. simplex* cultures DPS increased of ~ 30% after only 1 min (Fig. 6.9a). A similar pattern was observed in *M. comicus*, with an increase of ~25% (data not shown). By contrast, in CC culture of *I. rotunda* DPS showed a less pronounced increase than the PA one (8% and ~30% respectively after 1min) (Fig. 6.9b). The lowest DPS changes were recorded in the PA culture of *M. pusilla* (Tab. 6.7; Fig. 6.9c).

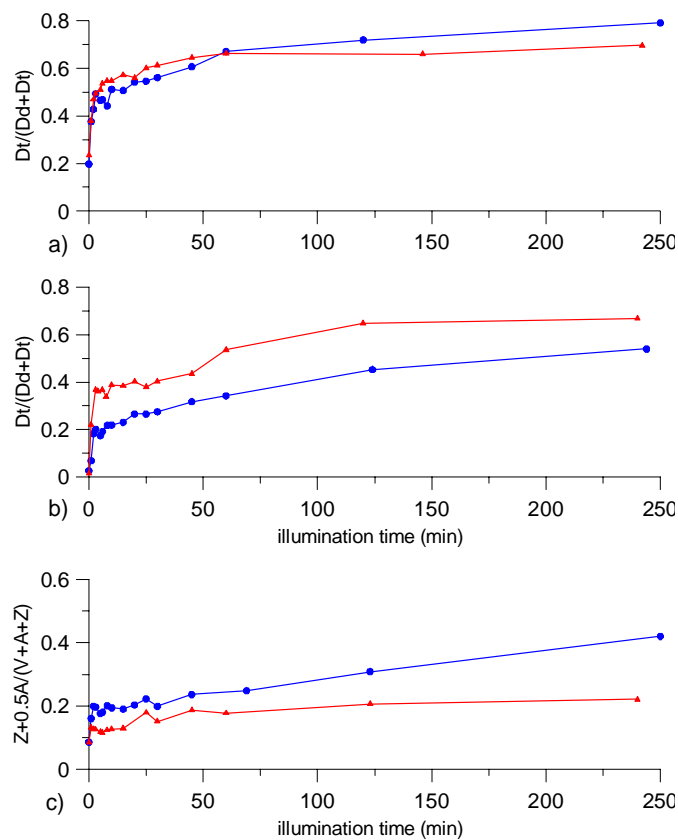


**Figure 6.9** – DPS state in CC (●) and PA (▲) cultures of *P. simplex* (a), *I. rotunda* (b), and *M. pusilla* (c) during CULT-2 experiment.

In CULT-2 experiment the *de novo* synthesis of D-cycle pigments (essentially Diadinoxanthin) was higher in the PA cultures than in the CC ones (Fig. 6.10). By contrast, in *M. pusilla* a new synthesis occurred only in the CC culture (data not shown).

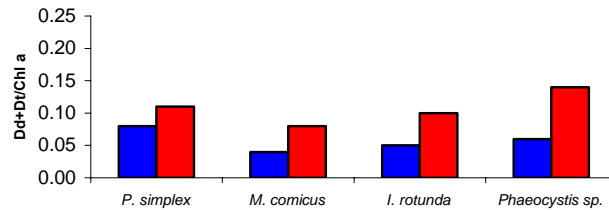


**Figure 6.10** –Newly synthesized (Dd+Dt)/Chl *a* ratio after high-light treatment (4h) of CC (blue area) and PA (red area) in CULT-2 experiments.

In the golden-brown algae, the V-cycle pool showed an increase at the end of the experiment, however not clear pattern was recognizable in the DPS state, since almost the main pool was in the de-epoxidized form just at the beginning of the experiment. The only exception was *P. simplex*: both CC and PA cultures displayed DPS values quite constant in the first 30 min of exposure and then they increased until the end of the experiment (Fig. 6.11).

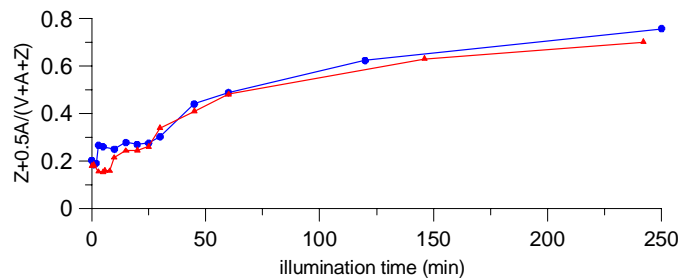


**Figure 6.11** – DPS state of Violaxanthin cycle in CC (●) and PA (▲) cultures of *P. simplex* during CULT-2 experiment.

The lower importance of V-cycle in the photoprotection of golden-brown algae was indicated by their contribution to the newly synthesized xanthophylls during the high-light treatment of both CULT-1 and CULT-2 experiment (Tab. 6.8).

	CULT-1		CULT-2	
	LL	ML	CC	PA
<i>P. simplex</i>	28.7	25.5	9.6	5.6
<i>M. comicus</i>	28.3	25.7	14.8	9.1
<i>I. rotunda</i>	14.3	0.9	10.4	5.5
<i>Phaeocystis</i> sp.	12.4	15.9	9.6	4.3

**Table 6.8** – Percentage of newly synthesized V-cycle pigments (normalized for Chl *a* content) after the 4h treatment, CULT-1 and CULT-2 experiments.

In all the cultures the other photoprotective carotenoids and the photosynthetic pigments did not change, with the only exception of Lutein in *M. pusilla* (data not shown).

When cultures were put back to the initial growth irradiance (i.e. 40  $\mu\text{mol photons m}^{-2} \text{s}^{-1}$ ) the DPS state decreased and after 150 min reached values generally similar to the pre-treatment ones, though higher (Tab. 6.7). However, the kinetics of epoxidation was generally more rapid in the PA cultures than in the CC ones (Fig. 6.12). For instance, after 30 min, DPS reached 40% and 54% of total decrease in CC and PA cultures of *P. simplex* respectively (Fig. 6.12a). *M. comicus* and *Phaeocystis* sp. showed a pattern similar to that of *P. simplex* (data not shown); while in *I. rotunda* the highest differences between the two cultures were observed. In particular the DPS varied linearly in the CC culture (Fig. 6.12b). Again, the lowest change was observed in the PA culture of *M. pusilla* (Tab. 6.7; Fig. 6.12c).

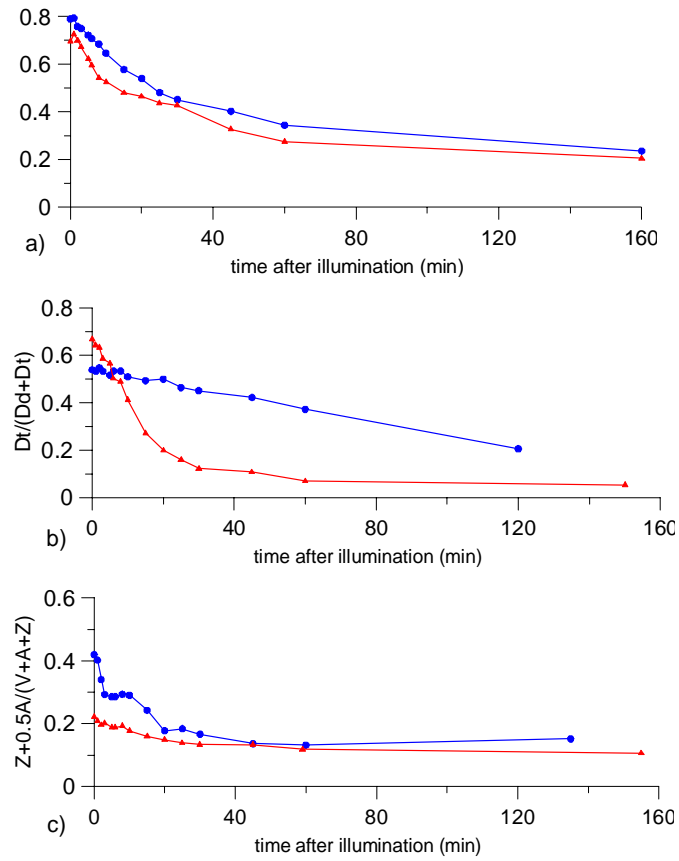


**Figure 6.12** – DPS state in CC (●) and PA (▲) cultures of *Papiliocellulus simplex* (a), *I. rotunda* (b) and *M. pusilla* (e) after the high-light treatment of CULT-2 experiment.

### 6.3.2 Phyto-PAM coefficients

In CULT-2 the Phyto-PAM coefficients showed differences in the photophysiological responses between CC and pre-adapted (PA) cultures (Tab. 6.9 and 6.10; Fig. 6.13). Unlike LL and ML cultures of CULT-1, initial CC values of  $\alpha_{\text{PAM}}$  were almost all the same of the PA ones in all the species. The pre-treatment (0h)  $r\text{Etr}_{\text{max}}$  values were quite similar in the cultures of *P. simplex* and *M. comicus*, while in the other species the PA cultures exceeded the values of the CC ones by more than 2 fold.

In *P. simplex* and *M. comicus* the two cultures showed very similar variations in  $F_v/F_m$  ratio and  $\alpha_{\text{PAM}}$ , while the two prymnesiophytes, *I. rotunda* and *Phaeocystis* sp., displayed a higher decrease in the CC cultures than in the PA one. For both coefficient the highest variations were observed in the CC culture of *I. rotunda* (Tab. 6.9, 6.10), which showed also the “sharp” decrease (60% of change after 30 min) (Fig. 6.13e,f); while the lowest variations were recorded in the PA culture of *M. pusilla* (Fig. 6.13i,l).

$r\text{Etr}_{\text{max}}$  followed the patterns of the other two coefficients: a decrease, but less pronounced in the PA cultures. The highest changes were observed in *I. rotunda*. At the end of the experiment (4h), the  $r\text{Etr}_{\text{max}}$  was 5 and 3 fold lower than the pre-treatment ones in the CC and PA culture respectively (Fig. 6.13g).

$E_{\text{kPAM}}$  values were characterized by an increase, although marked differences were observed between the species. In particular, in *P. simplex*  $E_{\text{kPAM}}$  increased in the first 30 min of exposure (from 71.0 to 95.1  $\mu\text{mol photons m}^{-2} \text{s}^{-1}$  in CC culture and from 83.4 to 129.8  $\mu\text{mol photons m}^{-2} \text{s}^{-1}$  in the PA one) and subsequently decreased until the end of the experiment (Fig.6.13d). In the other diatom, *M. comicus*, there was a regular increase, with higher change in the PA culture than in the CC one (Tab. 6.9-6.10).

*I. rotunda* was the species with the most pronounced increase of  $E_{\text{kPAM}}$  (Fig. 6.13h). As in *Phaeocystis* sp.,  $E_{\text{kPAM}}$  values showed only a slight increase in *M. pusilla* CC culture; while in the PA one the values were quite constant in the first 2h of high-light exposure and after showed a sharp increase (Fig. 6.13n).

**CC (Phyto-PAM coefficients)**

Species	$F_v/F_m$			$\alpha_{PAM}$			$rEtr_{max}$			$E_{kPAM}$		
	0h	4h	AI	0h	4h	AI	0h	4h	AI	0h	4h	AI
<i>P. simplex</i>	0.70	0.42	0.64	0.29	0.17	0.27	20.5	12.0	15.6	71	76	59
<i>M. comicus</i>	0.68	0.25	0.44	0.26	0.12	0.20	28.8	16.3	22.3	110	133	110
<i>I. rotunda</i>	0.67	0.04	0.24	0.29	0.02	0.10	10.3	1.9	7.8	36	126	75
<i>Phaeocystis</i> sp.	0.66	0.29	0.47	0.29	0.12	0.20	16.3	6.9	11.0	57	58	55
<i>M. pusilla</i>	0.65	0.27	0.50	0.26	0.11	0.20	16.1	8.1	15.0	63	77	75

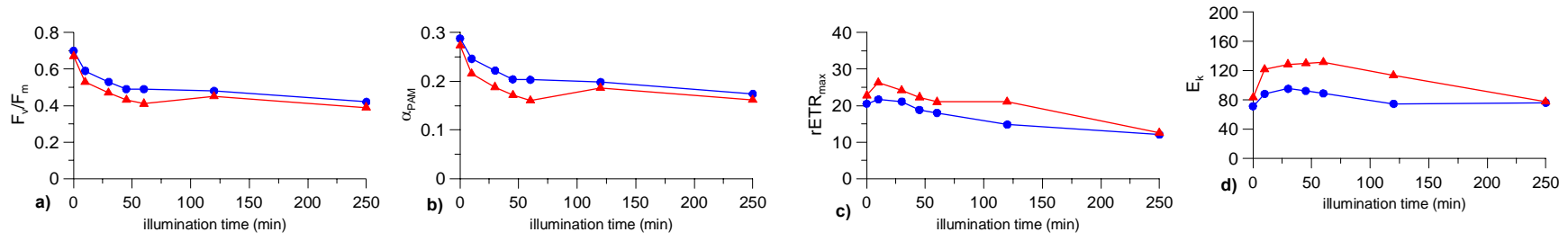
**Table 6.9** – Phyto\_PAM derived coefficients in the CC cultures, before (0h), after 4h of high-light and after 150 min (AI) at growth irradiance (see text), CULT-2 experiment.

**PA (Phyto-PAM coefficients)**

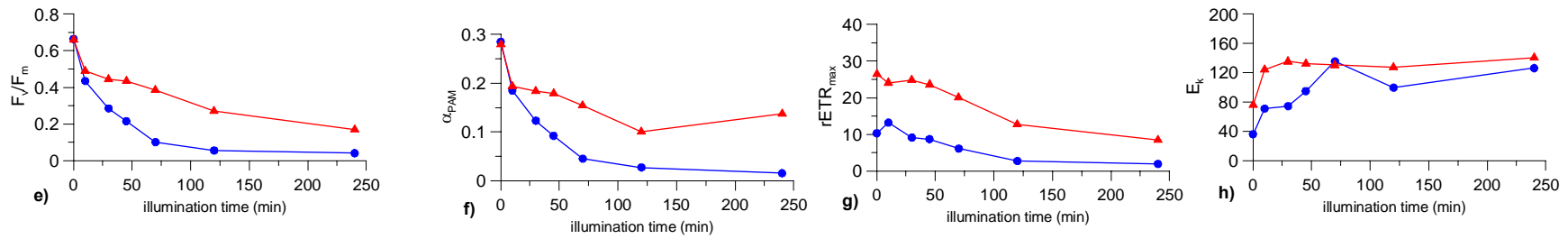
Species	$F_v/F_m$			$\alpha_{PAM}$			$rEtr_{max}$			$E_{kPAM}$		
	0h	4h	AI	0h	4h	AI	0h	4h	AI	0h	4h	AI
<i>P. simplex</i>	0.67	0.39	0.62	0.27	0.16	0.26	22.8	12.6	16.3	83	77	64
<i>M. comicus</i>	0.57	0.29	0.52	0.24	0.10	0.21	24.6	12.8	15.4	73	126	72
<i>I. rotunda</i>	0.66	0.17	0.41	0.28	0.14	0.17	26.5	8.4	7.3	76	141	43.8
<i>Phaeocystis</i> sp.	0.68	0.49	0.59	0.28	0.19	0.24	41.3	26.0	41.7	146	136	171
<i>M. pusilla</i>	0.68	0.55	0.64	0.27	0.21	0.25	33.0	23.2	29.8	23	108	119

**Table 6.10** – Phyto-PAM derived coefficients in the PA cultures, before (0h), after 4h of high-light and after 150 min (AI) at growth irradiance (see text), CULT-2 experiment.

*P. simplex*



*I. rotunda*



*M. pusilla*

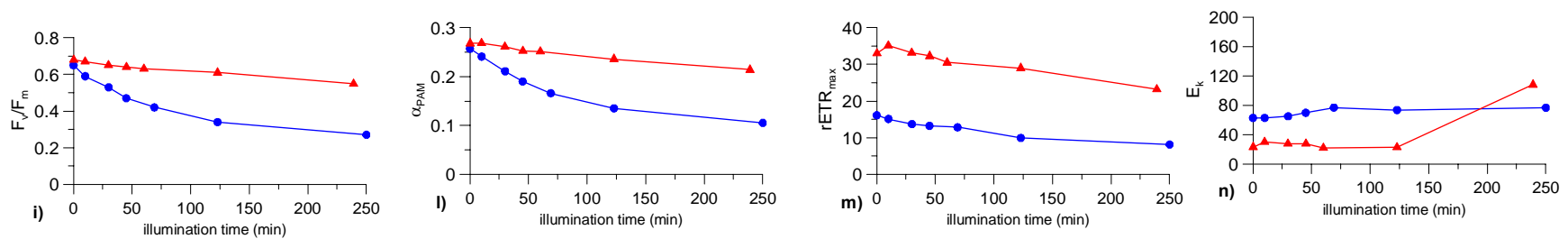


**Figure 6.13** – Variations in time of  $F_v/F_m$ ,  $\alpha_{PAM}$ ,  $rETR_{max}$  and  $E_{kPAM}$  of *P. simplex* (a,b,c,d), *I. rotunda* (e,f,g,h) and *M. pusilla* (i,l,m,n) in CC (●) and PA (▲) cultures during CULT-2 experiment.

When CC and PA cultures of each species were put back to the growth irradiance (i.e. 40  $\mu\text{mol photons m}^{-2} \text{s}^{-1}$ ) the Phyto-PAM derived coefficients showed a general tendency to return to the pre-treatment values.

As during high-light exposure, the  $F_v/F_m$  ratio and the  $\alpha_{\text{PAM}}$  values of the two diatoms *P. simplex* and *M. comicus* displayed a very similar pattern in both CC and PA cultures, reaching almost all the initial values after 150 min (Fig. 6.14a). In the other species there was a less pronounced change in the PA cultures than in the CC one. In particular, the CC culture of *I. rotunda* showed the highest variations, but the values reached after 150 min were still far from the initial pre-treatment ones.

Furthermore, this culture displayed a linear increase of  $F_v/F_m$  and  $\alpha_{\text{PAM}}$  values (Fig. 6.14e,f) as just observed for the DPS state (Fig. 6.12b). *M. pusilla* showed the lowest changes in the two coefficients described, especially for the PA culture (Fig. 6.14i,l).

A negative linear correlation was found between DPS state and  $F_v/F_m$  not only during the high-light treatment, but also when the cultures were carried back to the growth irradiance (Tab. 6.11). The highest values of correlation coefficient ( $r$ ) was found in the CC culture of *I. rotunda* after illumination period (AI), while the PA cultures of *Phaeocystis* sp. and *M. pusilla* showed the lowest ones.

	CC		PA	
	DI	AI	DI	AI
<i>P. simplex</i>	0.98	0.97	0.98	0.98
<i>M. comicus</i>	0.96	0.92	0.94	0.94
<i>I. rotunda</i>	0.96	0.99	0.95	0.96
<i>Phaeocystis</i> sp.	0.94	0.98	0.89	0.89
<i>M. pusilla</i>	0.96	0.85	0.88	0.88

**Table 6.11** – Linear correlation coefficient ( $r$ ) between DPS and  $F_v/F_m$  during high-light treatment (DI) and when the culture returned at growth irradiance (AI) in CULT-2 experiment.

The  $rE_{\text{tr,max}}$  showed only a slight increase in all the cultures (Tab. 6.9-6.10; Fig. 6.14). As for the other parameters, in the two diatoms CC and PA cultures had a similar pattern (Fig. 6.14c). In *I. rotunda* the most pronounced variation was observed again in the CC culture (Fig. 6.14g), while in *Phaeocystis* sp. and in *M. pusilla* (Fig. 6.14m) it was recorded in the PA ones. In these cases  $rE_{\text{tr,max}}$  quite reached the pre-treatment value.

The  $E_{\text{kPAM}}$  values decreased and partially returned to the pre-treatment conditions. In *P. simplex*  $E_{\text{kPAM}}$  decrease was almost all identical in the two cultures (Fig. 6.14d).

By contrast, in *M. comicus* the  $E_{kPAM}$  decrease was more rapid in the PA culture (78% of total change after 10 min) than in the CC one (58%) (data not shown).

A similar pattern was observed in *I. Rotunda* (61% of total change after 10 min in PA culture), while in the CC culture the  $E_{kPAM}$  value recorded after 140 min exceeded by ~ 2 fold the pre-treatment one (Fig. 6.14h).

In *Phaeocystis* sp. (data not shown) and in *M. pusilla* (Fig. 6.14n)  $E_{kPAM}$  values were quite constant in CC cultures, while they slightly increased in the PA ones.

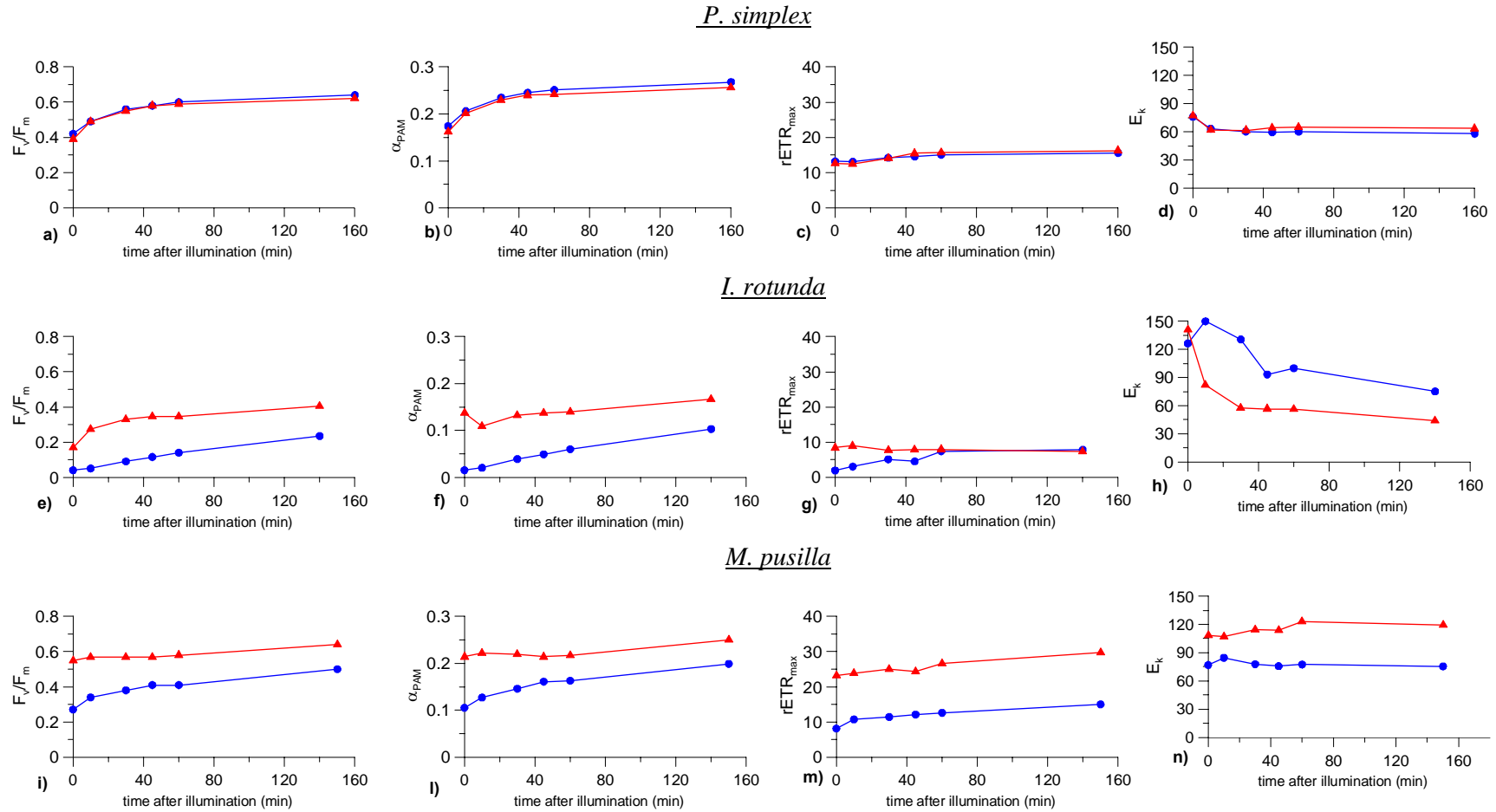


**Figure 6.14** – Variations in time of  $F_v/F_m$ ,  $\alpha_{PAM}$ ,  $rETR_{max}$  and  $E_{kPAM}$  of *P. simplex* (a,b,c,d), *I. rotunda* (e,f,g,h) and *M. pusilla* (i,l,m,n) in CC (●) and PA (▲) cultures after high-light treatment (phase AI); CULT-2 experiment.

## 6.4 Discussion

The CULT-1 and CULT-2 experiments were aimed at study photoprotection mechanisms in ultraphytoplankton species. In fact, as said in the section 1.2, the spatial distribution and the contribution to primary productivity of different ultraphytoplankton groups could be related to their capacity to acclimate to unpredictable fluctuations of natural light fields. The two experiments showed evident changes in both xanthophyll pools and Phyto-PAM derived coefficients of all the five species. Although it was not possible to discern directly any differences in photophysiological response as related to cell size since the species under investigation are all small than 5 $\mu$ m, we have tried to compare our results with the data available in literature on “model” species.

### *Golden-brown algae photoprotection*

As a first point, the four golden-brown algae under investigation showed a clear involvement of Diadinoxanthin (Dd) cycle in the photoprotection. In both the experiments the reaction of de-epoxidation was a very rapid process, while the epoxidation process was slower. This general scheme is not different from the picture emerged in the previous studies focused above all on large diatoms (Arsalane *et al.*, 1994; Olaizola *et al.*, 1994; Lavoud *et al.*, 2002a,b,c).

However, inter-specific differences can be pointed out. DPS state rose slightly faster in the two prymnesiophytes (*Imantonia rotunda* and *Phaeocystis* sp.) than in the two diatoms. After 1min of high-light treatment the DPS values exceeded by 1.5 and 2.6 the initial ones in diatoms and prymnesiophytes respectively (CULT-2 experiment). By contrast, no difference was found between cultures of the same species comparing the two experiments (e.g. CC vs. PA). The speed of the de-epoxidation is generally explained taking into account that Dd-Dt conversion is a one-step process (Ruban *et al.*, 2004), but other hypotheses are under investigation. The Dd de-epoxidase could be activated at lower  $\Delta$ pH than the V-cycle or related to the more appressed position of thylakoids (Lavoud *et al.*, 2002b). We may reasonably suppose that just this variability in the photosynthetic apparatus organization explain the observed differences among the species.

With the regard to the epoxidation process, the four species did not show significant difference. By contrast, the CULT2 experiment outlined that the epoxidation process was faster in the PA cultures than in the CC ones. Furthermore, during the high-light exposure *de-novo* synthesis of xanthophylls pool (i.e. Diadinoxanthin) was higher and started earlier in the PA cultures than in the CC ones. In addition, the periodic high light exposure in PA

cultures determined an increase of Diadinoxanthin pool size, but no contemporary change in the pigment composition of the antenna (such as Fucoxanthin content), which was quite similar in both CC and PA cultures. A similar pattern was observed in *P. tricornutum* cultures exposed to intermittent light-regime (Lavoud *et al.*, 2002c; 2003). These strategies have a high adaptive significance: modulating the Dd content and the velocity of recovery, the cell can regulate its capacity to cope with possible excessive irradiance without changing significantly the light harvesting under limiting irradiance. This is an obvious advantage in mixed water, where the irradiance regime changes very rapidly and the cells could be alternatively exposed to excessive and sub-saturating irradiance.

The negative correlation between the DPS state and the quantum yield of photosystem II ( $F_v/F_m$ ) indicates that in all the golden-brown algae the dissipative processes during the high-light treatment were modulated by the xanthophyll pool changes, i.e. Dt formation. In particular, the  $\alpha_{PAM}$  decrease observed in both CULT-1 and CULT-2 experiments clearly indicates that a reduction in the absorption cross section of antenna took place. However, as discussed in the section 2.3.3 if Dt play a direct or/and an indirect role in this process is far to be elucidated.

Again, the effectiveness of this photoprotection mechanism seems different between diatoms and prymnesiophytes. In particular, during CULT-1 experiment, when the light supply was very high ( $PFD = 1200 \mu\text{mol photons m}^{-2} \text{s}^{-1}$ ) electron turn-over rate ( $rEtr_{max}$ ) showed a dramatic decrease in the LL cultures of *I. rotunda* and *Phaeocystis* sp. (photoinhibition occurred), while in the diatoms the decrease was limited (Tab. 6.12). On the other hand, the  $rEtr_{max}$  decrease recorded in both ML and PA of prymnesiophytes was less pronounced. At the same time, the cultures showed lower changes in DPS state and  $F_v/F_m$  as well as a reduction in the correlation between these two parameters (Tab. 6.11). All these elements suggest that other photoprotection mechanisms could be involved when acclimation occurs. For instance, Lavoud *et al.* (2002a) found evidence for the induction of an electron transfer cycle around PSII in *P. tricornutum* at high light intensity. This chlororespiration is thought to proceed via the plastoquinol pool and to use reductants to ATP synthesis (Bennoun, 2001; Behrenfeld *et al.*, 2004). In this way the cell can contemporary reduce photodamage and extend the range of useful electron transport. However, no significant difference existed in  $rEtr_{max}$  reduction between LL and ML or CC and PA cultures of the two diatoms species. If these alternative patterns in diatoms are always “ready to start”, could be an interesting point of investigation. For instance,

Allakhverdiev *et al.*, (1997) postulated an involvement of Cyt<sub>b559</sub> in the switching mechanism ensuring that the cyclic pathway is activated only at high light intensity.

	CULT-1		CULT-2	
	LL	ML	CC	PA
<i>P. simplex</i>	41.2	35.2	41.5	44.7
<i>M. comicus</i>	37.8	27.1	43.4	47.0
<i>I. rotunda</i>	98.1	-	81.6	68.3
<i>Phaeocystis</i> sp.	96.4	59.6	57.76	37.0

**Table 6.12** – Percentage of rEtr<sub>max</sub> decrease after the 4h high-light treatment of CULT-1 and CULT-2 experiments.

#### *Violaxanthin cycle in golden-brown algae*

In Both CULT-1 and CULT-2 experiments, the four golden-brown algae showed the presence of the Violaxanthin-cycle (V-cycle) too. To date, few studies indicated the contemporary presence of both Dd- and V-cycle in golden-brown algae (Lohr and Wilhelm, 1999; 2001). On the other hand, some species (e.g. in Chrysophyceae) possess the V-cycle but not the D-cycle (Hager and Stranski, 1970, Lichtlé *et al.*, 1995). Lohr and Wilhelm (1999) proposed that Violaxanthin is an obligate precursor of Diadinoxanthin and Zeaxanthin can compete with Diadinoxanthin synthesis (Fig. 6.15).

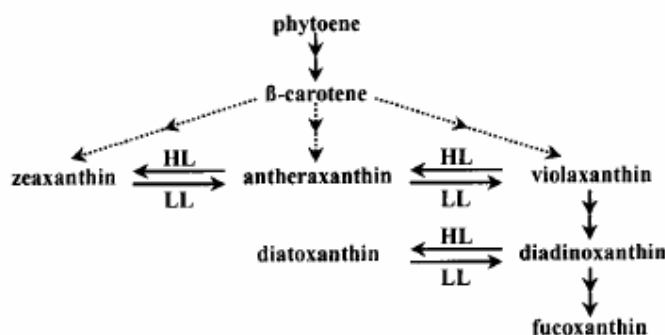


**Figure 6.15** – Hypothetical coupling between xanthophylls-cycle pools and Fucoxanthin biosynthetic pathway, proposed by Lohr and Wilhelm (1999).

In their studies on *P. tricornutum*, they found that increasing amounts of newly synthesized Violaxanthin are converted in Zeaxanthin more than in Diadinoxanthin, when the cells are subjected to increasing irradiance.

By contrast, in our experiments the contribution of V-cycle to the photoprotective carotenoids pool (PPC) resulted negligible, accounted always for less than 10% of the PPC.

Further, the newly synthesized xanthophylls were allocated only for ~10% in the V-cycle during CULT-2 experiment and ~20% during CULT-1 (Tab. 6.8).

The data emerging from our results indicated some factors influencing V-cycle pigments accumulation in the investigated species. At first, the duration of high-light treatment: Zeaxanthin accumulation increased after at least 60 min of high-light exposure. Secondly, the light intensity: as previous said the de novo synthesis of V-cycle pigments was higher in the CULT-1, with a PFD of 1200  $\mu\text{mol photons m}^{-2}\text{s}^{-1}$ . Since these factors are the same proposed by Lohr and Wilhelm (1999) for *P. tricornutum*, we may hypothesize that the general pathway was identical for all the golden-brown algae, but the importance of V-cycle in the photoprotection of each species could be subjected to an evolutionary constraint.

In particular our results showed clearly that in the four species under investigation the Diadinoxanthin pathway was preferred to the Zeaxanthin one, probably since Diadinoxanthin is a better substrate for de-epoxidase and, consequently more favorable in the short-term regulation (Lohr and Wilhelm, 1999).

#### *Green algae photoprotection*

In our experiments on *M. pusilla* the small changes in DPS state and quantum yield of PSII ( $F_v/F_m$ ) in ML and, above all, PA cultures, suggest that acclimation promotes other photoprotective mechanisms in this species rather than the V-cycle. For instance, the low increase of DPS state during the exposure to excessive light indirectly confirms the pathway proposed by Gilmore (2001) for the “model” species *Arabidopsis thaliana*: only a small proportion of the Zeaxanthin pool is “active” and directly involved in the energy dissipation processes. Havelková-Doušová *et al.* (2004) hypothesized that a combination of other mechanisms (e.g. state transition, dimension of antenna) more than the xanthophylls cycle operate at short time scales in *Dunaliella tertiolecta* cultures exposed to fluctuating irradiance. Further, Horton and Ruban (2005) outlined a role of PsbS protein complex in the photoprotection mechanism of plant and green algae, though the available data were not adequate to explain it in detail. Just this brief description clearly indicate that to date, the exact role of V-cycle in the green algae photoprotection is even more disputed (Masojidek *et al.*, 1999; Garcia-Mendoza *et al.*, 2002).

However, our result indicated that in PA culture of *M. pusilla*, as just observed in golden-brown algae, a series of physiological adjustment (e.g. pigment synthesis) are adopted to cope simultaneously with low and high irradiance. The effectiveness of this strategy is

proved by the high photosynthetic performance of PA culture ( $rEtr_{max}$  exceed by 2fold that of CC culture).

In this general picture an important role could be play by Lutein, since *M. pusilla* showed an increase of Lutein content per Chl *a* in both experiments. This pigment may have a direct role in photoprotection since it is low efficient in light energy transfer (see section 2.3.3), but recent studies explored other hypotheses (Niyogi *et al.*, 1997a,b; Pineau *et al.*, 2001). For instance, Lokstein *et al.*, 2002 working on *Arabidopsis thaliana* mutants, suggest that Lutein is involved in correct assembly of PSII antenna system rather than directly in NPQ. In particular, this pigment seems to control the functional antenna size and the connectivity between the reaction centers. By contrast, no change in Lutein content was observed in the two prymnesiophytes, which also contain this pigment. We may hypnotize that in the golden-brown algae the evolution of a different xanthophyll cycle (D-cycle) determined a different organization of the antenna and hence Lutein lose its original function.

In summary, all the five species under investigation showed efficient mechanisms of photoprotection to excessive irradiance, albeit some differences emerge between them (e.g. different role of xanthophylls cycle in the green algae compared with the golden-brown ones).

In the four golden-brown algae the V-cycle seems only an unavoidable competitive pathway, probably heritage of an ancestor, while the faster Diadinoxanthin de-epoxidation is the effective process involved in the mechanism of energy dissipation.

Furthermore, when acclimated to fluctuating irradiance regime (CULT-2 experiment) all the species show adaptative strategies in the photophysiological parameters geared toward optimizing fitness. A consequence of this flexibility is the capacity of maximizing the growth rate in spite of both predictable (circadian cycle) and unpredictable (e.g. turbulent water) irradiance fluctuations. On the other hand, clear differences exist between the investigated species: the two diatoms seem to have efficient photoprotective “machinery” even in absence of photoadaptation. By contrast, *I. rotunda* showed dramatic differences between pre-adapted and non adapted cultures.

These results can be helpful to interpret the pattern of occurrence of the species. For instance, the seasonal cycle of *I. rotunda* at st. MC is generally characterized by a maximum in spring (April) when the first stratification takes place and the water column is less dynamic (Sarno, personal communication). This kind of distribution is coherent with the less flexibility to unpredictable changes of the light field observed in this species during our

experiment. For the other prymnesiophytes *Phaeocystis* sp. it is not possible to compare its distribution with its photophysiology since it is still a little known species. To date it was found only in the Northern –Western Mediterranean Sea during the early spring bloom.

In the case of *M. pusilla*, the effectiveness of its photoprotection mechanism, above all in the pre-adapted species is surely one of the explanation for its presence at st. MC over the major part of the annual cycle (Zingone *et al.* 1999a) and for its world-wide distribution (Not *et al.*, 2004).

However, the pattern of occurrence of the two diatom species suggests that other factor may influence the distribution of a single species. In fact, *M. comicus* showed a peak during the autumnal bloom at st. MC (Ribera d'Alcalà *et al.*, 2004) and was found in high number also during the early spring bloom in the Northern –Western Mediterranean Sea (Sarno *et al.*, 2004); while *P. simplex* was less abundant in the Northern –Western Mediterranean and it has been never found at st. MC (Zingone, personal communication). In spite of these clear differences in the distribution of these two diatoms, our experiments showed identical photoprotection mechanisms and effectiveness. In our opinion, the spatial and temporal distribution of phytoplankton species could be regulated by endogenous clock, activated by environmental factors, such as photoperiod.

It would be a very interesting point for further investigation to test mechanisms of adaptation to fluctuating light in different strains of a same species which occur at different moments of the year. In this way, possible intra-specific differences could be highlighted and compared with the inter-specific ones.

The analysis of Phyto-Pam derived coefficients has permitted to obtain very reliable information on photophysiological state of cells during the experiments (i.e. changes in the electron transport rate). On the other hand, it is evident that the determination of *NPQ* would provide a more complete picture in order to clarify the links between DPS state and photosynthetic apparatus conditions. The contemporary definition of Phyto-PAM coefficients and *NPQ* would be another stimulating point for further investigation.

## **CONCLUSIONS**

As widely discussed in the first chapter, this project was focused on a better understanding of the role of ultraphytoplankton ( $<5\mu\text{m}$ ) in marine ecosystems, with specific attention to small eukaryotes, since their contribution to phytoplankton community would be largely underestimated. To date, few studies (e.g. Moon-van der Staay *et al.*, 2001; Zhu *et al.*, 2005) were performed on the taxonomic composition (only ~40 species have been formerly described) and the contribution to total phytoplankton biomass of the smallest eukaryotes. Previous results (Vaulot *et al.*, 2001; Bec *et al.*, 2005) seem to indicate that small eukaryotes are more abundant in coastal waters. To test these hypotheses, we have studied the distribution of ultraphytoplankton as compared to the entire phytoplankton biomass and productivity over an annual cycle at a long-term sampling station in the Gulf of Naples (st. MC). Further, the seasonal evolution of taxonomic composition (main algal groups) of this fraction has been determined by means of HPLC.

Our results showed that ultraphytoplankton accounted on average for ~50% of both phytoplankton biomass and primary production. It results a structural elements of phytoplankton community of coastal areas, even in sites subjected to important land run-off as the case of st. MC. However, the mean percentage contribution of ultraphytoplankton to total phytoplankton biomass decreased significantly during bloom conditions. This trend is similar to that found by Agawin *et al.* (2000) and Bell and Kalff (2001) for picoplankton ( $<2\mu\text{m}$ ) on world data sets. By contrast, our data did not show a positive correlation between ultraphytoplankton contribution and temperature, as found by the same authors. In our opinion, an explanation of this discrepancy was the presence at st. MC of episodic and variable inputs of new nutrients even in summer. As a consequence, warm temperatures often were not characterized by a low nutrients content and large cells were dominant (see chapter IV). This picture is quite different from the classic scheme of temperate areas where warm temperature coincide with a stratified and nutrient poor water column dominated by small cells. In this scenario the nutrients availability more than a direct effect of temperature on ultraphytoplankton growth rate seems to modulate the phytoplankton community at st. MC.

The results over the annual cycle indicated small eukaryotes as by far the main component of ultraphytoplankton community. In details, the eukaryotes accounted on average for  $84.1 \pm 11.0\%$  of the ultraphytoplankton biomass. In addition, our results have outlined a pattern in the distribution of eukaryotes and prokaryotes within the ultraphytoplankton fraction: the first are more important during the blooms, while prokaryotes show the highest percentage contribution in oligotrophic conditions. We have showed the presence of a correlation between prokaryotes and nutrients: the percentage of this group decreased at higher nitrate concentration. This relationship highlights an higher efficiency in nutrient up-take of prokaryotes at low nutrient concentrations. In particular, the prochlorophytes more than the cyanobacteria showed the highest differences in contribution to phytoplankton community over the annual cycle: they are practically undetected during the blooms. These results are supported by the recent studies of Zubkov *et al.* (2003), which indicated *Prochlorococcus* as generally dominant in systems based on recycled production since it turns out more efficient in  $\text{NH}_4$  and organic nitrogen compounds uptake.

By contrast, the success of small eukaryotes may be explained by their high competitiveness in exploiting the episodic arrival of new nutrients as compared to prokaryotes. Further, as shown by the experiments on monospecific cultures (see below), these eukaryotes have a very adaptable photosynthetic apparatus that proves to be successful in a water column subject to the alternation between stratification and mixing (e.g. in spring and autumn). In addition, their productive capacity was similar to that of large cells. All these elements may suggest that the lower contribution of ultraphytoplankton eukaryotes during bloom periods could be related to an efficient grazing pressure from the microzooplankton than to a less growth rate. In fact, previous studies at st. MC (Modigh 2001; Modigh and Castaldo, 2001) showed that there is no lag in the time response of microzooplankton to increase in chlorophyll *a* concentration. By contrast, the growth rate of mesozooplankton seems inadequate to exploit the sudden availability of preys (i.e. large cells) due to episodic inputs of new nutrients. Such grazing pressure on small cells suggests a high transfer efficiency to higher trophic levels, tuning the fate of carbon through the food-web.

The impact of size-selective microzooplankton grazing on small cells was demonstrated in different coastal sites (Jochem 2003; Mousseau *et al.*, 1996; Bec *et al.*, 2005) and some recent studies may support the hypothesis of an essential biotic control on phytoplankton community size-structure. For instance, Jiang *et al.* (2005) using an Evolutionary Nutrient-Phytoplankton-Zooplankton (ENPZ) model showed that increasing nutrient flux tends to increase phytoplankton cell size in the presence of phytoplankton-zooplankton coevolution, but have no effect in the absence of zooplankton. On the other hand, Collos *et al.* (2005) demonstrated that the  $K_s$  for nitrate up-take changes according to its environmental availability and independently from size. The authors suggest the presence of different nutrient carriers, which are activated at different nutrient concentrations. Clearly if this hypothesis is confirmed, the general concept that large cells are more efficient at high nutrient concentrations and, for this reason, dominant in eutrophic conditions would be completely re-examined.

The HPLC data over the annual cycle indicated that the  $>5\mu\text{m}$  fraction is a low diversified fraction at least on the pigment composition view, since Fucoxanthin is the main pigment of this fraction. This result is confirmed by the previous microscopic studies (Marino *et al.*, 1984, Zingone *et al.*, 1990), which indicated that diatoms are always dominant during phytoplankton blooms at st. MC. By contrast, ultraphytoplankton is a very diversified group, showing a clear seasonal successional pattern in both surface and sub-surface layer.

The golden-brown algae were the dominant group in the ultraphytoplankton fraction, according to the previous considerations about the importance of an adaptable photosynthetic apparatus, successful in a dynamic water column. One of the most interesting results of our data is the importance of the cryptophytes during the winter-early spring and the autumn blooms, when this class accounted for ~40% of the ultraphytoplankton biomass. In our opinion, this result underlines the importance of finding suitable methods to determine and quantify this group, probably underestimated by traditional techniques.

The recent works of Not *et al.* (2004; 2005) indicated the Prasinophyceae, as one of the main and constant component of small eukaryotes community in different ecological contexts. By contrast, our results showed the presence of this family (i.d. *Micromonas*

*pusilla*) only during the late winter-early spring bloom (March). Since Prasinoxanthin is completely separated by our HPLC method only at quite high concentration, the presence of this group in little number could be undetected during the samplings. Really previous studies based on Serial Dilution Cultures (SDC) showed the presence of *Micromonas pusilla* at st. MC also in winter (Zingone *et al.*, 1999a).

Prokaryotes were more abundant in low chlorophyll conditions. In particular, prochlorophytes were practically undetected during the spring, while cyanobacteria were recorded all over the annual cycle. In summer these two groups presented an opposite distribution along the water column: cyanobacteria at surface and prochlorophytes placed deeper. A similar pattern of occurrence was observed during the TRI2 experiment (see chapter V) and was reported in the Gulf of Naples by Casotti *et al.* (2000) and in other different ecological contexts (Worden *et al.*, 2004). This distribution could be explained by the higher sensitivity of prochlorophytes to UV radiations, as demonstrated by Sommaruga *et al.*, (2005) and by their higher efficiency to absorb blue light (Ting *et al.*, 2002).

On a methodological point of view, the application of size-fractionated pigments to define the main phytoplankton groups has highlighted that the use of pigments as size indicators, proposed by some authors (Gibb *et al.*, 2000) can imply significant errors in the estimate of size-classes distribution. In fact, our results clearly indicated that the main pigments (such as Fucoxanthin) are generally not confined in a specific size-class.

In order to interpret ultraphytoplankton distribution and possible differences in its photophysiology compared to the “model” species, ultraphytoplankton specific responses to predictable changes in the irradiance regime (circadian patterns) were studied.

Since during the circadian experiments the ultraphytoplankton fraction always accounted for  $\geq 90\%$  of total phytoplankton biomass, it was not possible to discern directly any differences in photophysiological response as related to cell size. However, comparing our data to the photosynthetic parameters oscillations reported in literature for phytoplankton community dominated by large cells (Prezelin *et al.*, 1987; Putt *et al.*, 1988) relevant differences in the circadian patterns are not outlined. In addition, diel fluctuations of *in vivo* fluorescence and photoprotective pigments pool found in the

natural ultraphytoplankton populations during our experiments are quite similar to that observed in *Phaeodactylum tricornutum* (a micro-plankton specie) cultures (Ragni, 2005).

All the photophysiological parameters showed diel fluctuations more pronounced in the surface samples than the deeper ones. This highlights that the irradiance regime experienced by the ultraphytoplankton community is crucial in triggering the cellular response. On the other hand, the taxonomic composition of the phytoplankton community may have a role in the observed differences among the surface samples of the three experiments. For instance, cyanobacteria population, during TRI-3, showed the lowest diel fluctuations of the photosynthetic parameters, in spite of the widest variation in the irradiance regime. Further, the experimental evidences suggest that in natural populations the description of photophysiological adjustments is further complicated by other environmental factors, e.g. nutrients, which interact with endogenous signals, modulating them.

In all the experiments and despite the differences in community composition, ultraphytoplankton populations of the surface layer showed a photosynthetic machinery “ready” to answer to environmental changes, trough the regulation of both antenna and reaction center systems. As a consequence, they were able to avoid photodamage and to maximize carbon fixation rates also at excessive light levels. Further, the organization and timing over the day of the different cellular activities (such as pigments synthesis) not only would increase the efficiency in responding to environmental perturbation but in the use of the resources too. This efficiency and flexibility, as previous said, are not significant different from that observed in large cells and, consequently, further suggest that biotic controls (such as grazing) more than physic ones are responsible of the less contribution of ultraphytoplankton during the bloom periods at st MC.

Finally, the photoprotection mechanisms of ultraphytoplankton were studied in monospecific cultures of some eukaryotes species (chosen for their different pigment composition) in order to compare their photophysiology with that of large species and to interpret their patterns of occurrence. Our experiments did not permit to outline directly any differences in photophysiological response as related to cell size. However, we have

tried to compare our result with the data available in literature on “model” species. As a general feature, the scheme of photoprotection in the golden-brown species is not different from the picture emerged in the previous studies focused on large diatoms (Arsalane *et al.*, 1994; Olaizola *et al.*, 1994; Lavoud *et al.*, 2002a,b,c). It is based on the involvement of Diadinoxanthin (Dd) cycle, with a very rapid de-epoxidation process. By contrast, the results found in *Micromonas pusilla* seem to indicate that the corresponding V-cycle is less important in the photoprotection of green algae, while lutein seems involved in the response to excessive irradiance. The effectiveness of photoprotection in the acclimated cultures of *M. pusilla* suggests the presence of other and more rapid photophysiological responses (such as state transition) as proposed by Havelková-Doušová *et al.* (2004) for *Dunaliella tertiolecta* cultures exposed to fluctuating irradiance.

In truth, our results do not exclude that other mechanisms (e.g. chlororespiration) and alternative carbon pathways (e.g. reductants) may play an important role also in the photoprotection of the golden-brown algae, as proposed by Lavoud *et al.* (2002b) and Behrenfeld *et al.* (2004). To better understand the complex interactions among all these elements some aspects need more attention in the future, including pigment synthesis pathways and exact position of pigments within the antenna.

To our knowledge the presence of Violaxanthin-cycle in golden-brown algae containing a Diadinoxanthin-cycle was described until now only for the diatom *P. tricornutum* (Lohr and Wilhelm, 1999). Our results suggest that V-cycle is more diffuse within this group than previously suspected and so it seems surprising that the accumulation of these pigments has never been reported for a long time. Lohr and Wilhelm (1999) hypothesized that the accumulation of V-cycle pigments could be observed best on algae with a high rate of *de novo* carotenoid synthesis in combination with high deepoxidase activity, since Violaxanthin is an intermediate in the biosynthetic pathway of Diadinoxanthin.

In contrast with the results of Lohr and Wilhelm (1999) the contribution of V-cycle to the photoprotective carotenoids pool (PPC) resulted negligible in both our experiments, accounted always for less than 10% of the PPC. So it seems only an unavoidable competitive pathway of Diadinoxanthin synthesis, probably heritage of an ancestor, while

the faster Diadinoxanthin de-epoxidation is the effective process involved in the mechanism of energy dissipation.

The CULT-2 experiment was aimed at investigating photophysiological responses in species acclimated to fluctuating irradiance regime. The results of this experiment showed that all the species show adaptative strategies, when acclimated. For instance, the pre-adapted cultures of each species showed an higher *de-novo* synthesis of xanthophylls pool during the high-light exposure. In addition, in these cultures there were a greater Diadinoxanthin pool size, but no contemporary change in the pigment composition of the antenna (such as Fucoxanthin content). A similar patter was observed in *P. tricornutum* cultures exposed to intermittent light-regime (Lavoud *et al.*, 2002c; 2003). In our opinion, these strategies have a high adaptative significance: modulating the Dd content and the velocity of recovery, the cell can regulate its capacity to cope with possible excessive irradiance without changing significantly the light harvesting under limiting irradiance. This is an obvious advantage in mixed water, where the irradiance regime changes very rapidly and the cells could be alternatively exposed to excessive and sub-saturating irradiance. A consequence of this flexibility is the capacity of maximizing the growth rate in spite of unpredictable (e.g. turbulent water) irradiance fluctuations.

On the other hand, clear differences exists between the investigated species: the two diatoms seem to have an efficient photoprotective “machinery” even in absence of photoadaptation. By contrast, *Imantonia rotunda* showed dramatic differences between pre-adapted and non adapted cultures.

These results can be helpful to interpret the pattern of occurrence of the species. For instance, the seasonal cycle of *I. rotunda* at st. MC is generally characterized by a maximum in spring (April) when the first stratification takes place and the water column is less dynamic (Sarno, personal communication). This kind of distribution is coherent with the less flexibility to unpredictable changes of the light field observed in this species during our experiment. For the other prymnesiophytes *Phaeocystis* sp. it is not possible to compare its distribution with its photophysiology since it is still a little known species. To date, it was found only in the Northwestern Mediterranean Sea during the early spring bloom (Zingone, personal communication). In the case of *M. pusilla*, the effectiveness of its photoprotection mechanism, above all in the pre-adapted species is surely one of the

explanation for its presence at st. MC over the major part of the annual cycle (Zingone *et al.* 1999a) and for its world-wide distribution (Not *et al.*, 2004). However, the pattern of occurrence of the two diatom species suggests that other factor may influence the distribution of a single species. In fact, *Minidiscus comicus* showed a peak during the autumnal bloom at st. MC (Ribera d'Alcalà *et al.*, 2004) and was found in high number also during the early spring bloom in the Northwestern Mediterranean Sea (Sarno *et al.*, 2004); while *Papiliocellulus simplex* was less abundant in the same area and it has never been found at st. MC (Zingone, personal communication). In spite of these clear differences in the distribution of these two diatoms, our experiments showed identical photoprotection mechanisms and effectiveness. In our opinion, a possible explanation could be the presence in the phytoplankton cells of an endogenous clock activated by environmental factors, which regulates the temporal and spatial distribution of each species.

### *Perspectives*

The main results of this project, on one hand outlined some interesting features about the role of ultraphytoplankton in marine ecosystems, on the other hand they highlighted emerging “open question”, which could be the bases for further researches.

First, the use of fractionated pigment analyses (HPLC) showed to be an effective and rapid tool to describe the assemblage of the smallest phytoplankton and to uncover the contribution of algal classes that are generally underestimated with traditional techniques (e.g. cryptophytes). On the other hand, the HPLC method remains quite inadequate to determine the contribution of groups with highly diversified and overlapping pigment compositions such as diatoms, prymnesiophytes and crysophytes. Comparative studies along HPLC and other methods, such as molecular markers, are surely one of the most promising fields for a better understanding of the diversity of small-size phytoplankton communities.

Another interesting aspect to point out is which implications and of what extent have the inter-specific differences observed in photoprotection responses in the formulation of photoacclimation models. In fact, both the “logistic” model proposed by Cullen and Lewis (1988) and the “dynamic” model proposed by Geider *et al.* (1996) used mean

parameters derived from very few model species: *Phaeodactylum tricornutum* and *Thalassiosira pseudonana*. Thus, it would be very helpful using the experimental data derived, for example, from our experiments to test the prediction of these models about photoacclimation state characteristics. In fact, an accurate study of at least some crucial species and a parameterization of the results in the models could provide more reliable tools in primary productivity estimates.

As previous said, we did not investigate directly whether the patterns in photophysiological responses observed in both circadian and photoprotection experiments, were exclusive of the size class we focused on. In order to clarify whether size effect exists in photophysiological responses it would be more effective a comparative experiments among different size morphotype of the same species rather than among species of different size. In this way, we can exclude the possible inter-specific differences and, at the same time we could explore the intra-specific ones.

On a methodological point of view, the application of *in vivo* fluorescence approaches in both circadian and photoacclimation experiments points out that they provide a powerful tool in the study of phytoplankton photophysiology and modelling. However, it is essential for their routinely use to achieve standardized and international protocols. Since the fluorescence approaches cope with the “light reaction” of photosynthesis they are more adapted to study the variations in the status of photosystems II and photoacclimation processes. On the other hand, the observed uncoupling between fluorescence parameters (e.g. electron transport rate) and carbon fixation demonstrates the need of flanking the use of these methods with standard primary production techniques, if we want to test to what extent the organization rates are really affected by variations in irradiance field.

# APPENDIX

Abbreviation	Definition	Algal group	Used unit of measurement
19'Bf	19'Butanoiloxifucoxantin	pelagophytes, some diatoms and prymnesiophytes	mg m <sup>-3</sup> pg cell <sup>-1</sup>
19'Hf	19'Hexanoiloxifucoxantin	prymnesiophytes and some diatoms	mg m <sup>-3</sup> pg cell <sup>-1</sup>
Allo	Alloxanthin	cryptophytes	mg m <sup>-3</sup> pg cell <sup>-1</sup>
Ant, A	Antheraxanthin	green algae	mg m <sup>-3</sup> pg cell <sup>-1</sup>
Chl <i>a</i>	Chlorophyll <i>a</i>	all phytoplankton groups, except prochlorophytes	mg m <sup>-3</sup> pg cell <sup>-1</sup>
Chl <i>b</i>	Chlorophyll <i>b</i>	green algae	mg m <sup>-3</sup> pg cell <sup>-1</sup>
Chl <i>c</i> <sub>3</sub>	Chlorophyll <i>c</i> <sub>3</sub>	pelagophytes, some diatoms and prymnesiophytes	mg m <sup>-3</sup> pg cell <sup>-1</sup>
Chl <i>c</i> <sub>2</sub>	Chlorophyll <i>c</i> <sub>2</sub>	golden-brown algae	mg m <sup>-3</sup> pg cell <sup>-1</sup>
Chl <i>c</i> <sub>1</sub>	Chlorophyll <i>c</i> <sub>2</sub>	golden-brown algae	mg m <sup>-3</sup> pg cell <sup>-1</sup>
Diado, D	Diadinoxanthin	golden-brown algae	mg m <sup>-3</sup> pg cell <sup>-1</sup>
Diato, Dt	Diatoxanthin	golden-brown algae	mg m <sup>-3</sup> pg cell <sup>-1</sup>
Div- Chl <i>a</i>	Divinyl- Chlorophyll <i>a</i>	prochlorophytes	mg m <sup>-3</sup> pg cell <sup>-1</sup>
Fuco	Fucoxantin	diatoms, some pelagophytes and prymnesiophytes	mg m <sup>-3</sup> pg cell <sup>-1</sup>
Lut	Lutein	green algae	mg m <sup>-3</sup> pg cell <sup>-1</sup>
Neox	Neoxanthin	green algae	mg m <sup>-3</sup> pg cell <sup>-1</sup>
Perid	Peridinin	dinoflagellates	mg m <sup>-3</sup> pg cell <sup>-1</sup>
Prasino	Prasinoxanthin	prasinophytes	mg m <sup>-3</sup> pg cell <sup>-1</sup>
Viola, V	Violaxanthin	green algae	mg m <sup>-3</sup> pg cell <sup>-1</sup>
Zea, Z	Zeaxanthin	Cyanophyta	mg m <sup>-3</sup> pg cell <sup>-1</sup>
β - carot	β - carotene	golden-brown algae	mg m <sup>-3</sup> pg cell <sup>-1</sup>
PPC	Photoprotective carotenoids		mg m <sup>-3</sup> pg cell <sup>-1</sup>
PSP	Photosynthetic pigments		mg m <sup>-3</sup> pg cell <sup>-1</sup>
T Chl <i>a</i>	Chlorophyll <i>a</i> + Divinyl- Chlorophyll <i>a</i>		mg m <sup>-3</sup> pg cell <sup>-1</sup>

**Table I** – List of principal photosynthetic pigments, their distribution in algal groups and abbreviations used in the text.

Abbreviation	Definition	Used unit of measurement
$\alpha^B$	Photosynthetic efficiency (light limited slope of PvsE curve)	mgC (mgChl $a \mu$ molphotons $m^{-2} s^{-1} h$ ) <sup>-1</sup>
$\alpha_{PAM}$	Light limited slope of rETR curve (Phyto-PAM technique)	$\mu$ molelectrons photons <sup>-1</sup>
$\beta$	index of photoinhibition	mgC (mgChl $a \mu$ molphotons $m^{-2} s^{-1} h$ ) <sup>-1</sup>
CC	Colture Control (acclimated at 40 $\mu$ molphotons $m^{-2} s^{-1}$ )	
CHEMTAX	matrixfactorisation program for estimate algal abundance	
CP	Core Proteins	
CZCS	Coastal Zone Color Scanner	
CULT-1, CULT-2	First and second photoacclimation experiments on cultures	
DPS	De-epoxidation state of the xanthophylls cycles	
$E_k, E_{kPAM}$	Compensation irradiance, or photoacclimation index	$\mu$ molphotons $m^{-2} s^{-1}$
$E_D(\lambda, z)$	Scalar downwellig irradiance at the depth z and wavelenght $\lambda$	$W m^{-2} nm^{-1}$
$F_0, F_m$	Minimum and maximum fluorescence yield measured in the dark	r.u.
$F_0', F_m'$	Minimum and maximum fluorescence yield measured under a background irradiance	r.u.
$F_v/F_m$	Maximum quantum yield of PSII	r.u.
$F_v'/F_m'$	Maximum quantum yield of PSII under a background irradiance	r.u.
FRRF	Fast Repetition Rate Fluorometry	
FCM	Flow citometry	
$\Phi_f$	Fluorescence quantum yield	
HPLC	High liquid Pressure Cromatography	
$K_d$	Diffuse attenuation coefficient for downwelling irradiance	$m^{-1}$
LHCP	Light-Harvesting Chloropyll-Protein complex	
LL	Low Light culture (acclimated at 80 $\mu$ molphotons $m^{-2} s^{-1}$ )	
MC	Marechiarra, sampling station in the Gulf of Naples	
ML	Medium Light colture (acclimated at 300 $\mu$ molphotons $m^{-2} s^{-1}$ )	
NPQ	Non-Photochemical Quencing	

**Table II** – List of principal symbols and abbreviation used in the text – Continue-

PA	Pre-Adapted culture (grown at 40 $\mu\text{molphotons m}^{-2} \text{s}^{-1}$ and exposed to 10 cycle of high-light)	
PAM	Pulse Amplitude Modulate technique	
PAR	Photosynthetic Available Radiation	$\mu\text{molphotons m}^{-2} \text{s}^{-1}$
$P^B_{\text{max}}$	maximum photosynthetic capacity	$\text{mgC mgChl a}^{-1} \text{h}^{-1}$
PFD	Photon Flux Density	$\mu\text{molphotons m}^{-2} \text{s}^{-1}$
PSI, PSII	Photosystem I and II	
$r\text{ETR}$ , $r\text{ETR}_{\text{MAX}}$	Relative electron transport rate, maximum relative electron transport rate	$\mu\text{molelectrons m}^{-2} \text{s}^{-1}$
$Q_A$	Quinone, second acceptor in electron transport	
RC	Reaction Center	
SDC	Serial Dilution Culture	
SeaWiFS	Sea-viewing Wide Field-of-view Sensor	
$\sigma_{\text{PSII}}$	Effective cross section of PSII	$\text{A}^2 \text{q}^{-1}$
TRI-1, TRI-2, TRI-3	First, second and third circadian experiments	

**Table II** – List of principal symbols and abbreviation used in the text.

**REFERENCES**

- Adir N., Zer H., Shochat S., Ohad I. (2003). Photoinhibition – a historical perspective. *Phot. Res.*, 76: 343-370.
- Agawin N. S. R., Duarte C. M., Agustì S. (1998). Growth and abundance of *Synechococcus* sp. in a Mediterranean bay: a seasonality and relationship with temperature. *Mar. Ecol. Prog. Ser.*, 170: 45-53.
- Agawin N. S. R., Duarte C. M., Agustì S. (2000). Nutrient and temperature control of the contribution of picoplankton to phytoplankton biomass and production. *Limnol. Oceanogr.*, 45(3): 591-600.
- Akè-Castillo J. A., Hernandez-Becerril D. U., Meave del Castillo M. E., Bravo-Sierra E. (2001). Species of *Minidiscus* (Bacillariophyceae) in the Mexican Pacific Ocean. *Cryptogamie Algol.*, 22(1): 101-107.
- Allakhverdiev S. I., Klimov V., Carpentier R. (1997). Evidence for the involvement of cyclic electron transport in the protection of Photosystem II against photoinhibition: influence of a new phenolic compound. *Biochemistry*, 36: 4149-4154.
- Anagnostidis K., Komárek J. (1990). Modern approach to the classification system of cyanophytes. 5. Stigonematales. *Arch. Hydrobiol. Suppl.* 73: 157-226.
- Ansotegui A., Sarobe A., Trigueros J. M., Urrutxurtu I., Orive E. (2003). Size distribution of algal pigments and phytoplankton assemblages in a coastal-estuarine environment: contribution of small eukaryotic algae. *J. Plank. Res.*, 25 (4): 341-355.
- Arsalane W., Rousseau B., Duval J-C. (1994). Influence of the pool size of the xanthophyll cycle on the effects of light stress in a diatom: competition between photoprotection and photoinhibition. *Photochem. Photobiol.*, 60: 237-243.
- Azam F., Fenchel T., Field J. G., Gray J. S., Meyer-Reil R. A., Thingstad F. (1983). The ecological role of water column microbes in the sea. *Mar. Ecol. Prog. Ser.*, 10: 257-263.
- Babin M., Morel A., Gagnon R. (1994). An incubator designed for extensive and sensitive measurements of phytoplankton photosynthetic parameters. *Limnol. Oceanogr.*, 39: 694-702.
- Banase K. (1992). Grazing, temporal changes of phytoplankton concentrations, and the microbial loop in the open sea. In: *Primary productivity and biogeochemical cycles in the sea*. Falkowski P.G. and Woodhead A. D. (eds.), Plenum Press, New York and London, pp. 409-440.
- Barber R. T., Hilting A. K. (2002). History of the study of plankton productivity. In: *Phytoplankton Productivity – Carbon assimilation in marine and freshwater ecosystems*. Williams P. J. le B., Thomas D. N., Reynolds C. S. (Eds), Blackwell Science, pp. 16-43.

- Barlow R. G., Mantoura R. F. C., Cummings D. G., Fileman T. W. (1997). Pigment chemotaxonomic distributions of phytoplankton during summer in the Western Mediterranean. *Deep Sea Res. II*, 44: 833-850.
- Barlow R. G., Mantoura R. F. C., Cummings D. G., Fileman T. W. (1999). Monsoonal influence on the distribution of phytoplankton pigments in the Arabian Sea. *Deep Sea Res. II*, 46: 677-699.
- Behrenfeld M., Bale A., Kolber Z., Aiken J., Falkowski P. G. (1997). Confirmation of iron limitation of phytoplankton photosynthesis in the equatorial Pacific Ocean. *Nature*, 383: 508-511.
- Bec B., Husseini-Ratrema J., Collos Y., Souchu P., Vaquer A. (2005). Phytoplankton seasonal dynamics in a Mediterranean coastal lagoon: emphasis on the picoeukaryote community. *J. Plank. Res.*, 27 (9): 881-894.
- Beherfield M. J., Prasil O., Kolber Z., Babin M., Falkowski P. G. (1998). Compensatory changes in Photosystem II electron turnover rates protect photosynthesis from photoinhibition. *Phot. Res.*, 58: 259-268.
- Behrenfeld M. J., Esaias W. E., Turpie K. R. (2002). Assessment of primary production at the global scale. In: *Phytoplankton Productivity – Carbon assimilation in marine and freshwater ecosystems*. Williams P. J. le B., Thomas D. N., Reynolds C. S. (Eds), Blackwell Science, pp. 156-186.
- Behrenfeld M. J., Prasil O., Babin M., Bruyant F. (2004). In search of a physiological basis for covariations in light-limited and light-saturated photosynthesis. *J. Phycol.*, 40: 4-25.
- Bell T., Kalff J. (2001). The contribution of picophytoplankton in marine and freshwater systems of different trophic status and depth. *Limnol. Oceanogr.*, 46(5): 1243-1248.
- Bennon P. (2001). Chlororespiration and the process of carotenoid biosynthesis. *Biochem. Biophys. Acta*, 1506: 133-142.
- Berges J. A., Harrison P. J. (1993). Relationship between nucleoside diphosphate kinase activity and light-limited growth rate in the marine diatom *Thalassiosira pseudonana* (Bacillariophyceae). *J. Phycol.* 29: 45 -53.
- Bidigare R. R., Schofield O., Prezelin B. B. (1989). Influence of zeaxanthin on quantum yield of photosynthesis of *Synechococcus* clone WH7803 (DC2). *Mar. Ecol. Prog. Ser.*, 56: 177-188.
- Biegala I. C., Not F., Vaultot D., Simon N. (2003). Quantitative assessment of picoeukaryotes in the natural environment by using taxon-specific oligonucleotide probes in association with tyramide signal amplification-fluorescence in situ hybridization and flow cytometry. *Appl. Environ Microbiol.*, 69: 5519-5529.

- Brunet C., Lizon F. (2003). Tidal and diel periodicities of size-fractionated phytoplankton pigment signatures at an offshore station in the southeastern English Channel. *Est. Coast. Shelf Sci.* 56: 833-843.
- Bryant D. (1994). *The molecular biology of Cyanobacteria*. Kluwer Academic publishers, Dordrecht, the Netherlands, pp. 323.
- Bustillos-Guzman J., Claustre H., Marty J. C. (1995). Specific phytoplankton signatures and their relationship to hydrographic conditions in the coastal northwestern Mediterranean Sea. *Mar. Ecol. Prog. Ser.*, 124: 247-258.
- Butcher R. W. (1952). Contributions to our knowledge of the smaller marine algae. *J Mar Biol Assoc UK*, 31: 175–191.
- Caroppo C., Fiocca A., Sammarco P., Magazzù G. (1999). Seasonal variations of nutrients and phytoplankton in the coastal SW Adriatic Sea (1995-1997). *Bot. Mar.*, 42: 389-400.
- Carr, M.G., Whitton, B.A. (1982). *The Biology of Cyanobacteria*. *Botanical Monographs*. Blakwell Science, pp. 688.
- Carrada G.C., (1983). The gulf of Naples and its data base. Quantitative analysis and simulation of Mediterranean coastal ecosystem: The gulf of Naples a case of study, *Unesco Rep. Mar. Sci.*, 20: 70-79.
- Carrada G.C., Hopkins T.S., Bonaduce G., Ianora A., Marino D., Modigh M., Ribera d'Alcalà M., Scotto di Carlo B. (1980). Variability in the hydrographic and biological features of the gulf of Naples. *P.S.Z.N.I.: Marine Ecology*, 1: 105-120.
- Carrada G.C., Fresi E., Marino D., Modigh M., Ribera d'Alcalà M. (1981). Structural analysis of winter phytoplankton in the gulf of Naples. *J. Plank. Res.* 3 (2): 291-313.
- Casotti R., Brunet C., Arnone B., Ribera d'Alcalà (2000). Mesoscale features of phytoplankton and planktonic bacteria in a coastal areas induced by external water masses. *Mar. Ecol. Prog. Ser.*, 195: 15-27.
- Casper-Lindley C., Björkman O. (1998). Fluorescence quenching in four unicellular algae with different light-harvesting and xanthophyll-cycle pigments. *Phot. Res.*, 56: 277-289.
- Cerino F. (2004). Cryptophyceae of the Mediterranean Sea: morphology, ecology and genetic diversity. PhD Thesis, University of Messina, pp. 112.
- Chisholm S. W. (1992). Phytoplankton size. In: *Primary productivity and biogeochemical cycles in the sea*. Falkowski P.G. and Woodhead A. D. (eds.), Plenum Press, New York and London, pp. 213-237.
- Chisholm S. W., Olsen R. J., Zettler E. R., Goericke R., Watterbury J. B., Welschmeyer N. A. (1988). A novel free-living prochlorophyte abundant in the oceanic euphotic zone. *Nature*, 334: 340-343.

- Chisholm S. W., Falkowski P. G., Cullen J. J. (2001). Dis-crediting ocean fertilization. *Science* 294: 309-310.
- Collos Y., Vaquer A., Souchu P. (2005). Acclimation of nitrate uptake by phytoplankton to high substrate levels. *J. Phycol.*, 41: 466-478.
- Courtiers C., Vaquer A., Troussellier M., Lautier J. (1994). Smallest eukaryotic organism. *Nature*, 370: 255.
- Cox G. (1993). Phrochlorophyceae. In: *Ultrastructure of microalgae*. Berner T. (ed.), CRC Press, Boca Raton, pp. 53-70.
- Cullen J., Lewis M. R. (1988). The kinetics of algal photoadaptation in the context of vertical mixing. *J. Plank. Res.*, 10 (5): 1039-1063.
- Demers S., Roy S., Gagnon R., Vignault C. (1991). Rapid light-induced changes in cell fluorescence and in xanthophyll-cycle pigments of *Alexandrium excavatum* (Dinophyceae) and *Thalassiosira pseudonana* (Bacillariophyceae) a photo-protection mechanism. *Mar Ecol. Prog. Ser.*, 76: 185-193.
- Demmig-Adams B. (2003). Linking the xanthophylls cycle with thermal energy dissipation. *Phot. Res.*, 76: 73-80.
- Dortch Q., Thompson P. A., Harrison P. J. (1991). Variability in nitrate uptake kinetics in *Thalassiosira pseudonana* (Bacillariophyceae). *J. Phycol.* 27: 35-39.
- Drebes G. von (1974). *Marines Phytoplankton*. Georg Thieme Verlag, Stuttgart, pp. 186.
- DuRand M. D., Green R. E., Sosik H. M., Olson R. J. (2002). Diel variations in optical properties of *Micromonas pusilla* (Prasinophyceae). *J. Phycol.* 38: 1132-1142.
- Durnford D. G., Falkowski P. G. (1997). Chloroplast redox regulation of nuclear gene transcription during photoacclimation. *Phot. Res.*, 52: 229-241.
- Egeland E. S., Liaaen-Jensen S. (1995). Ten minor carotenoids from prasinophyceae (Chlorophyta). *Phytochemistry*, 40 (2): 515-520.
- Egeland E. S., Eikrem W., Throndsen J., Wilhelm C., Zapata M., Liaaen-Jensen S. (1995). Caratenoids from further prasinophytes. *Biochem. System. Ecol.*, 23 (7/8): 747-755.
- Eilers P. H. C., Peeters J. C. H. (1993). Dynamic behaviour of a model for photosynthesis and photoinhibition. *Ecol. Modell.*, 69: 113-133.
- Falkowski P. G. (2002). On the evolution of the carbon cycle. In: *Phytoplankton Productivity – Carbon assimilation in marine and freshwater ecosystems*. Williams P. J. le B., Thomas D. N., Reynolds C. S. (Eds), Blackwell Science, pp. 318-349.

- Falkowski P. G., La Roche J. (1991). Acclimation to spectral irradiance in algae. *J. Phycol.* 27: 8-14.
- Falkowski P. G., Raven J. A. (1997). *Aquatic photosynthesis*. Blackwell Science, pp. 375.
- Falkowski P. G., Katz M. E., Knoll A. H., Quigg A., Raven J. A., Schofield O., Taylor F. J. R. (2004). The evolution of modern eukaryotic phytoplankton. *Science*, 305: 354-360.
- Fay P., Van Baalen C. (1987). *The cyanobacteria*. Elsevier Science Publisher, Amsterdam, The Netherlands, pp. 545.
- Fietz S., Nicklish A. (2002). Acclimation of the diatom *Stephanodiscus neoastraea* and the cyanobacterium *Planktotryx agardhii* to simulated natural light fluctuations. *Phot. Res.*, 72: 95-106.
- Forbes J. R., Denman K. L., Mackas D. L. (1986). Determinations of photosynthetic capacity in coastal marine phytoplankton: effects of assay irradiance and variability of photosynthetic parameters. *Mar. Ecol. Prog. Ser.*, 32: 181-191.
- Garcia-Mendoza E., Matthijs H. C. P., Schubert H., Mur L. R. (2002). Non-photochemical quenching of chlorophyll fluorescence in *Chlorella fusca* acclimated to constant and dynamic light conditions. *Phot. Res.*, 74: 303-315.
- Gardner C., Crawford R. M. (1992). A description of the diatom *Papiliocellulus simplex* sp. Nov. (Cymatosiraceae, Bacillariophyta) using light and electron microscopy. *Phycologia*, 31(3/4): 246-252.
- Gargas E., Hare I., Martens P., Edler L. (1979). Diel change in Phytoplankton photosynthetic efficiency in brackish waters. *Mar. Biol.*, 52: 113-122.
- Geider R. J., MacIntyre H. L., Kana T. M. (1996). A dynamic model of photoadaptation in phytoplankton. *Limnol. Oceanogr.*, 41: 1-15.
- Geider R. J., MacIntyre H. L. (2002). Physiology and biochemistry of Photosynthesis and algal carbon acquisition. In: *Phytoplankton Productivity – Carbon assimilation in marine and freshwater ecosystems*. Williams P. J. le B., Thomas D. N., Reynolds C. S. (Eds), Blackwell Science, pp: 44-77.
- Gibb S. W., Barlow R. G., Cumming D. G., Rees N. W., Trees C. C., Holligan P., Suggett D. (2000). Surface phytoplankton pigment distributions in the Atlantic Ocean: an assessment of basin scale variability between 50°N and 50°S. *Prog. Oceanogr.*, 45: 339-368.
- Gilmore A. M. (2001). Xanthophyll cycle-dependent nonphotochemical quenching in photosystem II: mechanistic insights gained from *Arabidopsis thaliana* L. mutants that lack violaxanthin deepoxidase activity and/or lutein. *Phot. Res.*, 67: 89-101.
- Glover H. E., Smith A. E., Shapiro L. (1985). Diurnal variations in photosynthetic rates: comparison of ultraphytoplankton with a larger phytoplankton size fraction. *J. Plank. Res.*, 7(4): 519-535.

- Glover H. E., Keller M. D., Guillard R. R. L. (1986). Light quality and oceanic ultraphytoplankters. *Nature*, 319: 142-143.
- Glover H. E., Keller M. D., Spinrad R. (1987). The effects of light quality and intensity on photosynthesis and growth of marine eukaryotic and prokaryotic phytoplankton clone. *J. Exp. Mar. Biol. Ecol.*, 105: 137-159.
- Goericke R., Repeta D. G. (1992). The pigments of *Prochlorococcus marinus*: the presence of divinyl chlorophyll *a* and *b* in a marine prokaryote. *Limnol. Oceanogr.*, 37: 425-433.
- Goldman J. C., Glibert P. M., (1983). Kinetics of inorganic nitrogen uptake by phytoplankton. In: *Nitrogen in the marine environment*. Carpenter E. J. and Capone D. G. (eds). Academy Press, New York, pp. 233-274.
- Guillard, R. R. L. (1983). Culture of phytoplankton for feeding marine invertebrates. In: *Culture of Marine Invertebrates Selected Readings*. Berg C.J.J. (Eds.), Hutchinson Ross Publishing Co., Stroudsburg, PA, pp. 108-132.
- Guillou L., Eikrem W., Chretiennot-Dinet M. J., Le Gall F., Massana R., Romari K., Pedros-Aliò C., Vaulot D. (2004). Diversity of picoplanktonic Prasinophytes assessed by direct nuclear SSU rDNA sequencing of environmental samples and novel isolates retrieved from oceanic and coastal marine ecosystems. *Protist* 155: 193-214.
- Hager A., Stranski H. (1970). The carotenoid pattern and the occurrence of the light-induced xanthophylls cycle in various classes of algae. V. A few members of Cryptophyceae. *Arch. Microbiol.*, 73: 77-89.
- Hanson R., Ducklow H. W., Field J. (1999). *The Changing Ocean Carbon Cycle, a midterm synthesis of Joint Global Ocean Flux Study*. International Geosphere-Biosphere Programme Book Series Nr. 5. Hanson R., Ducklow H. W., Field J. (Eds) Cambridge University Press, pp. 378.
- Harding L.W., Meeson B. W., Prezelin B. B., Sweeney B. M. (1981). Diel periodicity of photosynthesis in marine phytoplankton. *Mar. Biol.* 61: 95-105.
- Harris G. P. (1986). *Phytoplankton ecology. Structure, function and fluctuation*. Chapman and Hall, London, pp. 384.
- Havelková-Doušova Prasil O., Behrenfeld M. J. (2004). Photoacclimation of *Dunaliella tertiolecta* (Chlorophyceae) under fluctuating irradiance. *Photosynthetica*, 42(2): 273-281.
- Hill R., Bendel R. (1960). Function of two cytochrome components in chloroplast: a working hypothesis. *Nature*, 186: 136-137.
- Holm-Hansen O., Lorenzen C. J., Holmes R. W., Strickland J. D. H. (1965). Fluorimetric determination of chlorophyll. *J. du Conseil perm. internat. Expl. de la Mer*, 30: 3-15.

- Hopkins T. S. (1986). Recent observation on the intermediate and deep water circulation in the southern Tyrrhenian sea. *Oceanologica Acta*, 34: 4-5.
- Horton P., Ruban A. (2005). Molecular design of the photosystem II light-harvesting antenna : photosynthesis and photoprotection. *J. Exp. Botany*, 56 (411): 365-373.
- Ianora A., Mazzocchi M.G., Scotto di Carlo B. (1985). Zooplankton community structure for coastal waters of the gulf of Naples. Summer of 1983. *Rapp. Comm. int. Mer. Medit.*, 29: 299-300.
- Jacquet S., Partensky F., Lennon J.-F., Vaultot D. (2001). Diel patterns of growth and division in marine picoplankton in culture. *J. Phycol.* 37: 357-369.
- Jeffrey S. W. (1997). Application of pigment methods to oceanography. In: *Phytoplankton pigments in oceanography*. Jeffrey S.W., Mantoura R. F. C. e Wright S. W. (eds), UNESCO publishing, pp. 127-166.
- Jeffrey S. W., Vesik M. (1997). Introduction to marine phytoplankton and their pigment signatures. In: *Phytoplankton pigments in oceanography*. Jeffrey S. W., Mantoura R. F. C. e Wright S. W. (eds), UNESCO publishing, pp. 37-84.
- Jeffrey S. W., Mantoura R.F.C., Wright S.W. (1997). *Phytoplankton pigments in oceanography*. UNESCO publishing, pp. 662.
- Jensen T. E. (1993). Cyanobacterial ultrastructure. In: *Ultrastructure of microalgae*. Berner T. (ed.), CRC Press, Boca Raton, p. 7-51.
- Jiang L., Schofield O. M. E., Falkowski P. G. (2005). Adaptive evolution of phytoplankton cell size. *Amer. Nat.*, 166 (4): 496-504.
- Jochem F. J. (2003). Photo- and heterotrophic pico- and nanoplankton in the Mississippi River plume: distribution and grazing activity. *J. Plank. Res.*, 25 (10): 1201-1214.
- Johnson Z., Barber R. T. (2003). The low-light reduction in the quantum yield of photosynthesis: potential errors and biases when calculating the maximum quantum yield. *Phot. Res.*, 75: 85-95.
- Kaftan D., Meszaros T., Whitmarsh J., Nebdal L. (1999). Characterization of Photosystem II activity and heterogeneity during the cell cycle of the green alga *Scenedesmus quadricauda*. *Plant Physiol.*, 120: 433-441.
- Kana T. M., Watts J. L., Gilbert P. M. (1985). Diel periodicity in the photosynthetic capacity of coastal and offshore phytoplankton assemblages. *Mar. Ecol. Prog. Ser.*, 25: 131-139.
- Kana T. M., Gilbert P. M., Goericke R., Welshmeyer N. A. (1988). Zeaxanthin and  $\beta$ -carotene in *Synechococcus* WH7803 respond differently to irradiance. *Limnol. Oceanogr.*, 33: 1623-1627.

- Keller M. D., Selvin R. C., Claus W., Guillard R. R. (1987). Media for the culture of oceanic ultraphytoplankton. *J. Phycol.*, 23: 633-638.
- Kjørbe T. (1993). Turbulence, phytoplankton cell size, and the structure of pelagic food webs. *Mar. Biol.*, 29: 1-72.
- Kirk J. T. O. (1992). The nature and measurement of the light environment in the Ocean. In: *Primary productivity and biogeochemical cycles in the sea*. Falkowski P.G. and Woodhead A. D. (eds.), Plenum Press, New York and London, pp. 9-30.
- Kirk J. T. O. (1994). *Light and photosynthesis in aquatic ecosystems*. Cambridge University press, Cambridge, pp. 509.
- Kohata K., Watanabe M. (1988). Diel changes in the composition of photosynthetic pigments and cellular carbon and nitrogen in *Pyramimonas parkeae* (Prasinophyceae). *J. Phycol.*, 24: 58-66.
- Kolber Z. S., Falkowski P. G. (1993). Use of active fluorescence to estimate phytoplankton photosynthesis in situ. *Limnol. Oceanogr.*, 38(8): 1646-1665.
- Kolber Z. S., Prasil O., Falkowski P. G. (1998). Measurement of variable chlorophyll fluorescence using fast repetition rate techniques: defining methodology and experimental protocols. *Biochim. Biophys. Acta* 1367: 88-106.
- Lally C. M., Parson T. R. (1997). *Biological Oceanography an introduction*. The Open University, Oxford, pp. 314.
- Latasa M., Berdalet E., Estrada M. (1992). Variation in biochemical parameters of *Heterocapsa* sp. and *Olisthodiscus luteus* grown in 12:12 light:dark cycles. II. Changes in pigment composition. *Hydrobiologia*, 238: 149-157.
- Latasa M., Bidigare R. R. (1998). A comparison of phytoplankton populations of the Arabian Sea during the Spring Intermonsoon and Southwest Monsoon of 1995 as described by HPLC-analyzed pigments. *Deep-Sea Res. II*, 45: 2133-2170.
- Lavaud J., van Gorkom H. J., Etienne A.-L. (2002a). Photosystem II electron transfer cycle and chlororespiration in planktonic diatoms. *Phot. Res.*, 74: 51-59.
- Lavaud J., Rousseau B., Etienne A.-L. (2002b). In diatoms, a transthylakoid proton gradient alone is not sufficient to induce a non-photochemical fluorescence quenching. *FEBS letters*, 523: 163-166.
- Lavaud J., Rousseau B., van Gorkom H. J., Etienne A.-L. (2002c). Influence of the diadinoxanthin pool size on the photoprotection in marine planktonic diatom *Phaeodactylum tricorutum*. *Plant. Physiol.* 129: 1398-1406.
- Lavaud J., Rousseau B., Etienne A.-L. (2003). Enrichment of the light-harvesting complex in diadinoxanthin and implications for the non photochemical fluorescence quenching in diatoms. *Biochemistry*, 42: 5802-5808.

- Laybourn-Parry J. (1992). *Protozoan Plankton Ecology*. Chapman&Hall, London, pp. 231.
- Legendre L., Michaud J. (1998). Flux of biogenic carbon in oceans: size-dependent regulation by pelagic food webs. *Mar. Ecol. Prog. Ser.*, 164: 1-11.
- Lewis M. R. (2002). Variability of plankton and plankton processes on the mesoscale. In: *Phytoplankton Productivity – Carbon assimilation in marine and freshwater ecosystems*. Williams P. J.le B., Thomas D. N., Reynolds C. S. (Eds), Blackwell Science, pp. 109-137.
- Li, W. K. W., Subba Rao D. V., Harrison W. G., Smith J. C., Cullen J. J., Irwin B., Platt T., (1983). Autotrophic picoplankton in the tropical ocean. *Science*, 219: 292-295.
- Li W. K. W., Zohary T., Yacobi Y. Z., Wood A. M. (1993). Ultraphytoplankton in the eastern Mediterranean Sea: towards deriving phytoplankton biomass from flow cytometric measurements of abundance, fluorescence and light scatter. *Mar. Ecol. Prog. Ser.*, 102: 79-87.
- Lichtlé C., Arsalane W., Duval J.-C., Passaquet C. (1995). Characterization of the light-harvesting complex of *Giraudyopsis stellifer* (Chrysophyceae) and effects of light stress. *J. Phycol.*, 31: 380-387.
- Lin S., Knox R.S. (1991). Studies of excitation energy transfer within the green alga *Chlamydomonas reinhardtii* and its mutants at 77-K. *Photo. Res.*, 27(3): 157-168.
- Lizon F., Lagadeuc Y., Brunet C., Aelbrecht D., Bentley D. (1995). Primary production and photoadaptation of phytoplankton in relation with tidal mixing in coastal waters. *J. Plank. Res.*, 17(5): 1039-1055.
- Lohr M., Wilhelm C. (1999). Algae displaying the diadinoxanthin cycle also possess the violaxanthin cycle. *Proc. Natl. Acad. Sci. USA*, 96: 8784-8789.
- Lohr M., Wilhelm C. (2001). Xanthophyll synthesis in diatoms: quantification of putative intermediates and comparison of pigment conversion kinetics with rate constants derived from a model. *Planta*, 212: 382-391.
- Lokstein H., Tian L., Polle J. E. W., DellaPenna D. (2002). Xanthophyll biosynthetic mutants of *Arabidopsis thaliana*: altered nonphotochemical quenching of chlorophyll fluorescence is due to changes in photosystem II antenna size and stability. *Biochim. Biophys. Acta*, 1553: 309-319.
- MacCaull W. A., Platt T (1977). Diel variations in the photosynthetic parameters of coastal marine phytoplankton. *Limnol. Oceanogr.*, 22: 723-31.
- MacIntyre H. L., Kana T. M., Anning T., Geider R. J. (2002). Photoacclimation of photosynthesis irradiance response curves and photosynthetic pigments in microalgae and cyanobacteria. *J. phycol.*, 38: 17-38.

- Mackey M. D., Mackey D. J., Higgins H. W., Wright S. W. (1996). CHEMTAX – a program for estimating class abundances from chemical markers – application to HPLC measurements of phytoplankton. *Mar. Ecol. Prog. Ser.*, 144: 265-283.
- Malone T. C. (1971). Diurnal rhythms in netplankton and nanoplankton assimilation ratios. *Mar. Biol.*, 10: 285-289.
- Mangoni O., Modigh M., Mozetic P., Saggiomo V. (2004). Mesoscale variability of photosynthetic parameters in a highly dynamic frontal area (Northern Adriatic Sea). *American Society of Limnology and Oceanography. Ocean Research Conference*. February 15-20, Hawaii.
- Mann K. H., Lazier J. R. N. (1991). *Dynamics of marine ecosystems*. Blakwell, Boston, pp466.
- Manton I. and Parke M. (1960). Further observations on small green flagellates with special reference to possible relatives of *Chromulina pusilla* Butcher. *J. Mar. Biol. Ass. U.K.* 39: 275-298.
- Mantoura R. F. C. e Repeta D. J. (1997). Calibration methods for HPLC. In: *Phytoplankton pigments in oceanography*. Jeffrey S.W., Mantoura R. F. C. e Wright S. W. (eds), UNESCO publishing, pp. 407-428.
- Margalef R. (1978). Life-forms of phytoplankton as survival alternatives in an unstable environment. *Oceanologica Acta*, 1: 493-509.
- Marie D., Brussard C., Partensky F, Vaultot D. (1999). Enumeration of phytoplankton, bacteria and viruses in marine samples. *Current protocols in Cytometry*. J. Wiley & Sons, Inc. Suppl. 10: 11.11.1-11.11.15.
- Marino M., Modigh M., Zingone A. (1984). General features of phytoplankton communities and primary production in the gulf of Naples and adjacent waters Coastal and Estuarine Studies. In: *Marine phytoplankton and productivity*. Holm-Hansen L.B.O., Gilles R. (eds), Springer Varlagh, Berlin, 8: 89-100.
- Marra J., Heinemann K. (1982). Photosynthesis response by phytoplankton to sunlight variability. *Limnol. Oceanogr.*, 27 (6): 1141-1153.
- Marty J.-C., Chiavérini J., Pizay M.-D., Avril B. (2002). Seasonal and interannual dynamics of nutrients and phytoplankton pigments in the western Mediterranean Sea at the DYFAMED time-series station (1991-1999). *Deep Sea Res. II*, 49: 1965-1985.
- Masojídek J., Torzillo G., Koblížek M., Kopecký J., Bernardini P., Sacchi A., Komeda J. (1999). Photoadaptation of two members of the Chlorophyta (*Scenedesmus* and *Chlorella*) in laboratory and outdoor cultures: changes in chlorophyll fluorescence quenching and the xanthophyll cycle. *Planta*, 209: 126-135.

- Masojídek J., Grobbelaar J. U., Pechar L., Koblížek M. (2001). Photosystem II electron transport rates and oxygen production in natural waterblooms of freshwater cyanobacteria during a diel cycle. *J. Plank. Res.*, 23 (1): 57-66.
- Mobley C. D. (1994). *Light and water. Radiative transfer in natural waters*. Academic press, London, pp. 592.
- Modigh M. (2001). Seasonal variations of photosynthetic ciliates at a Mediterranean coastal site. *Aquat. Microb. Ecol.*, 23: 163-175.
- Modigh M., Ribera d'Alcalà M., Saggiomo V., Forlani G., Tosti E. (1985). Time relationship between physical-chemical and biological properties of phytoplankton blooms in the inner part of the Gulf of Naples, summer 1983. *Rapp. Comm. Int. Mer. Médit.*, 29: 109-110.
- Modigh M., Saggiomo V., Ribera d'Alcalà M. (1996). Conservative features of picoplankton in a Mediterranean eutrophic area, the Bay of Naples. *J. Plank. Res.*, 18 (1): 87-95.
- Modigh M., Castaldo S. (2001). Variability and persistence in tintinnid assemblages at a Mediterranean coastal site. *Aquat. Microb. Ecol.*, 28: 299-311.
- Moon-van der Staay S. Y., van der Staay G. W. M., Guillou L., Vaultot D., Claustre H., Medlin L. K. (2000). Abundance and diversity of Prymnesiophytes in the picoplankton community from the Equatorial Pacific Ocean inferred from 18S rDNA sequences. *Limnol. Oceanogr.*, 45: 98-109.
- Moon-van der Staay S. Y., De Wachter R., Vaultot D. (2001). Oceanic 18S rDNA sequences from picoplankton reveal unsuspected eukaryotic diversity. *Nature*, 409: 607-610.
- Morel A., Ahn Y. W., Partenski F., Vaultot D., Claustre H. (1993). *Prochlorococcus* and *Synechococcus*: a comparative study of their size, pigmentation and related optical properties. *J. Mar. Res.*, 51: 617-649.
- Mousseau L., Legendre L., Fortier L. (1996). Dynamics of size-fractionated phytoplankton and trophic pathways on the Scotian Shelf and at the shelf break, Northwestern Atlantic. *Aquat. Microb. Ecol.*, 10: 149-163.
- Moutin T., Raimbault P. (2002). Primary production, carbon export and nutrients availability in western and eastern Mediterranean Sea in early summer 1996 (MINOS cruise). *J. Mar. Syst.*, 33-34: 273-288.
- Mura M. P., Agustì S., Cebrian J., Satta P. (1996). Seasonal variability of phytoplankton biomass and community composition in Blanes Bay (1992-1994). *Publ. Espec. Inst. Esp. Oceanogr.*, 22: 23-29.
- Niyogi K. K., Björkman O., Grossman A. R. (1997a). The roles of specific xanthophylls in photoprotection. *Proc. Natl., Acad. Sci. USA*, 94: 14162-14167.

- Niyogi K. K., Björkman O., Grossman A. R. (1997b). Chlamydomonas xanthophylls cycle mutants identified by video imaging of chlorophyll fluorescence quenching. *Plant Cell*, 9: 1369-1380.
- Not F., Latasa M., Marie D., Cariou T., Vaultot D., Simon N. (2004). A single species, *Micromonas pusilla* (Prasinophyceae), dominates the eukaryotic picoplankton in the Western English Channel. *Appl. Environ. Microbiol.*, 70 (7): 4064-4072.
- Not F., Massana R., Latasa M., Marie D., Colon C., Eikrem W., Pedros-Alio C., Vaultot D., Simon N. (2005). Late summer community composition and abundance of photosynthetic picoeukaryotes in Norwegian and Barents Seas. *Limnol. Oceanogr.*, 50(5): 1677-1686.
- Olaizola M., Laroche J., Kolber Z. and Falkowski P. G. (1994). Non photochemical fluorescence quenching and the diadinoxanthin cycle in a marine diatom. *Phot. Res.*, 41: 357-370.
- Owens T. G., Falkowski P. G., Withledge T. E. (1980). Diel periodicity in cellular chlorophyll content in marine diatoms. *Mar. Biol.*, 59: 71-77.
- Palenik, B. (2001). Chromatic adaptation in marine *Synechococcus* strains. *Appl. Environ. Microbiol.*, 67: 991-994.
- Palenik B., Brahmsha B., Larimer F.W., Land M., Hauser L., Chain P., Lamerdin J., Regala W., Allen E. E., McCarren J., Paulsen I., Dufresne A., Partensky F., Webb E. A., Waterbury J. (2003). The genome of a motile marine *Synechococcus*. *Nature*, 424: 1037-1042.
- Pineau B., Gerard-Hirne C., Selve C. (2001). Carotenoid binding to photosystems I and II of *Chlamydomonas reinhardtii* cells grown under weak light or exposed to intense light *Plant Physiol. Biochem.*, 39: 73-85.
- Platt T., Gallegos C., Harrison W.G., (1980). Photoinhibition of photosynthesis in natural assemblages of marine phytoplankton. *J. Mar. Res.*, 38 (4): 687-701.
- Platt T., Sathyendranath S. (1988). Oceanic primary production: estimation by remote sensing at local and regional scales. *Science*, 241: 1613-1620.
- Porra R. J., Pfündel E.E., Engel N. (1997). Metabolism and function of photosynthetic pigments. In: *Phytoplankton pigments in oceanography*. Jeffrey S.W., Mantoura R. F. C. e Wright S. W. (eds), UNESCO publishing, pp. 85-126.
- Post A. F., Dubinsky Z., Wyman K., Falkowski P. G. (1984). Kinetics of light intensity adaptation in a marine planktonic diatom. *Mar. Biol.*, 83: 231-238.
- Prezelin B.B. (1992). Diel periodicity in phytoplankton productivity. *Hydrobiologia* 238: 1-35.
- Prezelin B. B., Ley A. C. (1980). Photosynthesis and Chlorophyll a fluorescence rhythms of marine phytoplankton. *Mar. Biol.*, 55: 295-307.

- Prezelin B. B., Putt M., Glover H. E. (1986). Diurnal patterns in photosynthetic capacity and depth-dependent photosynthesis irradiance relationships in *Synechococcus spp.* and larger phytoplankton in three water masses in the Northwest Atlantic Ocean. *Mar. Biol.*, 91: 205-217.
- Prezelin B. B., Bidigare R. R., Matlick H. A., Putt M., Ver Hoven B. (1987). Diurnal patterns of size-fractionated primary productivity across a coastal front. *Mar. Biol.*, 96: 563-574.
- Prezelin B. B., Glover H. E. (1991). Variability in time/space estimates of phytoplankton, biomass and productivity in the Sargasso Sea. *J. Plank. Res.*, 13 (suppl.): 45-67.
- Psarra S., Tselepides T., Ignatiades L. (2000). Primary productivity in oligotrophic Cretean Sea (NE Mediterranean): seasonal and interannual variability. *Prog. Oceanogr.*, 46: 187-204.
- Pugnetti P., Camatti E., Mangoni O., Morabito G., Oggioni A., Saggiomo V. (in press). Phytoplankton production in Italian freshwater and marine ecosystems: state of the art and perspectives. *Chemistry and Ecology*.
- Putt M., Rivkin R. B., Prezelin B. B. (1988). Effects of altered photic regimes on diel patterns of species-specific photosynthesis. I. Comparison of polar and temperate phytoplankton. *Mar. Biol.*, 97: 435-433.
- Ragni, M. (2005) Circadian patterns in key physiological processes of the marine diatom *Phaeodactylum tricornutum*. PhD Thesis, The Open University. London, pp. 168.
- Ragueneau O., Treguer P., Leynaert A., Anderson R. F., Brzezinski M. A., DeMaster D. J., Dugdale R. C., Dymond J., Fischer G., Francois R., Heinze C., Maier-Reimer E., Martin-Jezequel V., Nelson D. M., Queguiner B. (2000). A review of the Si cycle in the modern ocean: recent progress and missing gaps in the application of biogenic opal as a paleoproductivity proxy. *Global Planet Change*, 26: 317-365.
- Raven J. A. (1998). Small is beautiful: the picophytoplankton. *Func. Ecol.*, 12: 503-513.
- Redfield A. C., Ketchum B. H., Richards F. A. (1963). The influence of organism on the composition of sea water. In: *The Sea*, Vol.2 (ed. Hill M. N.), Interscience, New York, pp.26-77.
- Reinfelder J. R., Kraepiel A. M., Morel A. (2000). Unicellular C4 photosynthesis in a marine diatom. *Nature*, 407 (26): 996-999.
- Reynolds, N. (1974). *Imantonia rotunda* gen. et sp. nov., a new member of the Haptophyceae. *Bri. Phycological J.*, 9: 429-434.
- Ribera d'Alcalà M., Modigh M, Moretti M., Saggiomo V., Scardi M., Spezie G., Zingone A. (1989). Una storia infinita. Eutrofizzazione nella baia di Napoli. *Oebalia*, 15: 491-501.

- Ribera d'Alcalà M., Conversano F., Corato F., Licandro P., Mangoni O., Marino D., Mazzocchi M. G., Modigh M., Montresor M., Nardella M., Saggiomo V., Sarno D., Zingone A. (2004). Seasonal patterns in plankton communities in a pluriannual time series at a coastal Mediterranean site (Gulf of Naples): an attempt to discern recurrences and trends. *Sci Mar.* 68 (suppl. 1): 65-83.
- Riebesell U., Wolf-Gladrow D. a. (2002). Supply and uptake of inorganic nutrients. In: *Phytoplankton Productivity – Carbon assimilation in marine and freshwater ecosystems*. Williams P. J.le B., Thomas D. N., Reynolds C. S. (Eds), Blackwell Science, pp. 109-137.
- Rocap G., Larimer F. W., Lamerdin J., Malfatti S., Chain P., Ahlgren N. A., Arellano A., Coleman M., Hauser L., Hess W.R., Johnson Z. I., Land M., Lindell D., Post A. F., Regala W., Shah M., Shaw S. L., Steglich C., Sullivan M. B., Ting C. S., Tolonen A., Webb E. A., Zinser E. R., Chisholm S. W. (2004). Genome divergence in two *Prochlorococcus* ecotypes reflects oceanic niche differentiation. *Nature*, 424: 1042-1047.
- Rodríguez F., Pazos Y., Maneiro J., Zapata M. (2003). Temporal variation in phytoplankton assemblages and pigment composition at a fixed station of the Ría of Pontevedra (NW Spain). *Est. Coast. Shelf Sci.*, 58: 499-515.
- Ruban A., Lavaud J., Rousseau B., Guglielmi G., Horton P., Etienne A. (2004). The super-excess energy dissipation in diatom algae: comparative analysis with higher plants. *Phot. Res.*, 82: 165-175.
- Sakshaug E., Bricaud A., Dandonneau Y., Falkowski P. G., Kiefer D. A., Legendre L., Morel A., Parslow J., Takahashi M. (1997). Parameters of Photosynthesis: definitions, theory and interpretation of results. *J. Plankton Res.*, 19: 1637-1670.
- Sarno D., Iennaco I., Siano R., Montresor M., Zingone A. (2004). Phytoplankton physiognomy during the spring bloom in the North Balearic Front (North Western Mediterranean). *Atti Incontro scientifico congiunto CoNISMa – AIOL*, Città del Mare, Terrasini (PA), 18-22 October 2004.
- Scanlan D. J.; West N. J. (2002.) Molecular ecology of the marine cyanobacterial genera *Prochlorococcus* and *Synechococcus*. *FEMS Microbiology Ecology* 40: 1-12.
- Schulter L., Mohlenberg F., Havskum H., Larsen S. (2000). The use of phytoplankton pigments for identifying and quantifying phytoplankton groups in coastal areas: testing the influence of light and nutrients on pigment/chlorophyll *a* ratios. *Mar. Ecol. Prog. Series*, 192: 49-63.
- Scotto di Carlo B., Tomas C.R, Ianora A., Marino D., Mazzocchi M.G., Modigh M., Montresor M., Petrillo L., Ribera d'Alcalà M., Saggiomo V., Zingone A. (1985). Uno studio integrato dell'ecosistema pelagico costiero del Golfo di Napoli. *Nova Thalassia*, 7: 98-128.

- Sommaruga R., Hofer J. S., Alonso-Saez L., Gasol J. M. (2005). Differential sunlight sensitivity of picophytoplankton from surface Mediterranean coastal waters. *Appl. Environ. Microb.*, 71 (4): 2154-2157.
- Sournia A. (1974). Circadian periodicities in natural populations of marine phytoplankton. *Adv. Mar. Biol.*, 12: 325-389.
- Stockner J. G. (1988). Phototrophic picoplankton: an overview from marine and freshwater ecosystems. *Limnol. Oceanogr.* 33 (4): 765-775.
- Takano H. (1981). New and rare diatoms from Japanese marine water –VI. Three new species in Thalassiosiraceae. *Bull. Tok. Reg. Fish. Res. Lab.*, 105: 31-43.
- Tandeau de Marsac N. (2003). Phycobiliproteins and phycobilisomes: the early observations. *Phot. Res.*, 76: 197-205.
- Thompson P. (1999). The response of growth and biochemical composition to variations in day length, temperature and irradiance in the marine diatom *Thalassiosira pseudonana* (Bacillariophyceae). *J. Phycol.* 35: 1215-1223.
- Thomsen H. A., Buck K. R. (1998). Nanoflagellates of the Central California waters: taxonomy, biogeography, and abundance of primitive, green flagellates (Pedinophyceae, Prasinophyceae). *Deep Sea Res. II*, 45: 1687-1707.
- Thronsdon J., Zingone A. (1994). Micronomads of the Mediterranean Sea. *Giornale Botanico Italiano*, 128 (6): 1031-1044.
- Ting C. S., Rocap G., King J., Chisholm S. W. (2002). Cyanobacterial photosynthesis in the oceans: the origins and significance of divergent light-harvesting strategies. *Trends Microbiol.* 10(3): 134-142.
- Vandevolve T., Legendre L., Demers S., Therriault J. C. (1989). Circadian variations in photosynthetic assimilation and estimation of daily phytoplankton production. *Mar. Biol.*, 100: 525-531.
- Vaulot D., Partenski F., Neveux J., Mantoura R. F. C., Llewellyn C. A. (1990). Winter presence of prochlorophytes in surface waters of the northern western Mediterranean Sea. *Limnol. Oceanogr.*, 35: 1156-1164.
- Vaulot D., Romari K., Valentin K., Not F., Simon N., Biegala I., Le Gall F., Medlin L. K., Eikrem W. (2001). Diversity of eukaryotic picoplankton in coastal waters. *J. Phycol.*, 37 (3): 50.
- Vaulot D., Le Gall F., Marie D., Guillou L., Partenski F. (2004). The Roscoff Culture Collection (RCC): a collection dedicated to marine picoplankton. *Nova Hedwigia*, 79: 49-70.
- Vidussi F., Claustre H., Bustillos-Guzman J., Cailliau C., Marty J.-C. (1996). Determination of chlorophylls and carotenoids of marine phytoplankton: separation of chlorophyll a from divinyl-chlorophyll a and zeaxanthin from lutein. *J. Plank. Res.*, 18: 2377-2382.

- Williams P.J., Thomas D. N., Reynolds C. S. (2002). *Phytoplankton Productivity – Carbon assimilation in marine and freshwater ecosystems*. Blackwell Science, pp. 387.
- Worden, A. Z., Nolan J. K., Palenik B. (2004). Assessing the dynamics and ecology of marine picophytoplankton: The importance of the eukaryotic component. *Limnol. Oceanogr.* 49(1): 168-179.
- Wright S. W. (2001). Application of pigment analysis and CHEMTAX to field studies of phytoplankton communities. *Workshop “Pigments as a tool to estimate the biomass of a different phytoplankton groups”* Institut de Ciències del Mar, Barcellona 29 April-1 May: 17.
- Young A. J., Frank H. A. (1996). Energy transfer reactions involving carotenoids: quenching of chlorophyll fluorescence. *J. Photochem. Photobiol Biology*, 36: 3-15.
- Zapata M., Rodríguez F., Garrido J. L (2004). Separation of chlorophylls and carotenoids from marine phytoplankton: a new HPLC method using a reversed phase C8 column and pyridine-containing mobile phases. *Mar Ecol Prog Ser.*, 195: 29-45.
- Zingone A., Montresor M., Marino D., (1990). Summer phytoplankton physiognomy in coastal waters of the gulf of Naples. *Mar. Ecol.*, 11 (2): 157-172.
- Zingone A., Casotti R., Ribera d’Alcalà M., Scardi M., Marino D., (1995). “St Martin’s Summer”: the case of an autumn phytoplankton bloom in the gulf of Naples (Mediterranean Sea). *J. Plank. Res.*, 17 (1): 575-593.
- Zingone A., Sarno D., Forlani G. (1999a). Seasonal dynamics of *Micromonas pusilla* (Prasinophyceae) and its viruses in the Gulf of Naples (Mediterranean Sea). *J. Plank. Res.*, 21: 2143-2159.
- Zingone A., Chrétiennot-Dinet M.-J., Lange M., Medlin L. (1999b). Morphological and genetic characterization of *Phaeocystis cordata* and *P. jahnii* (Prymnesiophyceae), two new species from the Mediterranean Sea. *J. Phycol.*, 35: 1322-1337.
- Zhu F., Massana R., Not F., Marie D., Vaulot D. (2005). Mapping of picoeukaryotes in marine ecosystems with quantitative PCR of the 18S rRNA gene. *FEMS Microb. Ecol.*, 52: 79-92.
- Zubkov M. V., Fuchs B. M. Tarran G. A., Burkill P. H., Amann R. (2003). High rate of uptake of organic nitrogen compounds by *Prochlorococcus* cyanobacteria as a key to their dominance in oligotrophic oceanic waters. *Appl. Env. Microbiol.* 69 (2): 1299-1304.

## *Acknowledgments*

Durante questi tre anni tante sono le persone che mi hanno accompagnato, permettendomi di arrivare alla fine di questo percorso e a cui va la mia sincera gratitudine.

Il grazie più grande è per il mio tutor Dr. Vincenzo Saggiomo, per aver creduto in me, offrendomi la possibilità di compiere questo cammino di crescita e per essere un punto di riferimento importante sia sul piano scientifico che umano.

Un grazie sincero va anche al mio co-tutor Dr. Adriana Zingone, che con i suoi consigli mi ha aiutato a guardare sempre le questioni sotto diverse prospettive.

Alla Dr. Monica Modigh va un ringraziamento speciale per aver condiviso con me tante avventure e tante infinite discussioni, e per avermi aiutato nello stesura finale della tesi.

Un grande grazie al Dr. Maurizio Ribera d'Alcalà, che con la sua inesauribile energia e profonda conoscenza, mi ha sempre ricordato quanto possa essere affascinante questa nostra scienza.

Non avrò mai parole sufficienti per ringraziare Francesca Margiotta, per aver vissuto e condiviso con me, letteralmente gomito a gomito, i mille eventi lavorativi e non che hanno riempito questi tre anni, per essere una cara amica, prima che una collega.

Vorrei ringraziare di cuore anche Mariella Ragni per avermi introdotto al problema dei cicli circadiani e per essermi stata vicina sin dalla mia prima crociera.

La mia più sincera gratitudine va a tutto il laboratorio di Oceanografia Biologica, per avermi accolta e aver rappresentato il substrato ideale per la mia crescita scientifica e personale, non facendomi mai mancare il confronto con persone esperte e motivate. Il mio affetto va soprattutto a Serena, Enzo e Rosario che hanno condiviso con me le giornate, soprattutto quelle interminabili di quest'ultimo periodo. Un grazie affettuoso, in particolare, lo devo a Ferdinando Tramontano per l'aiuto durante i campionamenti a Marechiarà e ad Italia, per avermi più volte aiutato a districarmi fra i "tranelli" della burocrazia.

L'Area Gestione Ambiente ed Ecologia Costiera delle Aree Temperate e Polari è stata un indispensabile supporto nello svolgimento delle analisi e delle attività di campo. Un grazie immenso a Ciro Chiese ed Augusto Passarelli, per la disponibilità e l'amicizia dimostratami in mille occasioni.

La mia gratitudine va anche al laboratorio di Botanica Marina per aver messo a disposizione gli spazi, i mezzi, ma soprattutto l'esperienza per portare avanti gli esperimenti sulle colture. Un grazie particolare a Raffaele Siano che mi ha aiutato più volte a "salvare" le mie specie e ad Isabella Piercopo per avermi gentilmente fornito le immagini al microscopio. A Mariella, poi, va l'affetto per i tanti momenti vissuti insieme.

Un grazie sincero è per la dott.ssa Raffaella Casotti e Françoise Ribalt che hanno guidato con pazienza i miei primi passi nel mondo della citofluorimetria.

Il laboratorio di Biologia Marina del Dipartimento di Zoologia dell'Università "Federico II", dove ho mosso i primi passi da giovane tesista è stato anche in questi anni un punto di riferimento importante. Un grazie di cuore al prof. Gian Carlo Carrada e alla prof.ssa. Olga Mangoni per avermi fatto sentire sempre a casa; a Maria Grieco per l'amicizia sincera dimostratami e a Raffaella Balzano, con cui ho condiviso l'esperienza del dottorato.

Un ringraziamento speciale va a Giuseppe Giordano per aver trascorso con me le interminabili giornate nelle “fredde” celle e aver sempre mostrato lo stoicismo del perfetto tesista.

Al personale tecnico scientifico e all’equipaggio delle N/O *Vettoria*, *Coopernaut* ed *Urania*, va un grandissimo grazie per aver reso possibile l’attività di campo, soprattutto durante gli “insonni” esperimenti sui cicli circadiani.

A questo punto è per me importante ringraziare di cuore tutti gli amici che mi accompagnano da una vita, non facendomi mai mancare il loro sostegno e con cui divido da anni l’esperienza meravigliosa e complicata del diventare adulti. Un grazie fortissimo a Rosalba, Adele, Stefania, Anna, Giovanni, Giovanna, Maria, Nando, Barbara M., Barbara T., Giancarlo, Eugenia, Francesco, Luca.

Un semplice grazie non può racchiudere tutte le emozioni che Federico mi ha donato in questi anni... Ma grazie per essere ancora “sale” della mia vita, invito continuo ad esprimere il meglio di me.

A mamma, papà e Vincenzo va il grazie più grande per essere da sempre e per sempre luogo di crescita e di confronto, ma soprattutto luogo d’amore.